DEVELOPMENT AND APPLICATION OF LINEAR STATE ESTIMATORS IN CONTROL OF REACTIVE DISTILLATION

BY

Olanrewaju Moshood Jide

A Thesis Presented to the
DEANSHIP OF GRADUATE STUDIES

KING FAHD UNIVERSITY OF PETROLEUM & MINERALS
DHAHRAN, SAUDI ARABIA

In Partial Fulfillment of the
Requirements for the Degree of

MASTER OF SCIENCE

In
CHEMICAL ENGINEERING

May 2005

KING FAHD UNIVERSITY OF PETROLEUM & MINERALS
DHAHRAN 31261, SAUDI ARABIA

DEANSHIP OF GRADUATE STUDIES

This thesis, written by **Olanrewaju Moshood Jide** under the direction of his thesis advisor and approved by his thesis committee, has been presented to and accepted by the Dean of Graduates Studies, in partial fulfillment of the requirement for the degree of

MASTER OF SCIENCE IN CHEMICAL ENGINEERING.

Thesis Committee

MAArfaj
Dr. M. A. Al-Arfaj
(Thesis Advisor)

Esam Hamad
Prof. Esam Hamad
(Member)

H. Duwaish
Dr. H. Al-Duwaish
(Member)

Prof. Mohammed B. Amin
(Department Chairman)

Dr. Mohammad A. Al-Ohali
(Dean of Graduate Studies)

هـ١٤٢٦/٤/٢٢
Date 30-5-2005

Dedicated to

My parents, wife and son

Acknowledgements

All thanks to Allah, The Beneficent and Merciful, for given me the opportunity to pursue my M.S. degree and the capability to complete this work successfully. I express my profound gratitude to my thesis advisor, Dr. Muhammad A. Al-Arfaj, for his guidance, encouragement and invaluable contributions towards the success of this work. Indeed, I am very fortunate to have him as my advisor because he has trained me on how to thrive for the highest quality of research standards. His enthusiasm and innovative thinking were a great inspiration for me throughout my research work. I gratefully acknowledge my committee members, Dr. Hussain N. Al-Duwaish and Professor Esam Hamad for their co-operation, support and contributions to make this work a reality. The suggestions and advice they rendered to me are highly valued and appreciated. The financial support provided by King Fahd University of Petroleum & Minerals under the project CHE/DISTILLATION/272 is highly appreciated. Also, the assistance and support provided to me by the faculties, staffs and colleagues at Chemical Engineering Department of KFUPM is deeply acknowledged. Last but not the least, I thank my parents, wife and son for their love, sacrifice, affection and understanding.

Table of Contents

Acknowledgements iv
Table of Contents v
List of Tables ix
List of Figures x
THESIS ABSTRACT (ENGLISH) xvi
THESIS ABSTRACT (ARABIC) xvii
CHAPTER 1 1
1 Introduction 1
  1.1 Background 1
  1.2 Previous Work 3
    1.2.1 Reactive Distillation Control 3
    1.2.2 State Estimators and their Applications 8
  1.3 Scope and Objectives 11
  1.4 The Significance of this Work 12
  1.5 References 13
CHAPTER 2 16
2 Linearized State Space Formulation for Nonlinear Generic Reactive Distillation 16
  2.1 Introduction 16
  2.2 Reactive Distillation System 18
    2.2.1 Nonlinear Process Model 20
    2.2.2 Linear State Space Model Formulation 23
  2.3 Steady State Design Data. 24
  2.4 Model Linearity 28
  2.5 System Stability 28
  2.6 Conclusion 29
  2.7 References 34
CHAPTER 3 36

3 Dynamic Comparison of Linear and Nonlinear Models for Generic Reactive Distillation System 36
3.1 Introduction 36
3.2 Error Index 37
3.3 Steady State Design Data 38
3.4 Steady State Sensitivity 40
3.5 Robustness of a Linear Model 45
3.5.1 Open-loop Model (OL) 50
3.5.2 Open-loop Model with Internal Composition Controller (OL+IC) 56
3.6 Accuracy of a Linear Model 63
3.7 Conclusion 68
3.8 References 69
CHAPTER 4 70
4 Impact of Disturbance Magnitudes and Directions on the Dynamic Behavior of Reactive Distillation 70
4.1 Introduction 70
4.2 Dynamic Scenarios 72
4.3 Open-loop Model (OL) 73
4.3.1 Feed Flowrates 73
4.3.2 Feed Composition 82
4.3.3 Vapor Boilup 83
4.4 Open-loop Model with Internal Controller (OL) 86
4.4.1 Feed Flowrates 87
4.4.2 Vapor Boilup 91
4.5 Single-end Control (CL) 93
4.6 Conclusion 97
4.7 Reference 98
CHAPTER 5 99
5 Performance Assessment of Different Control Structure for Generic Reactive Distillation Using Linear and Nonlinear Process Models 99
5.1 Introduction 99

5.2 The Process 100
5.3 Control Structures 101
5.3.1 Control Structure I 102
5.3.2 Control Structure II 109
5.3.3 Control Structure III 119
5.3.4 General Comparisons and Observations 125
5.4 Conclusion 126
5.5 Reference 127
CHAPTER 6 128
6 Design and Implementation of Linear State Estimators in Reactive distillation 128
6.1 Introduction 128
6.2 Reactive Distillation Models 129
6.3 Observability, Location and Number of Measurements 133
6.3.1 Observability 133
6.3.2 Measurement Location 133
6.3.3 Number of Measurements 134
6.4 State Estimator Structure 138
6.4.1 Base Initial Condition Errors, Measurement and Plant Noise 139
6.4.2 Luenberger Observer (LO) 140
6.4.3 Kalman Filter (KF) 146
6.5 Results and Discussion 149
6.5.1 The Estimators Performance 149
6.5.2 Effect of the Initial Conditions Errors 154
6.5.3 Effect of the Measurement Noise 156
6.5.4 Plant-model Mismatch 158
6.5.5 The Linear Estimators Using Measurement Data Predicted by the Nonlinear Equation 160
6.6 Conclusion 164
6.7 References 165
CHAPTER 7 167
7 The State Estimator-Based Control of Reactive Distillation System 167

7.1 Introduction 167
7.2 The Process 168
7.3 State Estimator Structure 168
7.4 Control System Configuration 170
7.5 Results and Discussion 174
7.5.1 Control Performance 174
7.5.2 Effect of Erroneous Initial Conditions 182
7.5.3 Effect of Measurement Error 186
7.5.4 Plant-Model mismatch 189
7.6 Conclusion 190
7.7 References 192
CHAPTER 8 193
8 Conclusions and Future Research Directions 193
8.1 Conclusions 193
8.2 Future Research Directions 194
NOMENCLATURE 197
APPENDICES 202
Appendix A 202
Appendix B 214
Appendix C 215
Appendix D 216
VITA 217

List of Tables

Table 2.1 Kinetic and physical properties.. 26
Table 2.2 Optimum steady state conditions.. 27
Table 2.3 Eigenvalues of matrix A (5N X 5N), N=22, column configuration ($N_S/N_{RX}/N_R$): 7/6/7 column stages, 1 reboiler and 1 condenser. 33
Table 3.1 Base steady state conditions for a high and low-conversion region. 39
Table 3.2 The Average Relative Error (ARE) of open-loop model (OL), without internal controller 46
Table 3.3 The Average Relative Error (ARE) for open-loop model (OL), without internal controller 47
Table 3.4 The Average Relative Error (ARE) for open-loop model with internal composition controller (OL+IC) 48
Table 3.5 The Average Relative Error (ARE) for open-loop model with internal composition controller (OL+IC) 49
Table 4.1 Effect of disturbance magnitudes and directions on the system stability 96
Table 6.1 Optimum base steady state conditions.. 132
Table 6.2 Number of the measurement versus the rank of the system. 137
Table 7.1 Base steady state conditions 175

List of Figures

Figure 2.1 (a) Reactive distillation column, (b) a reactive tray. 19

Figure 2.2 Steady state composition profile (in deviation form) of the reactant A on the tray nf1, the reactant B on the tray nf2, the product C in the distillate and the product D in the bottoms with ±2% & ±4% change in F_B 30

Figure 2.3 Steady state temperature profiles after ±2% & ±4% changes are made in F_B: (a) column temperature profiles in deviation form. (b) column temperature profiles. 31

Figure 2.4 Dynamic composition profile of the reactant A on the tray nf1, the reactant B on the tray nf2, the product C in the distillate and the product D in the bottoms with ±2% & ±4% change in F_B 32

Figure 3.1 (a) Composition profiles with 2% increase in F_B, (b) temperature profiles with 2% increase in F_B: (---) base steady state profile with no disturbance; (— —) linear model; (——) nonlinear model.. 41

Figure 3.2 (a) Composition profiles with 2% increase in F_A, (b) temperature profiles with 2% increase in F_A: (---) base steady state profile; (— —) linear model ;(——) nonlinear model. 43

Figure 3.3 Composition profiles with 2% increase in F_A: (---) base steady state profile; (— —) linear model; (——) nonlinear model.. 44

Figure 3.4 (a) Composition profiles with 1% increase in F_B: (b) temperature profiles with 1% increase in F_B: (---) base steady state profile; (— —) linear model; (——) nonlinear model. 51

Figure 3.5 (a) Composition profiles with 5% increase in F_B: (b) temperature profiles with 5% increase in F_B: (---) base steady state profile; (— —) linear model; (——) nonlinear model. 52

Figure 3.6 (a) Composition profiles with 10% increase in F_B: (b) temperature profiles with 10% increase in F_B: (---) base steady state profile; (— —) linear model;........ 53

Figure 3.7 Dynamic responses of bottoms flowrate (B) to different magnitude of increase in F_B: (— —) linear model; (——) nonlinear model... 54

Figure 3.8 Dynamic responses of the composition of component D to different magnitude of increase in F_B: (— —) linear model; (——) nonlinear model. 55

Figure 3.9 OL+IC. Composition profiles with 5% increase in F_B: (---) base steady state profile; (— —) linear model; (——) nonlinear model. 58

Figure 3.10 OL+IC. Composition profiles with 5% increase in F_B: (---) base steady state profile; (— —) linear model; (——) nonlinear model. 59

Figure 3.11 OL+IC. Composition profiles with 5% increase in F_B: (---) base steady state profile; (— —) linear model; (——) nonlinear model. 60

Figure 3.12 OL+IC. Dynamic responses of flowrate (F_A) and composition of reactant A on tray nf1to different magnitude of increase in F_B: (— —) linear model; (——) nonlinear model. 61

Figure 3.13 OL+IC. Dynamic responses of bottoms flowrate (B) to different magnitude of increase in F_B: (— —) linear model; (——) nonlinear model. 62

Figure 3.14 OL+IC. Dynamic responses of the composition of component D to different magnitude of increase in F_B: (— —) linear model; (——) nonlinear model. 62

Figure 3.15 The ARE of the bulk steady state composition profiles with disturbance in F_B: OL (b) OL+IC. 66

Figure 3.16 The ARE of the individual dynamic (Dyn) and steady state (s.s) of bottoms flowrate (B) with disturbance in F_B: (——) OL; (----) OL+IC. 66

Figure 3.17 The ARE of the bulk steady state temperature profiles with disturbances in Vs, F_B, %mol B in F_A: (—) OL; (---) OL+IC. 67

Figure 4.1 Dynamic responses of the system to different magnitude changes in feed F_B. (a) total reaction rate; (b) bottoms flowrate; (c) composition of product D in the bottoms; (d) internal composition of reactant A in tray nf1. 75

Figure 4.2 Dynamic responses of the system to different magnitude changes in feed F_A. (a) total reaction rate; (b) bottoms flowrate; (c) composition of product D in the bottoms; (d) internal composition of reactant A in tray nf1. 76

Figure 4.3 Responses of the reaction rate in reactive trays to step changes in F_B and F_A. (a) reactive tray nf1; (b) reactive tray nf1+2; (c) reactive tray nf2. 77

Figure 4.4 Dynamic responses of total reaction rate to step changes in feed flowrates of reactant A and B. (—) OL-I; (---) OL-II. 80

Figure 4.5 Temperature distribution in the column with disturbance in feed streams: 81

Figure 4.6 Dynamic response of the total reaction rate (TR) of products in reactive zone to different magnitude changes in feed compositions.. 84

Figure 4.7 Dynamic responses of the system to different magnitude changes in vapor boilup. (a) total reaction rate; (b) bottoms flowrate; (c) composition of product D in the bottoms; (d) internal composition of reactant A in tray nf1. 85

Figure 4.8 Dynamic responses of total reaction rate (TR) of products in reactive zone (a) step changes in vapor boilup. (b) step changes in reflux rate. 88

Figure 4.9 Responses of the system in presence of an internal composition controller to ±10% change in feed F_B. (a) total reaction rate; (b) bottoms flowrate; (c) composition of product D in the bottoms; (d) internal composition of reactant A in tray nf1. 89

Figure 4.10 Steady state profiles of composition of A, B, C and B with change in F_B in presence of internal composition controller.. 90

Figure 4.11 Response bottoms flowrate (B) the total reaction rate (TR) to different magnitudes change in vapor boilup in presence of an internal composition controller. 92

Figure 4.12 The responses of the system with single-end composition controller when step changes are made in the vapor boilup (V_S). 95

Figure 5.1 Dual-end composition control structure 103

Figure 5.2 Dual-end composition control responses, -20%, +10%, +20% F_B:............... 105

Figure 5.3 Dual-end composition control responses, 5%, 10% mol of reactant A in Z_b:107

Figure 5.4 Dual-end composition control responses, setpoint changes $X_{bot,B}$ from 95% to 92% and 98%: (- - -) linear model; (—); nonlinear model. 108

Figure 5.5 Three alternative control schemes for single-end control structure: (I) fixed reflux ratio and control level by the reflux flowrate; (II) fixed reflux ratio and control level by the distillate flowrate (D); (III) fixed reflux flowrate and control level by the distillate flowrate.. 113

Figure 5.6 Single-end composition control responses base on Scheme 3 with -20%, +10% and +20% disturbances in F_B: (---) linear model; (—) nonlinear model. 114

Figure 5.7 Single-end composition control structure.. 115

Figure 5.8 Single-end composition control responses: -20%, +10%, +20% F_B. 116

Figure 5.9 Single-end composition control responses, 5%, 10% mol of A in Z_b: 117

Figure 5.10 Single-end composition control responses, setpoint changes $X_{bot, B}$ from 95% to 92% and 98%: (- - -) linear model; (—); nonlinear model. 118

Figure 5.11 Single-end temperature control structure. 121

Figure 5.12 Single-end temperature control responses, -20%, +10%, +20% F_B: 122

Figure 5.13 Single-end temperature control responses, 5%, 10% mol of reactant A in Z_b: 123

Figure 5.14 Single-end temperature control responses, ±2 K degree changes in temperature on tray 2: (- - -) linear model; (—); nonlinear model. 124

Figure 6.1 Algorithm for determining the number of measurements needed for system observability.. 135

Figure 6.2 Linear state estimator structure. 141

Figure 6.3 The base initial condition error ($x_0 err$) and base measurement noise ($v(t)$). 142

Figure 6.4 [A] The eigenvalues of matrix (A-KC), [B] effect of the eigenvalues selection on the performance of Luenberger observer: (a) the same as eigenvalues of matrix A; (b) the slowest two eigenvalues are shifted to higher magnitudes; (c) the slowest seven eigenvalues are shifted to higher magnitudes: (–––) actual state profile; (----) estimated state profile. 145

Figure 6.5 Dynamic composition profiles: (–––) actual state profile; (----) LO estimated state profile; (— —) KF estimated state profile. 151

Figure 6.6 Kalman filter dynamic profiles : (–––) actual state profile; (----) estimated state profile when a steady state Ricatti equation is used in KF design; (— —) estimated state profile when a differential Ricatti equation is used in KF design.. 152

Figure 6.7 Kalman filter dynamic profiles : (–––) actual state profile; (----) estimated state profile when a steady state Ricatti equation is used in KF design; (— —) estimated state profile when a differential Ricatti equation is used in KF design.. 153

Figure 6.8 Effect of initial condition errors on the performance of the state estimators with a 10% F_B disturbance, [A] initial condition errors; [B] response from the Luenberger observer; [C] response from Kalman filter, (I) $x_0 err$; (II) 4 $x_0 err$; (III)

$\hat{X}(0)$ = 0.25/0.25/0.25/0.25:(——) actual state profile; (----) estimated state profile. 155

Figure 6.9 Effect of measurement noise on the performance of the estimators with a 10% F_B disturbance, (a) measurement noise; (b) response of the Luenberger observer; (c) response of the Kalman filter: (——) actual state profile; (----) estimated state profile. 157

Figure 6.10 Effect of plant-model mismatch on the performance of the linear state estimators with a 10% F_B disturbance. (----) KF estimated state profile; (— —) LO estimated state profile; (——) actual state profile. (I) $\hat{\alpha} = 4.2/2.2/8.2/1$; (II) $\hat{\alpha} = 4.4/2.4/8.4/1$. 159

Figure 6.11 [A] The shifted eigenvalues for the Luenberger observer (LO) with a 10% F_B disturbance, [B] Steady state composition profiles from LO as: (a) predicted by nonlinear process model; (b) predicted by LO using nonlinear equation for measurement; (c) predicted by LO using linearized equation for measurement. ... 162

Figure 6.12 Steady state composition profiles from Kalman filter (KF) as: (a) predicted by nonlinear process model; (b) predicted by KF using nonlinear equation for measurement; (C) predicted by KF using linearized equation for measurement.... 163

Figure 7.1 The estimator-based control system structure. 171

Figure 7.2 Dual-end control structure. 172

Figure 7.3 The base initial condition errors ($x_0 err$) and base measurement noise (v). 176

Figure 7.4 The Pseudo Rectangular Random Sequence (PRRS) forcing function on F_B. 176

Figure 7.5 Control performance when all the composition controllers rely on the KF. The base initial condition errors, $\delta_m = 10\%$ and $\delta_p = 1\%$ are used for KF design. +10% and -10% F_B disturbance. (——) CS-Analyzer; (----) CS-Estimator....................... 179

Figure 7.6 Control performance when all the composition controllers rely on the KF. The base initial condition errors, $\delta_m = 10\%$ and $\delta_p = 1\%$ are used for KF design. PRRS forcing function on F_B. (——) CS-Analyzer; (----) CS-Estimator. 180

Figure 7.7 Control performances when the only internal composition controller relies on the KF: the base initial condition errors, $\delta_m = 10\%$ and $\delta_p = 1\%$ are used for KF design +20% and -20% F_B disturbance, (——) CS-Analyzer; (----) CS-Estimator.. 181

Figure 7.8 Effect of the erroneous initial conditions. [a] (I) $\hat{X}(0) = X_0 + 4x_0 err$; 184

Figure 7.9 Effect of the erroneous initial conditions on the control performance: (I) $\hat{X}(0) = X_0 + x_0 err$; (II) $\hat{X}(0) = X_0 + 4x_0 err$;(III) $\hat{X}(0) =$ 0.25/0.25/0.25/0.25, 10% F_B disturbance, (——) CS-Analyzer; (----) CS-Estimator. $\delta_m = 10\%$ and $\delta_p = 1\%$ are used for KF design. 185

Figure 7.10 Effect of measurement error in the measurement data with a +10% F_B disturbance. The base initial condition errors, $\delta_m = 10\%$ and $\delta_p = 1\%$ are used for KF design. (——) CS-Analyzer; (----) CS-Estimator. (a) no error (b) +1 ^{0}C (c) -1 ^{0}C error located in 3 stages. 187

Figure 7.11 Temperature profile on tray nf1 of the CS-Estimator system. The measurement error of 1 ^{0}C present in the thermocouples located on the reboiler, the tray nf1 and the top plate. The base initial condition errors, $\delta_m = 10\%$ and $\delta_p = 1\%$ are used for KF design. +10% F_B disturbance. 188

Figure 7.12 Effect of errors in relative volatility. The base initial condition errors, $\delta_m = 10\%$ and $\delta_p = 1\%$ are used for KF design. +10%F_B disturbance. (——) CS-Analyzer; (----) CS-Estimator. 191

THESIS ABSTRACT (ENGLISH)

NAME:	OLANREWAJU MOSHOOD JIDE
TITLE OF STUDY:	DEVELOPMENT AND APPLICATION OF LINEAR STATE ESTIMATORS IN CONTROL OF REACTIVE DISTILLATION
MAJOR FIELD:	CHEMICAL ENGINEERING
DATE OF DEGREE:	MAY, 2005

Effective control and monitoring of a process requires sufficient information on the state of the process, which is uniquely specified by the process state variables. In practice, online measurements of all of the variables of a process are rarely available, and in such cases, reliable information on the immeasurable state variables is obtained by using the state estimator. This work presents the design, implementation and application of linear state estimators, which can infer the column composition from the temperature measurements or other process states in a reactive distillation process.

The accuracy of the developed estimators is checked by comparing the estimated states to the actual states as predicted by the process model of a reactive distillation system. The robustness and reliability of the linear state estimators are demonstrated against erroneous initial conditions, the measurement noise and plant-model mismatch. The estimator-based control system is developed and implemented on a reactive distillation process. The control performance of the system that relies on the estimator is examined and compared to that of the system which takes direct measurement from the process model using online perfect analyzer. It is found that a robust linear state estimator can be successfully designed and implemented on the feedback control of reactive distillation system.

Keywords: *Reactive distillation; Linear model; State estimator; Process control*

THESIS ABSTRACT (ARABIC)

إن التحكم والمتابعة الجيدة لأداء العمليات الكيميائية يتطلب الحصول على كمية كافية من المعلومات وذلك لتحديد حالة العملية. في حالات كثيرة يصعب الحصول على المعلومات المطلوبة عن العملية عن طريق أجهزة القياس وذلك يتطلب إستخدام مقدر للحالة. تقدم هذه الأطروحة طريقة تصميم وتطبيق مقدر الحالة الخطي في أبراج التقطير التفاعلية وذلك عن طريق تقدير تكوين السائل عن طريق معرفة درجة الحرارة.

لقد تم تقييم أداء هذه المقدرات عن طريق مقارنة نتائجها بنتائج النموذج الرياضي للعملية. لقد تم دراسة جودة أداء هذه المقدرات تحت ظرف تصاميم مختلفة كفرضية وجود خلل في قراءة الحرارة أو خطأ بين النموذج الرياضي والعملية وغيرها من ظروف مختلفة. لقد تمت مقارنة أداء عمل نظام التحكم القائم على أساس مقدر الحالة مع ذلك القائم على أساس أجهزة القياس وتم الوصول إلى نتيجة أن مقدر الحالات الخطي يمكن تطبيقة على عملية التقطير التفاعلية وبأداء جيد.

CHAPTER 1

1 Introduction

1.1 Background

The combination of reaction and distillation is an old idea that has received renewed attention recently. The importance and application of reactive distillation has captured the imagination of many because of the demonstrated potential for capital productivity improvements, increased reaction conversion, elimination of difficult separation, selectivity improvements, and reduced energy use through direct utilization of reaction heat. Therefore, reactive distillation technology has shown a significant growth in both patents and journal papers [1-5]. However, the reactive systems where the reactant and product volatilities differ considerably are ideally suited for reactive distillation [6].

The rising demand for saving energy and the increasing product quality requirements necessitate a better and more effective control system. However, the control of reactive distillation system is challenging because of its complex dynamics resulting from its integrated functionality of reaction and separation. Al-Arfaj and Luyben [3] discussed many control schemes for an ideal reactive distillation. They concluded that an internal composition control is important to have an effective control of the system. In their study, they assumed that the internal compositions are available for the control system by an accurate composition analyzer.

Although composition analyzers, like online chromatography have been used in the process industries for a long time, they usually suffer from many shortcomings. An online analyzer is expensive to acquire and requires a high investment. The reliability of online chromatography is not very good. Perhaps, the most important setback in the application of an online analyzer to measure process compositions in chemical process control is that it possesses a very large time delay and thereby lowers the achievable control performance [7]. Thus, it is of a major interest to develop an effective state estimator whenever a composition measurement is required in the control system.

Most of the early work on reactive distillation focused on its design and process modeling [6, 8-13]. A limited number of papers have been published on control of the reactive distillation [3]**.** In the same vein, many research papers have discussed the application of the state estimators in the control of conventional distillation column [14-20]. However, the application of the state estimators in the control of reactive distillation has not been reported in the open literature. Considering the numerous advantages of reactive distillation, and the effective application of the state estimation method to the conventional distillation system, this thesis work is aimed at developing the state estimators, which can infer the column compositions from the temperature measurement and other state of the process. The robustness and reliability of the developed state estimators are tested under a wide range of operating conditions. The developed state estimator is implemented in the feedback control system for reactive distillation process.

1.2 Previous Work

1.2.1 Reactive Distillation Control

Reactive distillation is the coupling of both physical separation and chemical reaction in one unit operation. It has been employed in industry for many decades, and its area of application has grown significantly. A reactive distillation column is usually split into three sections: reactive section, stripping section and rectifying section. In the reactive section, the reactants are converted into products, and where, by means of distillation, the products are separated out of reactive zone. The tasks of the rectifying and stripping sections depend on the boiling points of the reactant and product.

Several researchers have worked extensively on the conceptual design, steady state multiplicity and process optimization of reactive distillation [1, 6, 8]. However, only a few papers have appeared that discuss the closed-loop of reactive distillation column. No research has appeared in the open literature that utilizes the state estimators in the feedback control of distillation column.

Roat et al. [21] presented an industrial approach to the modeling and control of reactive distillation column systems. They proposed a control structure that uses two conventional proportional-integral (PI) temperature controllers to maintain two trays temperature in the two-product reactive distillation column by adjusting the two fresh feed streams. Sneesby et al. [22] proposed a two-point control scheme for ethyl *tert*-butyl ether (ETBE) reactive distillation column in which both product purity and conversion are controlled. They implemented conventional PI controller to control a temperature in the stripping section by manipulating the reboiler heat input and to the control conversion by manipulating the reflux flowrate.

Al-Arfaj and Luyben [3] studied the control of reactive distillation column that produced two products from a single reactive column by feeding exactly stoichiometric amount of the two fresh feed streams. They explored six alternatives control structures, all of which included the measurement of composition of one of the reactants inside the reactive section of the column. This composition is then used to adjust the appropriate fresh feed stream. They reported that unless an excess of one of the reactants in the column is incorporated in the design, the inventory of one of the reactants needs to be detected so that a feedback trim can balance the reactants feed stoichiometry. Therefore, the use of the compositional analyzer in the reactive zone was advocated.

Luyben [23] presented a quantitative comparison of the steady-state economics and the dynamic controllability of two alternative reactive distillation systems. He found out that even though there is a significant steady state penalty in using the two-column process, but the use of online analyzer is eliminated. Although, the one-column is more efficient than the two-column, but its operation depends on having a reliable composition measurement.

Al-Arfaj and Luyben [24] further investigated the control structures for *tert*-butyl ether (ETBE) reactive distillation column using the two different process configurations: a design with two fresh reactant feed streams and a design with a single reactant feed. They presented an optimum design for the double-feed case. In their study, several control structures were investigated, and their effectiveness in the ETBE case was compared with those in their previous study. Their results showed that the double-feed system requires internal composition control to balance the feeds stoichiometry, along with the temperature control to maintain the product purity. They extended their work to more control structure alternatives for the methyl acetate reactive distillation [4].

Al-Arfaj and Luyben [25] has also demonstrated that ethylene glycol reactive distillation columns can be controlled effectively by a simple PI control scheme. Their proposed control structure achieves the stoichiometric balancing of the reactants and maintains the product purity within reasonable bounds. In their work, only simple conventional PI loops are used, no composition analyzer is required and the structure shows that it can handle large disturbances. They reported that the structure can be generally applicable to other systems that are similar to the ethylene glycol system in stoichiometry, kinetics, vapor-liquid equilibrium (VLE), and design.

Estrada-Villagrana et al. [26] employed a dynamic model to study the control of MTBE reactive distillation. The control structures were constructed to control reflux drum level, the base level and MTBE purity in the bottoms. The distillate and the reflux flowrate were considered as possible manipulating variables to control the drum level. The bottoms flowrate controls the base level. A temperature in the stripping zone was selected to be controlled by the reboiler heat input to ensure MTBE purity at the bottoms. Even though the reactive columns are known to be highly nonlinear, they demonstrated the use of the linearized control analysis tools in the controllability of reactive distillation.

Vora et al. [27] presented the control of reactive distillation for the production of ethyl acetate. Utilizing the index two DAE model (i.e. Dynamic Algebraic Equation model), they analyzed the system from a steady-state and a dynamic point of view. Based on their results, they found that the process has two time scales caused by the liquid hydraulics. Motivated by this finding, a modified slow dynamics model was developed.

The nonlinear controllers were designed based on the two-time scale model. Those controllers performed well when the product purity setpoint was increased by 25%.

Wang et al. [5] further investigated the effect of interaction multiplicity on the control system design for a MTBE reactive distillation column. They found out that despite the presence of steady state multiplicities in the column, a linear control is still possible because a controlled and manipulated variable-pairing scheme that exhibits a sufficiently large range of near relations can be found.

Al-Arfaj and Luyben [28], in their recent study, presented a plantwide flowsheet that contains reactive distillation column for the production of *tert*-amyl methyl ether (TAME). The flowsheet consists of one reactor, one reactive column, two conventional columns and two recycles. They discussed the importance of the plantwide control and the role of reactive distillation. The reactive distillation column was found to be the central part of the whole flowsheet in terms of both the steady-state design and the dynamic controllability.

Engell and Fernholz [29] investigated the general aspect of controlling the reactive separation processes, and gave the example of the control of a semi-batch reactive distillation process. Utilizing a neural network model, the authors demonstrated that that more complicated controller structures, sophisticated controller design methods, and alternative, model-based nonlinear controllers are needed for reactive distillation processes when compared to conventional processes. The necessity of an accurate process model in control system design was also emphasized.

Huang et al. [30] explored a vapor-liquid-liquid equilibrium behavior of n-butyl propionate and presented a systematic procedure for the design and temperature control of the heterogeneous reactive distillation. The authors showed that a reactive distillation exhibits unique temperature sensitivities. As a result, a Nonsquare Relative Gain (NRG) was used to identify the temperature-control trays, which resulted in an almost one-way decoupled system. Motivated by this, a decentralized PI controller was used at the regulatory level. Because maintaining constant tray temperatures does not imply the same quality specification in a kinetically controlled distillation column, the authors demonstrated that feed forward temperature compensation is necessary to maintain the desired product composition. The proposed design method for butyl propionate reactive distillation can be easily adapted to butyl acetate reactive distillation because of their similarities in VLLE and process characteristics.

Luyben et al. [31] studied the design and control of two alternative processes for the production of butyl acetate from methyl acetate. The two process configurations are a conventional reactor/separator and a reactive distillation. The authors showed that despite both processes are capable of producing high purity butyl acetate and methanol without the use of an extractive agent, the reactive distillation process is more economical. Developing a plantwide control structure for each of the process, the authors showed that an effective control can be achieved by using conventional PI controllers.

Noeres et al. [32] investigated the benefits of using dynamic models of different complexity and size for process design, optimal operation and control of catalytic distillation processes. They studied the heterogeneously catalyzed reactive distillation of methyl acetate as a case study. An experimentally validated rate-based model was developed for process design and scale up issues. However, for optimization and control purposes, the authors used a simplified model as the rigorous rate-based model, as claimed, was not suitable for these tasks because of its complexity. A closed-loop optimization of the system was performed based on the developed linear control structure. The authors demonstrated that the linear controller performed well over a wide range of operating conditions. Because the developed linear controllers were not able to drive the process in arbitrary regions of operation, the use of nonlinear model-based controllers was suggested to be considered in future work.

1.2.2 State Estimators and their Applications

In most of the chemical, biochemical and petrochemical processes, effective monitoring and control is often difficult because of the absence of frequent and delay-free measurements of important process variables and the presence of unknown disturbances in the process, which cannot be modeled. As a result, the state estimator has been recognized as a tool that can be designed to estimate the values of these process variables from the available measurements. State estimators/observers can play a key role in the process control and monitoring wherein an early detection of hazardous conditions is needed for a safe operation. Several works have been done over a decade in the application of the state estimation method in the control of both batch and continuous distillation systems. Summarized below is the literature on the application of state estimator in conventional distillation system.

Lang and Gilles [14] presented a full-order nonlinear observer for distillation columns. The temperatures are measured at different points of the column and compared to the observer's output temperatures. Their results showed that it is possible to estimate temperature and concentration profiles for both binary and multicomponent distillation units by the nonlinear observer. The performance of the observer was tested through numerical simulation and it was found to be very robust toward model errors, wrong parameters or uncertain inputs.

Quintero-Marmol et al. [15] applied an Extended Luenberger Observers (ELO) to predict compositions in multicomponent batch distillation from temperature measurements. A general design procedure of an observer for a batch distillation column was presented. Even though, the linear observer in theory needs only Nc-1 measurements to be observable where Nc is the number of components in the mixture, it was found out that nonlinear observer needed at least Nc measurements to be effective. They presented two different observers: one using full order model and the other using reduced order model. They concluded that full order, though more complex to obtain, performed consistently better than the reduced order-model. But the reduced order is easier to implement.

Ruokang et al. [33] presented a strategy for fault detection and diagnosis in a closed-loop nonlinear distillation system. An extended Kalman filter was applied inside the control loop to recover information from noisy measurement signal and provide estimates of the state variables and unknown parameters of the process. The state estimates produced by an extended Kalman filter are the input for the controller. Meanwhile, Mejdell et al. [19] implemented a static partial least-square regression estimator for product compositions on a high-purity pilot-plant distillation column. The estimator was found to be static and its application is straight forward. An experimentally based estimator, with logarithmically transformed temperatures and compositions, was reported to give excellent performance over a wide range of operating points.

Roberto et al. [17] developed a nonlinear extended Kalman filter (EKF) estimator, which predicts the composition of the outlet streams of a binary distillation column from the temperature measurements. The performance of the estimator was evaluated by comparison with data obtained from the several transient experiments performed in a pilot plant. The EKF estimator was reported to be robust with respect to the model errors, which affect its response. They extended their work to the multicomponent distillation column where they reported that when moving from the binary distillation system to the multicomponent system, the need for an accurate description of the vapor-liquid equilibrium is more stringent [18].

Oisiovici et al. [20] developed a discrete extended Kalman filter for binary and multicomponent distillation systems. They developed it to provide reliable and real-time column composition profiles from few temperature measurements. Unlike off-line design of Extended Luenberger Observer (ELO) proposed by Quintero-Marmol and Luyben [15], the gains of EKF are calculated and updated online. They reported that EKF has the ability to incorporate the effects of noise from both measurement and modeling.

In a more recent work, Bahar *et al.* [34] recently developed an inferential control methodology, which utilizes an artificial neural network (ANN) estimator for a model predictive controller for an industrial multicomponent distillation column. The selection of the temperature measurement points for the inferential control is done by the help of singular value decomposition analysis together with the column dynamics information. A moving window ANN estimator is designed to estimate the product compositions from the tray temperature measurements. The composition predictions are further corrected with the actual composition data in 30-min intervals. A multi input multi output (MIMO) model predictive controller (MPC) is used with the developed ANN estimator for the dual composition control of the column. The performance of the developed control system utilizing ANN estimator is tested considering setpoint tracking and disturbance rejection performances for the unconstrained and constrained cases.

1.3 Scope and Objectives

Lack of appropriate, inexpensive online sensors, high costs of measurement methods, and time consuming offline measurement analysis are some of the reasons that make continuous measurement of the important state variables of a process difficult. Even when online measuring devices are available, in some cases, measurements cannot be obtained frequently without time-delay. The challenge in obtaining such important state variables for control purposes is to design a state estimator, which is robust against a noisy measurement, erroneous initial conditions and model uncertainties.

The present work describes the development, implementation and application of the linear state estimators in control of reactive distillation. Internal compositions which are needed in control system are estimated by the use of the state estimators instead of measuring them by an analyzer. The reliability of these estimators is examined and their impacts on the performance of the control system of reactive distillation are studied. The performance of the feedback control system using the state estimator is compared to that when a composition analyzer is used. The specific objectives of this work are:

1. Developing the linear and nonlinear process models in the state-space form that describes the reactive distillation system.
2. Investigating the impact of disturbance magnitudes and directions in the dynamic behavior of a reactive distillation.

3. Performing a closed-loop assessment of various control structures for reactive distillation using linear and nonlinear process models.
4. Developing the linear state estimators for composition estimation in reactive distillation system.
5. Implementing a linear state estimator in a feedback control of reactive distillation and investigating the reliability and robustness of the estimator-based system against the plant-model mismatch, erroneous initial conditions and measurement errors.

1.4 The Significance of this Work

Reactive distillation has commercially gained a separate status as a promising multifunctional reactor and separator in most of the world leading chemical industries. Locally, reactive distillation technology is used in more than one Saudi Basic Industries Cooperation (SABIC) affiliate. Controlling these processes at the desired conditions is an essential requirement for a better operation at a higher profitability. An effective way of controlling this process requires the knowledge of the internal composition of one of the reactants. This is hard to implement because of the online analyzer unreliability. This research develops a technique to provide the online controller with this information by the use of a state estimator and eliminate the use of the unreliable composition analyzer.

1.5 References

[1] K. Sundmacher and A. Kienle, "Reactive distillation: status and future directions." Weinheim: WILLEY-VCH, 2003.

[2] M. A. Isla and H. A. Irazoqui, "Modeling, analysis, and simulation of a methyl tert-butyl ether reactive distillation column," *Ind. Eng. Chem. Res.*, vol. 35, pp. 2696-2708, 1996.

[3] M. A. Al-Arfaj and W. L. Luyben, "Comparison of alternative control structures for an ideal two-product reactive distillation column," *Ind. Eng. Chem. Res.*, vol. 39, pp. 3298-3307, 2000.

[4] M. A. Al-Arfaj and W. L. Luyben, "Comparative control study of ideal and methyl acetate reactive distillation," *Chem. Eng. Sci.*, vol. 24, pp. 5039-5050, 2002.

[5] S. Wang, D. S. H. Wong, and E. Lee, "Control of a reactive Distillation Column in the kinetic Regime for the synthesis of n-Butyl Acetate," *Ind. Eng. Chem. Res.*, vol. 42, pp. 5182-5194, 2003.

[6] R. Taylor and R. Krishna, "Modeling reactive distillation," *Chem. Eng. Sci.*, vol. 55, pp. 5183-5229, 2000.

[7] T.-M. Yeh, M.-C. Huang, and C.-T. Huang, "Estimate of process compositions and plantwide control for multiple secondary measurements using artificial neural networks," *Comput. & Chem. Engng*, vol. 27, pp. 55-72, 2003.

[8] M. F. Doherty and G. Buzad, "Reactive distillation by design.," *Transactions of the Institution of Chemical Engineers, Part A*, vol. 70, pp. 448-458, 1992.

[9] G. Buzad and M. F. Doherty, "New tools for the design of kinetically controlled reactive distillation columns for ternary mixtures," *Comput. & Chem. Engng*, vol. 19, pp. 395-408, 1995.

[10] A. R. Ciric and P. Miao, "Steady state multiplicities in an ethylene glycol reactive distillation column," *Ind. Eng. Chem. Res.*, vol. 33, pp. 2738-2748, 1994.

[11] M. G. Sneesby, M. O. Tade, and T. N. Smith, "Multiplicity and pseudo-multiplicity in MTBE and ETBE reactive distillation," *Chem. Eng. Res. & Des.*, vol. 76, pp. 525-531, 1998.

[12] M. G. Sneesby, M. O. Tade , R. Datta, and T. N. Smith, "Detrimental influence of excessive fractionation on reactive distillation," *AIChE J.*, vol. 44, pp. 388-393, 1998.

[13] S. Hauan, T. Hertzberg, and K. M. Lien, "Why methyl *tert*-butyl ether production by reactive distillation may yield multiple solutions," vol. 34, pp. 987-991, 1995.

[14] L. Lang and E. D. Gilles, "Nonlinear observers for distillation columns," *Chem. Eng. Sci.*, vol. 14, pp. 1297-1301, 1990.

[15] E. Quintero-Marmol, L. W. Luyben, and C. Georgakis, "Application of an extended Luenberger observer to the control of multicomponent batch distillation," *Ind. Eng. Chem. Res*, vol. 30, pp. 1870-1879, 1991.

[16] E. Quintero-Marmol and W. L.Luyben, "Inferential Model-Based control of Multicomponent Batch distillation," *Chem. Eng. Sci*, vol. 47, pp. 887-898, 1992.

[17] R. Baratti, A. Bertucco, D. Alessandro, and M. Morbidelli, "Development of a composition estimator for binary distillation columns. Application to a pilot plant," *Chem. Eng. Sci.*, vol. 50, pp. 1541-1550, 1995.

[18] R. Baratti, A. Bertucco, D. Alessandro, and M. Morbidelli, "A composition estimator for multicomponent distillation columns development and experimental test on ternary mixtures," *Chem. Eng. Sci.*, vol. 53, pp. 3601-3612, 1998.

[19] T. Mejdell and S. Skogestad, "Composition estimator in a pilot-plant distillation column using multiple temperatures," *Ind. Eng. Chem. Res.*, vol. 30, 1991.

[20] R. M. Oisiovici and S. L. Cruz, "State estimation of batch distillation columns using an extended Kalman filter," *Chem. Eng. Sci.*, vol. 55, pp. 4667-4680, 2000.

[21] S. Roat, J. J. Downs, E. F. Vogel, and J. E. Doss, "Integration of rigorous dynamic modeling and control system synthesis for distillation columns,," *Chem. Pro. Control*, pp. 99-138, 1986.

[22] M. G. Sneesby, M. O. Tade, D. R., and T. N. Smith, " Two point control of reactive distillation column for composition and conversion," *J. Pro. Control*, vol. 9, pp. 19-31, 1999.

[23] W. L. Luyben, "Economic and dynamic impact of the use of excess reactant in reactive distillation systems," *Ind. Eng. Chem. Res*, vol. 39, pp. 2935-2946, 2000.

[24] M. A. Al-Arfaj and W. L. Luyben, "Control study of ethyl *tert*-butyl ether reactive distillation," *Ind. Eng. Chem. Res.*, vol. 41, pp. 3784-3796, 2002.

[25] M. A. Al-Arfaj and W. L. Luyben, "Control of ethylene glycol reactive distillation column," *AIChE J.*, vol. 48, pp. 905, 2002.

[26] A. D. Estrada-Villagrana, D. L. Boggles, E. S. Fraga, and R. Gani, "Analysis of input-output controllability in reactive distillation using the element model," *Comp. Aided Pross. Eng.*, vol. 10, pp. 57-162, 2000.

[27] N. Vora and P. Daoutidis, "Dynamics and control of an ethyl acetate reactive distillation column," *Ind. Eng. Chem. Res*, vol. 40, pp. 833-849, 2001.

[28] M. A. Al-Arfaj and W. L. Luyben, "Plantwide control for TAME production using reactive distillation," *AIChE J.*, vol. 50, pp. 1462-1473, 2004.

[29] S. Engell and G. Fernholz, "Control of a reactive separation process," *Chem. Eng. & Pro.,* 42, pp. 201-210, 2003.

[30] S. -G. Huang, C. -L. Kuo, S. -B. Hung, -W. Chen, and C. –C. Yu, "Temperature control of heterogeneous reactive distillation," *AIChE Journal*, 50, pp. 2203-2216, 2004.

[31] W. L. Luyben, M. K. Pszalgowski, M. R. Schaefer, and C. Siddons, “Design and control of conventional and reactive distillation processes for the production of butyl acetate," *Ind. Eng. Chem. Res.,* 43, pp. 8014-8025, 2004.

[32] C. Noeres, K. Dadhe, R. Gesthuisen, S. Engell, and A. Górak, "Model-based design, control and optimization of catalytic distillation processes," *Chem. Eng. and Pro.*, 43, pp. 421– 434, 2004

[33] L. Ruokang and J. H. Olson, "Fault detection and diagnosis in a closed-loop nonlinear distillation process: application of extended Kalman filters," *Ind. Eng. Chem. Res.*, vol. 30, pp. 898-908, 1991.

[34] A. Bahar, C. Ozgen, K. Leblebicioglu, and U. Halici, "Artificial neural network estimator design for the inferential model predictive control of an industrial distillation column," *Ind. Eng. Chem. Res.*, vol. 43, pp. 6102-6111, 2004.

CHAPTER 2

2 Linearized State Space Formulation for Nonlinear Generic Reactive Distillation

2.1 Introduction

The growing application of reactive distillation processes has necessitated a better understanding of its process dynamics and control. Reactive distillation columns are generally being modeled by a set of highly nonlinear first order differential equations [1-4]. However, many model-based controllers use linear models. Linear models are easier to understand and analyze than nonlinear models. Nonlinear systems often have the same general phase-plane behavior as the model linearized about the steady state condition when the system is close to that particular condition. Therefore, it is important to derive a suitable linearized dynamic model that when used in model-based control applications could yield an effective and robust control system.

Few papers have emerged on the development of a linear model for a typical distillation column. Marquardt and Amrhein [5] developed a linear distillation model for multivariable controller design of binary distillation columns. Their modeling idea draws on the wave propagation phenomena characterizing distillation column dynamics. The process nonlinearities were nicely averaged by using a 5th order linear model. Luyben [6] derived a simple but effective method to determine suitable linear transfer functions for highly nonlinear distillation columns. He presented an effective design procedure which uses Astrom’s method (relay feedback) to get critical gains and frequencies for each diagonal element of the plant transfer matrix. He concluded by emphasizing the effectiveness of the method in handling highly nonlinear column efficiently.

The use of linear transfer function becomes practically inapplicable when the knowledge of internal state variables is required because the method is based on input-output model which gives no information about the internal variables. Recent publications on control of reactive distillation columns have emphasized the need to have the knowledge of internal composition profiles in order to design an effective control for reactive distillation [7-11]. Unless an excess of one of the reactants is incorporated in the process design, some detection of the inventory of one of the reactants in the column is required so that a feedback trim can balance the reactants feed stoichiometry [7]. In such situations, the application of state space technique will be most suitable. Linear state space model can be easily transformed into linear transfer function model without loss of any system information.

The linearization of a nonlinear reactive distillation is challenging because of the reaction and separation combined in a single column. Complexity in its dynamics arises from the interaction of the reaction kinetics and distillation concept of vapor-liquid equilibrium in the system. A linearized state space model of reactive distillation system will help in investigating the stability, controllability and observability analysis of the system. Therefore, the objective of this present work is to develop a linearized state space model for a generic reactive distillation column.

2.2 Reactive Distillation System

Among several chemical systems, two-reactant-two-product reactions have received a wide application in reactive distillation technology [12]. In this work, we considered an ideal two-reactant-two-product reactive distillation column proposed by Al-Arfaj and Luyben [7] as shown in Figure 2.1. It consists of a reactive section in the middle with nonreactive rectifying and stripping sections at the top and bottoms respectively. The elementary, reversible and exothermic liquid-phase reaction occurring in the reactive zone is given as

$$A + B \Leftrightarrow C + D \tag{2.1}$$

The task of the rectifying section is to recover reactant B from the product stream C. In the stripping section, the reactant A is stripped from the product stream D. In the reactive section the products are separated in situ, driving the equilibrium to the right and preventing any undesired side reactions between the reactants A (or B) with the product C (or D). Therefore, reactants A and B are intermediate boilers while product C is the lightest and product D is the heaviest. This ensures that high concentration of the reactants A and B is maintained in the reactive zone, which is typical for reactive distillation application. The reactive section contains N_{RX} trays. The rectifying section contains N_R trays, and the stripping section below the reactive section contains N_S trays. The column is numbered from the reboiler to the condenser.

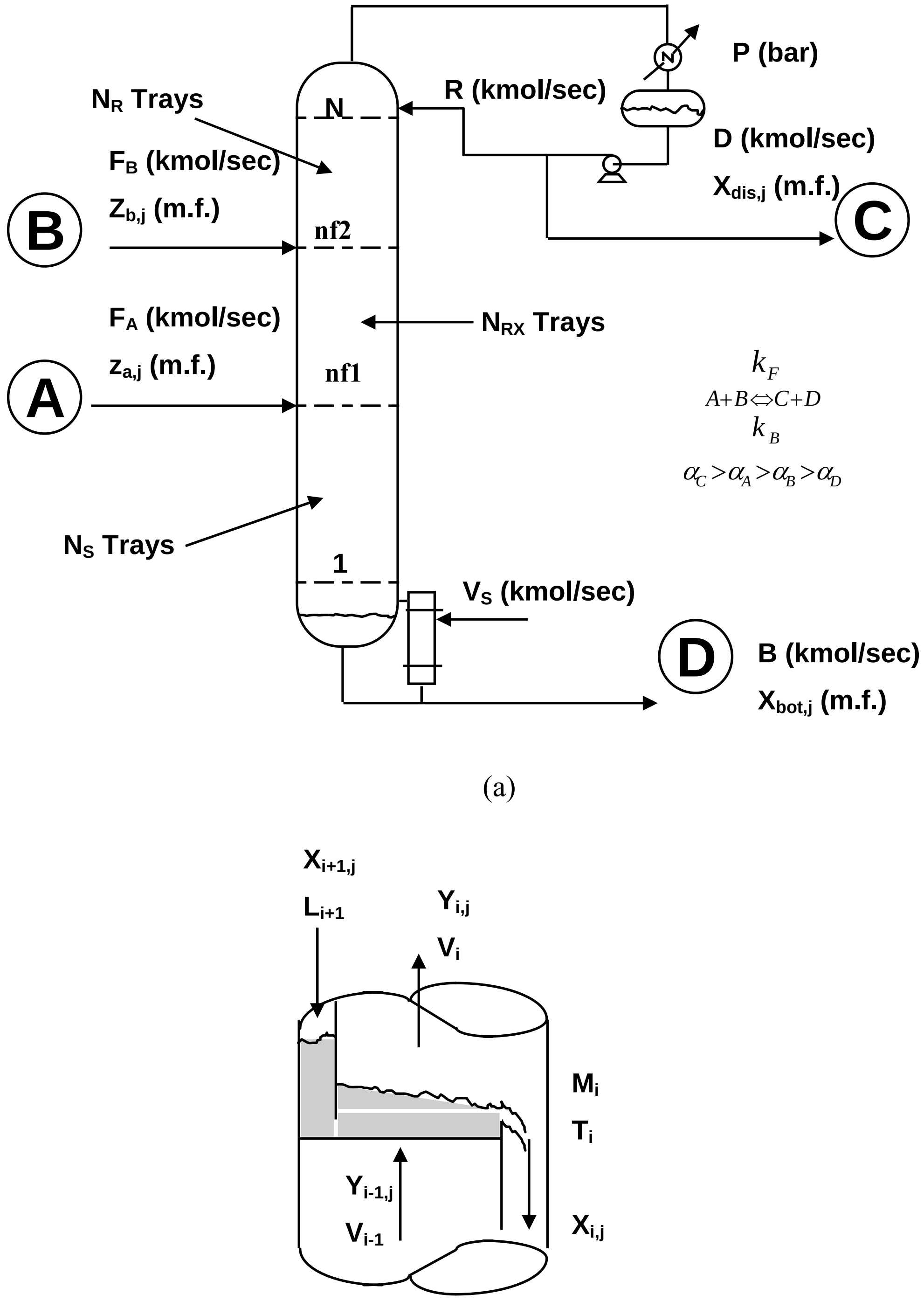
P (bar)
N_R Trays
N
R (kmol/sec)
F_B (kmol/sec)
Z_b,j (m.f.)
D (kmol/sec)
X_dis,j (m.f.)
B
C
nf2
F_A (kmol/sec)
z_a,j (m.f.)
N_RX Trays
nf1
A
k_F
A+B⇔C+D
k_B
α_C > α_A > α_B > α_D
N_S Trays
1
V_S (kmol/sec)
D
B (kmol/sec)
X_bot,j (m.f.)
X_i+1,j
L_i+1
Y_i,j
V_i
M_i
T_i
Y_i-1,j
V_i-1
X_i,j

(a)

(b)

Figure 2.1 (a) Reactive distillation column, (b) a reactive tray.

2.2.1 Nonlinear Process Model

A rigorous dynamic model for a typical reactive distillation column consists of a large number of nonlinear differential equations and demands much information about the system (compositions, vapor and liquid flowrates, liquid hold up in all stages at every instant, tray hydraulics, energy balances, and vapor-liquid equilibrium data). However, the system at hand is an ideal generic reactive distillation with simple vapor-liquid equilibrium, reaction kinetics, and physical properties. The model assumptions are summarized as follows:

1. Ideal vapor-liquid equilibrium.
2. Saturated liquid feed and reflux flowrate
3. The energy equations are neglected by assuming constant molar overflow except in the reactive zone where the vapor flowrate increases because of the heat of reaction which vaporizes some liquid on each tray.
4. Constant relative volatilities. The volatilities of the components are in such that

$$\alpha_D \langle \alpha_B \langle \alpha_A \langle \alpha_C \qquad (2.2)$$

5. Fixed heat of reaction and vaporization and saturated liquid feed and reflux.

The reactive distillation model is based on dynamic mass balance, while the energy equations are neglected by assuming constant molar overflow except in the reactive zone. Therefore, the nonlinear state space model can be described as follows:

Reboiler: $(i = 1)$

$$\frac{dx_{1j}}{dt} = \left[L_2(x_{2j} - x_{1j}) + V_s(x_{1j} - y_{1j})\right] / M_1, \quad \text{j=1:Nc} \qquad (2.3)$$

$$\frac{dM_1}{dt} = L_2 - V_s - B \qquad (2.4)$$

Stripping section: $(2 \le i \le N_S + 1)$

$$\frac{dx_{ij}}{dt} = \left[L_{i+1}(x_{i+1,j} - x_{i,j}) + V_s(y_{i-1,j} - y_{i,j})\right] / M_i \text{, j=1:Nc} \tag{2.5}$$

$$\frac{dM_i}{dt} = L_{i+1} - L_i \tag{2.6}$$

Reactive section: $(nf\ 1 \le i \le nf\ 2)$, $F_i = 0$, except at $i = nf\ 1, nf\ 2$

$$\frac{dx_{ij}}{dt} = \left[L_{i+1}(x_{i+1,j} - x_{i,j}) + V_{i-1}(y_{i-1,j} - x_{i,j}) + V_i(x_{i,j} - y_{i,j}) + R_i + F_i(Z_{ij} - x_{ij})\right] / M_i \text{,j=1:Nc} \tag{2.7}$$

$$\frac{dM_i}{dt} = L_{i+1} - L_i + R_i \lambda / \Delta H_v + F_i \tag{2.8}$$

Rectifying section: $(nf\,2 + 1 \le i \le Ns + N_{RX})$

$$\frac{dx_{ij}}{dt} = \left[L_{i+1}(x_{i+1,j} - x_{i,j}) + V_n(y_{i-1,j} - y_{i,j})\right] / M_i, \quad \text{j=1:Nc} \tag{2.9}$$

Condenser:

$$\frac{dx_{N,j}}{dt} = \left[V_n(y_{N_T} - x_{N,j})\right] / M_N \tag{2.10}$$

$$\frac{dM_N}{dt} = V_n - R - D \tag{2.11}$$

Tray i vapor flowrate in reactive zone is given as:

$$V_i = V_s + \frac{\lambda}{\Delta H_v} \sum_{k=1}^{i-Ns-1} R_{Ns+1+k} \tag{2.12}$$

while the vapor flowrate in rectifying section is expressed as:

$$V_n = V_s + \frac{\lambda}{\Delta H} \sum_{k=1}^{Nrx} R_{Ns+1+k} \tag{2.13}$$

Liquid flowrate is calculated from a linearized form of the Francis Weir formula:

$$L_i = \overline{L}_i + \frac{M_i - \overline{M}_i}{\beta} \tag{2.14}$$

where β is hydraulic time constant. Net reaction rate of component j on tray i is:

$$R_{i,j} = M_i \left(k_{F,i} x_{A,i} x_{B,i} - k_{B,i} x_{C,i} x_{D,i} \right) \tag{2.15}$$

The forward and backward specific reaction rates (kmol.s^{-1}.kmol^{-1}) on tray i:

$$k_{F,i} = a_F e^{-E_F / RT_i} \tag{2.16}$$

$$k_{B,i} = a_B e^{-E_B / RT_i}$$

where a_f and a_B are the pre-exponential factors, E_f and E_B are the activation energies, and T_i is the absolute temperature on tray i. Liquid-vapor equilibrium equations are:

$$y_{i,j} = \alpha_j x_{ij} / \sum_{k=1}^{Nc} \alpha_k x_{ik} \tag{2.17}$$

$$T_i = B_{vp,1} / [A_{vp,1} - \ln(\alpha_1 P / \sum_{k=1}^{Nc} \alpha_k x_{ik})] \tag{2.18}$$

Thus, nonlinear state space models would be of the form:

$$\frac{dX(t)}{dt} = f(X(t), U(t), d(t); \theta) \tag{2.19}$$

$$Y = h(X(t)) \tag{2.20}$$

where X is a vector of state variables, which are liquid mole fractions and holdup in all of the stages (including the reboiler and condenser);

$$X = \left[x_{1,1}, x_{2,1} \ldots x_{N,1}, x_{1,2}, x_{2,2} \ldots x_{N,2}, x_{1,3}, x_{2,3}, \ldots x_{N,3}, x_{1,4}, x_{2,4}, \ldots x_{N,4,} M_1, M_2, \ldots M_N \right]^T \tag{2.21}$$

"U" is a vector of input variables, which are vapor boilup (V_S) from the reboiler and reflux rate (R) from condenser; $U = [V_S, R]^T$. "d" is a vector of measurable disturbance variables, which are the fresh feed flowrates of reactant A and B with their feed compositions; $d = [z_{a,j}, z_{b,j}, F_A, F_B]^T$. "*Y*" is a vector of measurable outputs, which can either be column temperatures or the products compositions; $Y = [y_1 \ldots y_q]^T$. θ is the system constant parameters, which are component relative volatilities, reaction kinetics data and the column pressure. Note that the linearized model formulation considers the configuration where the reflux and steam flowrate are only available as manipulative variables. In general, other control configurations could be easily incorporated.

2.2.2 Linear State Space Model Formulation

The linearization of the nonlinear equations 2.19 and 2.20 is carried out by using the Taylor series expansion. This implies that these sets of nonlinear equations are approximated by a truncated Taylor series approximation around the steady state operating conditions. Although, the Taylor series-based linearization method is a well established technique, however, the most challenging aspect of its application is the formation of the resulting Jacobian matrices of the multivariable states for a coupled and highly nonlinear dynamic model [13]. If the general form of equations 2.19 and 2.20 is given as:

$$f(x)=\begin{bmatrix} f_1(x_1,x_2,...,x_{5N},u_1,u_2,...,u_p,d_1,d_2,...,d_q,\theta) \\ f_2(x_1,x_2,...,x_{5N},u_1,u_2,...,u_p,d_1,d_2,...,d_q,\theta) \\ . \\ . \\ . \\ f_{5N}(x_1,x_2,...x_{5N},u_1,u_2,...,u_p,d_1,d_2,...,d_q,\theta) \end{bmatrix} \quad Y=\begin{bmatrix} h_1(x_1,x_2,...,x_{5N}) \\ h_2(x_{1,}x_2,...,x_{5N}) \\ . \\ . \\ . \\ h_q(x_1,x_2,...,x_{5N}) \end{bmatrix} \tag{2.22}$$

then, the linearization version of the nonlinear functions is obtained by taking the first two terms of the Taylor series.

$$f(X)=f(\overline{X},\overline{U},\theta)+\frac{\partial f}{\partial X}\left(X-\overline{X}\right)+\frac{\partial f}{\partial U}\left(U-\overline{U}\right)+\frac{\partial f}{\partial d}\left(d-\overline{d}\right) \tag{2.23}$$

$$Y(X)=h(\overline{X})+\frac{\partial h}{\partial X}\left(X-\overline{X}\right) \tag{2.24}$$

In equation 2.23, the derivative of $f(X)$ is a derivative of 5N ×1 vector with respect to 5N ×1 state vector , P ×1 input vector and M × 1 disturbance vector.

This results in:

1. 5N ×5N Jacobian matrix "*A*" whose $(i, j)^{th}$ element is $\frac{\partial f_i}{\partial x_j}$
2. 5N × P input matrix "*B*" with $\frac{\partial f_i}{\partial u_j}$ coefficient as its elements
3. 5N × M disturbance matrix "*E*" with $(i, j)^{th}$ element as $\frac{\partial f_i}{\partial d_j}$
4. q × 5N output matrix "*C*" with $\frac{\partial h_i}{\partial x_j}$ coefficient as its element.

The steady state condition corresponds to $f(\overline{X}, \overline{U}, \theta) = 0$ and $h(\overline{X}) = 0$, and all the matrices elements are evaluated at steady state values. The deviation variables arise naturally out of the Taylor series expansion, and therefore, the linearized state space model in terms of deviation variable is:

$$\frac{dx'}{dt} = Ax' + Bu' + Ed' \tag{2.25}$$

$$Y' = Cx' \tag{2.26}$$

Formulation detail and entries of matrices *A, B, C* and *E* for a generic reactive distillation are given in the Appendix.

2.3 Steady State Design Data.

The formulation of a linearized model only requires the knowledge of the steady state design data, including the holdups and stationary concentration profiles. Considering the phenomena of steady state multiplicities of most reactive distillation systems as reported in the literature [14, 15], it is important to ensure that a unique and stable steady state conditions based on the desired specifications are obtained.

The kinetic, physical, and vapor-liquid equilibrium parameters for single-column reactive distillation were obtained from Luyben [16] and are summarized in Table 2.1. It is found that the design presented by Luyben [16] is stable only when the system is operated under closed-loop. Therefore, we modified this steady state design to ensure that the system is both open-loop and closed-loop stable. The procedure to obtain the modified design is the following:

1. The desired purity and conversion is kept the same (95%). The flowrate of the fresh reactants A and B entering into the column is fixed at 0.0126 kmol/s.
2. The initial holdups in all the trays are assumed to be 1 kmol and 10 s of holdup time is assumed in both the reboiler and condenser.
3. A dual composition control suggested by Al-Arfaj and Luyben [7] is implemented to obtain the desired manipulated variables. Composition of product C in the distillate is controlled by manipulating the reflux flowrate, while the vapor boilup is manipulated to control the bottoms composition of component D. The controllers automatically manipulated both the reflux flowrate and vapor boilup to the values that correspond to the desired conversion and purity.
4. The resulted steady state parameters are used as initial conditions to check for open-loop stability. The open-loop dynamic simulation had to be run for significantly long time to ensure open-loop stability. Table 2.2 shows the results of steady state conditions for which the system is open-loop and closed-loop stable.

Table 2.1 Kinetic and physical properties

activation energy (cal\mol)		forward	30000		
		backward	40000		
Specific reaction rate at steady state condition (kmols^{-1}kmol^{-1})		forward	0.008		
		backward	0.004		
heat of reaction (cal/mol)		-10 000	component	vapor pressure	
heat of vaporization (cal/mol)		6944		Avp	Bvp
relative volatilities	α_C	8	A	12.34	3862
	α_A	4	B	11.45	3862
	α_B	2	C	13.04	3862
	α_D	1	D	10.96	3862

Table 2.2 Optimum steady state conditions

	variables	steady state values
Column specifications	pressure (bar)	9
	stripping section	7
	reactive section	6
	rectifying section	7
flowrates	Vs (kmol/s)	0.0285
	R (kmol/s)	0.0331
	D (kmol/s)	0.0126
	B (kmol/s)	0.0126
X_{dis}	A	0.0467
	B	0.0033
	C	0.9501
	D	0.0000
X_{bot}	A	0.0009
	B	0.0445
	C	0.0000
	D	0.9545

2.4 Model Linearity

A linear system is one that satisfies both homogeneity and additivity property. For zero-state response, the model linearity can be assessed by

$$\begin{aligned} &X_1(t_0)=0 \\ &\Phi_1 U_1(t)+\Phi_2 U_2(t), t\geq t_0 \end{aligned} \qquad \Phi_1 Y_1(t)+\Phi_2 Y_2, t\geq t_0 \tag{2.27}$$

where Φ_1 and Φ_1 are constants.

Before the applicability of a linearized model is assessed, it is important to demonstrate that this principle of superposition is satisfied. The linearity of the proposed model was tested by exciting the system with the various magnitudes of input step changes. For illustration purposes, ±2% and ±4% step changes in feed flowrate of reactant B are introduced into the system as disturbances. Figure 2.2 shows the steady state composition profiles in deviation forms under various magnitudes of step input changes in feed flowrate of reactant B. The uniformity in the deviations of the compositions in both directions is a clear indication of model linearity. The model linearity of the system is equally observed in the column temperature profiles as shown in Figure 2.3. The dynamic composition profile of the reactant A on the tray nf1, the reactant B on the tray nf2, the product C in the distillate and the product D in the bottoms with ±2% & ±4% change in F_B are presented in the Figure 2.4. The output changes are symmetric, with the same speed of response. The behaviors of these responses are clear indicative of a linear system.

2.5 System Stability

Systems are generally designed to either process some signals or perform some tasks. Thus, if a system is unstable, it will grow unbounded, saturate and disintegrate when a signal, no matter how small, is applied. Therefore, stability is a basic requirement for all systems. We demonstrated one among many advantages of a linear system by investigating the model stability near the steady state conditions through the eigenvalues of its Jacobian matrix.

Because our system response is typical of zero-state, its stability can easily be verified using bounded-input-bound-output (BIBO) stability criteria. A multivariable process is open-loop stable if and only if all the eigenvalues of matrix A have negative real parts [17]. Table 2.3 shows the eigenvalues of matrix A for a linearized reactive distillation system with 20 trays, reboiler and condenser. As shown in Table 2.3, the system is stable because all the eigenvalues have negative real parts. This is inline with the dynamic stability test discussed earlier.

2.6 Conclusion

A linearized state space model for a generic reactive distillation has been formulated**.** The development of the model only requires information about the steady state design data, including the holdup in all the stages and the stationary composition profiles in the column. A detailed algorithm of the system sensitivity matrices is presented. The model obtained in this fashion is based on deviation variables. The developed approximate model is used to investigate the stability of the multivariable reactive distillation system. The linearity of the model is attested by the uniform and symmetric nature of the output responses to different magnitudes of the step inputs.

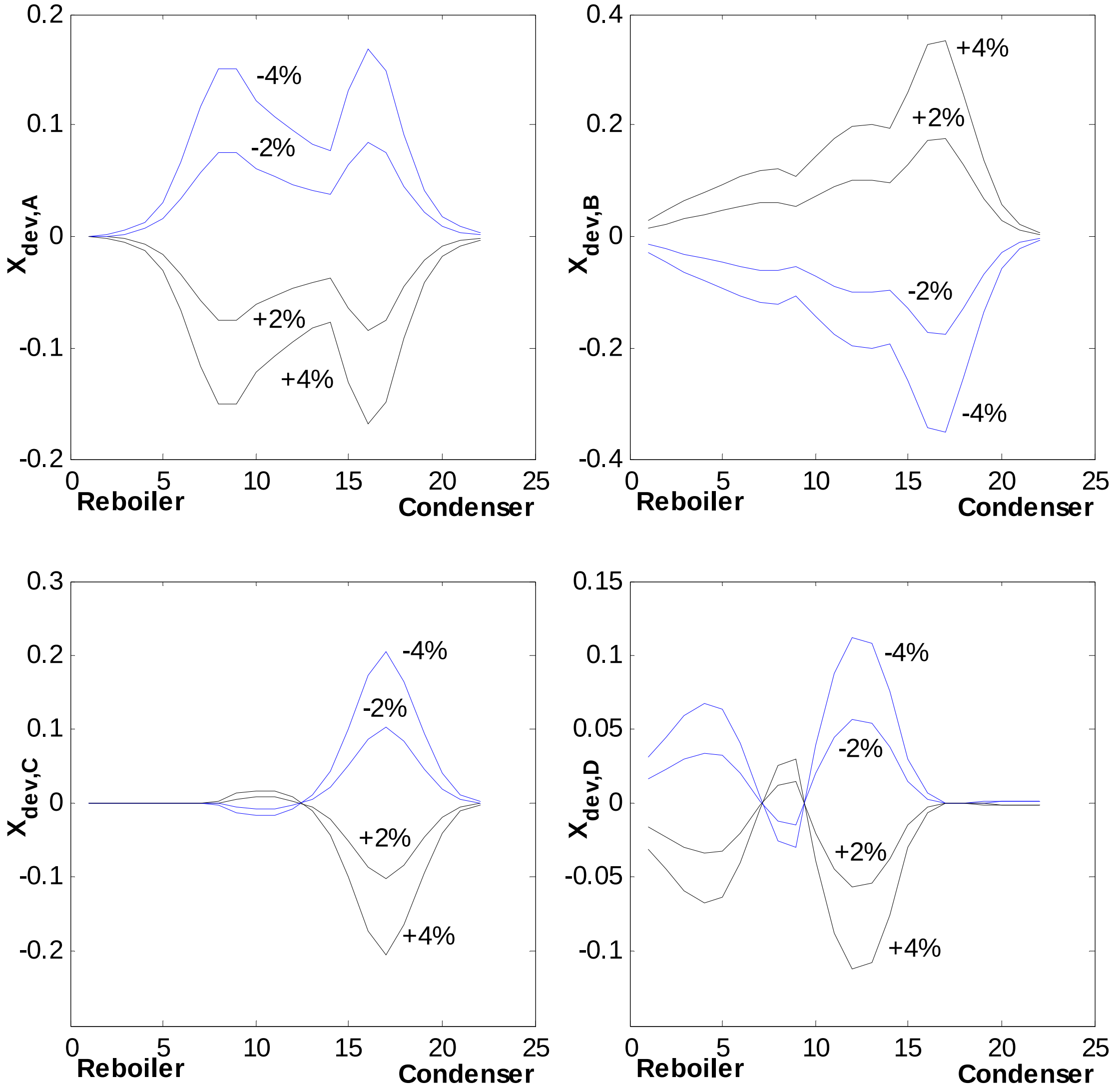

Figure 2.2 Steady state composition profile (in deviation form) of the reactant A on the tray nf1, the reactant B on the tray nf2, the product C in the distillate and the product D in the bottoms with ±2% & ±4% change in F_B

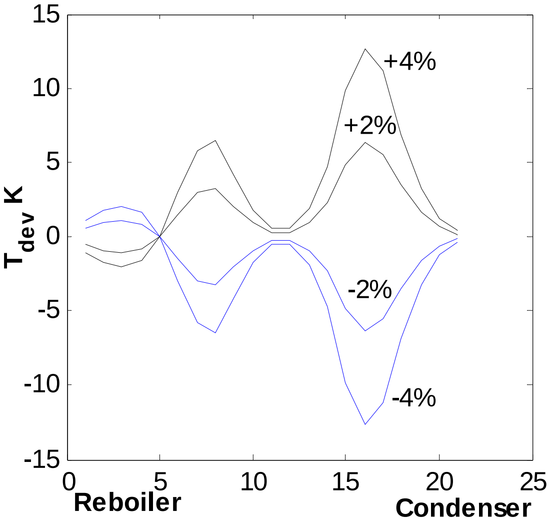

(a)

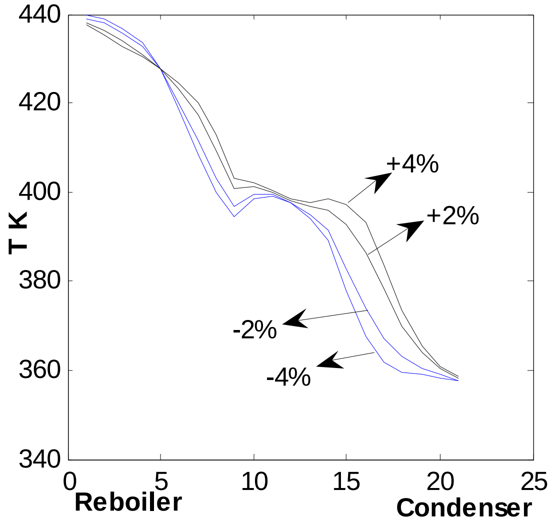

(b)

Figure 2.3 Steady state temperature profiles after ±2% & ±4% changes are made in F_B: (a) column temperature profiles in deviation form. (b) column temperature profiles.

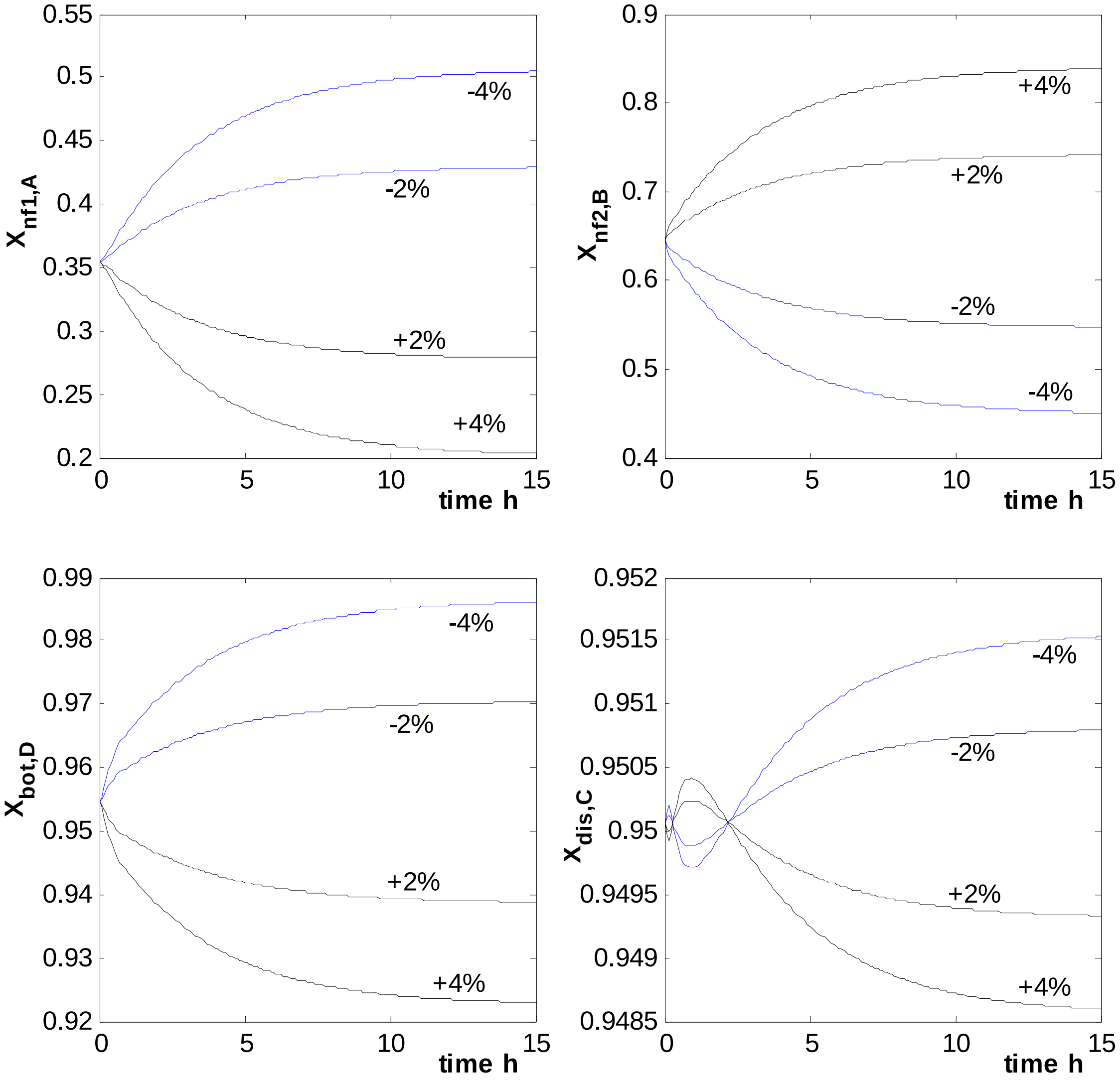

Figure 2.4 Dynamic composition profile of the reactant A on the tray nf1, the reactant B on the tray nf2, the product C in the distillate and the product D in the bottoms with ±2% & ±4% change in F_B.

Table 2.3 Eigenvalues of matrix A (5N X 5N), N=22, column configuration ($N_S/N_{RX}/N_R$): 7/6/7 column stages, 1 reboiler and 1 condenser.

-0.5221	-0.1592 + 0.0098i	-0.0747 + 0.0083i	-0.0323 + 0.0187i	-0.0097
-0.4483	-0.1592 - 0.0098i	-0.0747 + 0.0083i	-0.0458	-0.0074
-0.3935	-0.1571	-0.0728	-0.0267 + 0.0174i	-0.0001
-0.3894	-0.1506	-0.0685 + 0.0011i	-0.0267 - 0.0174i	-0.0005
-0.3564	-0.1267 + 0.0556i	-0.0685 - 0.0011i	-0.0398	-0.0011 + 0.0003i
-0.3170	-0.1267 - 0.0556i	-0.0588 + 0.0075i	-0.0365 + 0.0017i	-0.0011 - 0.0003i
-0.3016	-0.1086 + 0.0429i	-0.0588 - 0.0075i	-0.0365 - 0.0017i	-0.0046 + 0.0017i
-0.2898	-0.1086 + 0.0429i	-0.0595 + 0.0027i	-0.0365	-0.0046 - 0.0017i
-0.2502	-0.1308	-0.0595 - 0.0027i	-0.0226 + 0.0152i	-0.0013
-0.2347 + .0496i	-0.1285	-0.0554 + 0.0108i	-0.0226 - 0.0152i	-0.0053
-0.2347 - 0.0496i	-0.1210 + 0.0130i	-0.0554 - 0.0108i	-0.0289	-0.0035
-0.2369 + 0.0285i	-0.1210 - 0.0130i	-0.0515 + 0.0143i	-0.0166 + 0.0119i	-0.0034
-0.2369 -0.0285i	-0.1222 + 0.0029i	-0.0515 - 0.0143	-0.0166 - 0.0119i	-0.0025
-0.2016 + 0.0562i	-0.1222 - 0.0029i	-0.0471 + 0.0167i	-0.0249	-0.0025
-0.2016 + 0.0562i	-0.1027	-0.0471 - 0.0167i	-0.0214	-0.0046
-0.2064	-0.0935 + 0.0215i	-0.0547	-0.0153 + 0.0063i	-0.1667
-0.1792 + 0.0695i	-0.0935 - 0.0215i	-0.0426 + 0.0187i	-0.0153 - 0.0063i	-0.1667
-0.1792 - 0.0695i	-0.0973	-0.0426 - 0.0187i	-0.0181	-0.1667
-0.1941	-0.0868 + 0.0117i	-0.0530	-0.0169	-0.1667
-0.1562 +0.0633i	-0.0868 - 0.0117i	-0.0370 + 0.0193i	-0.0134	-0.1667
-0.1562 - 0.0633	-0.0836	-0.0370 - 0.0193i	-0.0093 + 0.0050i	-0.1667
-0.1619	-0.0791	-0.0323 + 0.0187i	-0.0093 - 0.0050i	-0.1667

2.7 References

[1] R. Taylor and R. Krishna, "Modeling reactive distillation," *Chem. Eng. Sci.*, vol. 55, pp. 5183-5229, 2000.

[2] A. Kumar and P. Daoutidis, "Modeling, analysis and control of an ethylene glycol reactive distillation column," *AIChE J.*, pp. 45- 51., 1999.

[3] R. Baur, R. Taylor, and R. Krishna, "Dynamic behavior of reactive distillation tray columns described with a nonequilibrium cell model," *Chem. Eng. Sci.*, vol. 56, pp. 1721-1729, 2001.

[4] S. Roat, J. J. Downs, E. F. Vogel, and J. E. Doss, "Integration of rigorous dynamic modeling and control system synthesis for distillation columns,," *Chem. Pro. Control*, pp. 99-138, 1986.

[5] W. Marquardt and M. Amrhein, "Development of a linear distillation model from design data for process control," *Comp. Chem. Engng*, vol. 18, pp. S349-S353, 1994.

[6] W. L. Luyben, "Derivation of transfer functions for highly nonlinear distillation columns," *Ind.Eng.Chem.Res.*, vol. 26, pp. 2490-2495, 1987.

[7] M. A. Al-Arfaj and W. L. Luyben, "Comparison of alternative control structures for an ideal two-product reactive distillation column," *Ind. Eng. Chem. Res.*, vol. 39, pp. 3298-3307, 2000.

[8] M. A. Al-Arfaj and W. L. Luyben, " Comparative control study of ideal and methyl acetate reactive distillation," *Chem. Eng. Sci.*, vol. 24, pp. 5039-5050, 2002.

[9] M. A. Al-Arfaj and W. L. Luyben, "Plantwide control for TAME production using reactive distillation," *AIChE J.*, vol. 50, pp. 1462-1473, 2004.

[10] M. A. Al-Arfaj and W. L. Luyben, "Control study of Ethyl *tert*-Butyl Ether reactive distillation, Ind. Eng. Chem. Res. (2002)," *Ind. Eng. Chem. Res.*, vol. 41, pp. 3784-3796, 2002.

[11] S. Wang, D. S. H. Wong, and E. Lee, "Control of a reactive distillation column in the kinetic regime for the synthesis of n-butyl acetate," *Ind. Eng. Chem. Res.*, vol. 42, pp. 5182-5194, 2003.

[12] K. Sundmacher and A. Kienle, "Reactive distillation: status and future directions." Weinheim: WILLEY-VCH, 2003.

[13] D. Wolbert, X. Joulia, B. Koehret, and L. T. Biegler, "Flowsheet optimization and optimal sensitivity analysis using analytical derivatives," *Comp. Chem. Engng*, vol. 18, pp. 1083-1095, 1994.

[14] M. G. Sneesby, M. O. Tade, and T. N. Smith, "Multiplicity and pseudo-multiplicity in MTBE and ETBE reactive distillation," *Chem. Eng. Res. & Des.*, vol. 76, pp. 525-531, 1998.

[15] A. R. Ciric and P. Miao, "Steady state multiplicities in an ethylene glycol reactive distillation column, Ind. Eng.," vol. 33, pp. 2738-2748, 1994.

[16] W. L. Luyben, "Economic and dynamic impact of the use of excess reactant in reactive distillation systems," *Ind.Eng.Chem.Res*, vol. 39, pp. 2935-2946, 2000.

[17] C.-T. Chen, *Linear system theory and design*. New York: Oxford University Press, 1999.

CHAPTER 3

3 Dynamic Comparison of Linear and Nonlinear Models for Generic Reactive Distillation System

3.1 Introduction

An understanding of the dynamic behavior of reactive distillation system is important from both process design and control perspectives. Moreover, the primary objective of process control is the design of effective and robust control systems that will keep the process conditions close to its desired steady state value. Even though the reactive distillation system is highly nonlinear, the influence of effective regulatory control is to ensure that the deviations from this steady state will be small, in which case the behavior will be essentially indistinguishable from that of linear system.

Nonlinear reactive distillation systems are notoriously difficult to analyze and solve, partially because they exist is such an infinite variety of forms, preventing any cohesive theory for analysis. Thus, it is very important to have an approximate linear model that will give good account of the process behavior near the desired operating conditions if we are to be able to use the powerful linear mathematical techniques in the system analysis and control. Nonlinearity in reactive distillation model arises because of complex processing configurations, which involves the interaction of the reaction kinetics and distillation concept of vapor-liquid equilibrium. Moreover, the desire for high conversion, selectivity and product purity increases the process nonlinearity. Luyben [1] pointed out that the response of distillation system becomes highly nonlinear as the purity level increases more than 98%.

Although simplified modeling of distillation columns for design of linear multivariable controllers has a long tradition [2-4], there is still no consensus on what constitute an adequate linear model of reactive distillation, on the physical effects to be retained, and on a recommended approximation method that will not lead to a false conclusion. These questions can only be addressed by a quantitative comparison of an approximate linear model to that of nonlinear rigorous model.

In the previous chapter, a linearized state space model for reactive distillation was formulated. The present work compares the performance of a linearized dynamic model of reactive distillation system with that of a nonlinear model with the sole aim to come up with some conditions and general guidelines under which a linear process model could be applied in model-based-control applications of reactive distillation. The effect of model stability on the performance of the approximate model is explored. The open-loop performance of both linear and nonlinear models in presence of an internal composition inventory control is demonstrated. An error index is developed to quantitatively analyze the accuracy of a linear process model.

3.2 Error Index

In order to quantitatively assess the performance and accuracy of a linear process model as compare to a nonlinear process model, an error index is defined in term of an Average Relative Error (ARE). The numerical values obtained from nonlinear model are considered as the real values for the system, while the values obtained from the linear model are taken as the approximate values. In this sense, an Average Relative Error is given as:

$$ARE = \frac{1}{n}\sum_{k=1}^{n} abs(\frac{\gamma_k^{real} - \gamma_k^{appr}}{\gamma_k^{real}}) X100 \qquad (3.1)$$

γ_k^{real} is the real value from the nonlinear model at point k, γ_k^{appr} is the approximate value from the linear model at the same point k. n is the number of data points.

3.3 Steady State Design Data

An availability of stable steady state values at the desired operating conditions is a fundamental prerequisite to developing a successful linear model. In the present study, two steady state designs are used to examine the system sensitivity to input disturbances (see Section 3.4). They are termed as a low-conversion and a high-conversion steady state designs. A high conversion is the steady-state conditions presented in Chapter 2 and is taken as the base design throughout this study. A low-conversion design is considered here to justify the consistency of a linearized model as long as the deviation in process variables due to a disturbance is within the region of the base steady states around which the model is linearized. Table 3.1 shows the summary of the of two steady state conditions for open-loop reactive distillation system.

Table 3.1 Base steady state conditions for a high and low-conversion region.

	Variables	high-conversion region	low-conversion region
flowrates	Vs (kmol/s)	0.0285	0.0281
	R (kmol/s)	0.0331	0.0328
	D (kmol/s)	0.0126	0.0119
	B (kmol/s)	0.0126	0.0133
X_{dis}	A	0.0467	0.0345
	B	0.0033	0.0008
	C	0.9501	0.9647
	D	0.0000	0.0000
X_{bot}	A	0.0009	0.0519
	B	0.0445	0.0822
	C	0.0000	0.0000
	D	0.9545	0.8658

3.4 Steady State Sensitivity

The performance of a linear model is based on the sensitivity of the steady state values to disturbances. The deviation from the steady states when disturbance is introduced into the system must be small enough and also be within the region of the steady states used in developing an approximate model. Thus, linearization may lead to an inaccurate or a false conclusion if the original model exhibits a drastic deviation from the base steady state region. This would also be true if the nonlinear process model is unstable under certain disturbances.

Figure 3.1a shows the composition profiles of the column comparing the linear and nonlinear models when component B fresh feed flowrate (F_B) is increased by 2%. The linear and nonlinear models show a consistent deviation within the vicinity of the base steady state composition profiles. As more of the B is fed into the column, the two models predict the shifting of reactant A profile in the middle of the column downward and of reactant B profile upward. The shifting down of product D profile in the stripping section showed by the two models indicates an increase in impurity in the bottoms as a result of excess of reactant B.

Figure 3.1b shows the steady state temperature profile of the linear and nonlinear models with 2% disturbance in F_B. There is a consistent deviation from the base steady state temperature profile, which indicates that a linear model predicts the original nonlinear model well within the desired steady state region. Note that both the two models show that the temperature in the stripping section is reduced as a result of more reactant B in the bottoms, and temperature in the rectifying section is increased because of the reactant B, which is lost to the overhead.

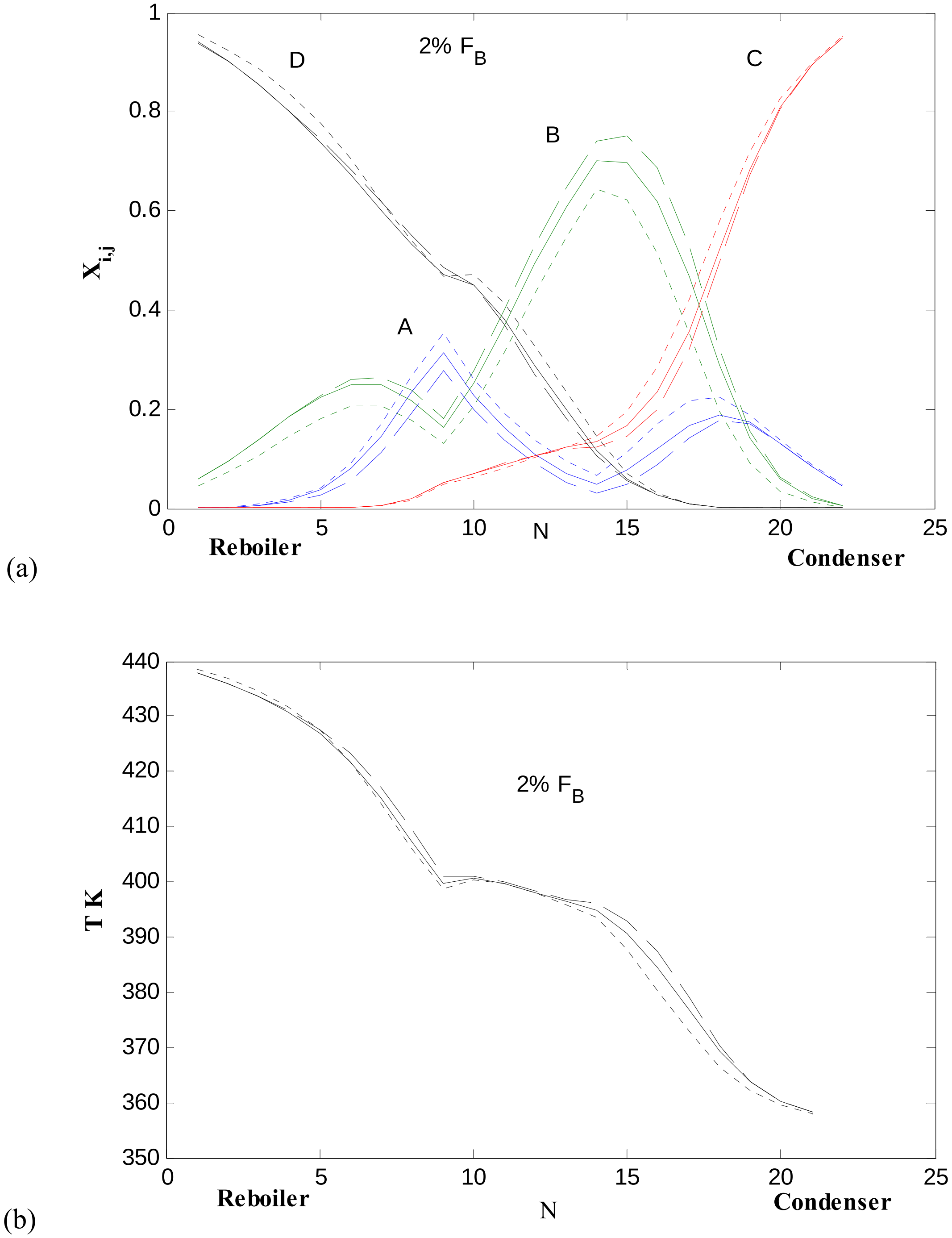

Figure 3.1 (a) Composition profiles with 2% increase in F_B, (b) temperature profiles with 2% increase in F_B: (---) base steady state profile with no disturbance; (— —) linear model; (——) nonlinear model.

Figure 3.2a compares the composition profile for both of the linear and nonlinear models when fresh feed flowrate of reactant A (F_A) is increased by 2%. A linear model predicts the composition profiles in the vicinity of the base composition profile as it was developed around that profile. In contrast, a nonlinear model shows a significant deviation in composition profile from the base steady state values. When there is an excess of reactant A, the light reactant, there must be an increase in the heat duty to strip out an unreacted A from product D. Because the heat duty is kept constant in this steady state analysis, this resulted in reactant A flooding the stripping section as predicted by nonlinear model. Figure 3.2b shows the temperature profiles of both models under the same conditions, i.e., +2% in F_A. The linear model shows a slight deviation around the base steady state, whereas the nonlinear model shows a significant change in the temperature profile along the column. The sharp drop in temperatures predicted by nonlinear model especially in the stripping section indicates excess of unreacted reactant A in the zone.

The nonlinear model behavior indicates that the system is open-loop pseudostable when F_A is increased by 2%. The system drifts to another low conversion state. It is expected that the linear model will not predict the drift since this is a nonlinear characteristics of the system. However, to verify the linear model applicability when the system is open-loop stable under a given disturbance, the low conversion state is taken as a new base (see Table 3.1) and the model is linearized around that design, then similar disturbance is introduced. Figure 3.3 shows the composition profiles at low conversion steady state region. Since the system of that state is stable under the same disturbance

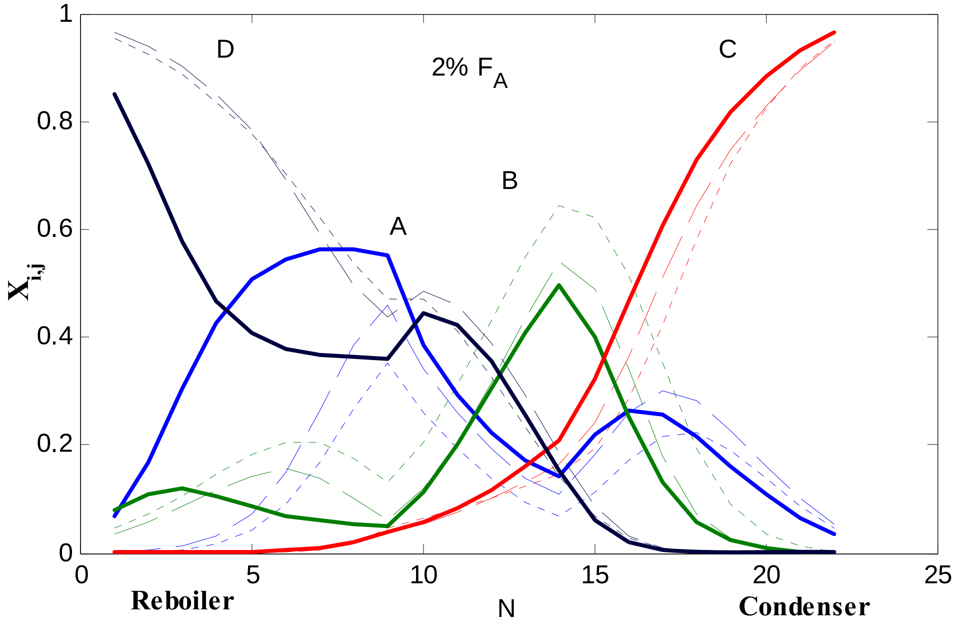

(a)

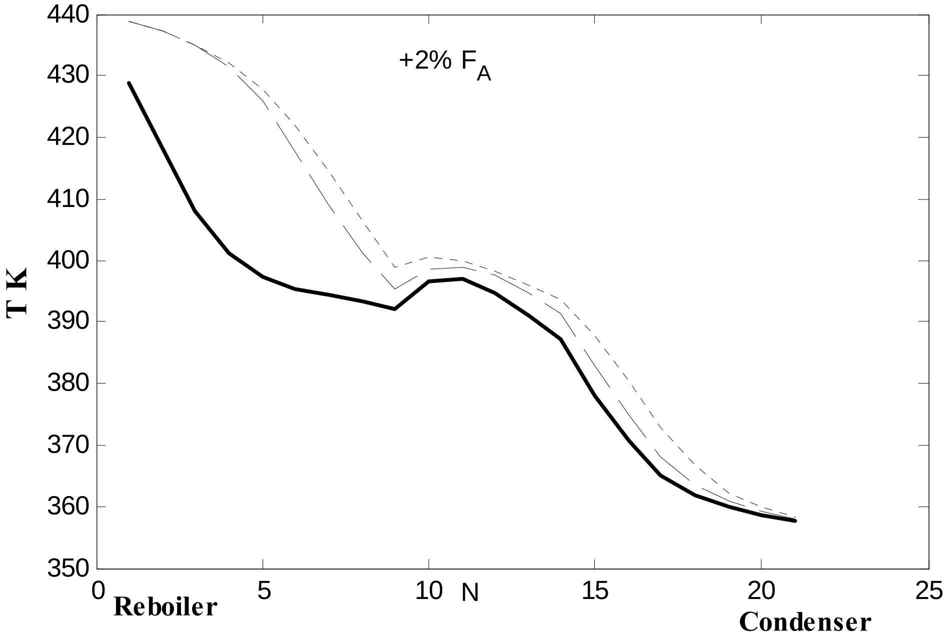

(b)

Figure 3.2 (a) Composition profiles with 2% increase in F_A, (b) temperature profiles with 2% increase in F_A: (---) base steady state profile; (— —) linear model ;(——) nonlinear model.

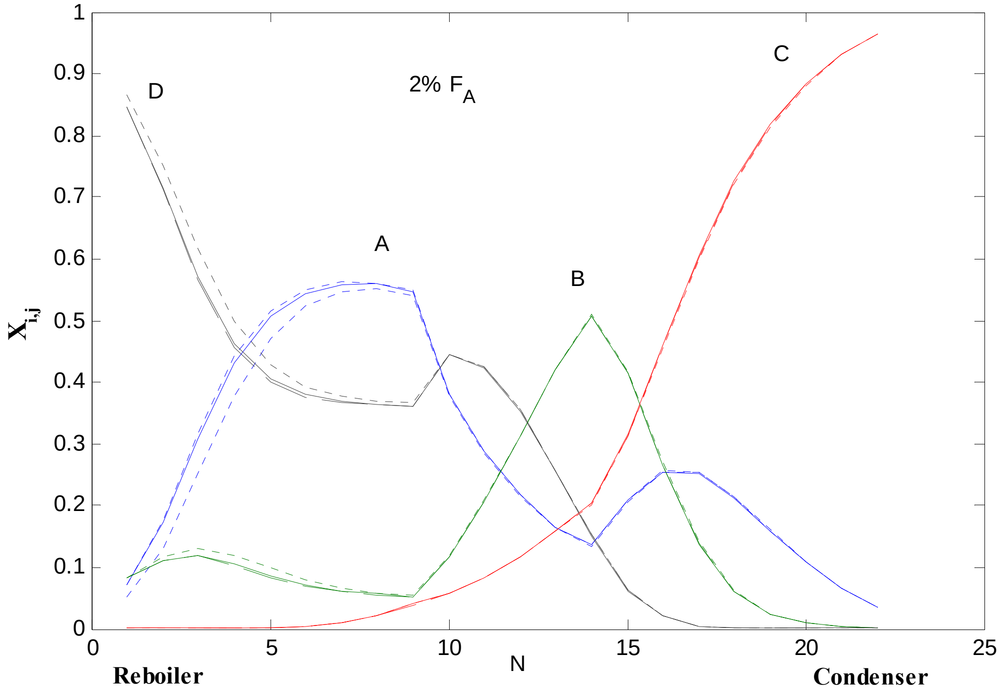

Figure 3.3 Composition profiles with 2% increase in F_A: (---) base steady state profile; (— —) linear model; (——) nonlinear model.

(+2%F_A), both linear and nonlinear models show a good matching and consistent deviations from the low conversion base steady state profiles. This indicates that a linear model will give good predictions of a nonlinear model when the base steady state design is open-loop stable under a given disturbance. In contrast, it may lead to a false predictions whenever the disturbance from the base design is either significant or results in a drift to another steady state region.

3.5 Robustness of a Linear Model

Assessing the robustness of a linear model under various magnitudes of disturbances is very important before its applicability can be considered. In this Section, the performance of an open-loop dynamic linear model is compared to that of a rigorous dynamic nonlinear model. Two dynamic scenarios are investigated:

1- Open-loop (OL): where only the pressure as well as the base and reflux drum level inventories are controlled while F_A, F_B, Z_a, Z_b, Vs and R are fixed.

2- Open-loop with internal composition control (OL+IC): in addition to level control loops, reactant A inventory is controlled through an the internal composition controller by manipulating the feed flowrate F_A.

The process variables considered as sources of disturbances are: feed flowrate of reactant B (F_B), feed composition of reactant A (Z_a) and vapor boilup (Vs). The two models are excited by a step change of magnitudes 1%, 2%, 5% and 10%. The changes in Z_a are the percentage amount of reactant B in reactant A fresh feed. The average relative error of all the disturbances studied under various magnitudes is summarized in Table 3.2-3.5. However, the system responses of the two models when F_B is changed are presented in detail.

Table 3.2 The Average Relative Error (ARE) of open-loop model (OL), without internal controller

SYSTEM			Open Model (OL)							
VARIABLE			F_B				%mol of B in feed A			
Magnitude / Variable			1%	2%	5%	10%	1%	2%	5%	10%
Bulk Steady state		$X_{i,A}$	4.09	8.51	23.82	67.64	15.55	29.73	44.69	72.10
		$X_{i,B}$	2.46	6.62	15.16	45.21	9.64	12.93	16.14	39.63
		$X_{i,C}$	2.24	6.21	14.71	20.09	8.62	18.33	23.33	33.29
		$X_{i,D}$	1.42	4.77	10.97	18.38	6.51	12.17	26.72	58.81
		T	0.05	0.21	0.54	0.98	0.29	0.72	0.84	1.34
Individual Variables	Steady State	D	0.02	0.06	0.67	2.60	0.02	0.26	4.24	11.87
		B	0.02	0.06	0.68	2.79	0.02	0.26	3.88	9.78
		$X_{bot,D}$	0.03	0.07	1.02	4.28	0.10	0.65	5.36	14.64
		$X_{dis,C}$	0.01	0.02	0.27	1.13	0.20	0.44	1.35	3.55
		$X_{nf1,A}$	3.37	10.55	18.74	23.89	14.21	23.24	32.09	36.30
		$X_{nf2,B}$	1.82	5.31	6.07	10.33	6.13	11.94	9.82	22.82
	Dynamic	D	0.03	0.09	0.62	2.58	0.02	0.24	3.90	11.38
		B	0.03	0.09	0.61	2.42	0.02	0.24	3.79	9.38
		$X_{bot,D}$	0.05	0.14	0.91	3.85	0.16	0.65	4.82	13.77
		$X_{dis,C}$	0.01	0.02	0.21	1.01	0.22	0.45	1.30	3.356
		$X_{nf1,A}$	2.31	7.30	16.41	17.76	10.29	27.23	30.84	35.75
		$X_{nf2,B}$	1.20	3.66	8.98	15.98	4.306	9.66	10.81	22.31

Table 3.3 The Average Relative Error (ARE) for open-loop model (OL), without internal controller

SYSTEM			Open Model (OL)			
VARIABLE			Vs			
Magnitude Variable			1%	2%	5%	10%
Bulk Steady state		$X_{i,A}$	14.88	23.99	36.34	71.55
		$X_{i,B}$	11.48	15.41	23.83	38.82
		$X_{i,C}$	17.63	31.48	50.86	62.13
		$X_{i,D}$	11.13	14.74	21.97	23.78
		T	0.55	0.88	1.01	1.98
Individual Variables	Steady State	D	0.06	0.67	3.01	6.85
		B	0.06	0.68	2.96	7.35
		$X_{bot,D}$	0.12	0.43	1.32	1.87
		$X_{dis,C}$	0.02	0.21	3.18	11.67
		$X_{nf1,A}$	17.21	23.12	33.12	59.34
		$X_{nf2,B}$	8.43	9.78	13.87	25.24
	Dynamic	D	0.07	0.67	2.96	6.58
		B	0.07	0.69	2.65	8.27
		$X_{bot,D}$	0.11	0.45	1.29	1.44
		$X_{dis,C}$	0.02	0.26	3.24	10.44
		$X_{nf1,A}$	15.80	21.08	32.23	58.68
		$X_{nf2,B}$	7.11	9.25	14.15	24.95

Table 3.4 The Average Relative Error (ARE) for open-loop model with internal composition controller (OL+IC)

SYSTEM			Open Model with Internal Controller (OL +IC)							
VARIABLE			F_B				%mol B in feed A			
Magnitude / Variable			1%	2%	5%	10%	1%	2%	5%	10%
Bulk Steady state		$X_{i,A}$	0.22	0.62	3.23	7.33	0.12	0.44	2.43	5.29
		$X_{i,B}$	0.18	0.64	3.00	8.35	0.12	0.44	2.17	6.02
		$X_{i,C}$	0.20	0.75	3.78	11.46	0.17	0.61	3.07	8.88
		$X_{i,D}$	0.19	0.54	2.91	10.60	0.10	0.32	1.42	6.67
		T	0.04	0.05	0.07	0.26	0.05	0.06	0.13	0.41
Individual Variables	Steady State	F_A	0.03	0.12	0.66	2.23	0.004	0.01	0.06	0.27
		D	0.03	0.11	0.61	2.05	0.01	0.05	0.32	1.20
		B	0.002	0.01	0.04	0.15	0.02	0.06	0.38	1.43
		$X_{bot,D}$	0.01	0.06	0.30	0.95	0.02	0.08	0.50	1.92
		$X_{dis,C}$	0.01	0.03	0.19	0.63	0.01	0.02	0.11	0.42
		$X_{nf1,A}$	0.01	0.07	0.39	1.34	0.001	0.01	0.04	0.20
		$X_{nf2,B}$	0.09	0.33	1.82	5.96	0.02	0.07	0.45	1.61
	Dynamic	F_A	0.02	0.09	0.48	1.67	0.01	0.02	0.13	0.51
		D	0.02	0.08	0.46	1.61	0.01	0.04	0.24	0.92
		B	0.002	0.006	0.04	0.13	0.02	0.06	0.36	1.40
		$X_{bot,D}$	0.01	0.04	0.25	0.87	0.02	0.07	0.42	1.68
		$X_{dis,C}$	0.005	0.02	0.10	0.37	0.002	0.01	0.07	0.26
		$X_{nf1,A}$	0.01	0.05	0.28	1.01	0.003	0.01	0.08	0.37
		$X_{nf2,B}$	0.06	0.25	1.36	4.54	0.01	0.05	0.28	1.03

Table 3.5 The Average Relative Error (ARE) for open-loop model with internal composition controller (OL+IC)

SYSTEM			Open Model with Internal Controller (OL +IC)			
VARIABLE			Vs			
Magnitude Variable			1%	2%	5%	10%
Bulk Steady state		$X_{i,A}$	2.69	8.99	34.75	55.65
		$X_{i,B}$	2.38	6.12	20.83	37.56
		$X_{i,C}$	3.20	10.83	43.06	59.55
		$X_{i,D}$	2.35	10.27	17.82	21.69
		T	0.08	0.28	0.71	1.21
Individual Variables	Steady State	F_A	0.26	0.92	1.30	0.37
		D	0.18	0.59	1.48	4.10
		B	0.07	0.34	0.25	5.62
		$X_{bot,D}$	0.06	0.12	1.17	1.21
		$X_{dis,C}$	0.09	0.34	2.21	10.44
		$X_{nf1,A}$	0.15	0.55	0.80	0.93
		$X_{nf2,B}$	0.92	3.14	3.76	1.64
	Dynamic	F_A	0.18	0.64	1.32	1.35
		D	0.15	0.48	1.48	3.93
		B	0.04	0.20	0.25	5.22
		$X_{bot,D}$	0.06	0.16	1.04	1.18
		$X_{dis,C}$	0.05	0.20	1.76	9.19
		$X_{nf1,A}$	0.11	0.40	0.84	0.92
		$X_{nf2,B}$	0.64	2.22	3.91	3.98

3.5.1 Open-loop Model (OL)

In this scenario, the inventory loops incorporated into the system are: the pressure (controlled by the heat removal from the condenser), the reflux drum level (controlled by the distillate flowrate) and the base level (controlled by the bottoms flowrate). Figure 3.4-3.6 show the steady state composition and temperature profiles of the linear and nonlinear models with 1%, 5% and 10% change in F_B. These results showed that the prediction of linear model becomes poor as the magnitude of the disturbance is increased. Note that both temperature and composition profiles along the length of the column show that the difference between the linear and nonlinear models is most significant at feed trays. This gives an indication of higher nonlinearity effect in feed trays than any other parts of the column. There are many reasons that could be responsible for this behavior. First, higher concentration of reactants in these trays indicates places with higher reaction rates than any other parts of reactive zone. Second, these trays serve as possible entrance of disturbances into the column. Third, these trays are the locations in the column with high interactive effect of reaction kinetics and separation.

Figure 3.7 shows the dynamic response of the bottoms flowrate (B) for both linear and nonlinear models to an increase with different magnitudes in F_B. This is shown as an illustration of the output performance of the linear model as compared to that of rigorous model. The two models show an increase in the bottoms flowrate (B) with increase in reactant B due to the excess of unreacted B that goes down to the bottoms of the column. Figure 3.8 compares the dynamic performance of the composition of product D for the linear model to that of nonlinear model at different magnitude of increase in F_B.

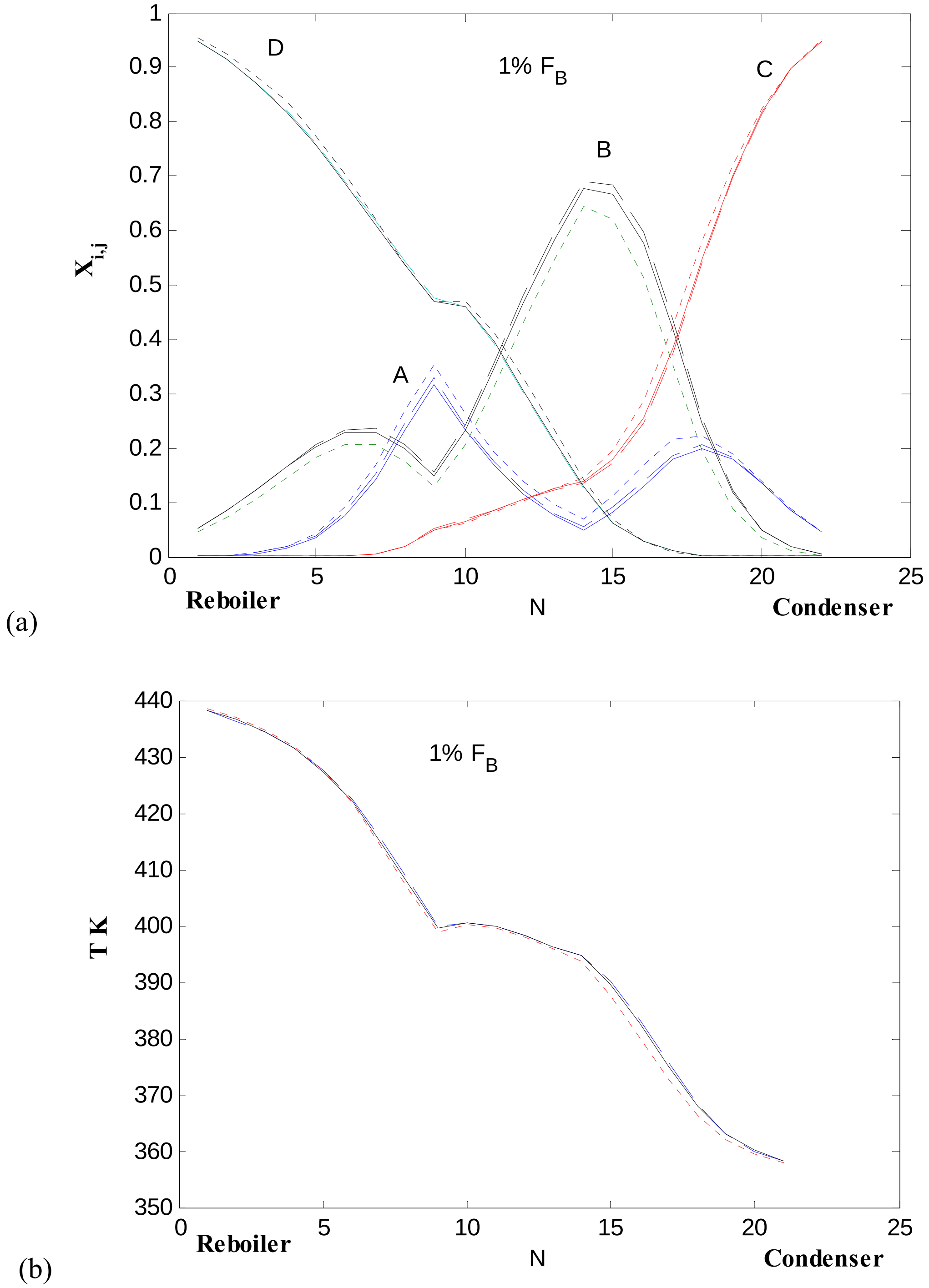

Figure 3.4 (a) Composition profiles with 1% increase in F_B: (b) temperature profiles with 1% increase in F_B: (---) base steady state profile; (— —) linear model; (——) nonlinear model.

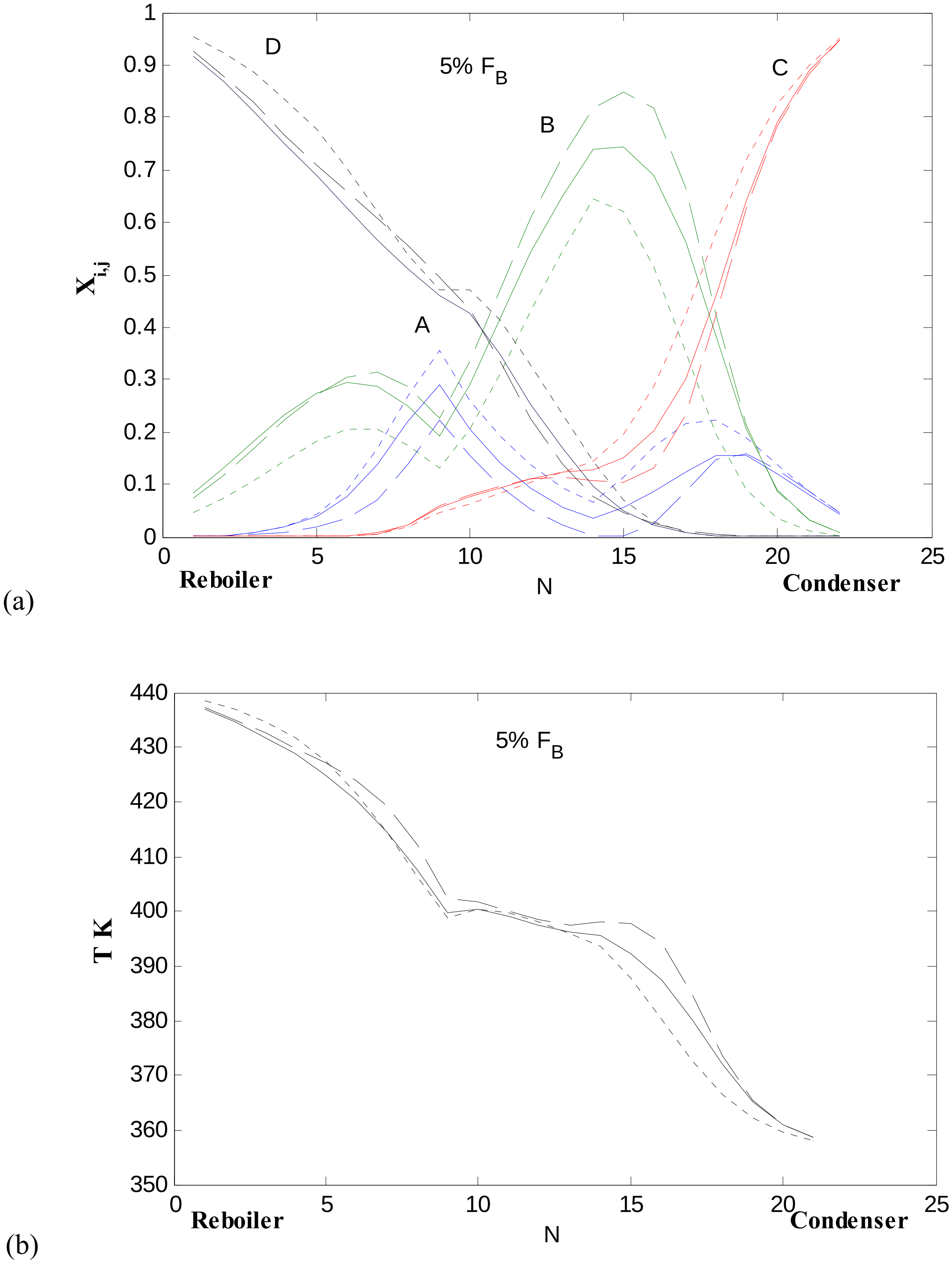

Figure 3.5 (a) Composition profiles with 5% increase in F_B: (b) temperature profiles with 5% increase in F_B: (---) base steady state profile; (— —) linear model; (——) nonlinear model.

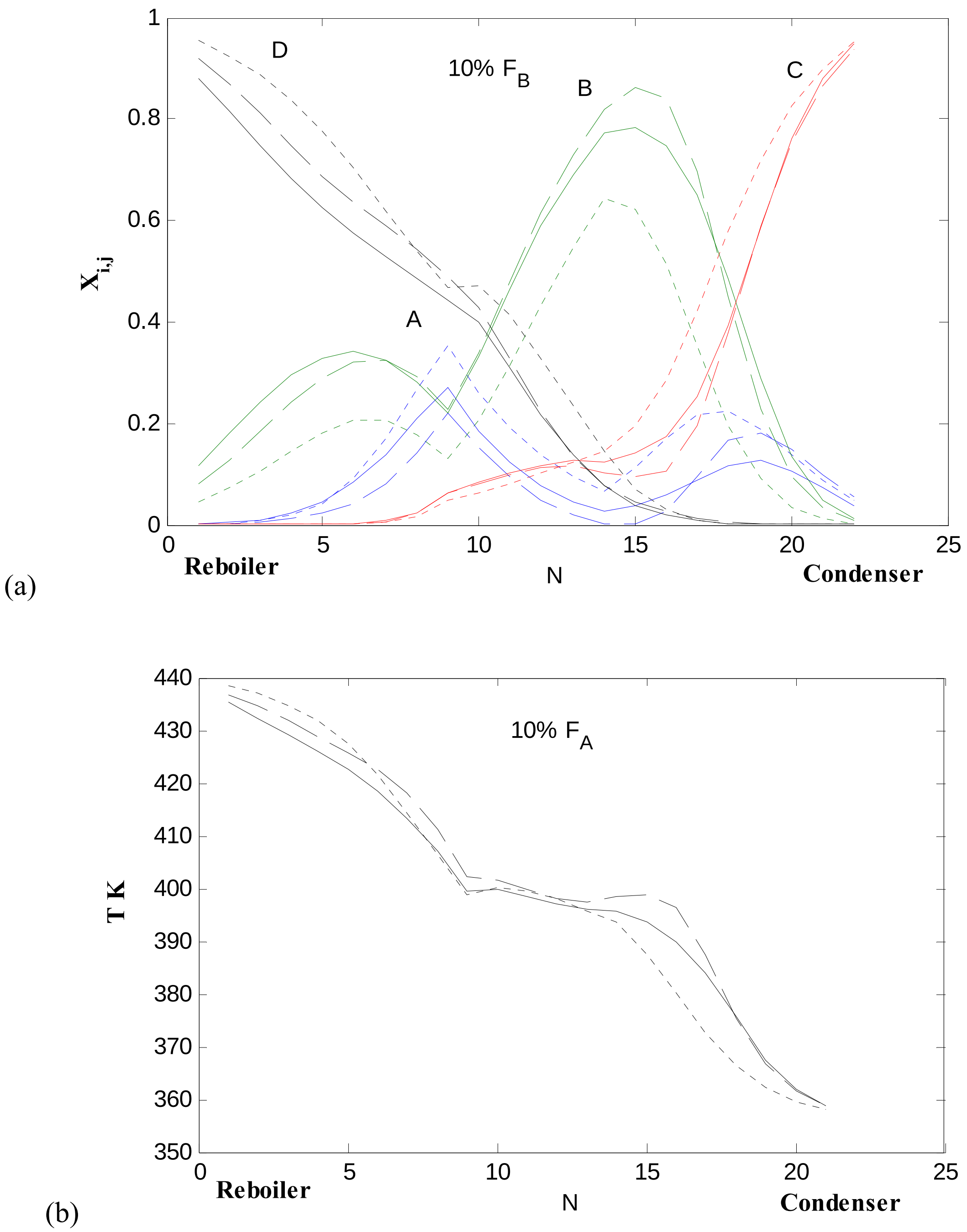

Figure 3.6 (a) Composition profiles with 10% increase in F_B: (b) temperature profiles with 10% increase in F_B: (---) base steady state profile; (— —) linear model; (——) nonlinear model.

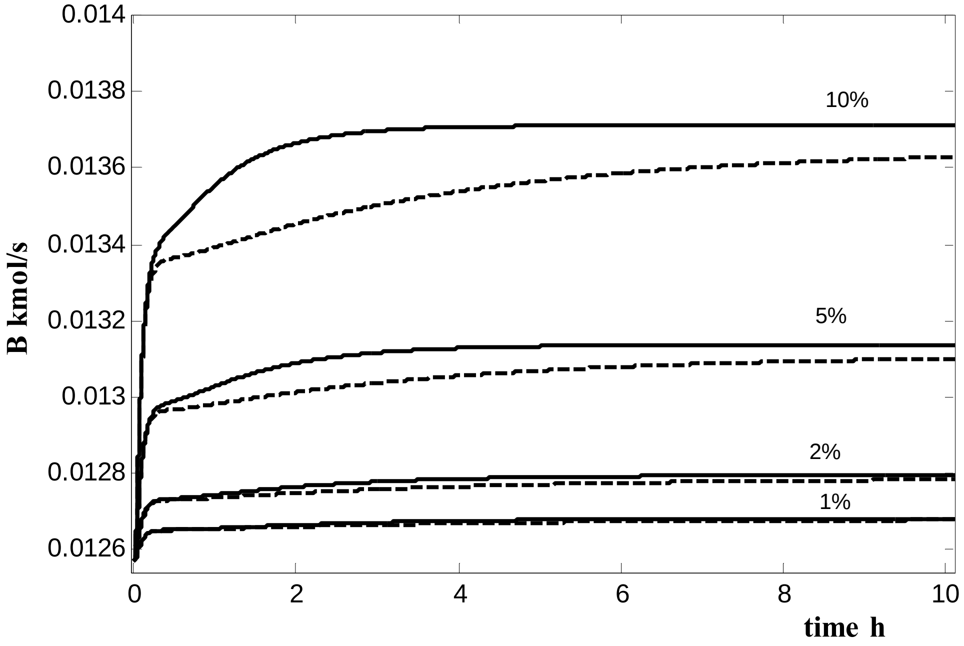

Figure 3.7 Dynamic responses of bottoms flowrate (B) to different magnitude of increase in F_B: (— —) linear model; (——) nonlinear model.

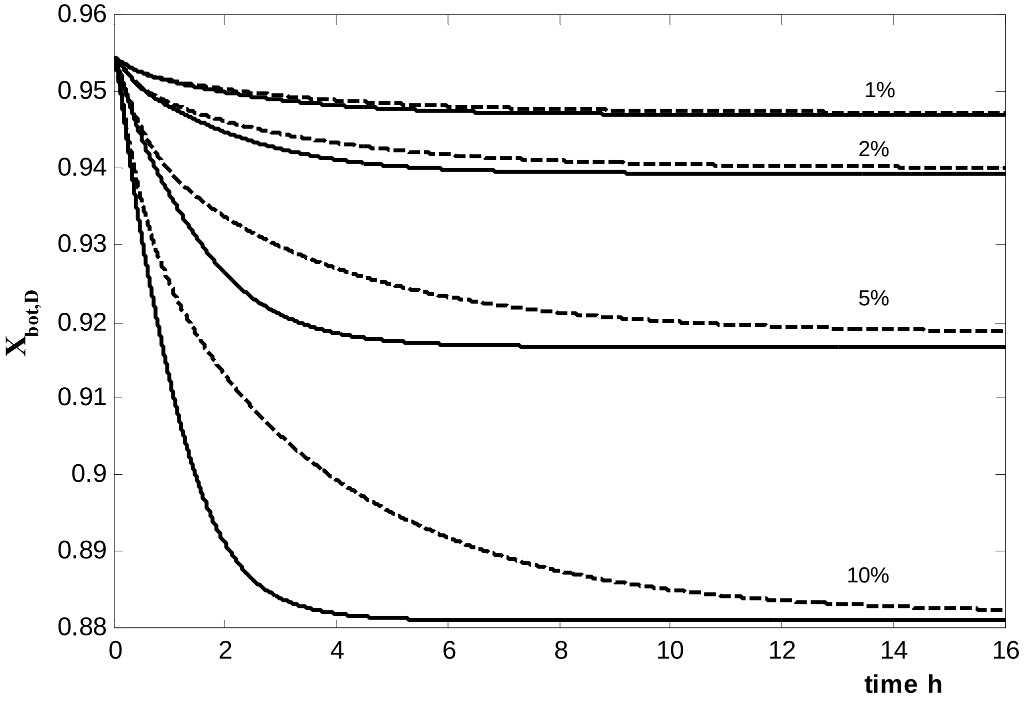

Figure 3.8 Dynamic responses of the composition of component D to different magnitude of increase in F_B: (— —) linear model; (——) nonlinear model.

The two models show a decrease in the concentration of D due to increase in concentration of reactant B in the bottoms.

In all of the dynamic comparisons that are carried out between the two models, the linear model shows a good performance at small magnitude of disturbance and the deviation between linear and nonlinear models increases with an increase in the magnitude of disturbances (see Table 3.2 an 3.3). The details of linear model accuracy are discussed in Section 3.6.

3.5.2 Open-loop Model with Internal Composition Controller (OL+IC)

Several papers have reported the use of an internal composition measurement in the closed-loop control of reactive distillation with multiple feeds to maintain the feeds stoichiometry [5-8]. The inclusion of an internal composition controller (to balance the reactants feed stoichiometry) is used to demonstrate the enhancement of open-loop performance of both linear and nonlinear models. The concentration of reactant A in the first tray of reactive zone (numbered from the bottoms) is controlled by manipulating the fresh feed flowrate of reactant A (F_A). The P-only controller is used because the objective of this internal controller is to maintain reactant A inventory and not to fix the composition at that stage.

Figure 3.9-3.11 show the steady state composition profiles for both linear and nonlinear models when an internal composition controller is included. The sources of disturbance are 1%, 2%, 5% and 10% increase in feed F_B. The linear model demonstrates a better performance and approximation of nonlinear model when compares with the same results shown in Figure 3.4-3.6, where no internal composition controller is used.

Figure 3.12 compares the dynamic response of the internal composition controller ($X_{nf1,A}$ and F_A) for both linear and nonlinear models. The disturbances are various magnitudes of positive step changes in F_B. The increase in the amount of reactant B fed into the column reduces the internal composition of reactant A. Controllers based on the two models respond adequately by increasing the feed flowrate F_A to counteract the gradual buildup of reactant B in reactive zone. The response time of the two models is comparable at lower magnitudes of disturbance. However, as the magnitude of disturbance increases linear model responds slower and predicted higher amount of F_A than that of the nonlinear model. The deviation between the two models increases with increase in disturbance magnitude.

Figure 3.13 shows the dynamic response of bottoms flowrate (B) for both linear and nonlinear models to different magnitude of changes in F_B, while the dynamic performance of the composition of product D for a linear model is compared to that of nonlinear model at different magnitude of changes in F_B as shown in Figure 14. The linear system response when an internal composition controller is included shows a good approximation of rigorous nonlinear model.

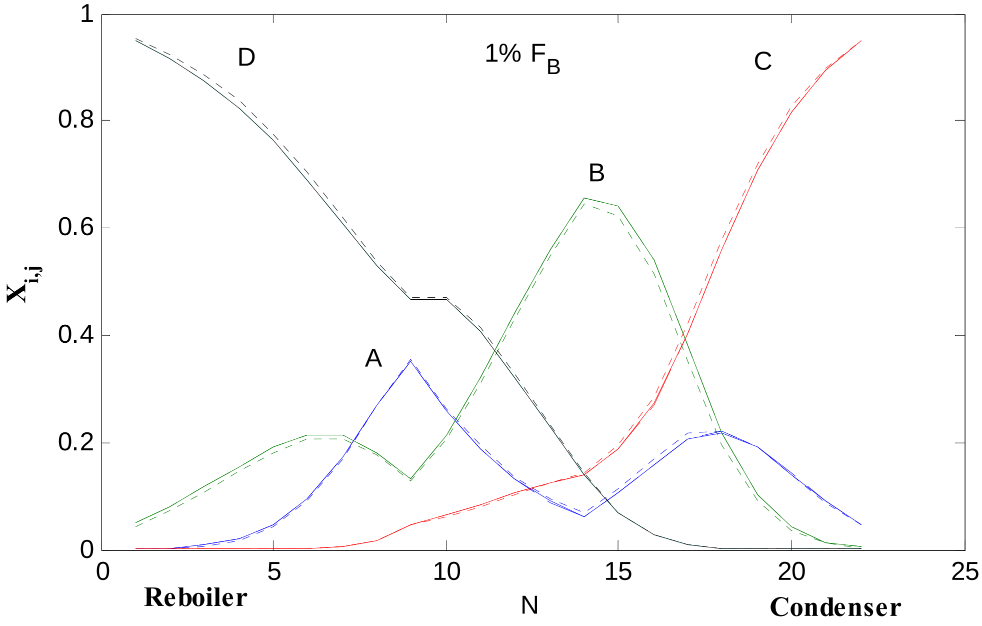

Figure 3.9 OL+IC. Composition profiles with 5% increase in F_B: (---) base steady state profile; (— —) linear model; (——) nonlinear model.

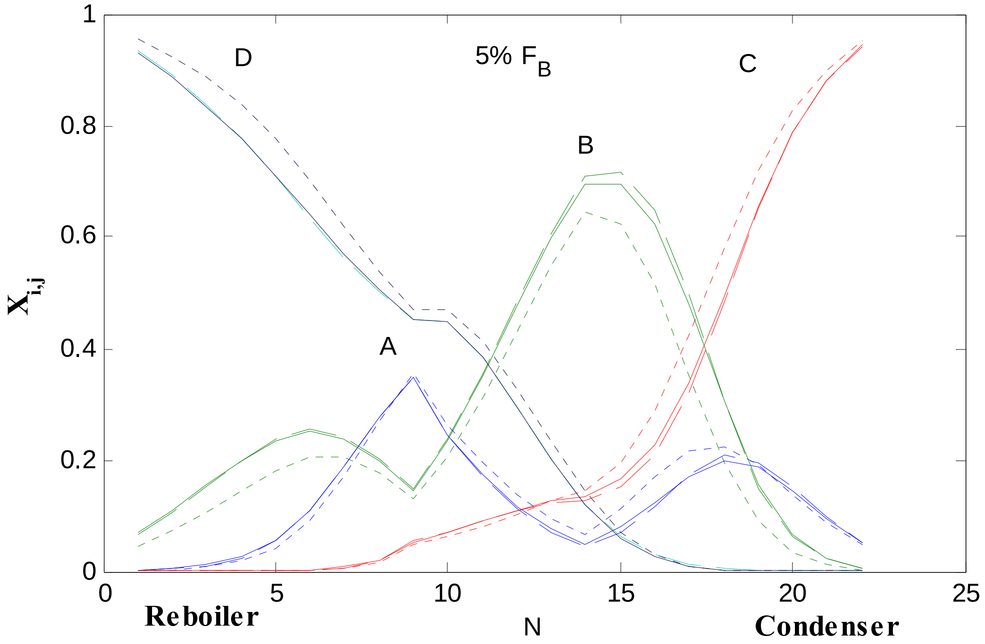

Figure 3.10 OL+IC. Composition profiles with 5% increase in F_B: (---) base steady state profile; (— —) linear model; (——) nonlinear model.

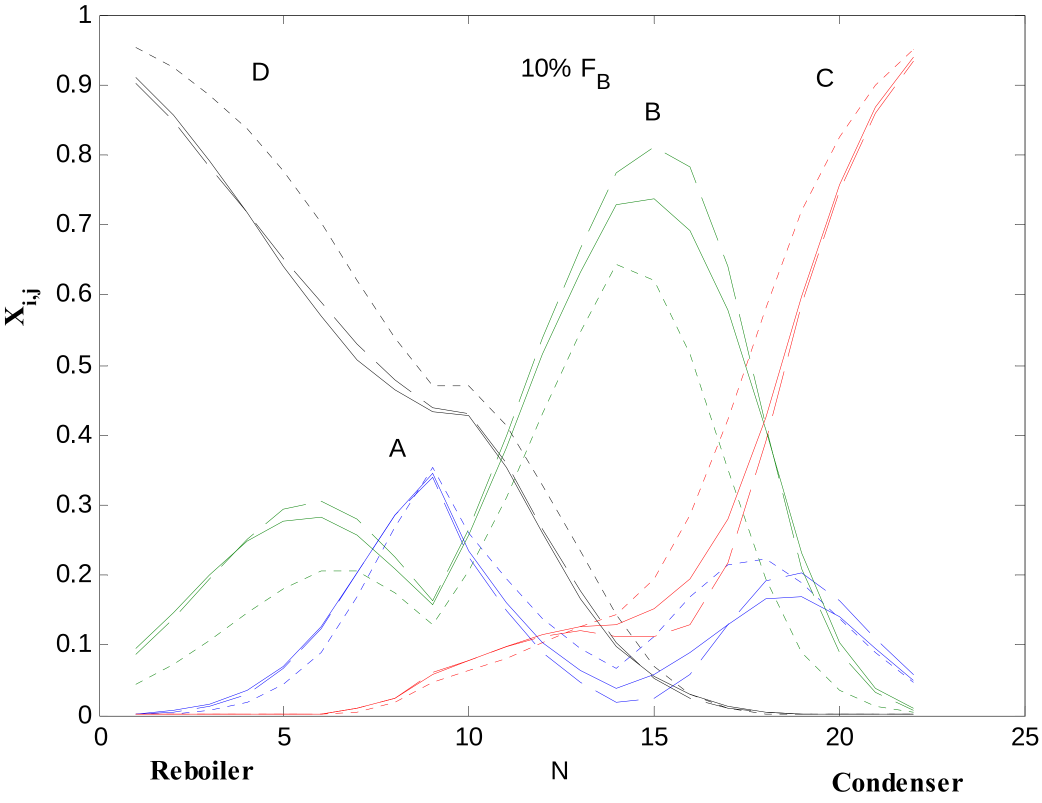

Figure 3.11 OL+IC. Composition profiles with 5% increase in F_B: (---) base steady state profile; (— —) linear model; (——) nonlinear model.

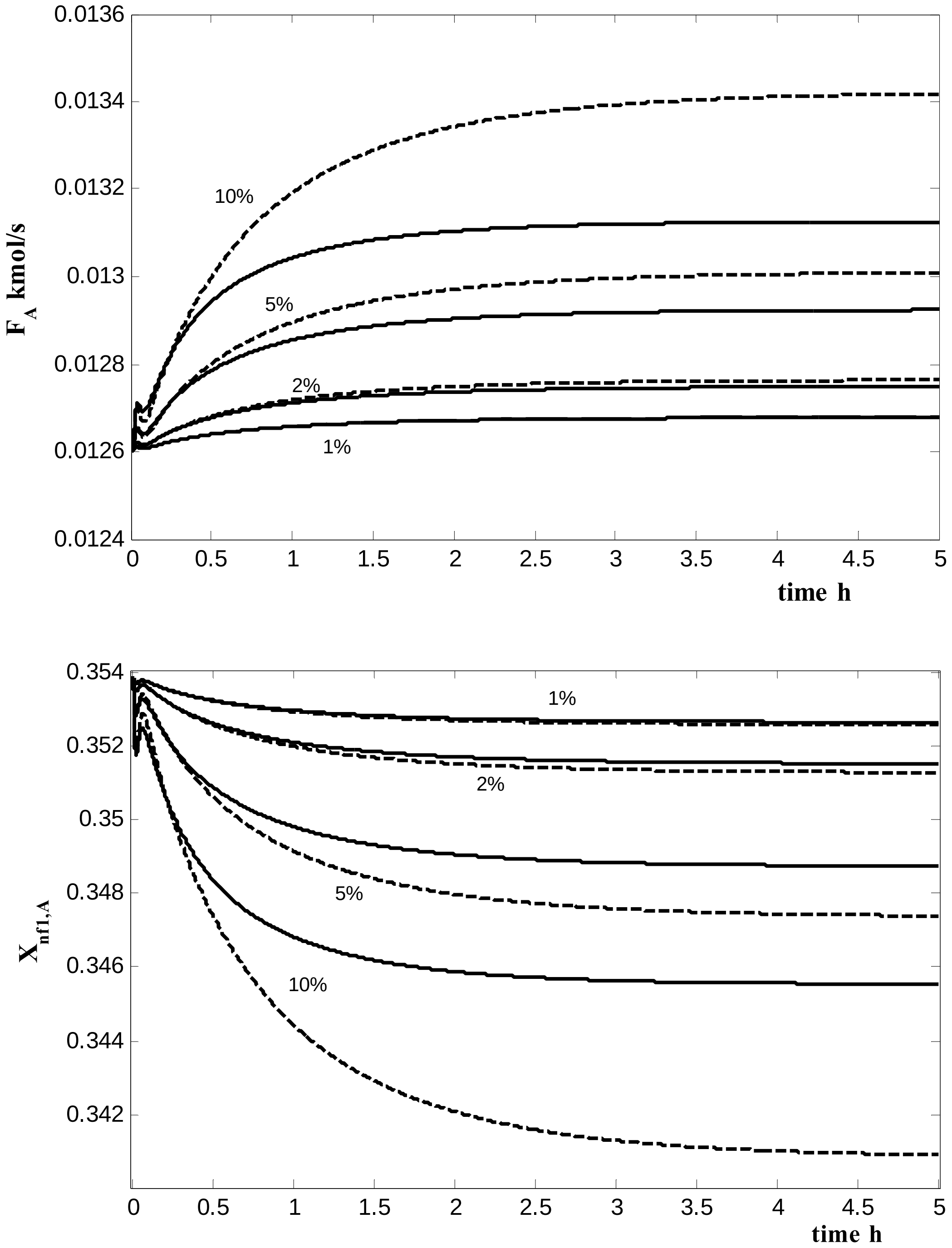

Figure 3.12 OL+IC. Dynamic responses of flowrate (F_A) and composition of reactant A on tray nf1to different magnitude of increase in F_B: (— —) linear model; (——) nonlinear model.

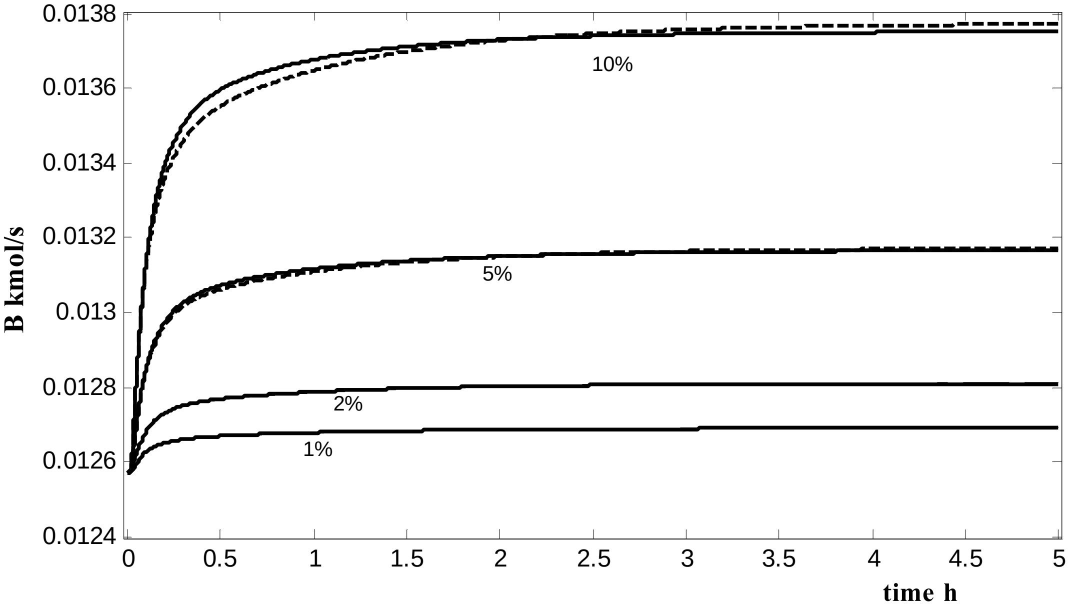

Figure 3.13 OL+IC. Dynamic responses of bottoms flowrate (B) to different magnitude of increase in F_B: (— —) linear model; (——) nonlinear model.

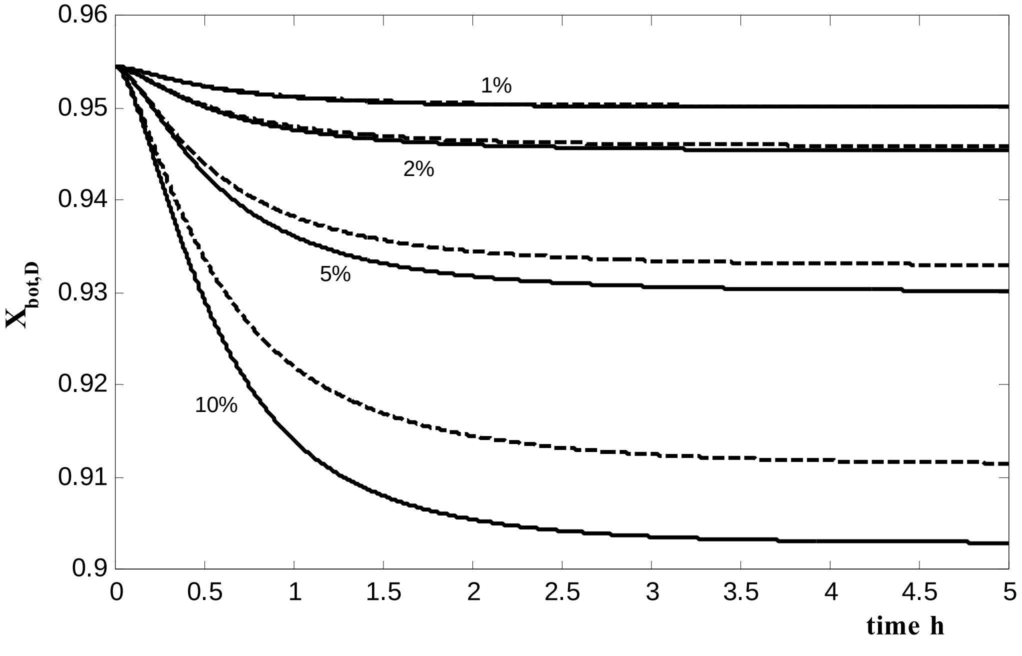

Figure 3.14 OL+IC. Dynamic responses of the composition of component D to different magnitude of increase in F_B: (— —) linear model; (——) nonlinear model.

3.6 Accuracy of a Linear Model

In this Section, the accuracy of a linear model with and without internal composition controller is quantified using the error index defined in Section 3.2. The quantification of model error based on various magnitudes of disturbance in feed flowrate $F_{B,}$ feed composition of reactant A (reactant B in F_A), and change in vapor boilup (Vs) are studied. Three major categories were used to classify the Average Relative Error (ARE) of the system.

1. Bulk steady state: in this category, the ARE of a given variable is averaged out over the number of stages. For example, the bulk steady state temperature is the sum of temperature in all the stages divided by the total number of stages.
2. Individual steady state: this is the ARE of a given variable at steady state.
3. Individual dynamic variable: this is the average ARE of a given variable over the time required to reach steady state.

Table 3.2 and 3.3 present the summary of the average relative error of the system without internal composition inventory. However, the ARE of the bulk steady state composition profiles with disturbance in F_B is shown in Figure 3.15. The results indicate that an approximation of the rigorous model with the linearized model without internal composition controller could be acceptable when the magnitude change in feed flowrate is below 6%. Similar conclusion could be reached when the ARE of the system are quantified based on individual dynamic and steady state of the system variables (see Figure 3.16). The ARE of the bulk composition in the OC+IC scenario is around 10% when F_B is increased by 10% while it is ranging between 20-40% if the internal composition is not included. The ARE of the system is significantly reduced when the internal controller is included in the open-loop system (see Figure 3.16 and 3.17), which suggest that the performance of linear system is acceptable with disturbance magnitude more than 10% if the ARE tolerance is less than 20%. The details of average relative error for the OL+IC scenario are presented in Table 3.3 and 3.4.

Figure 3.17 compares the impact of disturbance from different system variables (i.e. F_B, Z_a and Vs) on the performance of the linearized model using their average relative error (ARE). We have used the bulk steady state temperature profiles for this comparison because it represents the cumulative effect of system dynamics. Introduction of disturbance from the feed composition (reactant B in F_A) is shown to have higher ARE than from feed flowrate (F_B). This suggests that disturbance in feed composition affect the internal composition and increases the system nonlinearity more than that made by disturbing the system from feed flowrate. Exciting the system by changing the vapor boilup shows the highest trend of error because it impacts both the reaction kinetics and the separation capacity of the system, and thus, the system nonlinearity.

The critical performance comparison of the open-loop linear model with and without the internal composition controller reveals the following important points:

1. The performance of a linear model is improved with the inclusion of an internal composition controller, which suggests the degree of nonlinearity in a nonlinear model is reduced when the stoichiometry balance of the feed flowrates entering the reactive zone is maintained. The average relative error of a linear model when compared to a nonlinear model is reduced even at higher magnitude of disturbance when the internal composition controller is included. (see Table 3.2-3.4).

2. The settling time of a linear model with an internal controller is shorter than that without an internal controller, which is an indication of better system stability.
3. For implementation purposes, it is recommended to use the linearized model whenever the ratio of disturbance magnitude to the tolerable model error is not greater than 1 and that the system is open-loop stable under that magnitude of change. For example, if the tolerable model error is 20% then the linearized model could be used for disturbance magnitude up to 20%.
4. It is expected that the closed-loop performance (with either single-end or dual-end quality control) based on a linearized model will be reasonably close to the nonlinear model.

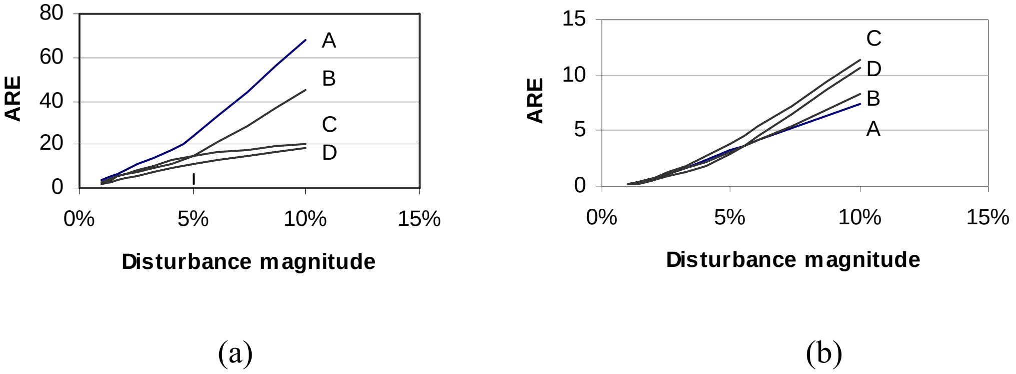

Figure 3.15 The ARE of the bulk steady state composition profiles with disturbance in F_B: OL (b) OL+IC.

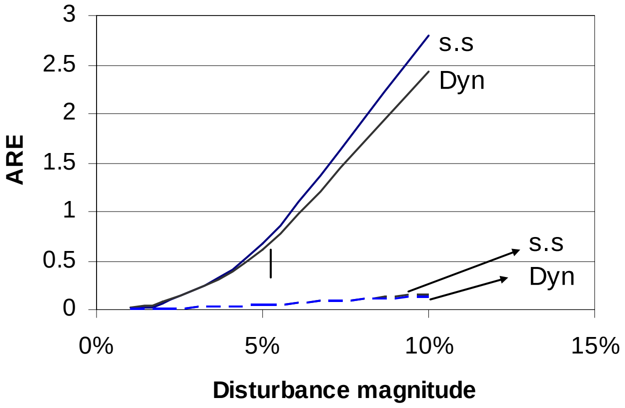

Figure 3.16 The ARE of the individual dynamic (Dyn) and steady state (s.s) of bottoms flowrate (B) with disturbance in F_B: (——) OL; (----) OL+IC.

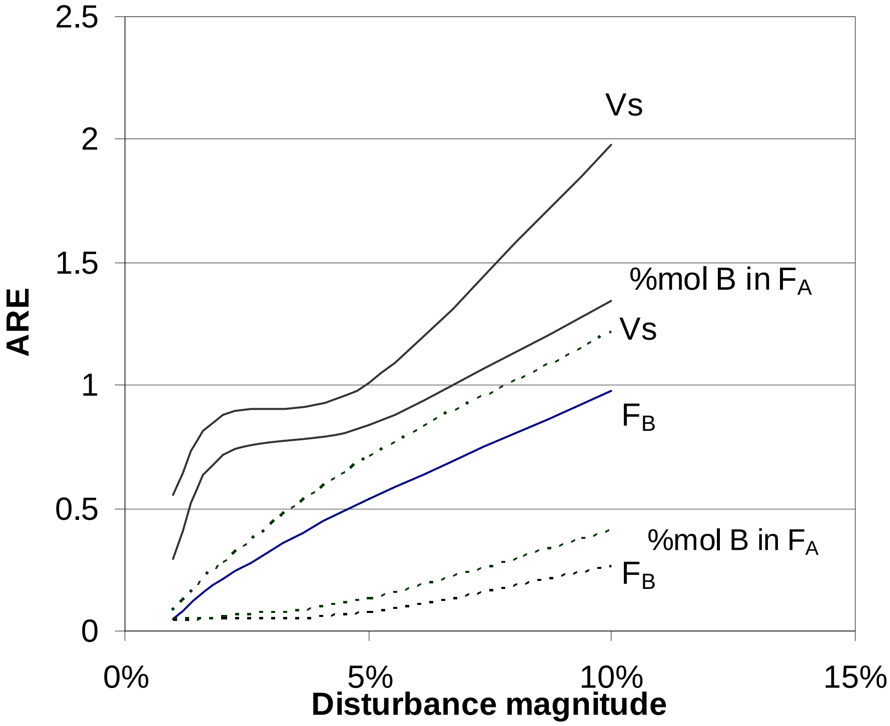

Figure 3.17 The ARE of the bulk steady state temperature profiles with disturbances in Vs, F_B, %mol B in F_A: (—) OL; (---) OL+IC.

3.7 Conclusion

In this study, we have compared the open-loop performance of a linearized dynamic model of generic reactive distillation system with that of a nonlinear model. An approximate linear model nicely averages the process nonlinearities when the magnitude of input change is small and becomes inadequate as the deviation from the base steady states increases with an increase in the magnitude of disturbance. The effect of various step input changes on the performance of an approximate model is explored. The linear model could be used to approximate the behavior of the system if the magnitude of the disturbance is less than 6% when there is no internal composition controller. When the internal composition controller is included, the linearized model could be used to approximate the nonlinear model up to a disturbance magnitude equals to the tolerable model error provided that the system is open-loop stable. If the system shifts from the base steady state to another under the influence of a disturbance, then linearizing around the base steady state will result in a model that provides false conclusion. The performance and robustness of a linear model is enhanced with the inclusion of an internal composition inventory control in the open-loop model of the system.

3.8 References

[1] C. Fuentes and W. L. Luyben, "Comparison of energy models for distillation columns," *Ind. Eng. Chem. Res.*, vol. 22, pp. 361, 1983.

[2] S. Skogestard and M. Morari, "The dominant time constant for distillation for distillation columns," *Compu. Chem. Engng*, vol. 11, pp. 607-617, 1987.

[3] W. L. Luyben, "Derivation of transfer functions for highly nonlinear distillation columns," *Ind. Eng. Chem. Res.*, vol. 26, pp. 2490-2495, 1987.

[4] W. Marquardt and M. Amrhein, "Development of a linear distillation model from design data for process control," *Computers Chem. Engng*, vol. 18, pp. S349-S353, 1994.

[5] M. A. Al-Arfaj and W. L. Luyben, "Comparison of alternative control structures for an ideal two-product reactive distillation column," *Ind. Eng. Chem. Res.*, vol. 39, pp. 3298-3307, 2000.

[6] M. A. Al-Arfaj and W. L. Luyben, "Comparative control study of ideal and methyl acetate reactive distillation," *Chem. Eng. Sci.*, vol. 24, pp. 5039-5050, 2002.

[7] M. A. Al-Arfaj and W. L. Luyben, "Comparative control study of ideal and methyl acetate reactive distillation," *Chem. Eng. Sci.*, vol. 24, pp. 5039-5050, 2002.

[8] M. A. Al-Arfaj and W. L. Luyben, "Plantwide control for TAME production using reactive distillation," *AIChE J.*, vol. 50, pp. 1462-1473, 2004.

CHAPTER 4

4 Impact of Disturbance Magnitudes and Directions on the Dynamic Behavior of Reactive Distillation

4.1 Introduction

Although reactive distillation might be an attractive alternative to the conventional multiunit processes, it can be effective for only a fairly small class of chemical systems because of some inherent limitations. Reactive distillation is particularly possible when reactants and products possess relative volatility such that a high concentrations of reactants and low concentrations of products are maintained in the reaction zone. The reaction rates must be comparable to those in the reactor at temperature suitable for distillation. The potential advantages of reactive distillation could be negated by improper choice of reactant to be run in excess in the reactive zone whenever it is needed to avoid substoichiometric balance. Thus, it is possible to decrease conversion by increasing the amount of catalyst under certain circumstances [1]. Increased separation capability could decrease process performance [2].

Successful commercialization of reactive distillation technology requires careful attention to the modeling aspects, including column dynamics, even at the conceptual design stage [3]. The design and operation issues for reactive distillation systems are considerably more complex than those involved for either conventional reactors or conventional distillation columns. The introduction of an in situ separation function within the reaction zone leads to complex interactions between thermodynamic vapor-liquid equilibrium, intra-catalyst dilution (for heterogeneously catalyzed processes) and chemical kinetics.

Another area of concerns in the study of reactive distillation system is the impact of disturbance magnitudes and directions in dynamic behavior of both open-loop and closed-loop model of reactive distillation. In a typical reactive distillation column, the regions of intense mass transfer are in the middle of the column where the reactive zone is usually located, while the ends of column are essentially used for purification. These regions are more sensitive to disturbance directions as compared to the ends of columns. The effectiveness of disturbance suppression in a multivariable control system can depend strongly on the direction of disturbance [4].

This work investigates the dynamic behavior of high-purity/high-conversion generic reactive distillation system. The effect of disturbance magnitudes and directions on the stability of both open-loop and closed-loop system of reactive distillation is quantitatively explored. The open-loop performance of the system is explored with and without the inclusion of internal composition inventory controller. The impact of certain inventory control loops on the dynamic stability of the system is studied. This investigation is essential to gain a better understanding of this generic class of reactive distillation and to examine the applicability of the developed process models in an advanced process control of the system.

4.2 Dynamic Scenarios

Considering the same reactive distillation process shown in Figure 2.1, the effect of disturbances is studied to investigate the system dynamic performance. The dynamics of the system under these changes were studied for three scenarios:

1- Open-loop (OL): Under this scenario, two cases are investigated:
    I. Open-loop dynamics I (OL-I): reflux rate is fixed by changing reflux ratio and reflux drum level is controlled by distillate flowrate.
    II. Open-loop dynamics II (OL-II): reflux ratio is fixed by changing the reflux rate and reflux drum level is controlled by distillate flowrate.

2- only the level control loops are closed while F_A, F_B, Z_a and Z_b, Vs and R could be sources of disturbance.

3- Open-loop with internal composition control (OL+IC): in addition to level control loops, the internal composition is controlled by feed flowrate. This reduces the number of disturbance by assigning one of the feed flowrates to control the composition

4- Single-end control (CL): in addition to OL+IC loops, a composition loop is closed by manipulating either Vs or R to control one of the product compositions which, in turn reduces the disturbance variables by one more.

The main process variables that are considered as sources of disturbances are:

1- Feed flowrates (F_A kmol/s, F_B kmol/s)

2- Vapor boilup (Vs kmol/s)

The effect of feed compositions (Z_a and Z_b) disturbance and reflux flowrate (R kmol/s) disturbance were studied and will be discussed briefly as they are somewhat similar to those of flowrates and vapor boilup disturbances. The kinetic and physical properties as well as the steady state operating conditions for the system is the same as presented in the Chapter 2.

This study considers the model configuration where vapor boilup and reflux flowrate could be the manipulated variables if the system is operated in closed-loop mode. In order to investigate the dynamic behavior of the system, three magnitudes (2%, 5%, and 10%) in both positive and negative directions are studied for each of the process disturbance variables.

4.3 Open-loop Model (OL)

4.3.1 Feed Flowrates

Figure 4.1 shows the responses of the system to different step changes in both magnitudes and directions of feed flowrate of reactant B (F_B). In this case, the reflux rate, vapor boilup, feed flowrate of reactant A and feed compositions are kept constant at their steady state values. Figure 4.1a shows the impact of this disturbance in the kinetic region of reactive distillation. Excess of reactant B, the heavier reactant, in the reactive zones slightly increases the rate of product formation. This is primarily due to fact that reactant B will concentrate more in the liquid phase and will react with the available reactant A whenever it is available in excess.

On the other hand, reducing F_B (see Figure 4.1) has a severe impact on the dynamic behavior of the system, and consequently its stability. Reducing F_B by 2% causes the total product formation rate to drift to another steady state. Further decrease in feed flowrate F_B will result in an unstable operation as the bottoms flowrate will increase unbounded (Figure 4.1) and consequently the distillate flowrate drops to zero. The impact of excess of reactant B concentration in the column is reflected by an increase in bottoms rate in similar proportions to the magnitude of disturbance as shown in Figure 4.1b. Increasing F_B has the advantage of increasing the conversion and enhancing the system stability, yet it decreases products purity as shown in Figure 4.1c as well as reducing reactant A concentration in the reactive zone as shown in Figure 4.1d.

Figure 4.2 shows the responses of the system when reactant A flowrate (F_A) is changed. Figure 4.2a shows a sharp drop in total product formation rate when F_A is increased. Increasing the flowrate of reactant A in the column seems to have the same effect as decreasing the flowrate of the reactant B (F_B), i.e. drift to new steady state. The rapid buildup of reactant A concentration in the reactive zone decreases the system stability because an excess of a more volatile reactant A will demand an increase in heat duty of the system (which is fixed in this scenario) in order to strip out any unreacted A from product D. On the other hand, decreasing the feed flowrate of reactant A decreases the total product formation rate in reactive zone without drifting or destabilizing the system.

Drifting the system either to another state or to completely unstable conditions when F_A is increased or when F_B is decreased is closely associated to the resulted substoichiometric balance of the reactants in the reactive zone. This is further studied by investigating the reaction kinetics on reactive trays by ±2% change in F_A and F_B as disturbances. Figure 4.3 shows the effect of disturbances on reaction rate in some selected reactive trays. The trays in reactive zone are numbered from bottoms to the top. Both decreasing the feed F_B and increasing the feed F_A in the column results in

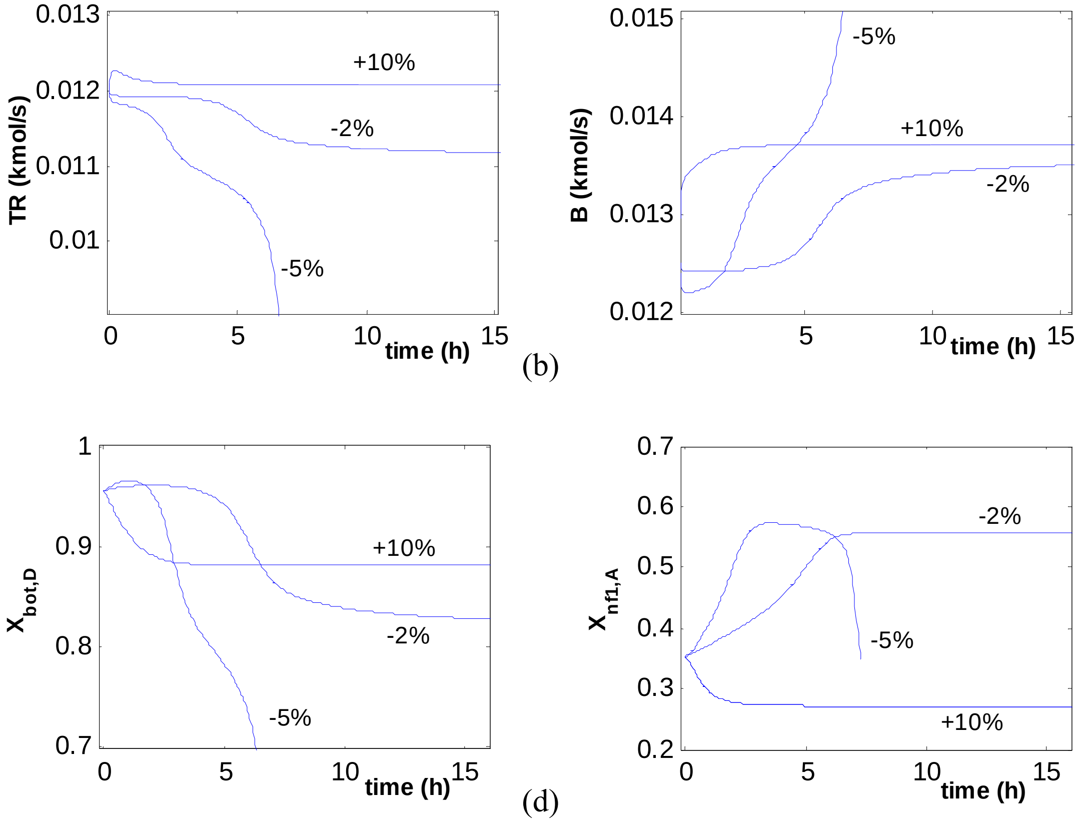

Figure 4.1 Dynamic responses of the system to different magnitude changes in feed F_B. (a) total reaction rate; (b) bottoms flowrate; (c) composition of product D in the bottoms; (d) internal composition of reactant A in tray nf1.

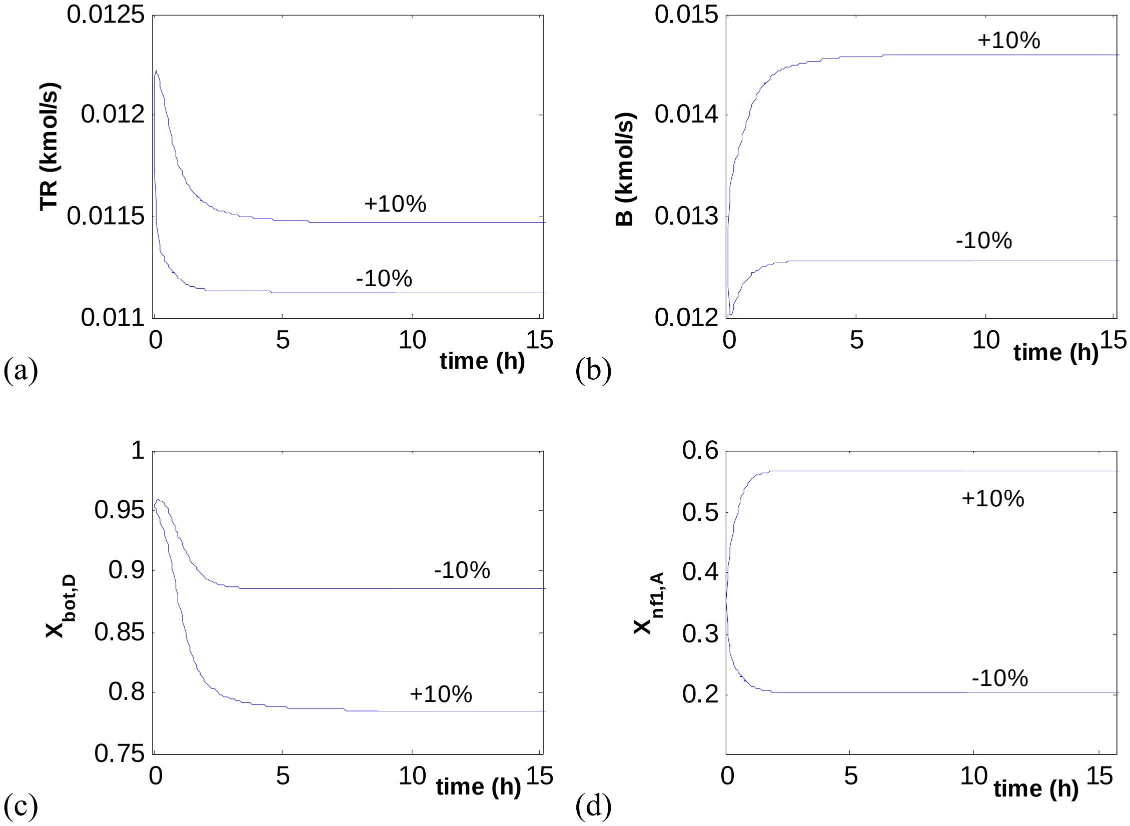

Figure 4.2 Dynamic responses of the system to different magnitude changes in feed F_A. (a) total reaction rate; (b) bottoms flowrate; (c) composition of product D in the bottoms; (d) internal composition of reactant A in tray nf1.

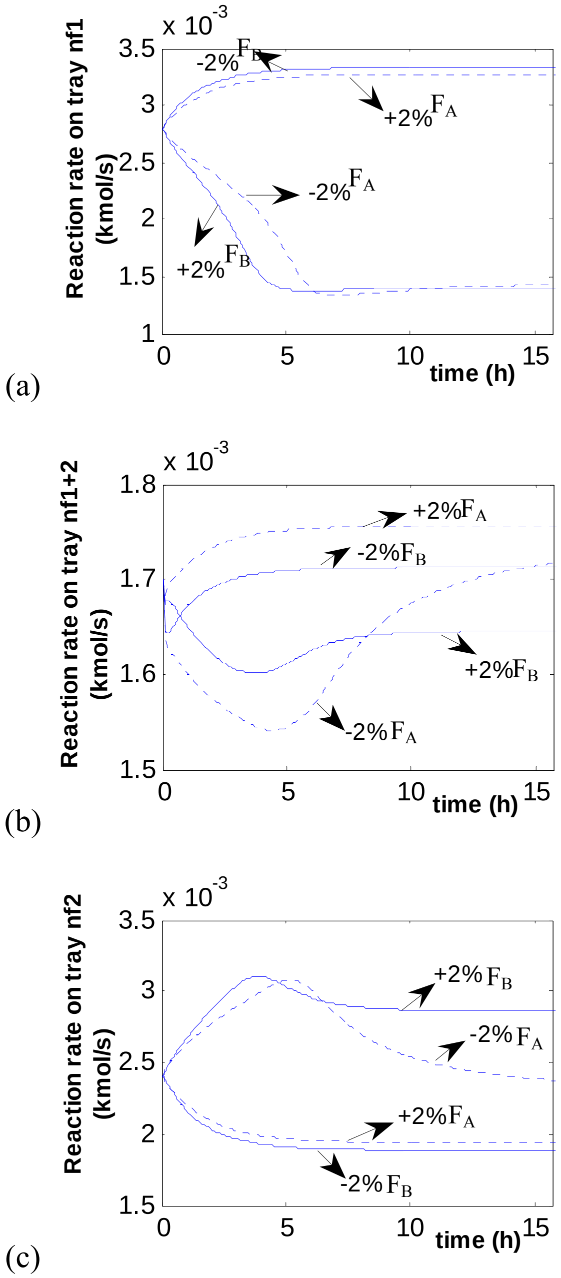

Figure 4.3 Responses of the reaction rate in reactive trays to step changes in F_B and F_A. (a) reactive tray nf1; (b) reactive tray nf1+2; (c) reactive tray nf2.

insufficient concentration of reactant B, and consequently decreases the rate of products formation in the reactive zone. The effect becomes most significant in the first reactive tray (nf1) where the product formation rate is the highest at the base steady state before introducing any disturbances. The highest steady state reaction rate is in tray nf1 of reactive zone which is reasonable as that is where we have the highest concentration of reactant A, the limiting reactant in liquid phase. The effect of reactant B deficiency is the rapid accumulation of concentration of reactant A in the stripping section, which will require more heat to vaporize it. Since in this scenario (OL) the separation capacity is fixed by keeping both the reflux rate and vapor boilup constant, decreasing the feed F_B or increasing the feed F_A will result in flooding the stripping section with an unreacted excess A, which in turn destabilizes the system or shift it to another state. Figure 4.5 shows how the temperature distribution in the column is affected with disturbance directions in feed streams.

In general, increase in F_B has similar effects as decrease in $F_{A.}$ One would expect the other way around is true, i.e. decrease in F_B or increase the feed $F_{A,}$ would have the same effect, but it is not. Reducing the feed flowrate of reactant B more than 2% is intolerable as it makes the system unstable, while increasing F_A up to 10% merely drift the system to another stable steady state. The reason behind that is as follows: when F_A is increased at fixed vapor boilup, more reactant A will leave the bottoms of the column as excess reactant. On the other hand, when F_B is reduced, less than the required amount of reactant B will be available, which upsets the reaction kinetics and thus destabilizes the system.

In order to assess the open-loop dynamics of the system when the reflux ratio is fixed, Figure 4.4a compares the total reaction rate responses of OL-I in the reactive zone to those of the OL-II when a 10% increase in feed flowrates is introduced. As can be seen, there is no much difference in the responses of OL-I and OL-II. On the other hand, Figure 4.4b shows the effect of negative disturbances in feed flowrate of reactant B (F_B) for the OL-I and OL-II cases. Introducing a negative disturbance in F_B has a more severe impact on the dynamics of the system, and consequently its stability when reflux rate is fixed (OL-I) than when reflux ratio is kept constant.

Generally, open-loop dynamics of reactive distillation will give a better performance when the reflux ratio is fixed instead of reflux rate. However, if fixing the reflux rate is preferable or needed, the inclusion of internal inventory composition controller and/or single-end controller (composition or temperature) as discussed in the next sections are expected to resolve most of the instability problems.

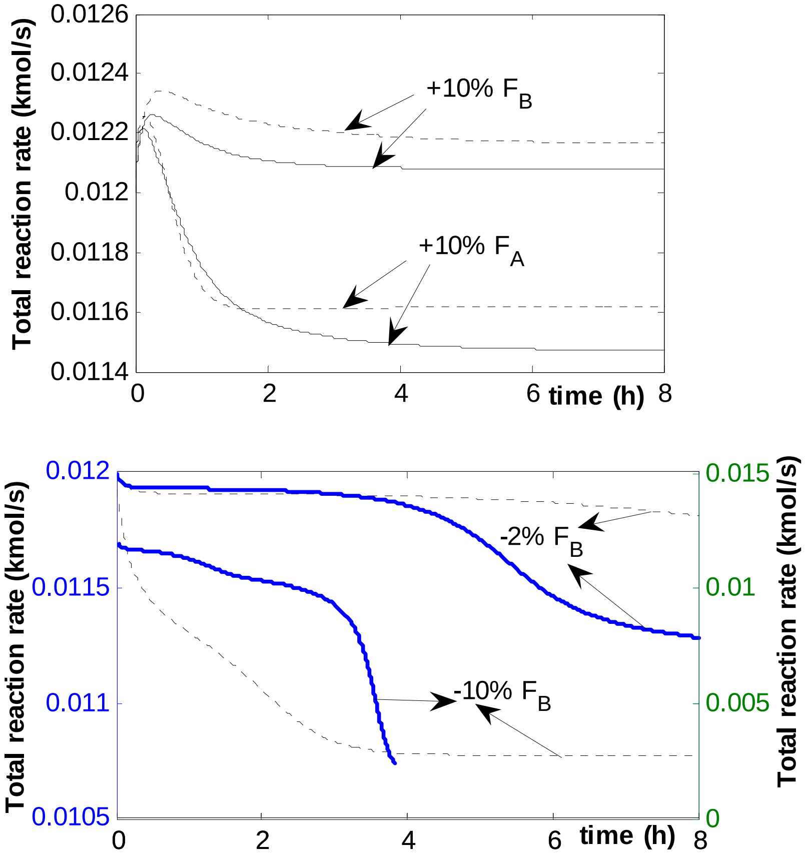

Figure 4.4 Dynamic responses of total reaction rate to step changes in feed flowrates of reactant A and B. (—) OL-I; (---) OL-II.

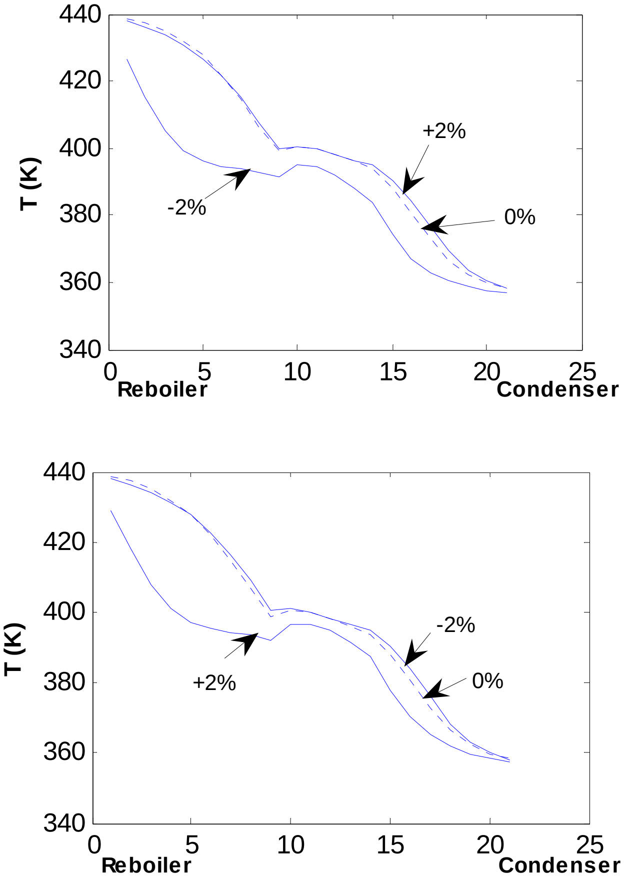

(a)

(b)

Figure 4.5 Temperature distribution in the column with disturbance in feed streams:

(a) ±2% F_B; (b) ±2% F_A

4.3.2 Feed Composition

In the steady state design, the feed composition of F_A is 100% A and similarly 100% B for F_B. In order to study the effect of feed composition, two cases are studied, in which feed composition is changed by introducing some impurities from the other reactant, i.e. impurity of reactant A in F_B and impurity of reactant B in F_A. Below are the two feed compositions considered:

1. 2%, 5% and 10% of reactant B in feed F_A
2. 2%, 5% and 10% of reactant A in feed F_B

Figure 4.6 shows the effect of change in feed compositions on the net reaction rate in the reactive zone. In general, introducing reactant B in F_A is expected to be tolerable similar to increasing F_B since both of these changes will result in more of reactant B in the system, but as they differ in the point where this increase is introduced, the dynamic behavior is different. The reaction rate decreases because of the reduction of reactant A in the reaction zone as a result of decrease in the amount of fresh reactant A entering the column.

In general, introducing reactant B in F_A is found to be tolerable similar to increasing F_B since both of these changes will result in more of reactant B in the system, but as they differ in the point where this increase is introduced, the dynamic behavior is different. The reaction rate decreases because of the reduction of reactant A in the reaction zone as a result of decrease in the amount of fresh reactant A entering the column. On the other hand, introducing reactant A in feed F_B is intolerable because of the same reason that makes a decrease in F_B intolerable, namely the excess of reactant A in the column while fixing separation capacity. The disturbance in feed compositions affects the system dynamics and increases its nonlinearity more than disturbance in feed flowrates.

4.3.3 Vapor Boilup

Figure 4.7 shows the dynamic responses of total product formation rate, bottoms flowrate and some compositions to different magnitude of changes in the vapor boilup from the reboiler. A small decrease in vapor boilup from its base steady state value makes the system unstable. This might be largely due to the interference effect of fractionation on the system's reaction kinetics. Reducing the heat duty of the reboiler, while the reflux rate and the feed inputs remain constant adversely affect the separation capacity of the column. Thus, less heat is available to vaporize unreacted A to the vapor phase. This in turn decreases the concentration of reactant A in the reflux rate and causes substoichiometric balance of the two reactants in reactive zone.

Increase in the amount of vapor flowrate at fixed reflux rate will increase the distillate flowrate and slightly decrease the bottoms product. In addition, the total reaction rate slightly decreases because the column fractionation capacity is affected, and more heat is available to enrich volatile components in vapor phase. This invariably increases bottoms product purity and leads to a gradual depletion of reactant A in the reactive zone as more of light reactant is being stripped out from the reactive zone. Thus, more of reactant A is lost in the overhead and the liquid concentration of reactant A is reduced. This suggests that increased separation capacity could decrease process performance (i.e. conversion and product purity).

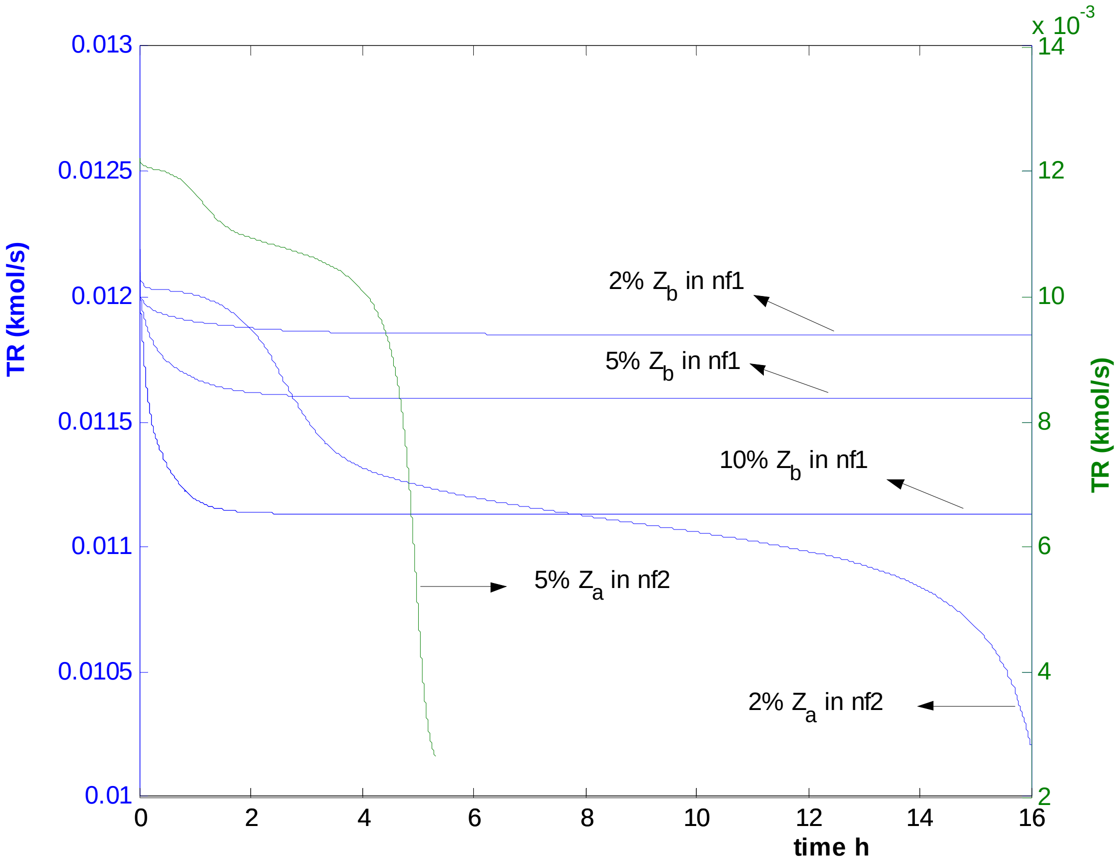

Figure 4.6 Dynamic response of the total reaction rate (TR) of products in reactive zone to different magnitude changes in feed compositions.

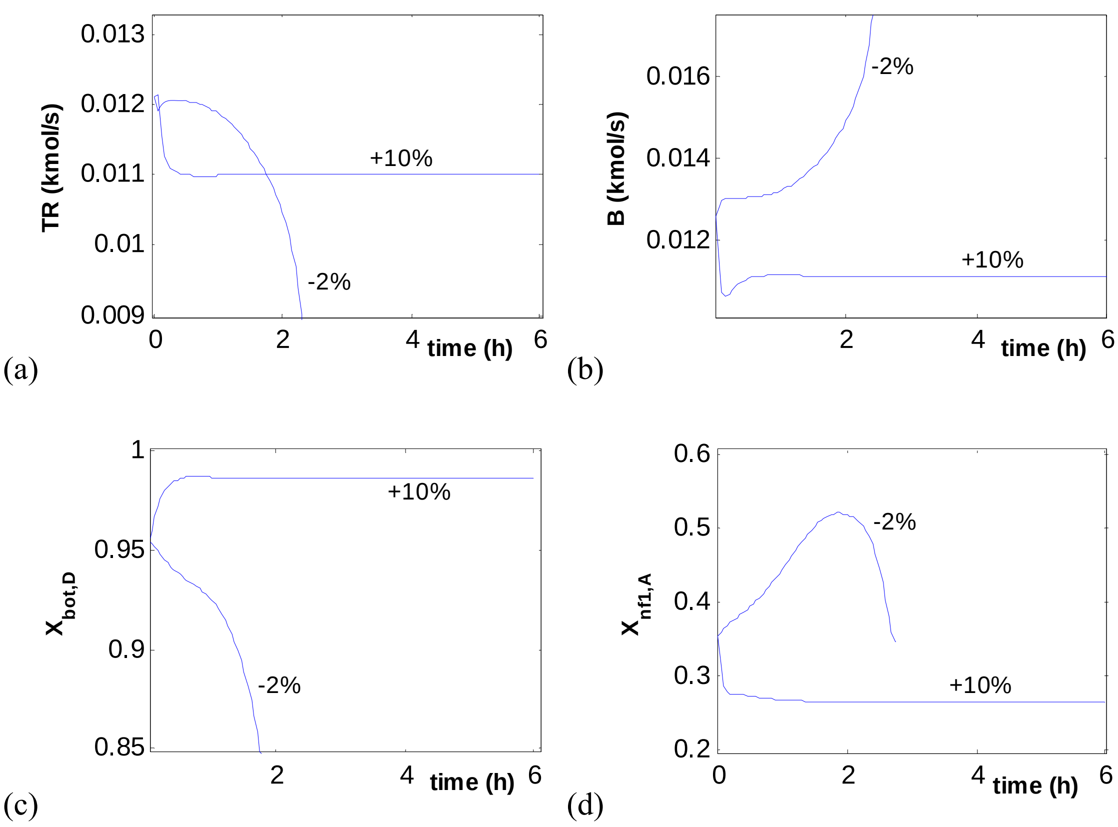

Figure 4.7 Dynamic responses of the system to different magnitude changes in vapor boilup. (a) total reaction rate; (b) bottoms flowrate; (c) composition of product D in the bottoms; (d) internal composition of reactant A in tray nf1.

It is observed that decreasing the vapor boilup has the same effect on the open-loop dynamics of the system as increasing the reflux flowrate at constant feed conditions as shown in Figure 4.8. Increasing the reflux rate with constant vapor boilup forces the bottoms flowrate to grow unbounded because it returns more volatile reactant A back into the reactive zone than needed. This will necessitate increase in energy consumption of the system.

4.4 Open-loop Model with Internal Controller (OL)

In a typical distillation column where the feed streams are considered to be set by upstream unit, and operating pressure is assumed fixed by heat removal from the condenser, the inventories that must be controlled are essentially the liquid level in the reflux drum and the base of the column. The investigation on the open-loop dynamics in the previous section has revealed the impact of stoichiometric imbalance of the reactants entering the column. Thus, the inclusion of internal composition inventory control is necessary to improve the system dynamics.

In this study, the concentration of reactant A on the first tray of reactive section is controlled by manipulating the fresh feed of component A using a Proportional-only controller. The P-only composition controller is used not necessarily to keep the internal composition of reactant A at constant value but to manipulate the fresh feed flowrate of reactant A to balance the feeds stoichiometry. The effect of disturbance in feed flowrate of reactant B, feed composition, vapor boilup and reflux rate have been investigated in this Section but only the results for changes in feed flowrate of reactant B and vapor boilup are shown.

4.4.1 Feed Flowrates

The responses of the system to different magnitudes of disturbances in feed F_B are shown in Figure 4.9. The system is found to be open-loop stable when the flowrate of reactant B is increased or decreased. By comparing the results shown in Figure 4.9 to those shown in Figure 4.1, the clear improvement in the system dynamics is the result of including the internal composition controller which enforces the stoichiometric balance in the reactive zone. Similar results are obtained when disturbance in feed composition is introduced.

Figure 4.10 summaries the steady state composition distributions in the column with different magnitudes of disturbance in feed flowrate of reactant B when the internal composition controller is included. As more of B is fed into the column, the internal composition of the reactant A is decreased and the controller responds appropriately by increasing F_A to balance the increase in F_B. The same argument is valid when F_B is reduced as well. Note that the system responses take a longer time to reach steady state when F_B is reduced as compare to when it is increased with equal magnitude. This indicates how the performance of any control structure on reactive distillation is dependent on the magnitude and direction of the disturbance.

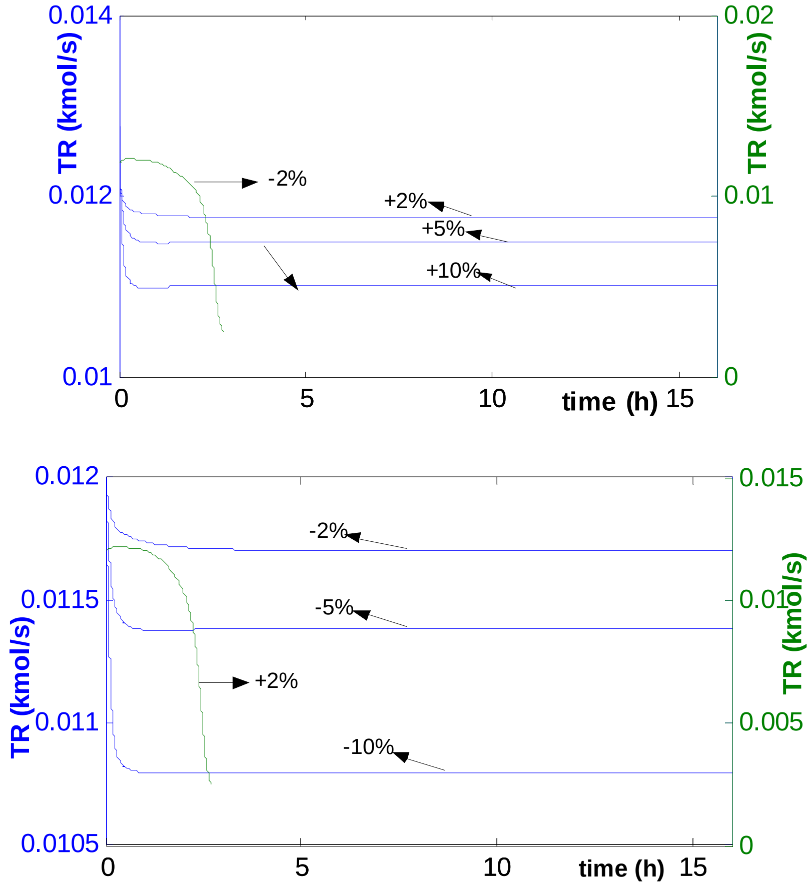

Figure 4.8 Dynamic responses of total reaction rate (TR) of products in reactive zone (a) step changes in vapor boilup. (b) step changes in reflux rate.

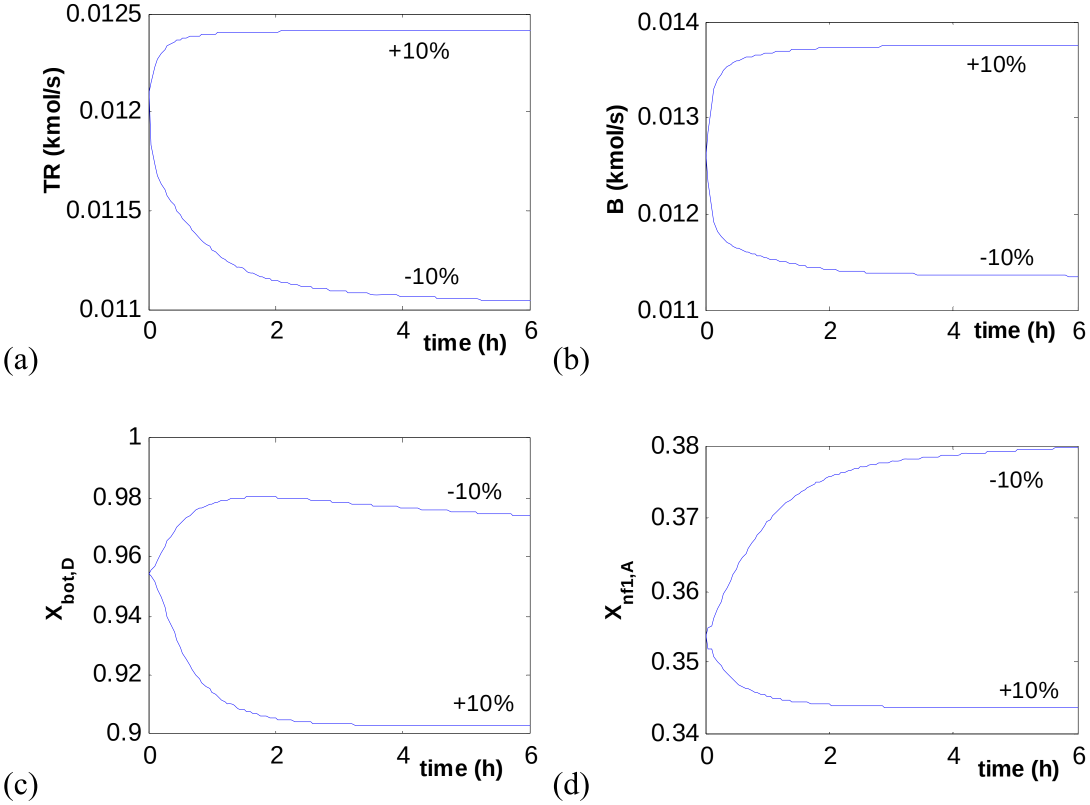

Figure 4.9 Responses of the system in presence of an internal composition controller to ±10% change in feed F_B. (a) total reaction rate; (b) bottoms flowrate; (c) composition of product D in the bottoms; (d) internal composition of reactant A in tray nf1.

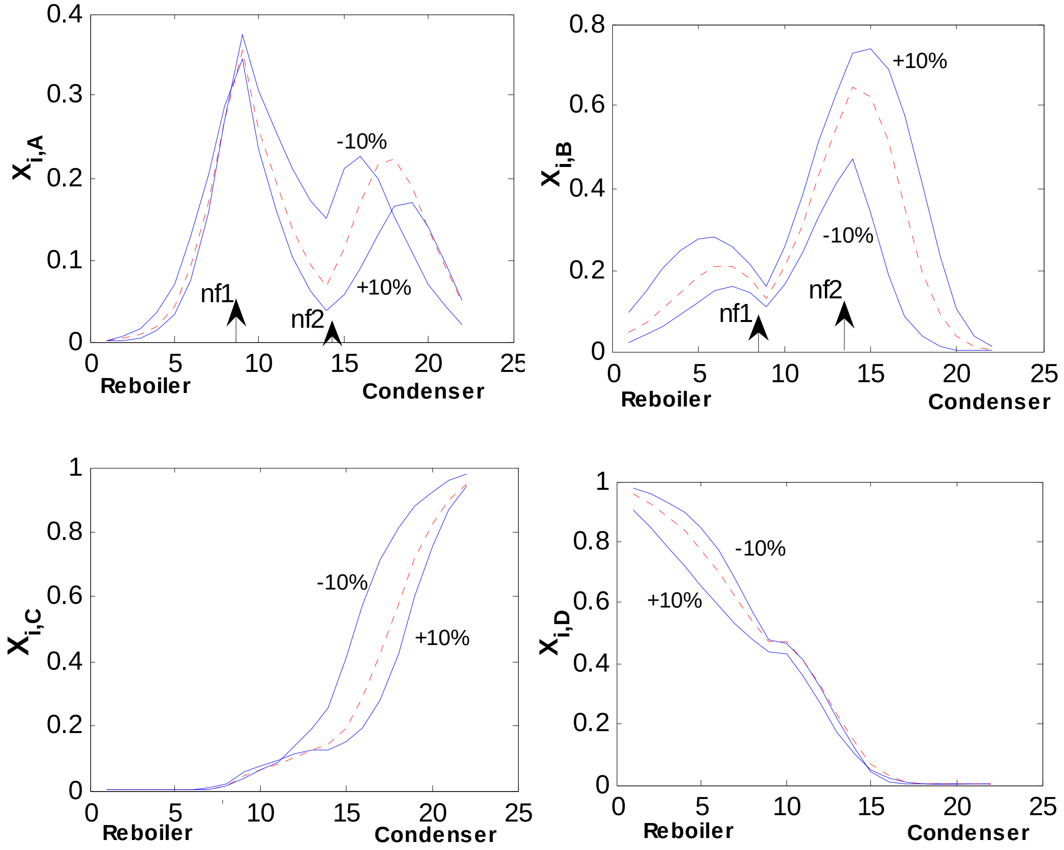

Figure 4.10 Steady state profiles of composition of A, B, C and B with change in F_B in presence of internal composition controller.

4.4.2 Vapor Boilup

Figure 4.11 shows the responses of the bottoms flowrate the total reaction rate when the vapor boilup is increased up to 10% and when decreased by 2%. Similar to OL scenario, the results show that the inclusion of internal composition inventory is insufficient to handle the decrease in vapor boilup below its optimum condition. The inclusion of internal composition controller does not address the problem of disturbing the separation capacity of the column when either the vapor boilup or reflux rate is changed. Therefore, it is expected that this scenario would be similar to the OL scenario for this class of disturbances.

In general, comparing the open-loop model with and without internal composition controller shows that disturbances in feed streams are better handled in presence of internal composition inventory controller because the controller acts to maintain the feeds stoichiometry. In addition, the settling time is generally far shorter when internal composition controller is included as compared to that without it.

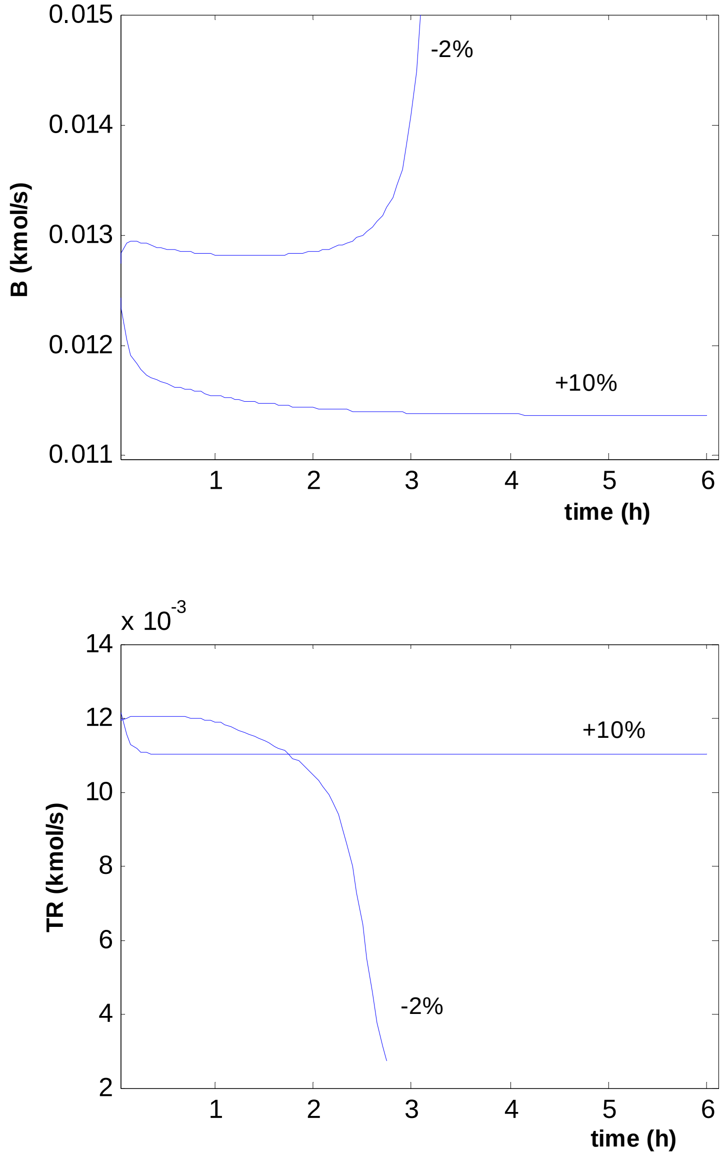

Figure 4.11 Response bottoms flowrate (B) the total reaction rate (TR) to different magnitudes change in vapor boilup in presence of an internal composition controller.

4.5 Single-end Control (CL)

The introduction of internal composition inventory controller improves the performance of open-loop reactive distillation system under disturbances in feed flowrate and composition in both directions. However, controlling the internal composition alone is shown in the earlier section to be inadequate to sustain the system stability whenever there is decrease in vapor boilup or increase in reflux rate. Steady state rating analysis [5] suggests that a simple single-end control structure could be developed for the system because keeping the reflux ratio of the system and not reflux rate constant enhance a better performance [6]. The composition of C in the distillate is controlled at 95% by manipulating the reflux rate. With the inclusion of this control loop, we are able to increase or decrease the vapor boilup to study its impact on both system stability and dynamic behavior.

Figure 4.12 shows the responses of the system when the vapor boilup is changed by ±10%. In this scenario, the system dynamics is improved to tolerate changes in vapor boilup as the overhead controller will adjust the reflux rate to maintain the required separation capacity. Changing the vapor boilup in either direction changes both the reflux and distillate flowrate in order to maintain the required separation capacity (i.e. maintaining the same reflux ratio). It is interesting to note that the total reaction rate does not change significantly from its base steady values of 0.01210 kmol/s when the vapor boilup is increased by 10%. (i.e., from 0.01210 kmol/s to 0.01211 kmol/s, which is about 0.08% increase in total reaction rate). On the other hand, decreasing the vapor boilup by the same magnitude of 10%, leads to a significant reduction in total reaction rate from 0.0121 kmol/s to 0.0112 kmol/s (i.e. 7.5% decrease in total reaction rate). This clearly demonstrates that a negative change in vapor boilup has more impact on the system behavior and influence the performance of the controller more than a positive change in vapor boilup. Examining closely the response of the product compositions, it can be easily noticed that the controller response is slower and has a longer settling time with a negative change than a positive change in vapor boilup. The impurity in the bottoms product is very significant with a negative change in vapor boilup due to the presence of more unreacted component B.

In general, the presence of single-end controller makes the system generally stable, but the effect of the disturbance magnitudes and directions as demonstrated in this work has a significant influence on the performance of the controller. Therefore this factor must be recognized and be considered in the designs and implementation of closed-loop reactive distillation system.

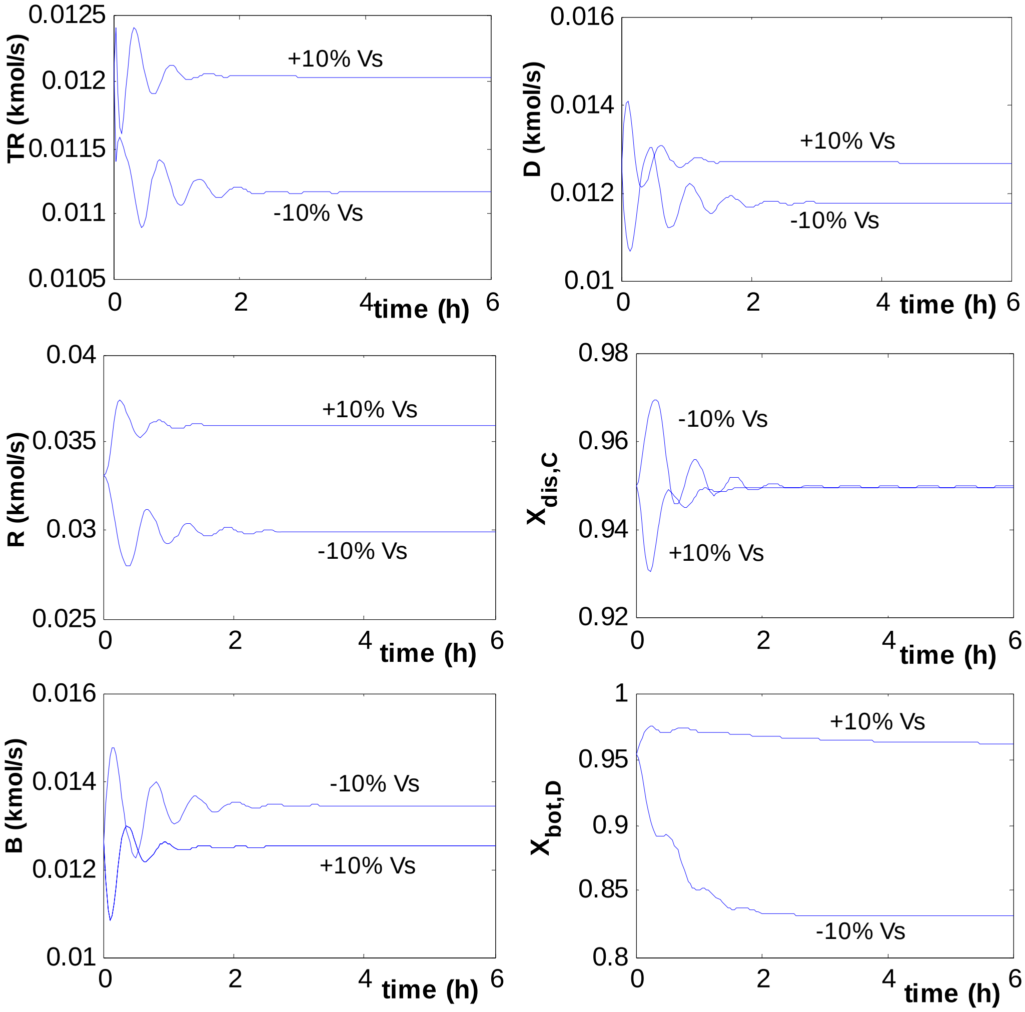

Figure 4.12 The responses of the system with single-end composition controller when step changes are made in the vapor boilup (V_S).

Table 4.1 Effect of disturbance magnitudes and directions on the system stability

Input	**Direction**	**OL**	**OL+IC**	**CL**
F_A	+	Trigger the system sharply to another steady state	N/A	N/A
	-	Stable		
F_B	+	Stable	Stable	Stable
	-	OL-I: trigger the system to another state with small disturbance and unstable with high disturbance, OL-II: stable	Stable	Stable
Vs	+	Stable	Stable	Stable
	-	OL-I: Unstable, OL-II: stable	Unstable	Stable
R	+	OL-I: Unstable, OL-II: stable	Unstable	Stable
	-	Stable	Stable	
Change in Z_b		OL-I: Trigger the system sharply to another steady state and unstable at high disturbance , OL-II: Stable	Stable	Stable
Change in Z_a		Stable	Stable	Stable

Note: OL = Open-loop
OL+IC = Open-loop with Internal Controller
CL = Closed-loop
N/A = Not a disturbance variable in this scenario

4.6 Conclusion

The effects of disturbance magnitudes and directions on the dynamic behavior of a high-purity\high-conversion reactive distillation have been investigated. Table 4.1 summarizes the dynamic responses of the system under the three scenarios and for the various disturbances that are investigated. This study demonstrates that open-loop reactive distillation system gives a better performance when operated with fixing reflux ratio instead of reflux rate. Excess of less volatile reactant in two-reactant-two-product generic reactive distillation has been found to enhance open-loop stability, but decreases the products purity. On the other hand, excess of more volatile reactant triggers the system to another steady state. Change in the manipulated variables (i.e. vapor boilup and reflux rate) in some directions in open-loop system is intolerable due to their effect on both the reaction kinetics and fractionation capacity of the column.

The performance of the open-loop system is improved significantly with the inclusion of an internal composition inventory control to balance the reactants feed stoichiometry. However, this has been shown to be insufficient when there is a change in either vapor boilup or reflux flowrate in certain directions due to the disturbance this makes to the separation capacity of the system. A single-end control along with internal composition controller is found to be the minimum required to ensure the systems stability.

4.7 Reference

[1] A. Higler, R. Krishna, and R. Taylor, "A non-equilibrium cell model for packed distillation columns," *Industrial and Engineering Chemistry Research*, vol. 38, pp. 3988-3999, 1999.

[2] M. G. Sneesby, M. O. Tade, R. Datta, and T. N. Smith, "Detrimental influence of excessive fractionation on reactive distillation," *AIChE J.*, vol. 44, pp. 388-393, 1998.

[3] R. Jacobs and R. Krishna, "Multiple solutions in reactive distillation for methyl tert-butyl ether synthesis," *Ind. Eng. Chem. Res.*, vol. 32, pp. 1706-1709, 1993.

[4] S. Skogestad and M. Morari, "Effect of disturbance directions on closed-loop performance," *Compt. & Chem. Eng.*, vol. 11, pp. 607-617, 1987.

[5] W. L. Luyben, "Steady state energy conservation aspects of distillation column control systems design," *Ind. Eng. Chem. Res*, vol. 14, pp.,321-325, 1975.

[6] M. J. Olanrewaju and M. A. Al-Arfaj, "Dynamic investigation of the high purity/ high conversion reactive distillation," 15th European Symposium on Computer Aided Process, Barcelona 2005, Accepted.

CHAPTER 5

5 Performance Assessment of Different Control Structure for Generic Reactive Distillation Using Linear and Nonlinear Process Models

5.1 Introduction

The main goal of process control is the design and implementation of effective control systems that will maintain the process conditions close to its desired steady-state value. Even though a reactive distillation system is inherently nonlinear, the essence of effective regulatory control is to ensure that deviations from base the steady state will be small, in which case the behavior will be essentially indistinguishable from that of a linear system. It is in this sense that the linear model-based controls could be applicable.

The present availability of computer software and hardware, which has made it possible to utilize a rigorous dynamic model in process control, will tend to pose a question as to why do we need an approximate linear model? The use of a linear model can enhance our understanding on the process observability and controllability. Without proper understanding, it is almost impossible to design a good control structure. The use of a linear model significantly reduces the speed of computation, which becomes very critical when a plant model, for instance, is needed for online control. Simple models are desirable in computer-based control for optimization and advanced regulatory control application, where online implementation limits the use of complex models. For proper control of reactive distillation, an internal composition needs to be obtained [1-3].

Most of the established estimation techniques (i.e., Kalman filter and Luenberger observer) that could be applied to obtain the internal composition use a linear model. Therefore, the use of a linear model in model-based control is needed and will significantly reduce the complexity involved in the design and implementation stages as compared to when a rigorous nonlinear model is used. Even nonlinear estimators such as an extended Kalman filter and an extended Luenberger observer use a linear model approximation in their design procedure. [4, 5]

The present work compares the performance of different control structures when implemented on a linearized process model to that when they are implemented on a nonlinear model for a generic reactive distillation. The idea is to investigate how good of a control can be achieved if a control structure is designed based on an approximate process model. This is an important assessment step before using the linearized model in model-based control applications. In this work, three control structures are implemented to assess the closed-loop performance of a linear process model compared to that of a rigorous nonlinear model. The control structures are dual-end composition control, single-end composition control and inferential composition control using temperature measurement. All of the control structures use a composition analyzer in the reactive zone to detect the inventory of one of the reactants so that a fresh feed can be manipulated to balance the feeds stoichiometry.

5.2 The Process

In this chapter, we considered the same reactive distillation system discussed in Chapter 2. An equal stoichiometric amount of fresh feed flowrate of 0.0126 kmol/s is used for both reactants A and B. The conversion and purity are fixed at 95%. The initial holdup in each tray is 1 kmol. The column has seven stripping trays, six reactive trays and seven rectifying trays. The operating pressure is 9 bar.

5.3 Control Structures

The operation of a multivariable process like reactive distillation column has to satisfy several control objectives. Typical objectives are to ensure the stability of the process, to produce specified products, and to optimize the operation economically. Because the various objectives may be of quite different importance and normally require different control actions, it is usually desirable to explore a wide variety of control structures in order to meet different objectives.

Three control structures are explored to compare and assess the closed-loop performance of a linearized model with that of a nonlinear model. All structures are single-input-single-output (SISO) structures with PI controllers except in level controls where P-only controllers are used. For each controller, a relay feedback test [6] is employed to obtain the ultimate gain and frequency. The controllers are tuned using the Tyreus-Luyben tuning method [7]. The design of inventory controllers is carried out first. The pressure is controlled by heat removal from the condenser. The assignment of manipulated variables for level controllers is based on the principle of choosing the stream with the most direct impact [8]. The base level is controlled by manipulating the bottoms flowrate, while the reflux drum level could either be controlled by manipulating either the distillate flowrate or the reflux flowrate. All of the valves are designed to be half open at the initial steady state. Two measurement lags of 30 s each are used in all composition or temperature loops.

All of the three control structures considered use a composition analyzer in the reactive zone as proposed by Al-Arfaj and Luyben[1] to detect the inventory of one of the reactants so that fresh feed can be manipulated to maitain the feeds stoichiometry. The concentration of reactant A on the first tray of the reactive zone (numbered from the bottoms) is controlled by manipulating the reactant A fresh feed flowrate. Three types of disturbances are investigated as follows:

1. Change in feed flowrate of component B (F_B): in this disturbance, F_B is increased by 10% and 20% and decreased by 20%. This disturbance is applied to all of the control structures.
2. Feed composition of reactant B: the reactant B feed is 100% mol of B. This feed composition disturbance will introduce reactant A in the feed composition of reactant B (Z_b). Two magnitudes are used: ΔZ_b= 5% (where the feed of reactant B becomes 95% mol of B and 5% mol of A). ΔZ_b= 10% (where the feed of reactant B becomes 90% mol B and 10% mol A). This disturbance is applied to all control structures.
3. Setpoint changes: in this disturbance, the composition setpoint of the composition controller is changed from 95% mol of D in the bottoms to 92% and 98%. This is applied to the first two control structures (see sections 4.1 and 4.2). For the third control structure (section 4.3), temperature setpoint changes of ± 2 K are tested.

5.3.1 Control Structure I

Figure 5.1 shows a dual-end composition control structure. The reflux drum level is controlled by manipulating the distillate flowrate. The purity of both products is maintained at 95%. In the distillate products, the composition of component C in the

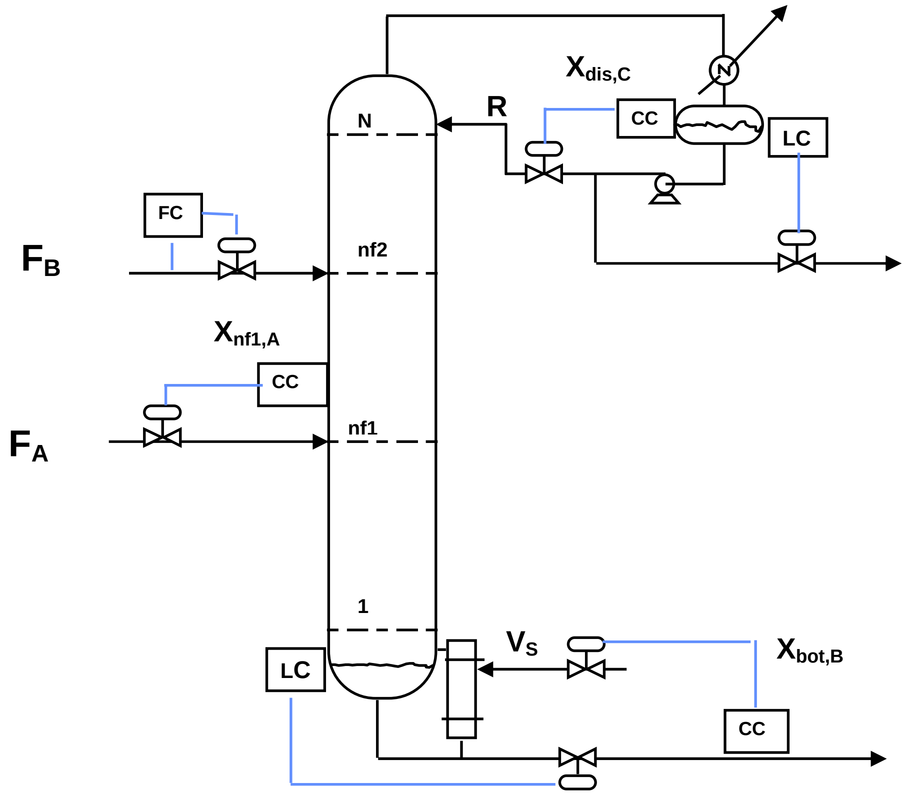

$X_{dis,C}$
R
CC
LC
N
FC
F_B
nf2
$X_{nf1,A}$
CC
F_A
nf1
1
V_S
$X_{bot,B}$
LC
CC

Figure 5.1 Dual-end composition control structure

distillate is controlled by manipulating the reflux flowrate from the condenser, while the bottoms composition of component D is controlled by manipulating the vapor boilup.

Various magnitudes of disturbance in the feed flowrate and feed composition are studied to assess the closed-loop performance of this control structure based on linear and nonlinear models. Figure 5.2 shows the response of the system for -20%, +10% and +20% changes in the feed flowrate of reactant B (F_B). Two curves are shown in each of the plots comparing the closed-loop performance of this control structure when a linear model is used to that when a rigorous nonlinear model is applied. The results show that this control structure is able to reject the load disturbance effectively with the two models. While the responses of controlled variables in both models show an excellent agreement, the responses of manipulated variables in linear model show a slight variation from that of a nonlinear model in an attempt to satisfy the same control objectives. This variation is seen to increase with an increase in the magnitude of the disturbance.

Under open-loop operation where only level inventories are controlled, the process will drift from the base steady state to a lower conversion state when F_B is decreased with small magnitude and will be unstable at higher magnitude of the disturbance [9]. The linearized model will not predict this drift because it is a nonlinear feature of the process. Even though the drift will not take place in the closed-loop scenario because the controllers will adjust the manipulating variables to maintain product purity, the process dynamics during transit region will not be properly described in the linear model. The open-loop stability of the nonlinear model must be investigated before the linearized model is used in model-based control applications. The use of a

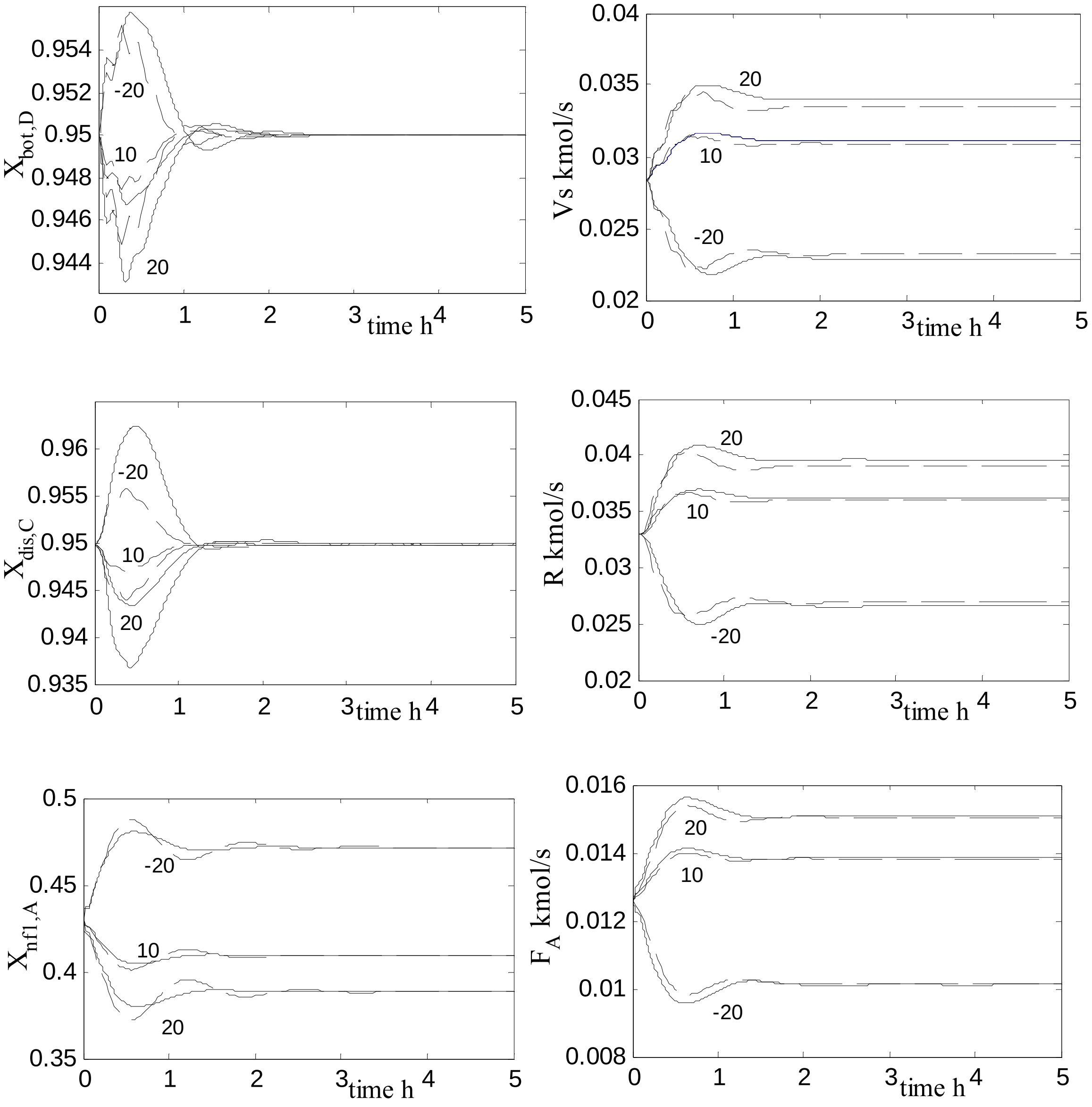

Figure 5.2 Dual-end composition control responses, -20%, +10%, +20% F_B:

(- - -) linear model; (—); nonlinear model.

linear model is inappropriate if the system is open-loop pseudo stable (drifts to another steady-state region) or unstable under disturbance.

Figure 5.3 compares the closed-loop performance of a linear model to that of a nonlinear model when 5% and 10% impurities of A are introduced in the feed composition of F_B. Under open-loop operation, introducing reactant A impurities in the reactant B feed allows the process to drift sharply to another state at lower impurity magnitudes and destabilizes the process completely at higher magnitudes of impurity [9]. Even though the composition controllers are able to meet the control objective of rejecting the feed composition disturbance, the response of a linear model is seen to be slower than that of a nonlinear model, thus making the time to reach the desired steady state longer than that when the controller is designed based on a linear model. The performance of this structure deteriorates with an increase in the magnitude of the disturbance when a linear model is used. Again, this shows the inapplicability of the use of linear models in control system design when the process is open-loop pseudostable or unstable under certain disturbances where the linear process model could not describe the nonlinear process behavior.

Figure 5.4 shows the responses of composition controllers with setpoint changes in the composition of component D in the bottoms product for both closed-loop linear and nonlinear models. The results show that setpoint changes by decreasing the bottoms purity from 95% to 92% or increasing the purity from 95% to 98% can be handled. The composition controllers appear to be effective and robust with both linear and nonlinear models. The results shown in Figures 5.2-5.4 point toward an interesting observation.

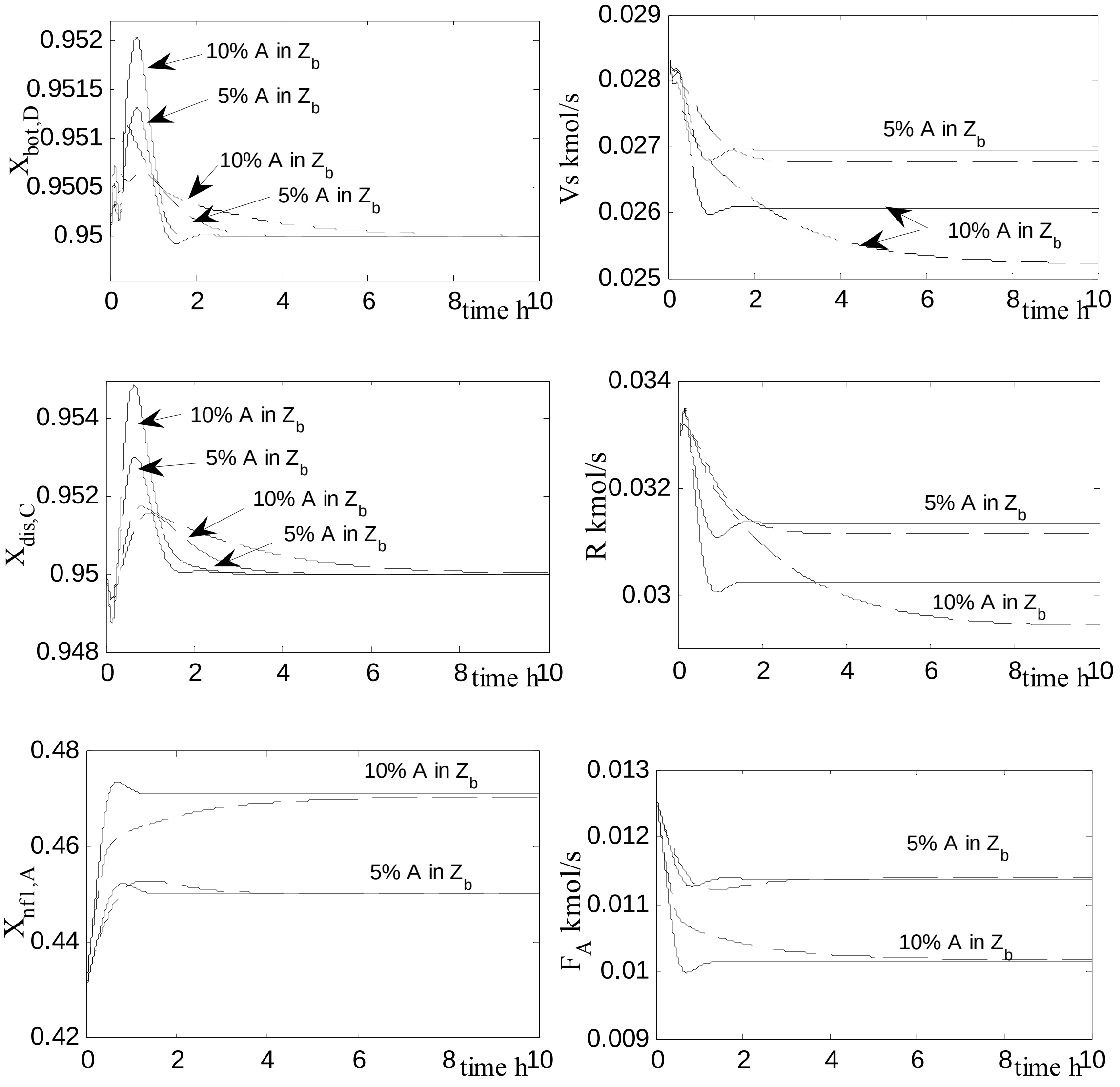

Figure 5.3 Dual-end composition control responses, 5%, 10% mol of reactant A in Z_b:

(- - -) linear model; (—); nonlinear model.

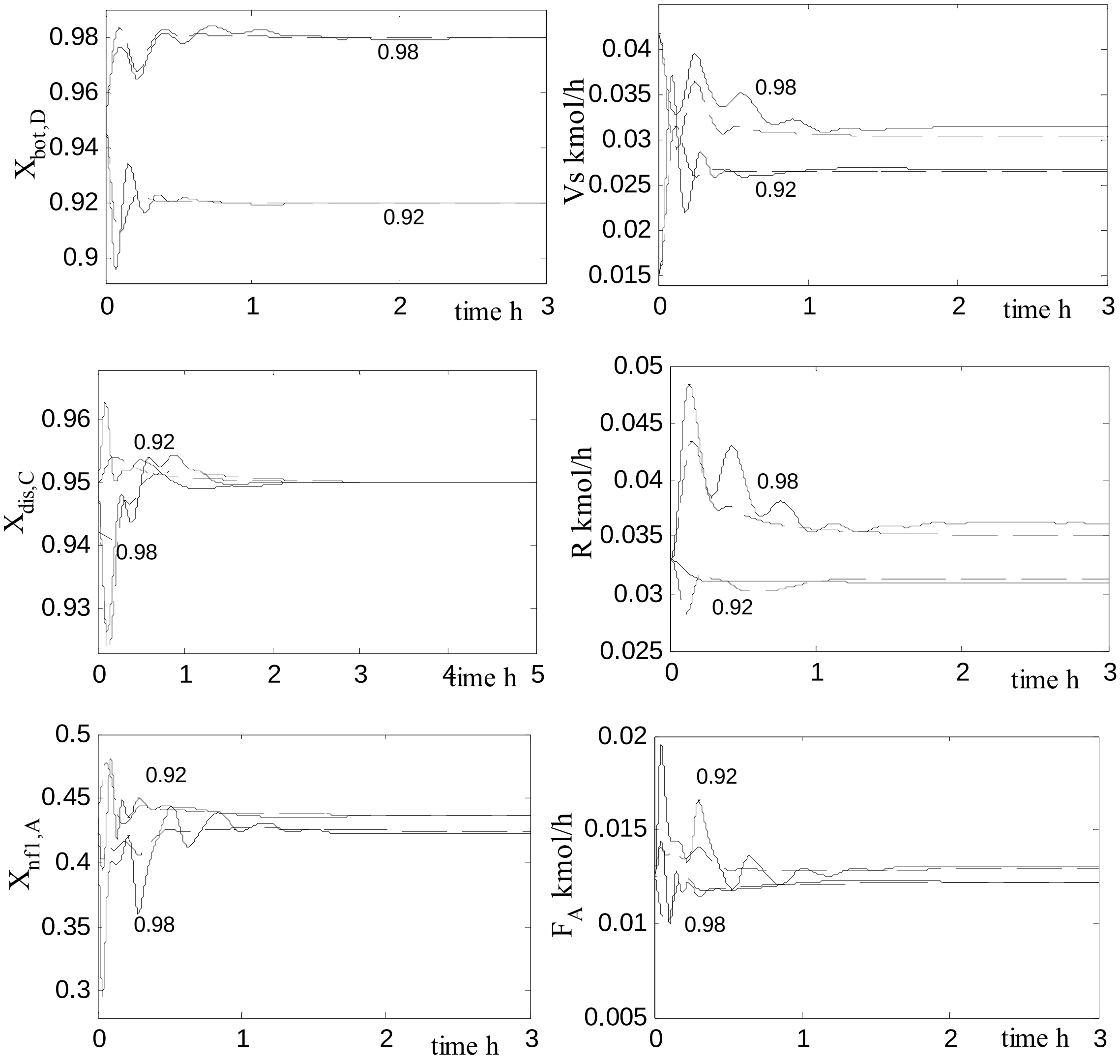

Figure 5.4 Dual-end composition control responses, setpoint changes $X_{bot,B}$ from 95% to 92% and 98%: (- - -) linear model; (—); nonlinear model.

The control system when controllers are designed based on a linear process model can achieve the control objectives but would typically underestimate some or all of the input characteristics (the magnitude, the rate, and the speed of change of manipulated variables) when the process is open-loop pseudo stable or unstable under the influence of disturbance. Even though the controlled variable will eventually settle to the required level, the manipulated variable may differ not only in the transit region but also in the amount required to get the controlled variable to the required level. If the resulting manipulated variables from the two models are comparable, then this underestimation in the input characteristics could be overcome by properly designing the control valves to be more aggressive than what would otherwise be designed based on the closed-loop performance of linear models.

5.3.2 Control Structure II

Although a dual-end composition control structure might have the advantage of energy savings, the additional expenses and the risk associated with designing and operating a more complex control system may not be justified in some systems where a single-end control system is feasible. The single-end composition control loop is a simple SISO system, so it can be easily tuned and give a faster response because of the reduced effect of loop interaction.

To further assess the impact of open-loop stability on the extendibility of control systems designed based on linear models, various control arrangements of the reflux drum level are investigated when the distillate product is not controlled. Three level control schemes are considered as follows:

III. Scheme I: the reflux ratio is fixed, and the reflux drum level is controlled by the reflux flowrate.

IV. Scheme II: the reflux ratio is fixed, and the reflux drum level is controlled by the distillate flowrate.

V. Scheme III: the reflux flowrate is fixed, and the reflux drum level is controlled by the distillate flowrate.

As discussed in section 4.1, a reduction on F_B by 20% destabilizes the system under the open-loop operation when both the reflux flowrate and vapor boilup are kept constant. Scheme 3 is mimicking that open-loop scenario because the reflux flowrate is kept constant, while the other two schemes are not because the reflux flowrate will vary to fix the reflux ratio. Therefore, it is expected that the linear process model will be useful for schemes 1 and 2 but will not be appropriate to use for scheme 3 because the open-loop instability.

Figure 5.5 shows the closed-loop response based on the two process models for the three schemes when a 20% reduction in F_B is introduced. The result in Figure 5.5 indicates that the process performance under schemes 1 and 2 are essentially similar and the control responses of both linear and nonlinear models are close and comparable. Therefore, which of the flowrates is used to control the drum level when the reflux ratio is fixed is not critical. This result also indicates that fixing the reflux ratio is more suitable when single-end control is used because it filters the disturbance impact on the system.

When the reflux flowrate is fixed (Scheme 3) instead of the reflux ratio, a different behavior is observed. Fixing the reflux flowrate will not filter the disturbance impact to the system and thus could destabilize the system if the process is operated at a critical region of stability. Similar to the observation in section 5.3.1 about the impact of open-loop stability on the closed-loop performance based on linear models, it is shown in Figure 5.5 that the response of the linear system when the reflux flowrate is kept constant is not matching the nonlinear response in the transit region. The prediction of the manipulated variable behavior from the linear model completely misses the trajectory suggested by the nonlinear model. The reason for this behavior is the fact that the system drifts to another state at this disturbance and the nonlinear model will calculate the required input to get the product purity to the required level from the new state. Because the linear model cannot predict the drift, the trajectory suggested by the linear model does not take this into consideration, which resulted in this inappropriate prediction of the transit behavior. In such a case, we cannot use the linear model as a basis for developing the control system of the process. On the other hand, when the change in F_B is made in the positive direction, the system is open-loop stable even with the fixed reflux flowrate configuration, and consequently it is expected that the performance based on the linear model will be similar to that based on the nonlinear model. A comparison of the performance based on the two models for this disturbance is shown in Figure 5.6, which is in line with our expectations.

The scheme 1 configuration is considered in detail to compare the closed-loop performance based on a linear model to that based on a nonlinear model for the single-end composition control structure. Figure 5.7 shows the single-end composition control structure based on the scheme 1 configuration. The composition of component D in the bottoms product is controlled by adjusting the vapor boilup. Figure 5.8 shows the performance of this control structure when F_B is increased by 10% and 20% and reduced by 20%. The responses from both controlled and manipulated variables when an approximate linear model is used are in agreement with those when a rigorous nonlinear model is used. The results demonstrated that changes in throughput can be handled using a linear model. The response of the distillate product composition of component C exhibits some variation from that of a nonlinear model because it is not controlled, and this difference increases greatly with an increase in the disturbance magnitudes. This is expected because the two models are not identical.

Figure 5.9 shows that a single-end composition control structure could also provide an effective regulatory control of the process when impurities of A are introduced in the feed composition of the reactant B stream. The linear process model demonstrates a better performance in feed composition disturbance rejection in a single-end composition control structure than in the dual-end control (compare the results shown in Figure 5.9 to those shown in Figure 5.3). Figure 5.10 compares the closed-loop performance of the linear and nonlinear models based on changes in the setpoint of the bottoms purity specification. The results demonstrate that a very high purity of the bottoms product could be achieved with a single-end controller by changing the setpoint from 95% to 98%.

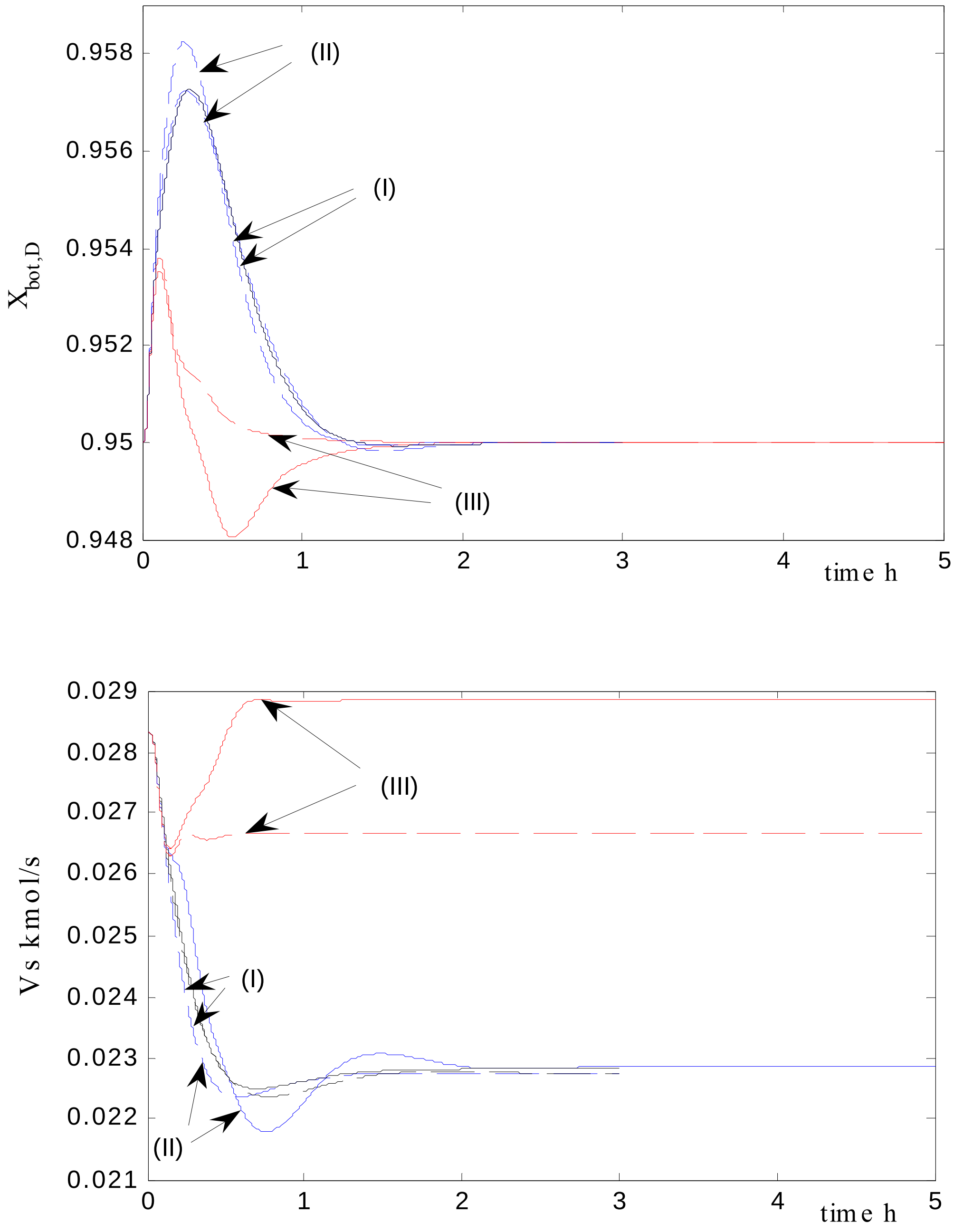

Figure 5.5 Three alternative control schemes for single-end control structure: (I) fixed reflux ratio and control level by the reflux flowrate; (II) fixed reflux ratio and control level by the distillate flowrate (D); (III) fixed reflux flowrate and control level by the distillate flowrate.

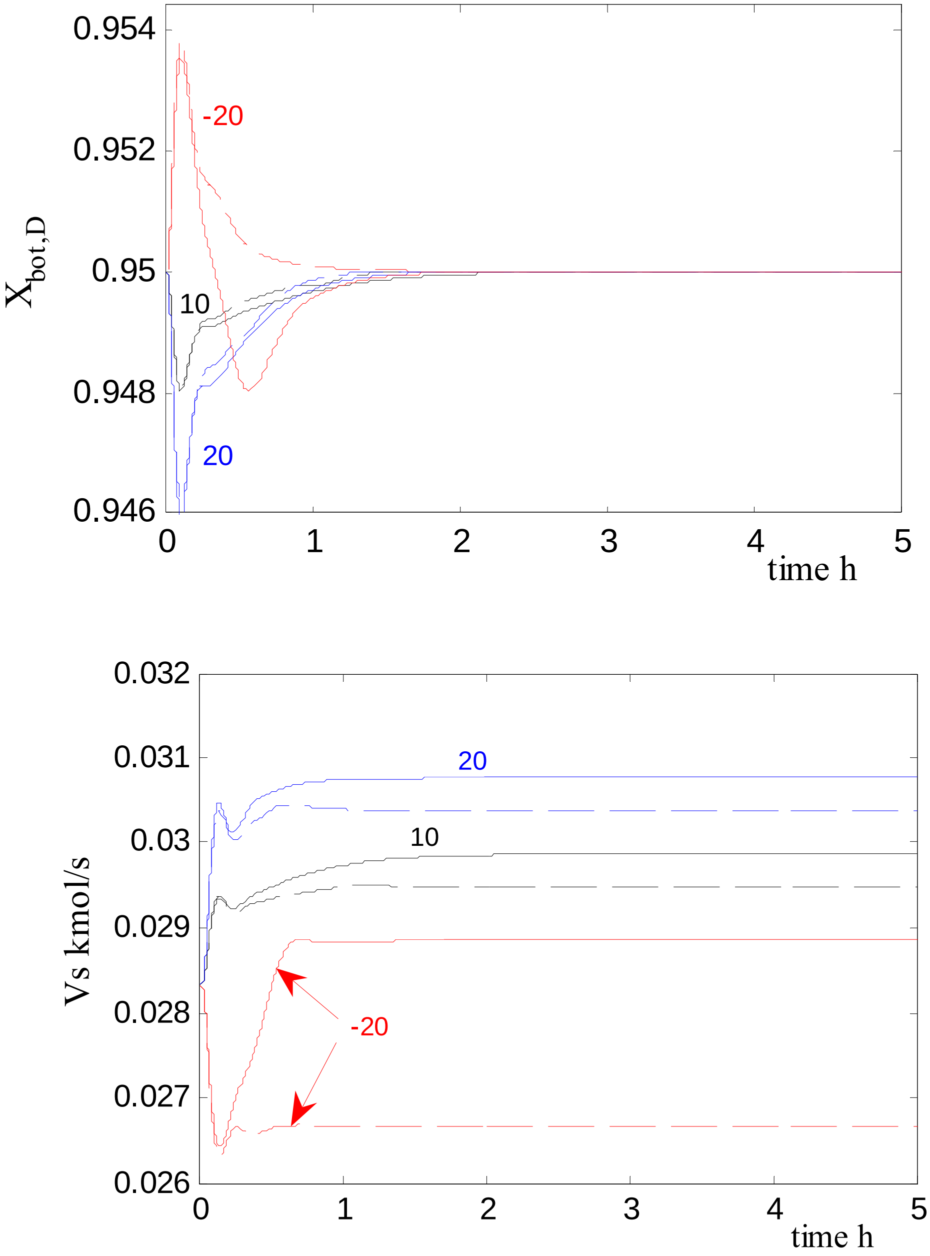

Figure 5.6 Single-end composition control responses base on Scheme 3 with -20%, +10% and +20% disturbances in F_B: (---) linear model; (—) nonlinear model.

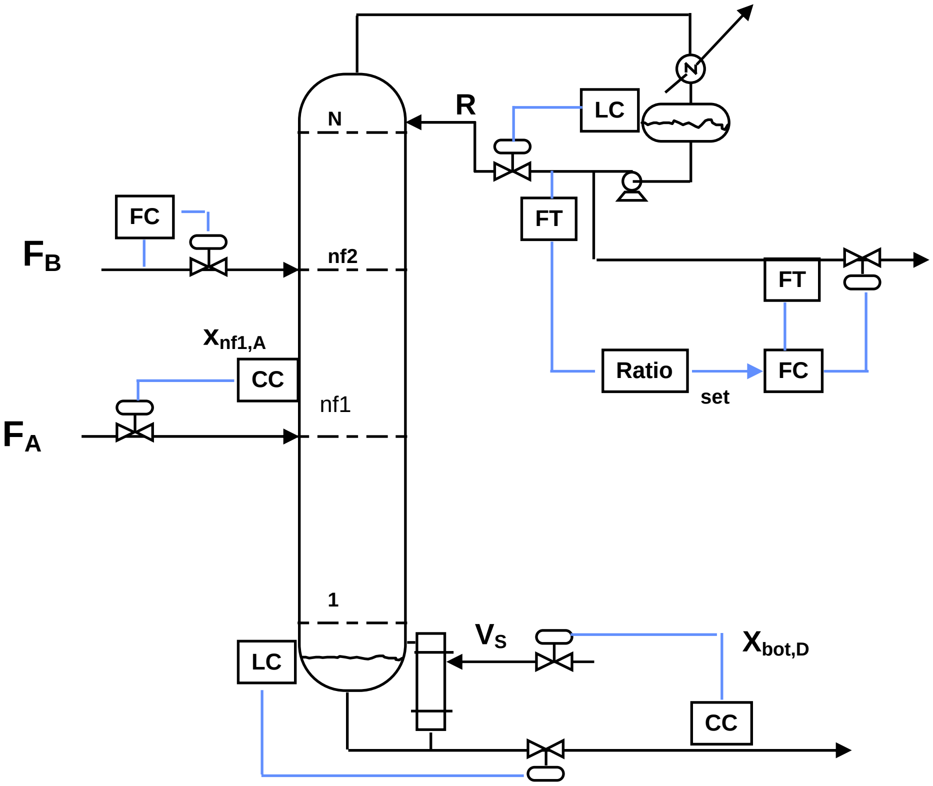

N
R
LC
FC
FT
F_B
nf2
FT
$X_{nf1,A}$
CC
Ratio
FC
set
nf1
F_A
1
V_S
$X_{bot,D}$
LC
CC

Figure 5.7 Single-end composition control structure.

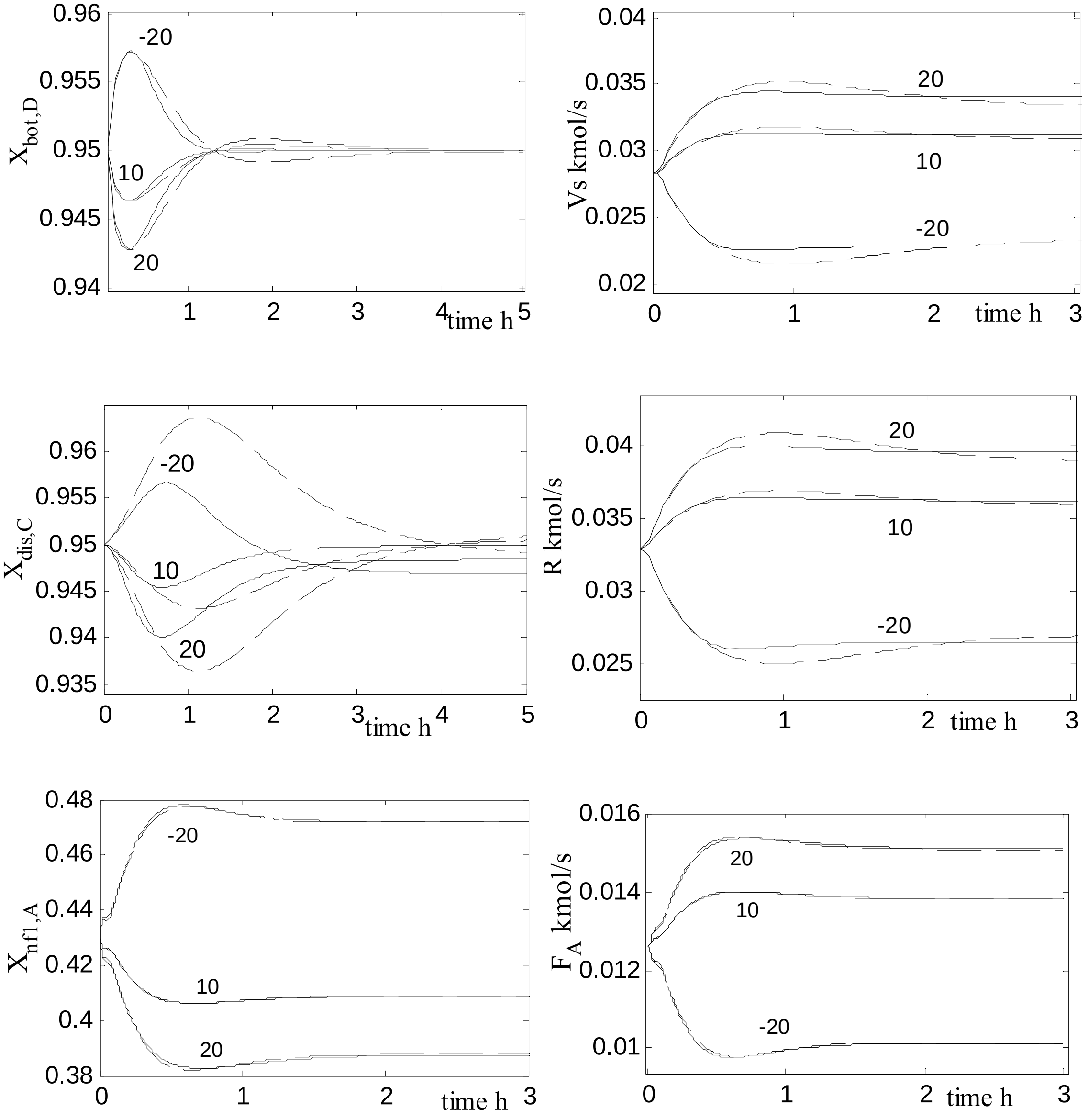

Figure 5.8 Single-end composition control responses: -20%, +10%, +20% F_B.

(---) linear model; (—) nonlinear model.

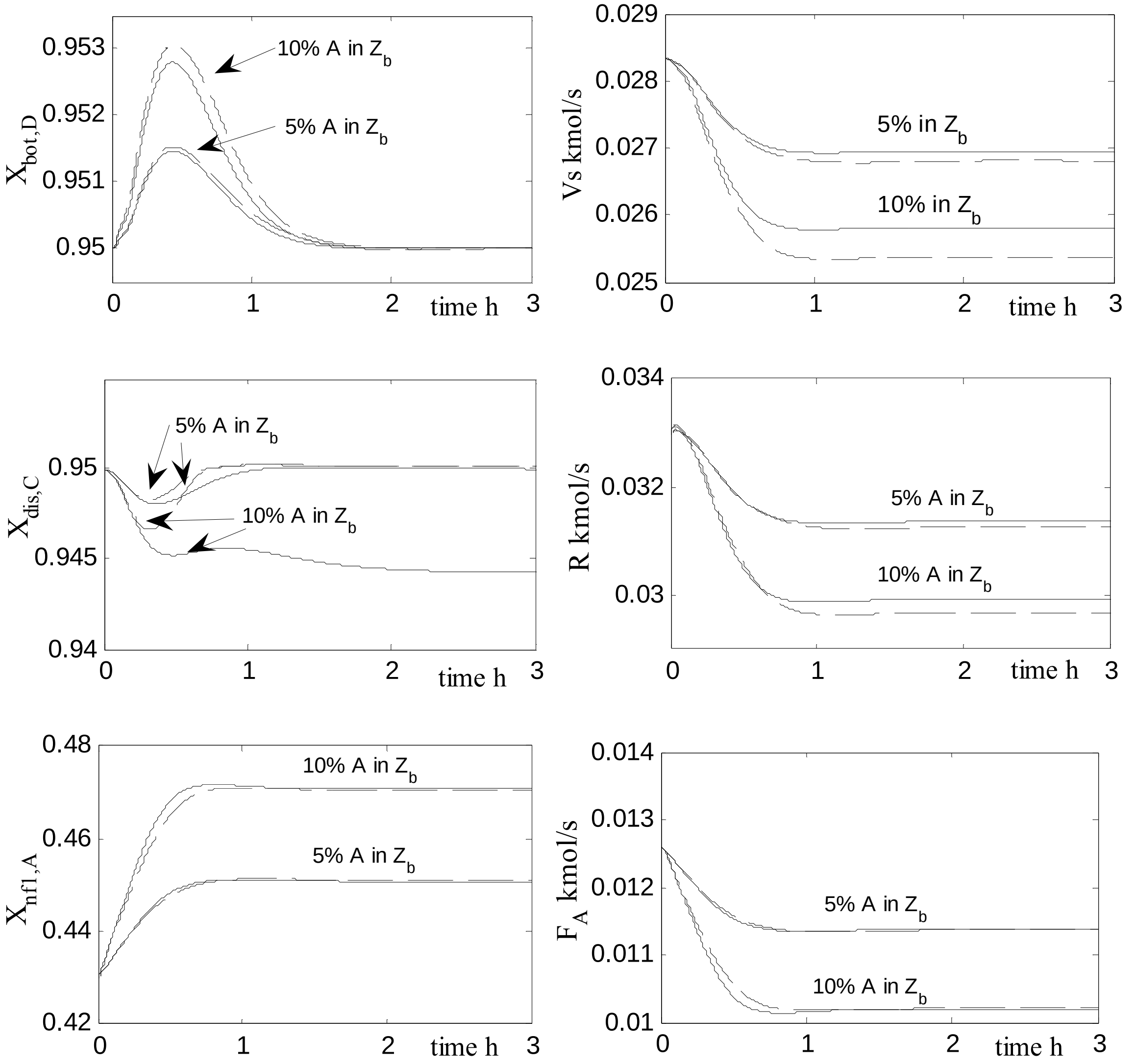

Figure 5.9 Single-end composition control responses, 5%, 10% mol of A in Z_b:

(- - -) linear model; (—); nonlinear model.

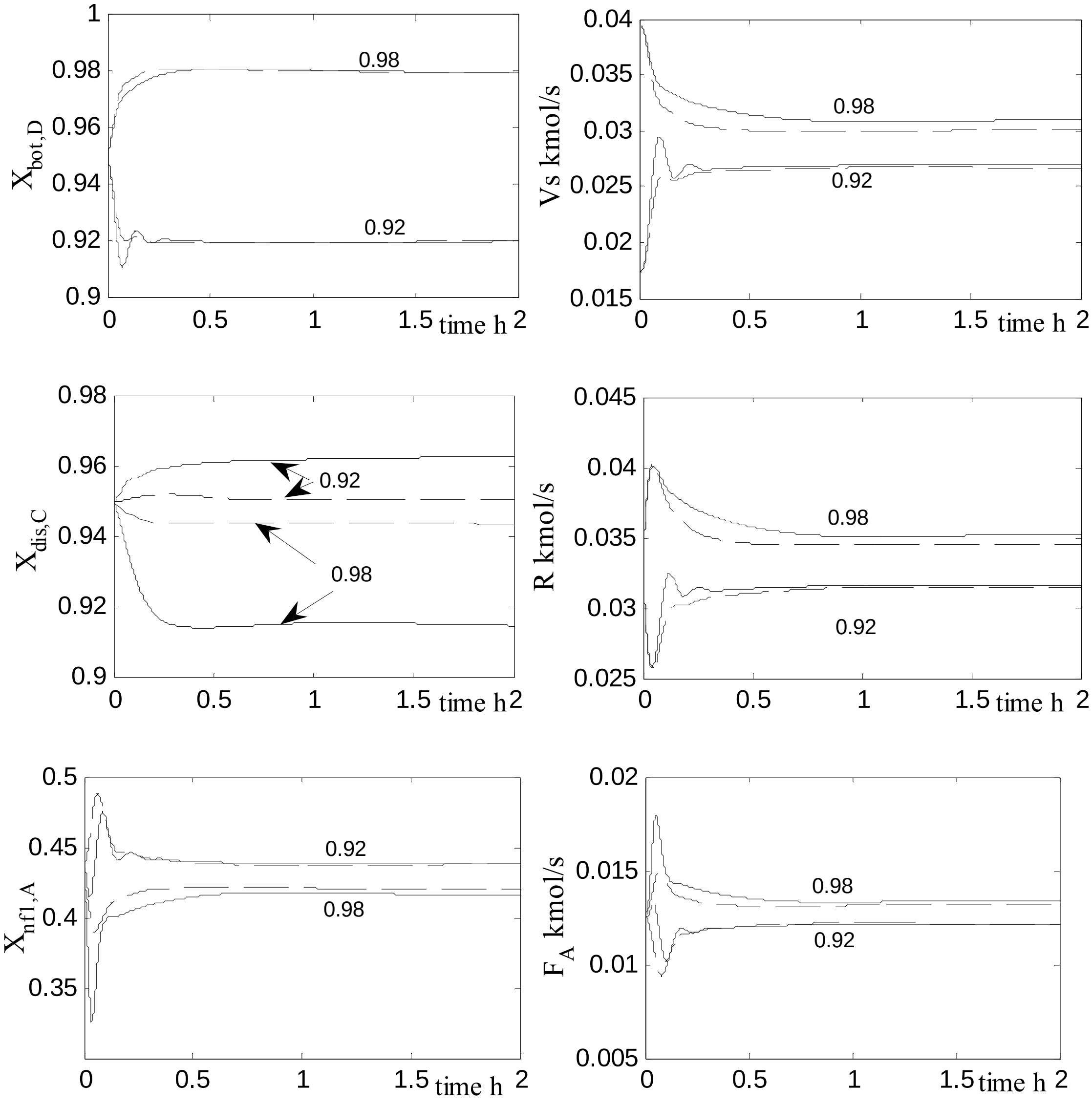

Figure 5.10 Single-end composition control responses, setpoint changes $X_{bot,\,B}$ from 95% to 92% and 98%: (- - -) linear model; (—); nonlinear model.

5.3.3 Control Structure III

Because the direct composition control structures discussed in the above Sections inevitably require the use of an expensive and unreliable composition analyzer, it is important to study how the linear model will behave when a simple temperature control system is used. The temperature sensor is typically fast, inexpensive and reliable. It could provide an indirect measurement of composition. Figure 5.11 shows a single-end temperature control structure. The reflux drum level is controlled by adjusting the reflux flowrate, while the reflux ratio is kept constant by changing the distillate flowrate. Because the control objective of this structure is to maintain the product composition as close as possible to its desired specification, the temperature measurement is placed on the most sensitive tray in the stripping section. The temperature on tray 2 (numbering from the bottoms) is measured and controlled by manipulating the vapor boilup.

Figure 5.12 compares the closed-loop performance of this control scheme using a linear model to that using a rigorous nonlinear model with different magnitudes of disturbance in the feed flowrate of reactant B. The results demonstrate that the temperature control performs well by keeping the purity of the bottoms product as close as possible to the desired value. The system responses under this control structure to feed composition disturbances are shown in Figure 5.13. Even though the bottoms purity is not maintained exactly at the desired level, this control structure is able to reject feed composition disturbances by keeping the bottoms purity within reasonable bounds using a linear process model. Note that there is a significant difference between the responses of linear and nonlinear process models for component C in the distillate product because it is not controlled. This signifies that the use of a linear model in a single-end control structure could be restricted to a chemical system where the purity of one component is desirable. Alternatively, the process could be designed with higher uncontrolled product purity to compensate for any inferior control performance.

The dynamic responses of the two models for ±2 K step changes in the temperature are shown in Figure 5.14. These results demonstrate that the temperature setpoint changes can be easily handled and the system responses of a linear model are comparable to those of a nonlinear model. An increase in the temperature causes the controller to increase the vapor boilup, and more heat is available to overpurify the bottoms product. The distillate purity changes in the opposite direction as expected. On the other hand, a decrease in the temperature results in a decrease in the amount of vapor boilup. The effects are an increase in impurity in the bottoms and overpurification of the distillate product.

All of the responses of a linear model using this structure show a good agreement when compared to the responses of a nonlinear model under the same control structure. The exception is in the distillate purity, where the difference in the responses of the two models becomes increasingly significant with an increase in the disturbance magnitude because that purity is not controlled.

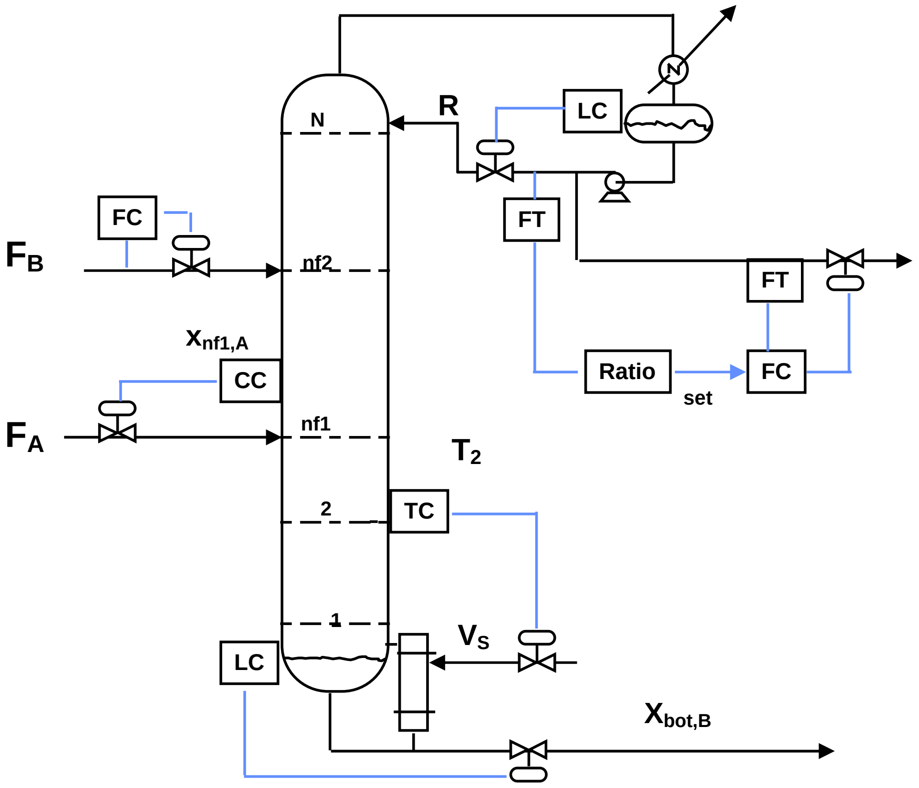
N
R
LC
FC
FT
F_B
nf2
FT
$X_{nf1,A}$
CC
Ratio
FC
set
F_A
nf1
T_2
2
TC
1
V_S
LC
$X_{bot,B}$

Figure 5.11 Single-end temperature control structure.

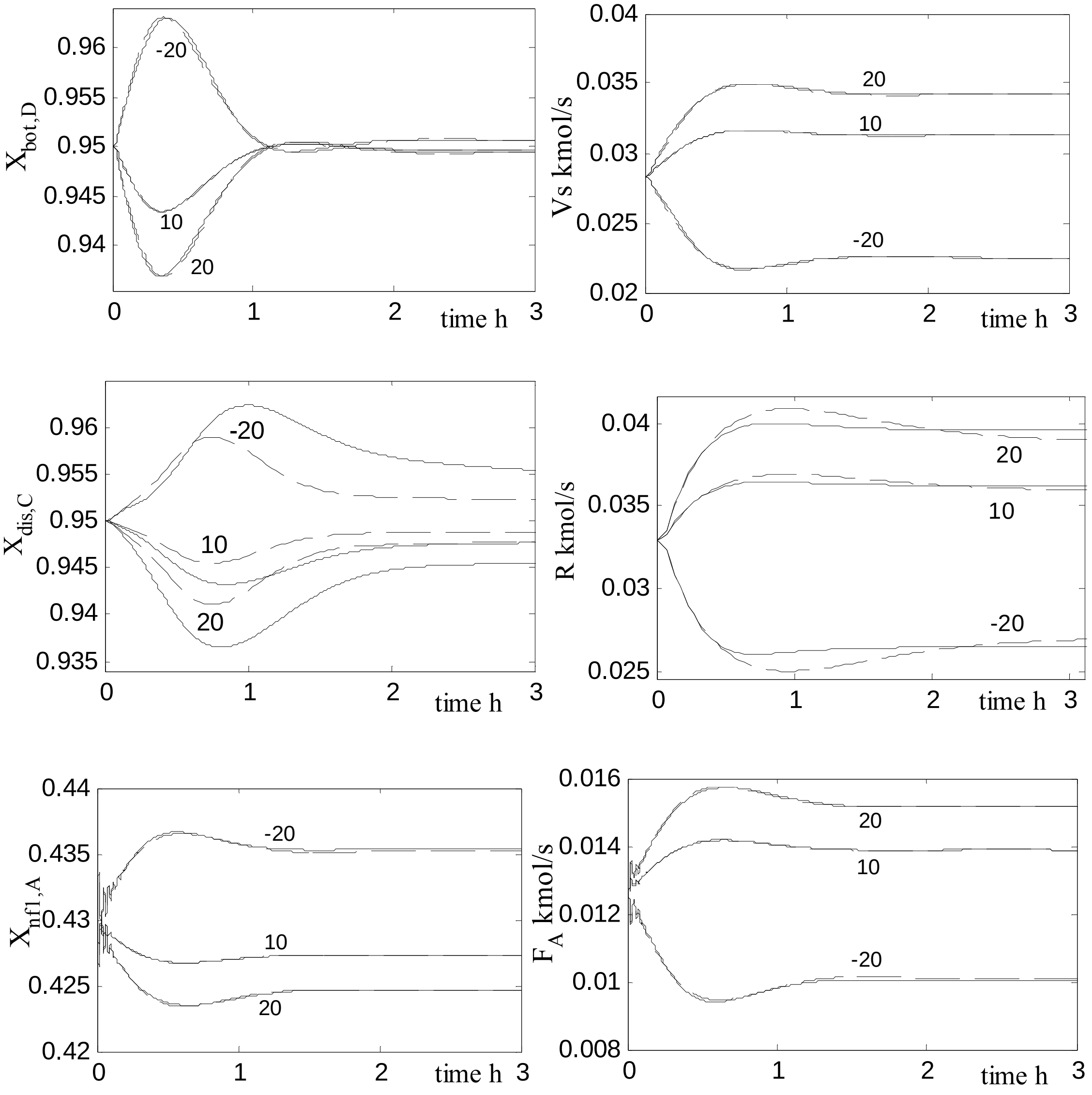

Figure 5.12 Single-end temperature control responses, -20%, +10%, +20% F_B:

(- - -) linear model; (—); nonlinear model.

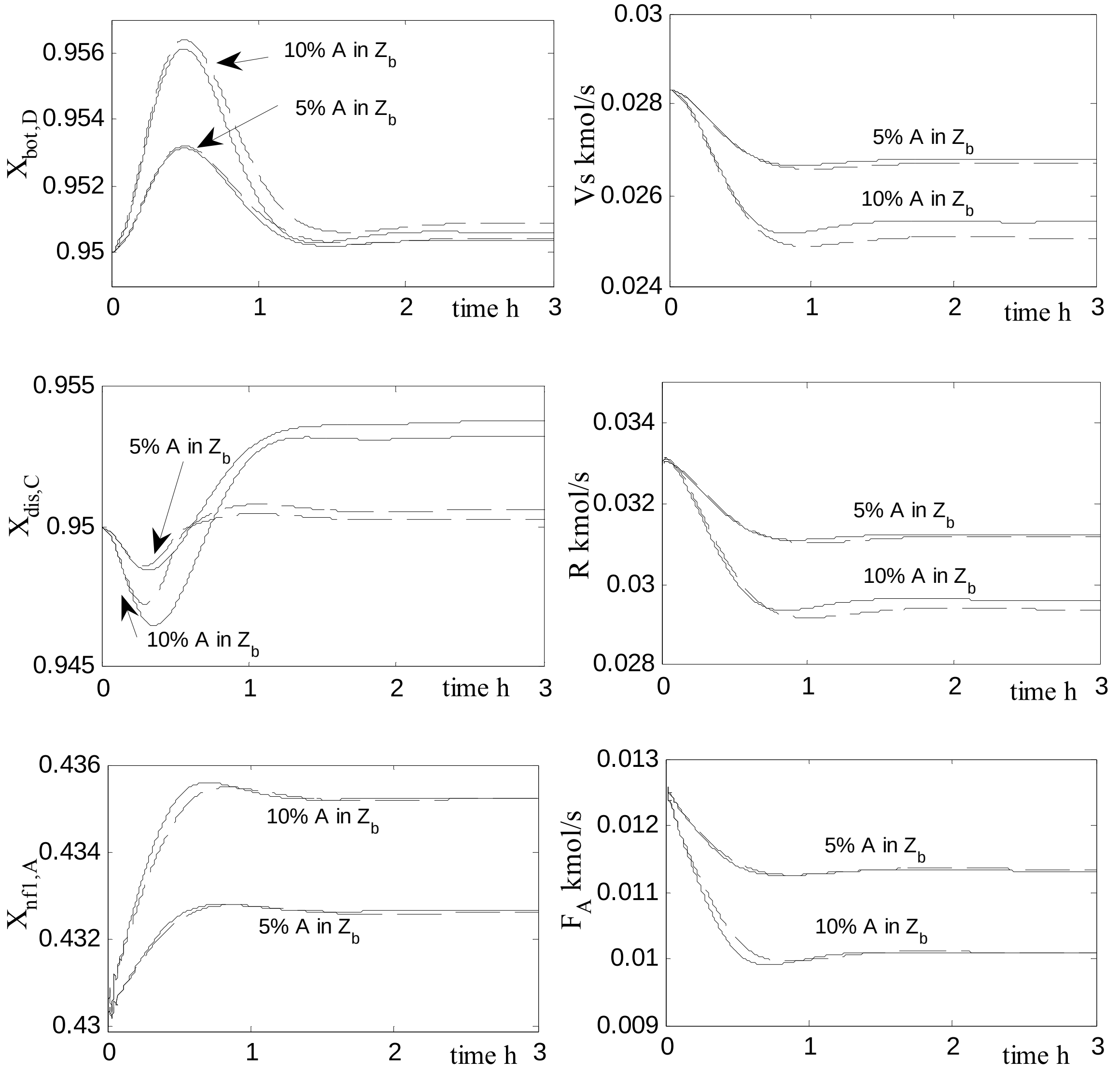

Figure 5.13 Single-end temperature control responses, 5%, 10% mol of reactant A in Z_b:

(- - -) linear model; (—); nonlinear model.

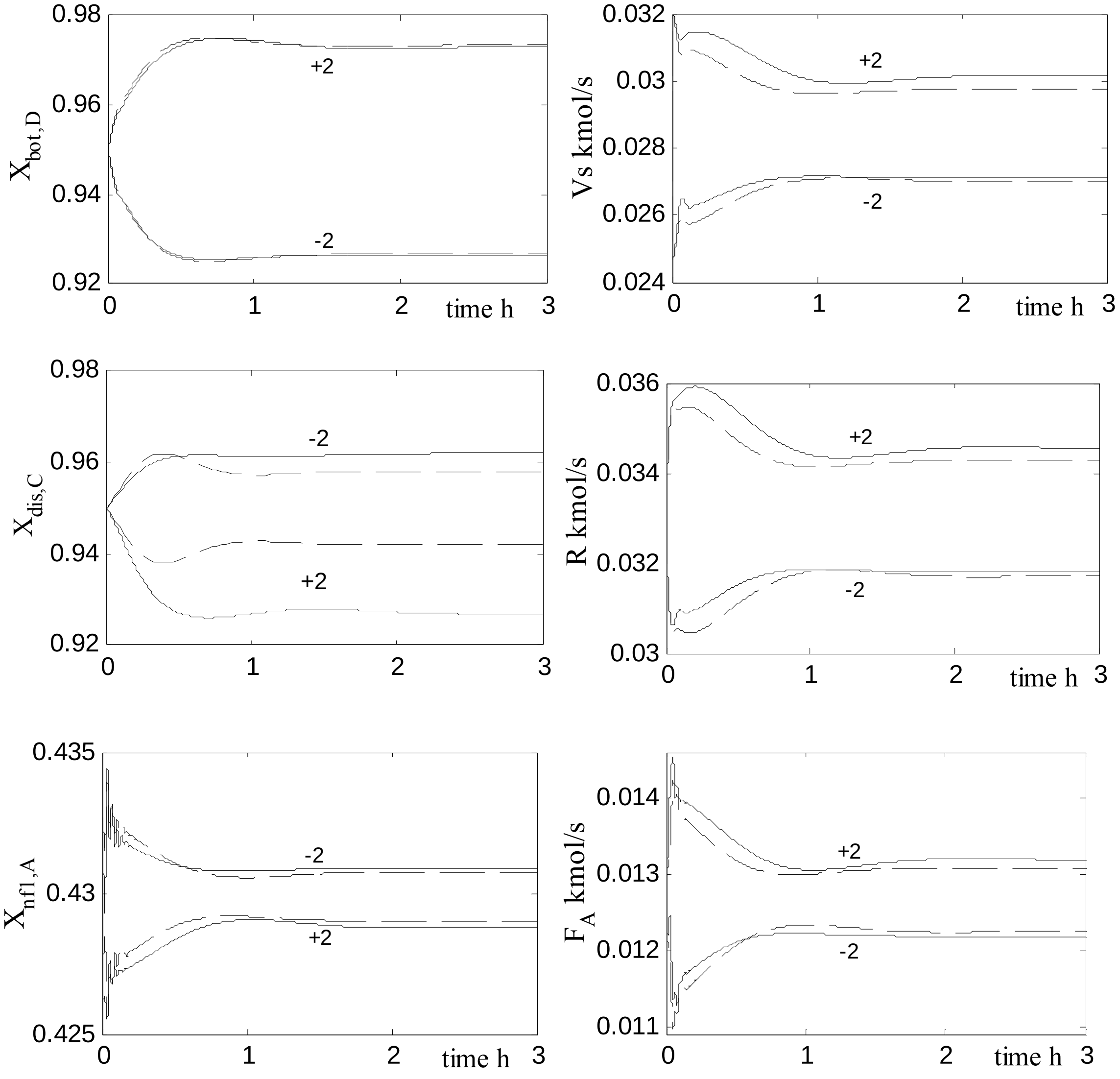

Figure 5.14 Single-end temperature control responses, ±2 K degree changes in temperature on tray 2: (- - -) linear model; (—); nonlinear model.

5.3.4 General Comparisons and Observations

Probably the most important finding of this work is the robustness and the extendibility of the control system when designed based on a linear process model. It is found that the linear process model could be used to develop a robust control system provided that the control valves are conservatively designed to compensate for the underestimation of the input characteristics by the linear model. That control system will be valid only if it is applied in the operating region where the model is linearized around and if the process is open-loop stable under disturbance. If the process shifts to another operating region for whatever reasons, then the process model must be linearized around the new operating region. This observation would be useful for the model-based control applications.

Comparing the closed-loop performance of linear and nonlinear models in a single-end (composition or temperature) control structure with that of a dual-end composition control discussed in section 5.3.1 reveals that the use of a linear model in single-end control structure gives a better agreement with the nonlinear model than when the linear model is used in dual-end composition control. The responses of both controlled and manipulated variables for the two models in single-end control structure are in better agreement when compare to that in dual-end composition control. The responses of the system with single-end control are also faster than the responses of the system with dual-end composition control. This could be due to an increase of nonlinearity in the system with a dual-end control structure which results from increased loop interactions. The single-end control suffers the ability to precisely control the uncontrolled end, but this could be compensated for by overdesigning the process (design at higher product purity). It is found that fixing the reflux ratio scheme in single-end control structure provides better disturbance filtration and process dynamics.

5.4 Conclusion

In this chapter, we have compared the closed-loop performance of three control structures when based on an approximate linear process model to that when based on a nonlinear process model for a generic two-product reactive distillation. The control structures examined are dual-end composition control, single-end composition control, and single-end temperature control. All of the structures use a composition analyzer in the reactive zone to detect the inventory of one of the reactants so that the fresh feed can be manipulated to balance the feeds stoichiometry.

It is shown that an approximate linear model behaves reasonably well compared to a nonlinear model in a closed-loop system when a disturbance in the process variables is introduced provided that the system is open-loop stable under that disturbance. Most of the responses of a closed-loop linear model using three alternative control structures show good agreement when compared to the responses of a closed-loop nonlinear model under the same process conditions. It is also shown that the performance of a linear model is better in a single-end control system than in a dual-end control system. It is generally recommended to fix the reflux ratio and not the reflux flowrate in the single-end control schemes.

5.5 Reference

[1] M. A. Al-Arfaj and W. L. Luyben, "Comparison of alternative control structures for an ideal two-product reactive distillation column," *Ind. Eng. Chem. Res.*, vol. 39, pp. 3298-3307, 2000.

[2] M. A. Al-Arfaj and W. L. Luyben, "Comparative control study of ideal and methyl acetate reactive distillation," *Chem. Eng. Sci.*, vol. 24, pp. 5039-5050, 2002.

[3] M. A. Al-Arfaj and W. L. Luyben, "Plantwide control for TAME production using reactive distillation," *AIChE J.*, vol. 50, pp. 1462-1473, 2004.

[4] R. Baratti, A. Bertucco, D. Alessandro, and M. Morbidelli, "Development of a composition estimator for binary distillation columns. Application to a pilot plant," *Chem. Eng. Sci.*, vol. 50, pp. 1541-1550, 1995.

[5] E. Quintero-Marmol, L. W. Luyben, and C. Georgakis, "Application of an extended Luenberger observer to the control of multicomponent batch distillation," *Ind. Eng. Chem. Res*, vol. 30, pp. 1870-1879, 1991.

[6] W. L. Luyben, "Derivation of transfer functions for highly nonlinear distillation columns," *Ind.Eng.Chem.Res.*, vol. 26, pp. 2490-2495, 1987.

[7] B. D. Tyreus and W. L. Luyben, "Tuning PI Controllers for integrator/dead time processes," *Ind. Eng. Chem. Res.*, vol. 31, pp. 2625-2628, 1992.

[8] B. D. Tyreus, "Optimization and multivariable control of distillation columns," *Adv. Instrum.*, vol. 42, pp. 25-44, 1987.

[9] M. J. Olanrewaju and M. A. Al-Arfaj, "Impact of disturbance magnitudes and directions on the dynamic behavior of a generic reactive distillation," *Submitted for publication*.

CHAPTER 6

6 Design and Implementation of Linear State Estimators in Reactive distillation

6.1 Introduction

The increasingly more aggressive global competition for the production of higher quality products at lower costs has placed considerable pressure on the process engineers to operate the existing plants more efficiently. Moreover, the effective control and monitoring of a process requires sufficient information on the state of the process, which is uniquely specified by the process state variables. In practice, online measurements of all the variables of a process are rarely available, and in such cases, reliable information on the immeasurable states is obtained by using the state estimator. The state observers/ estimators are dynamic models that are capable of inferring useful but inaccessible state variables from the available measurements. They can also play a key role in the process control and monitoring wherein an early detection of hazardous conditions is needed for a safe operation [1].

Several estimation techniques are available in the literature. These include the static partial least-square regression estimation [2], Kalman filtering [1, 3, 4], the state estimation through optimization formulation [5], high gain observers [6], Luenberger observer [7, 8], and a moving horizon state estimation [9]. Among these estimation techniques, the Kalman filter and the Luenberger observer, which have been in use since the early 60s have gained a wider application both in the academia and industry, though they have undergone several modifications over the years. Because, this work is the first on the application of state estimation in reactive distillation system, it is reasonable to start with these two techniques and assess their applicability in reactive distillation control.

In Chapter 5, we have presented different control structures for a generic reactive distillation using the linear and nonlinear process models. It is shown that an approximate linear model behaves essentially similar to a nonlinear model in a closed-loop system when the deviation of process variables resulting from the disturbance is within the region of the base steady state [10]. However, a composition analyzer was assumed available whenever a composition measurement is needed for control purposes.

This chapter focuses on developing and assessing the performance of the linear state estimators based on the Kalman filter and the Luenberger observer design methods for an ideal reactive distillation column. Internal compositions which are needed for proper control of reactive distillation will be estimated via the state estimator instead of measuring them by an analyzer. The design and implementation of linear observers are considered in the present work in order to give us a better insight and understanding on the feasibility of applying the state estimation techniques in the reactive distillation control.

6.2 Reactive Distillation Models

The development of a reliable and computationally efficient state estimator requires a mathematical model that is able to capture the main features of the system dynamics. Following the previous work on the reactive distillation shown in Figure 2.1, we considered here a reactive distillation model with constant liquid holdup in all the stages, negligible energy balance, constant relative volatility, and an equimolar overflow except in the reactive zone where the vapor and liquid flowrate changes because of heat of the reaction. Mole balances on all of the components and the algebraic equations describing the liquid and vapor flowrates in the reactive zone give the reactive distillation models:

$$\frac{dx_{ij}}{dt} = \left[L_{i+1}(x_{i+1,j} - x_{i,j}) + V_{i-1}(y_{i-1,j} - x_{i,j}) + V_i(x_{i,j} - y_{i,j}) + R_{i,j} + F_i(Z_{ij} - x_{ij})\right] / M_i \tag{6.1}$$

$$L_i = L_{i-1} - \frac{\lambda}{\Delta H_v} \sum_{k=1}^{i-Ns-1} R_{Ns+1+k,j} \tag{6.2}$$

$$V_i = V_S + \frac{\lambda}{\Delta H_v} \sum_{k=1}^{i-Ns-1} R_{Ns+1+k,j} \tag{6.3}$$

The nonlinear model of reactive distillation can be put in more compact vector form by decoupling all of the state variables in the models and represented it as nonlinear state space models

$$\frac{dX(t)}{dt} = f(X(t), U(t), d(t); \theta) \tag{6.4}$$

$$Y = h(X(t), \theta) \tag{6.5}$$

$$X = \left[x_{1,1}, x_{2,1} \ldots x_{N,1}, x_{1,2}, x_{2,2} \ldots x_{N,2}, x_{1,3}, x_{2,3}, \ldots x_{N,3}, x_{1,4}, x_{2,4}, \ldots x_{N,4,}\right]^T \tag{6.6}$$

X is n-dimensional and it represents the liquid composition of all components in the column. The p-dimensional U is a vector of manipulated variables, which in this study are considered to be the vapor boilup and reflux flowrate. d is m-dimensional vector included to depict system measurable disturbances which are feed flowrates and compositions. θ represents the model constant parameters, such as the relative volatilities, equilibrium constants and column pressure. Y is q-dimensional vector of the measured output variables (i.e. stage temperature measurements).

For the linear estimator design purposes, the nonlinearity of the dynamic equations must be removed. To accomplish this, the following fundamental assumptions are introduced as remark I.

Remark I: *A nominal solution of the nonlinear differential equation of reactive distillation must exist. This solution must well approximate the actual behavior of the system. The approximation is acceptable if the difference between the nominal and actual solutions can be described by a system of linear differential equations. These equations shall be termed "linear process modes".*

Linearizing the nonlinear process model of equation 6.4 and 6.5 using the Taylor series expansion method around the desired steady state operating conditions to yield

$$\dot{X}(t) = AX(t) + BU(t) + Ed(t) \tag{6.7}$$

$$Y = CX(t) \tag{6.8}$$

where the transition matrices A, B, C and E are evaluated at the desired steady state operating conditions (see the appendix for detail). The base steady state operating conditions considered in this work is given in Table 6.1. Taking into consideration the assumption given in remark I, the linear process model of equations 6.7 and 6.8 is assumed to be the plant model on which the design of estimators in this work is based.

Table 6.1 Optimum base steady state conditions.

	variables	steady state values
Column specifications	pressure (bar)	9
	stripping section (N_S)	7
	reactive section (N_{RX})	6
	rectifying section (N_R)	7
Equilibrium data	Relative volatilities: A/B/C/D	4/2/8/1
Flowrates (kmol/s)	Feed rate of reactant A	0.0126
	Feed rate of reactant B	0.0126
	Vapor boil up	0.0285
	Reflux rate	0.0331
	Distillate	0.0126
	Bottoms	0.0126
X_D	A	0.0467
	B	0.0033
	C	0.9501
	D	0.0000
X_B	A	0.0009
	B	0.0445
	C	0.0000
	D	0.9545

6.3 Observability, Location and Number of Measurements

6.3.1 Observability

The concept of the observability is very important and a necessity in the estimators design. The state equation is said to be observable when there exist a set of measurable outputs that contain information on all the state variables. Thus, it indicates the possibility of estimating the state from the available output. The criteria for determining observability for a linear system are well defined in the literature [7]. A linear system is observable if the matrix

$$\mathbf{O} = [C\ CA\ CA^2 \ldots CA^{n-1}] \tag{6.9}$$

is full column rank (i.e. of rank n). **O** is termed the observability matrix.

6.3.2 Measurement Location

An appropriate location of the measurements in the reactive distillation column is an important factor in the successful design and implementation of a state estimator, and in the control of the system as a whole. In the control of distillation system for instance, locating the temperature measurements far from the column ends is usually desirable because the products may be of a high purity where the temperature variations will be insignificant [2]. On the other hand, if the measurement is located too far from the end of the column, the temperature will be strongly influenced by the composition of the feeds and the product at the other column end [2]. The use of singular value decomposition (SVD) to determine the best measurement location as reported in the literature suggests the most sensitive trays are generally located approximately one-forth from each end of the column [11]. One major problem identified with this method is that it does not consider the load disturbance effects [11]. As the measurement location moves farther from the end of the column, the error in the overhead and bottoms compositions becomes greater, even when the measured variables remain constant, under load disturbances [11]. Therefore, the use of evenly spaced multiple measurements could provide an acceptable compromise and handle some of the interferences appropriately [2-4].

6.3.3 Number of Measurements

Intuitively, the more measurements there are, the more information and the greater the accuracy of the estimators. However, it is both technically and economically desirable to have small set of measurements. Yu and Luyben [12] established that a linear system of conventional distillation column is observable as long as the number of measurements is at least NC-1, where NC is the number of component. However, using the number of measurements more than the minimum required could increase the performance of the observer [12]. Unlike conventional distillation system, there are no specific guidelines from the literature on the minimum number of measurements required to make reactive distillation observable. Thus, it is part of this work to utilize the characteristics of a linear process model of reactive distillation to determine the number of measurements that will guarantee the observability of the system.

Figure 6.1 gives the simple and effective algorithm to determine the number of measurements for a linear process model of reactive distillation that will make the whole states observable. This algorithm examined the linear process model of reactive distillation with constant number of components (NC = 4) but at varying total number of

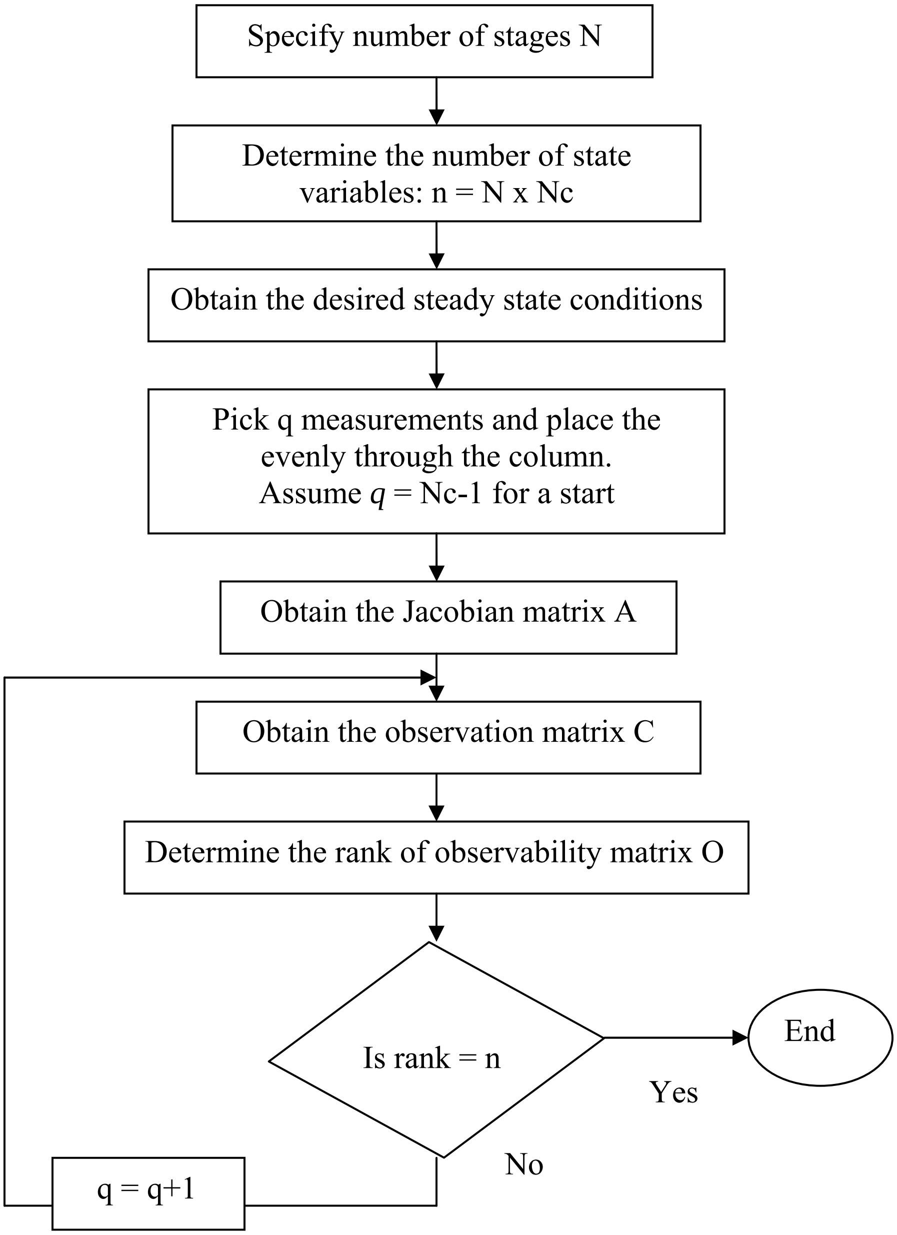
Specify number of stages N
Determine the number of state variables: n = N x Nc
Obtain the desired steady state conditions
Pick q measurements and place the evenly through the column. Assume q = Nc-1 for a start
Obtain the Jacobian matrix A
Obtain the observation matrix C
Determine the rank of observability matrix O
Is rank = n
End
Yes
No
q = q+1

Figure 6.1 Algorithm for determining the number of measurements needed for system observability.

stages N (from 16 to 37). The desired steady state operating conditions for the column at different number of stages were obtained using a steady state simulation program.

Using the desired steady state conditions to evaluate matrices A and C, observability condition (Equation 6.9) was used routinely to determine the minimum number of measurements that makes the system a full column rank. Table 6.2 summarizes the results obtained for different number of column stages. From these results, it can be concluded that the observability of a linear process model of reactive distillation depends strongly on the number of stages. Using only the temperature measurement evenly spaced in the reactive distillation column, the relationship between the number of measurement and the total number of stages is given by

$$\text{Number of measurement} = \frac{N}{2} \tag{6.10}$$

This result perhaps has a strong antecedent from the literature on distillation system. Luyben [13] suggested the tracking of the temperature front by using an average of as many trays temperature. Whitehead and Parnis [14] used a weighted average of many differential temperatures in a C_2 splitter. Mejdell and Skogestad [2] used temperature measurements in all the column stages in the development of static partial least-square regression estimator for product compositions on a high purity pilot-plant distillation column. The use of multiple temperature measurements by the estimators effectively counteracted the effect of pressure variations, measurement noise, off-key components, and the nonlinearity in the column [2].

Table 6.2 Number of the measurement versus the rank of the system.

N	$N_S/N_{RX}/N_R$	q	Rank / n
16	5/4/5	6 **7**	60/64 **64/64**
19	6/5/6	7 **9**	73/76 **76/76**
22	7/6/7	9 **11**	83/88 **88/88**
25	8/7/8	11 **13**	97/100 **100/100**
28	9/8/9	13 **14**	110/112 **112/112**
31	10/9/10	14 **16**	119/124 **124/124**
34	11/10/11	16 **17**	132/136 **136/136**
37	12/11/12	17 **19**	143/148 **148/148**

Remark II: *Using N/2 number of measurements is a sufficient condition to observe the whole states (liquid compositions) of reactive distillation.*

6.4 State Estimator Structure

The linear estimators are developed by using a linearized state-space model presented in section 6.2. The two different types of estimator design are considered: a Luenberger observer (LO) and a Kalman filter (KF). The general structure of the two estimators is essentially the same as presented in Figure 6.2. The main difference between these techniques is the design method of the filter gains. The theory and mathematical formulation of Luenberger observer and Kalman filter are detailed in the literature [7, 15] and only the required equations as it is relevant to this work are presented. The components of a linear state estimator are:

1. A linearized dynamic system: $\dot{X}(t) = AX(t) + BU(t) + Ed(t) + w(t)$ (6.11)
2. Measurement devices: $Z = CX(t) + v(t)$ (6.12)
3. Initial conditions: $X(0) = X_0 + x_0 err$ (6.13)

X_0 is a vector of the actual initial condition of the system taking at the steady state. w is a vector representing the plant noise, v represents measurement error vector and $x_0 err$ is a vector of the initial condition error. Equation 6.12 implies that at each independent time t there are q measurements available (i.e. Z is q-dimensional) that are linearly related to the states and are corrupted by the additive noise. All of these components will be combined into a state estimator of the form:

$$\hat{X}(0) = X_0 + x_0 err \tag{6.14}$$

$$Y = C\hat{X}(t) \tag{6.15}$$

$$\dot{\hat{X}}(t) = A\hat{X}(t) + BU(t) + Ed(t) + K[Z(X(t)) - Y(\hat{X}(t))] \tag{6.16}$$

where K is the estimator gains matrix. The estimator has two inputs U and Z with measurable disturbance d and its output yields the estimated state vector $\hat{X}$.

6.4.1 Base Initial Condition Errors, Measurement and Plant Noise

The development of an estimator usually assumes that the real initial conditions of the system are not known. Thus, a robust estimator should be able to start with approximate initial conditions. In this work, the guess initial conditions for the state estimator are defined as given in Equation 6.14. The initial condition errors are considered as the deviation from the actual initial conditions of the system obtained by solving the steady state model. The measurement noise v and the plant noise w are assumed to be uncorrelated (i.e. white noise) random sequence with known statistical properties.

$$E[w_k] = 0\,,\quad E[v_k] = 0 \tag{6.17}$$

$$E[w_k w_j{}^T] = Q_k \delta_{kj} \tag{6.18}$$

$$E[v_k v_j{}^T] = R_k \delta_{kj} \tag{6.19}$$

$$E[v_k w_j{}^T] = 0 \tag{6.20}$$

where δ_{kj} is the Kronecter delta. Note that subscripts i and k refer to the particular elements in the parameters vector or matrix.

In order to compare the performance of the two state estimators considered in this study, the same base initial condition errors, measurement noise and plant noise are used in the design, implementation and simulation of the two state estimators. Figure 6.3 gives the base initial condition errors and measurement noise for the estimators. The standard deviation of the base plant noise (*w*) is 0.1%. Unless otherwise stated, these base initial condition errors, measurement noise and plant noise are always present in all the simulation carried out in this work.

6.4.2 Luenberger Observer (LO)

For a Luenberger observer, Equation 6.16 can be rewritten as

$$\dot{\hat{X}}(t) = (A - KC)\hat{X}(t) + BU(t) + Ed(t) + KZ \tag{6.21}$$

The error between the actual state and estimated state is define as

$$e(t) = X(t) - \hat{X}(t) \tag{6.22}$$

Differentiating e*(t)* and then substituting equation 6.10 and 6.20 into it, we obtain

$$\dot{e}(t) = \dot{X}(t) - \dot{\hat{X}} \tag{6.23}$$

$$= AX(t) + BU(t) + Ed(t) - (A - KC)\hat{X} - BU(t) - Ed(t) - K(CX)$$

$$= (A - KC)X(t) - (A - KC)\hat{X}$$

$$\dot{e}(t) = (A - KC)e(t) \tag{6.24}$$

The equation 6.23 governs the estimation error ($e(t)$). If all eigenvalues of matrix (A-KC) can be assigned arbitrarily, then the rate of $e(t)$ to approach zero, or equivalently, for the estimated state to approach the actual state can be controlled. For example, if all

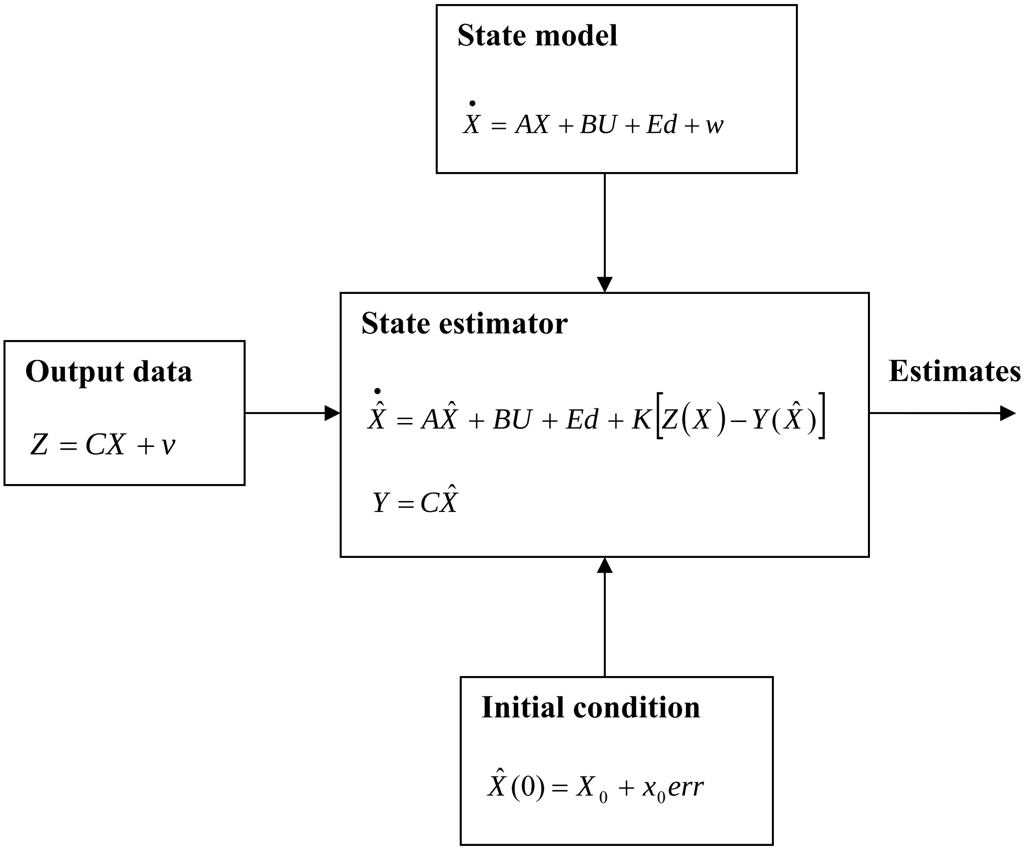
State model
$\dot{X} = AX + BU + Ed + w$
State estimator
$\dot{\hat{X}} = A\hat{X} + BU + Ed + K\left[Z(X) - Y(\hat{X})\right]$
$Y = C\hat{X}$
Output data
$Z = CX + v$
Estimates
Initial condition
$\hat{X}(0) = X_0 + x_0 err$

Figure 6.2 Linear state estimator structure.

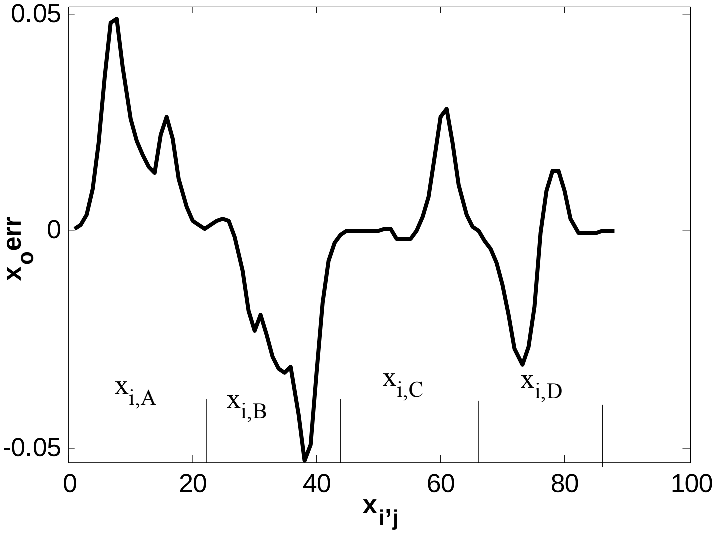

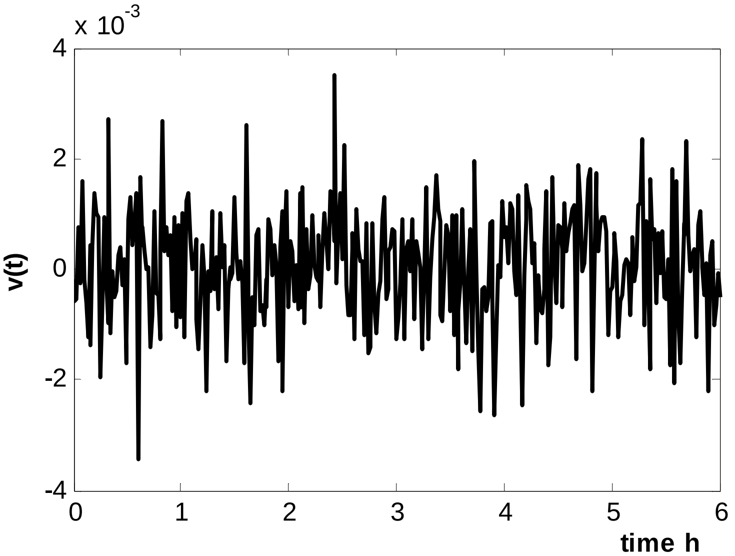

Figure 6.3 The base initial condition error ($x_0 err$) and base measurement noise ($v(t)$).

eigenvalues of matrix (A-KC) have negative real parts smaller than $-\mu$, then all the entries of the estimation error ($e(t)$) will approach zero at the rate faster than $e^{-\mu}$.

6.4.2.1 Design Procedure for a Luenberger Observer

The design procedure to obtain the gain matrix of the Luenberger observer is presented as follows:

(1) Using the algorithm presented in Figure 6.1, pick the number of measurements (q) such that the whole system's states are observable.

(2) Design the gain matrix K by using the duality theorem [7]. The pair (A, C) is observable if an only if (A^T, C^T) is controllable. If (A^T, C^T) is controllable, all eigenvalues of (A^T- $C^T I$) can be assigned arbitrarily by selecting a constant gain matrix I. The transpose of (A^T- $C^T I$) is (A- I^TC). If $K = I^T$, then (A- I^TC) is the same as (A- KC).

(3) Use Qunitero-Marmol method [8] to select suitable set of the eigenvalues for matrix (A-KC). This is carried out by increasing the magnitudes of the slowest eigenvalues of the system matrix A because the response of the estimator is expected to be faster than that of the real system.

(4) Evaluate the values of the gains (K) that place the selected eigenvalues at desired locations.

6.4.2.2 Tuning the Luenberger Observer

The design of the suitable observer gains is a major prerequisite for a successful implementation of the Luenberger observer method. Selecting an inadequate set of the eigenvalues could lead to the poor performance of the observer. To illustrate this, the different sets of eigenvalues as shown in Figure 6.4 are used in the Luenberger observer design. The eigenvalues of system matrix A is taken as the first set of eigenvalues for the state observer. In the second illustration, the magnitudes of the two slowest eigenvalues of matrix A are increased while in the third example, the slowest seven eigenvalues of matrix A are shifted. Figure 6.4B presents the performance of a Luenberger observer as a function of these different sets of eigenvalues to estimate the bottoms mol fraction of component D when the feed flowrate of reactant B is increased by 10%. Throughout this work, the reactant A flowrate, column pressure, reflux flowrate, and vapor boil up are kept constant, while the reflux drum and column base levels are controlled by manipulating the distillate and bottoms flowrates respectively. When the first set of the eigenvalues is used, it takes the observer estimate about 6 h to the approach the reference state, whereas using the third set, the observer estimate approaches the reference state in less than 20 min of the startup. Selecting higher magnitudes of the eigenvalues gives higher gains and faster response, but greater noise susceptibility, and often, lower margin of stability. Therefore, an appropriate selection of eigenvalues for the observer gains design is a key factor in the application of a Luenberger observer and should be selected carefully.

Remark III: *Because the gains of a Luenberger observer is designed offline, set the gains as high as the margin of stability will allow.*

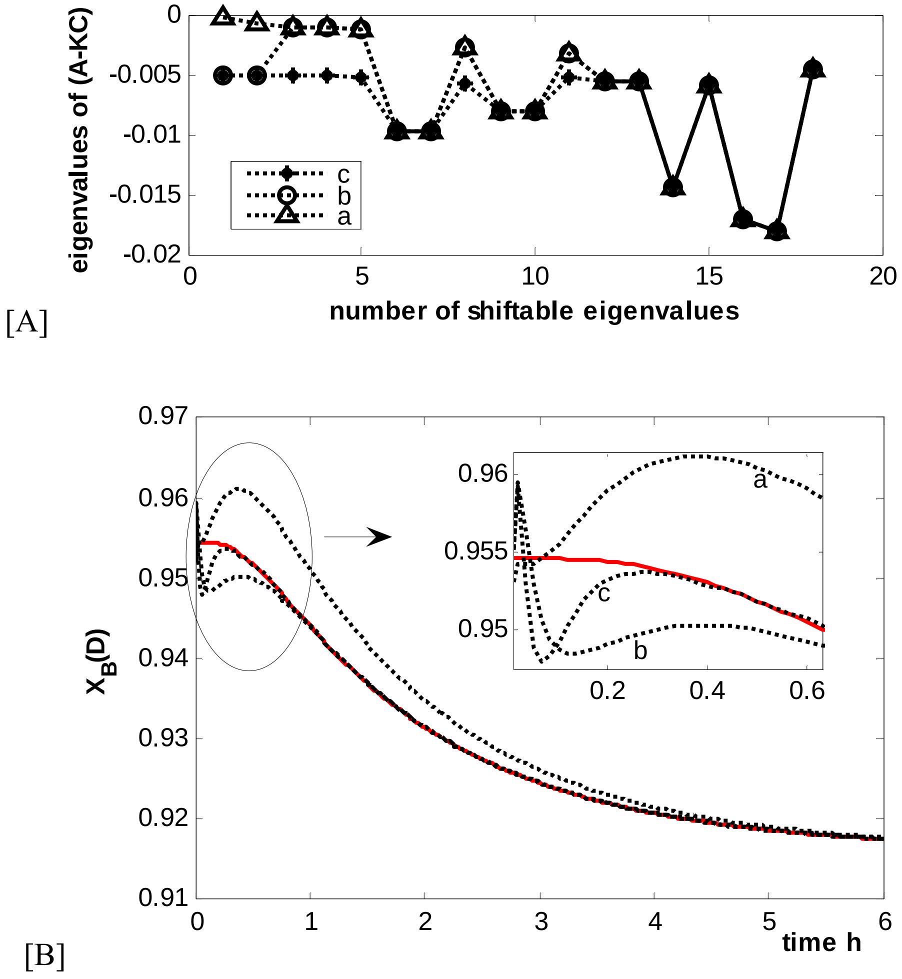

Figure 6.4 [A] The eigenvalues of matrix (A-KC), [B] effect of the eigenvalues selection on the performance of Luenberger observer: (a) the same as eigenvalues of matrix A; (b) the slowest two eigenvalues are shifted to higher magnitudes; (c) the slowest seven eigenvalues are shifted to higher magnitudes: (——) actual state profile; (----) estimated state profile.

6.4.3 Kalman Filter (KF)

The Kalman filter is an approximate optimal estimator of the state vector *X* at a given time value, based on the predictions of a given model and the measurements available up to that time. The detailed formulation of a Kalman filter is contained in [15]. Consider a continuous-time linear system derived previously and presented in the form

$$\overset{\bullet}{X}(t) = AX(t) + BU(t) + Ed(t) + v(t) \tag{6.25}$$

$$Z = CX(t) + w(t) \tag{6.26}$$

Analogously to the assumption made previously, we have included in this model the two white, zero-mean, mutually uncorrelated noise signals *v(t)* and *w(t)* and they have the same properties as discussed in section 6.4.1.

Again, we need to determine the estimator that best estimate the state of equation 6.25, while rejecting the influence of the noisy inputs and initial condition errors. As before, the estimator design objective is to design the gain that will minimize an error criterion as established by the equation 6.24.

First, let $\Phi(t, t_0)$ denote the state-transition matrix of the error system in equation 6.24, the complete solution of equation 6.24 is given as

$$e(t) = \Phi(t, t_0)e(t_0) + \int_{t_0}^{t} \Phi(t, \tau)[v(\tau) - w(\tau)]d\tau \tag{6.27}$$

Finding the error covariance *P* from this expression:

$$P(t) = E[e(t)e^T(\tau)] \tag{6.28}$$

By substituting equation 6.27 in equation 6.28 gives:

$$P(t) = \Phi(t,t_0)P_0\Phi^T(t,t_0) + \int_{t_0}^{t} \Phi(t,\tau)[Q+R]\Phi^T(t,\tau)d\tau \qquad (6.29)$$

Taking the derivative of equation 6.29 with respect to *t* to determine the dynamics of the error covariance P, and after simplification gives

$$\dot{P}(t) = (A-KC)P(t) + P(t)(A-KC)^T + Q + R \qquad (6.30)$$

This resulting equation is popularly known as differential matrix Riccati equation for the error covariance *P(t)* whose initial condition is $P(t_0) = P_0$. However, we have not yet optimized the norm of the error over all possible gain *K (t)*. To perform the optimization, we will attempt to minimize the squared error at any time *t*. This squared error may be expressed as

$$E[e^T(t)e(t)] = [P(t)] \qquad (6.31)$$

Therefore, the matrix gain *K* that minimizes the error criterion as expressed above is given as

$$\frac{\partial}{\partial K}[P(t)] = -2P(t)C^T + 2K(t)R = 0 \qquad (6.32)$$

which after further simplification gives the Kalman gain matrix K

$$K(t) = P(t)C^T R^{-1} \qquad (6.33)$$

Using this equation of the gain, the error covariance dynamics simplify as well to

$$\dot{P}(t) = AP(t) + P(t)A^T - P(t)C^T R^{-1} CP(t) + Q \qquad (6.34)$$

6.4.3.1 Kalman filter design procedure

Consider that the first observation occurs at time t_1. The Kalman filter design algorithm can be described by the following steps:

(1) Initialize P, $\hat{X}(0)$ and Q at time $t = t_0$, where P is a matrix of the estimate covariance error and Q is the covariance matrix of the measurement error. In this work, an arbitrary initial value to 10^{-5} is assumed for all of the elements of P, while Q is evaluated according to equation 6.18.

(2) Project the estimate of the covariance estimate error by integrating the simplified form of Riccati equation from t_0 to t_1.

$$\dot{\hat{P}}(t) = A\hat{P}(t) + \hat{P}(t)A^T + Q \tag{6.35}$$

(3) Compute the gain matrix K at time t_1

$$K(t) = \hat{P}(t)C^T R^{-1} \tag{6.36}$$

where R is the noise covariance matrix evaluated using equation 6.19 at time t_1.

(4) Estimate the state vector at t_1 by integrating the equation 6.25 from t_0 to t_1

(5) Update the covariance for the error in the state estimate vector at time t_1

$$P(t) = [I - CK]\hat{P}(t) \tag{6.37}$$

(6) Progress in time and move to step 2.

Because of the simulation difficulty usually involved when a differential Riccati equation is used, a Kalman filter algorithm utilizing a steady state Riccati equation is also considered and the KF design procedure is modified as follows:

(1) Initialize R and *Q*, where *Q* is the covariance matrix of the measurement error and R is the covariance matrix of the process noise.

(2) Obtain the covariance matrix *P* by solving the steady state Riccati equation as

$$AP + PA^T - PC^T R^{-1} CP + Q = 0 \tag{6.38}$$

(3) Compute the gain matrix *K*

$$K = PC^T R^{-1} \tag{6.39}$$

6.5 Results and Discussion

6.5.1 The Estimators Performance

The quality of the information to be derived from the estimators designed from the two methods can be judged from the results presented in Figure 6.5. The forcing function is a 10% increase in feed flowrate of reactant B. Note that the base initial condition errors and the measurement noise (in Figure 6.3) were added to the actual initial conditions and measurement data input into the state estimators. Following the heuristics stated in Remark III, the third set of eigenvalues (see Figure 6.4A) was used to design the estimator gains for Luenberger observer. The behavior of the two estimators is generally excellent with respect to the states from the linear process model. The results demonstrate that the estimators will be able to track asymptotically the reference states if the system is well described by a linear process model.

When the responses of a Luenberger observer is compared with those obtained with a Kalman filter observer, it can be easily noticed that a Luenberger observer seems to track the reference state faster than a Kalman filter. This is expected because the design of the gains for a Luenberger observer is carried out offline where the desired eigenvalues are suitably selected and the rate at which the estimation error is to approach zero is controlled. On the other hand, the gain matrix of a Kalman filter observer is calculated and updated online, thus making the response of the estimator a function of the system dynamics and nature of the disturbance input. As it will be discussed in the next sections, updating the gains online gives the Kalman filter the advantages of a better handling of plant-model mismatch and measurement errors.

One major concern in the application of the state estimators is the complexity it adds to the system and the target of any designer is to reduce the computational complexity as much as possible. In our study, we found out that implementing a Luenberger observer in the system is easier and require less computational time than a Kalman filter. It takes a Luenberger observer-based system less than one-forth of the time to simulate a Kalman-filter-based system under the same operating conditions. However, it is worth noting that using a steady Riccati equation in a Kalman filter design algorithm significantly reduces the computational time and at the same gives an acceptable result as shown in Figure 6.6 and 6.7.

The major setback in the Luenberger observer is in the design of the observer law (i.e. the gain matrix) for multivariable system such as the reactive distillation. Selecting the desired set of eigenvalues that will make the Luenberger observer applicable over a wide range of operating conditions is not a trivial task. It depends on many performance criteria such as rise time, settling time and overshoot of the system [7].

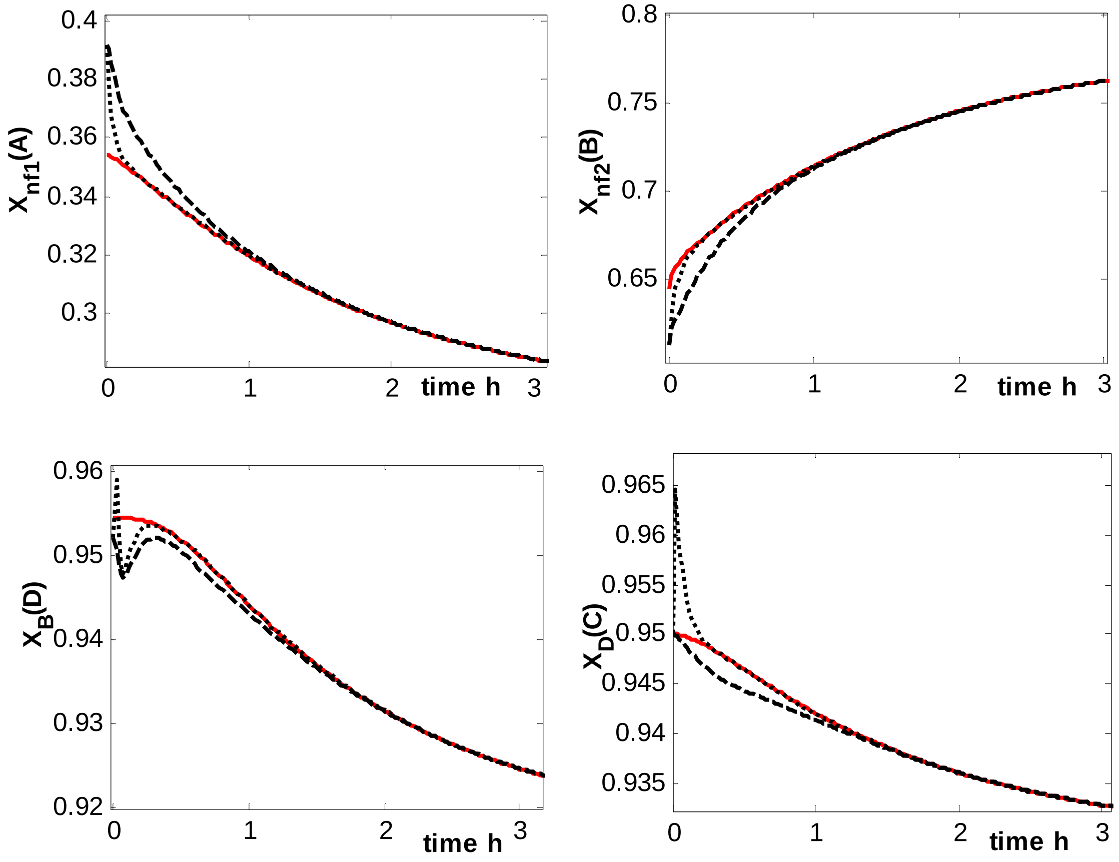

Figure 6.5 Dynamic composition profiles: (——) actual state profile; (----) LO estimated state profile; (— —) KF estimated state profile.

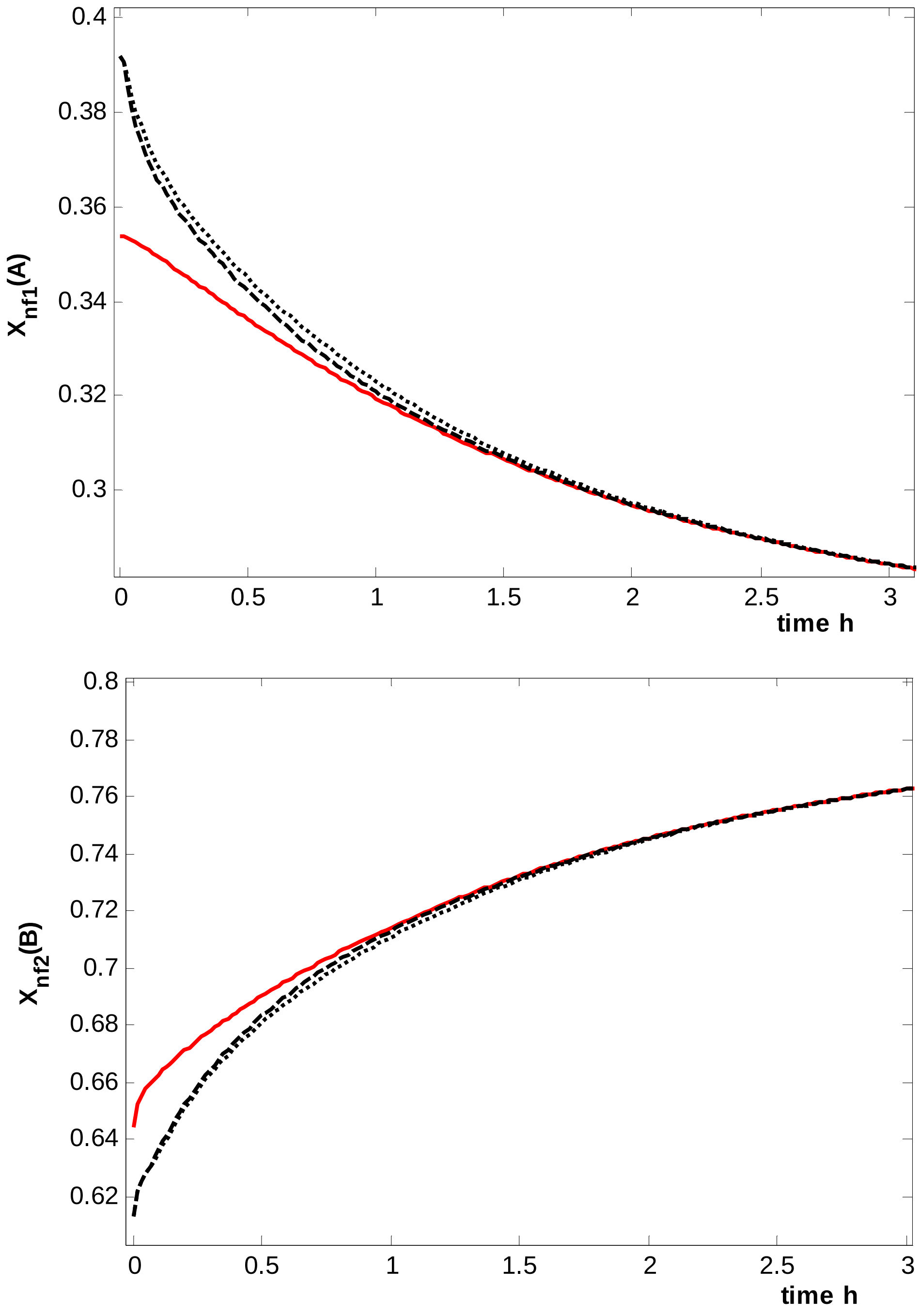

Figure 6.6 Kalman filter dynamic profiles : (——) actual state profile; (----) estimated state profile when a steady state Ricatti equation is used in KF design; (— —) estimated state profile when a differential Ricatti equation is used in KF design.

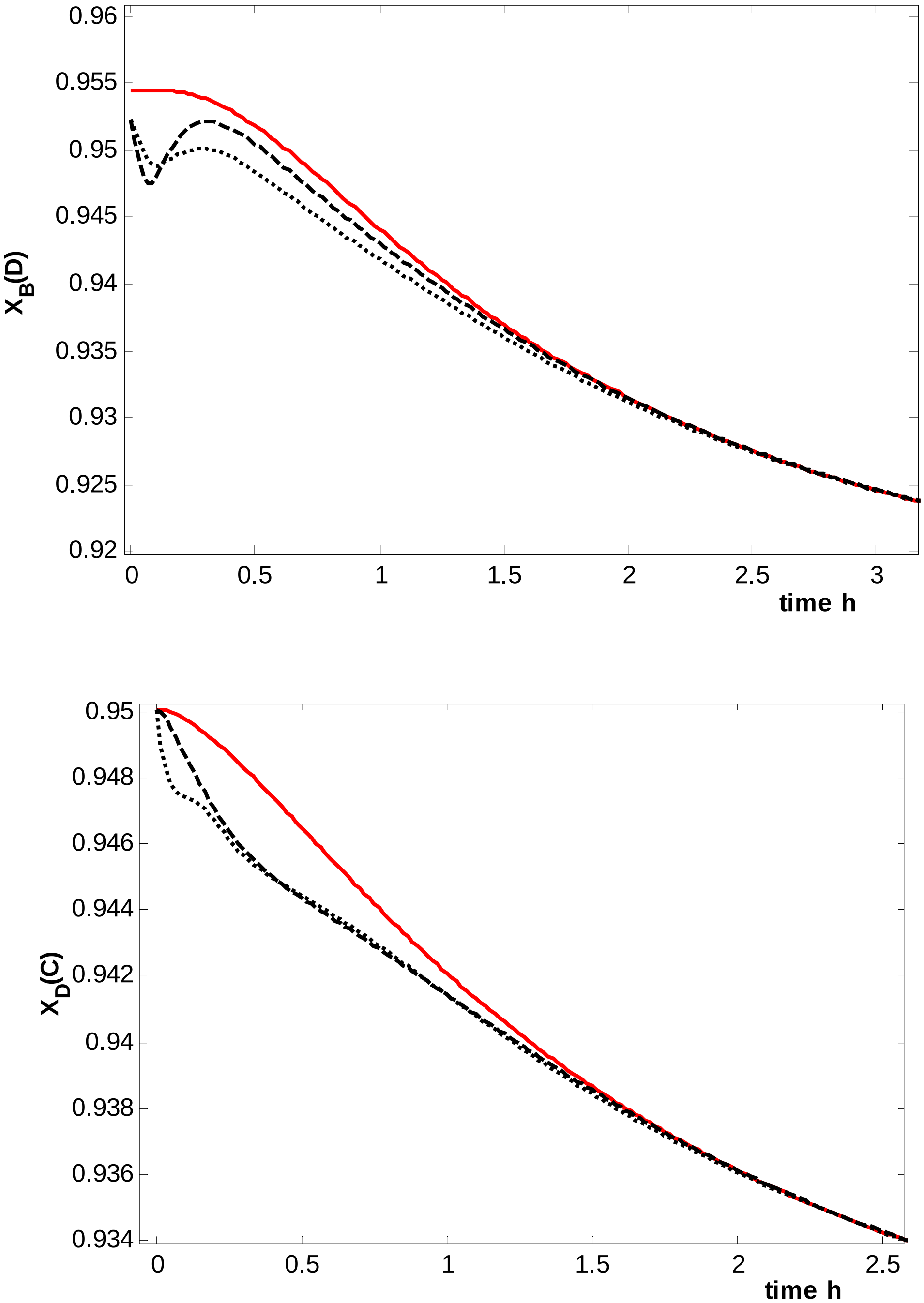

Figure 6.7 Kalman filter dynamic profiles : (——) actual state profile; (----) estimated state profile when a steady state Ricatti equation is used in KF design; (— —) estimated state profile when a differential Ricatti equation is used in KF design.

Remark IV: *A Luenberger observer requires less computational resources than a Kalman filter and the rate at which estimation error approaches zero can be set as a fast as desired provided the accurate models and low-noise sensors are available.*

6.5.2 Effect of the Initial Conditions Errors

In this section, the effect of the use of erroneous initial conditions on the estimators responses is studied. Figure 6.8A shows the three sets of initial condition errors used. These initial condition errors are added into the actual initial conditions (steady state values) of the system to serve as the initial estimator estimates. The first set of initial condition errors are the same as the base initial condition errors (x_0err) which were used in the previous section. The magnitudes of this base initial condition errors are increased by a factor of four ($4x_0err$) for the second illustration. The third set of the initial estimator estimates assumes an extreme case of equal composition of all of the components in all of the column stages (i.e. $\hat{X}(0)=$ 0.25/0.25/0.25/0.25). Figure 6.8 shows the performance of the two estimators to different set of the initial conditions. This result illustrates the capability of the estimators to start from the guessed or approximate initial conditions. However, it does show that the closer the initial estimates provided to the estimators to the actual initial conditions, the better the estimators performance. On the other hand, providing the estimators with the erroneous initial conditions could degrade their performance.

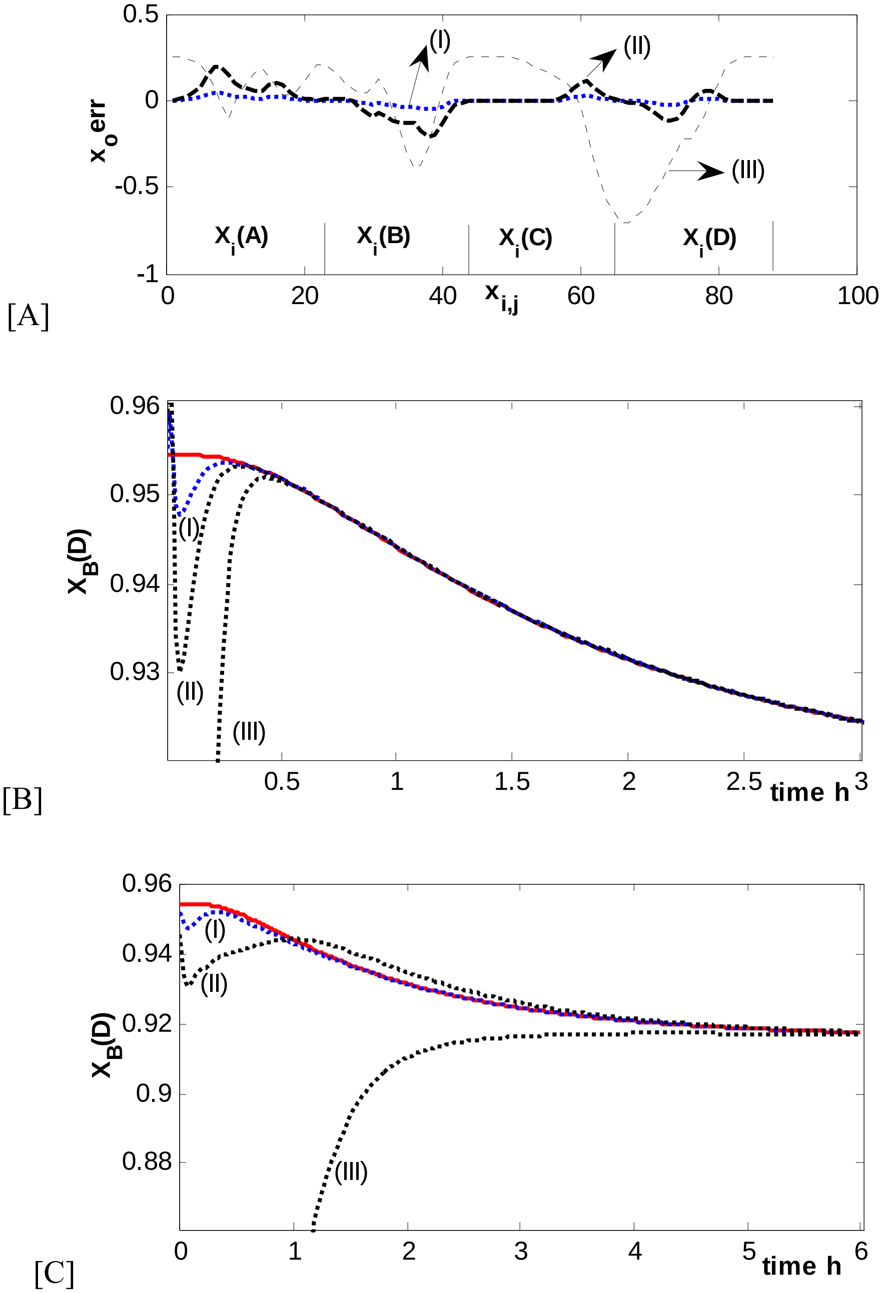

Figure 6.8 Effect of initial condition errors on the performance of the state estimators with a 10% F_B disturbance, [A] initial condition errors; [B] response from the Luenberger observer; [C] response from Kalman filter, (I) $x_0 err$; (II) $4x_0 err$; (III) $\hat{X}(0)$ = 0.25/0.25/0.25/0.25:(——) actual state profile; (----) estimated state profile.

6.5.3 Effect of the Measurement Noise

In order to demonstrate and assess the robustness of the two estimators to measurement noise as often the case in practical situation, the standard deviation of the base measurement noise is increased from 0.1% to 10%. Figure 6.9 shows the responses of both the Luenberger observer and Kalman filter. It can be clearly seen that Luenberger observer (Figure 6.9b) was unable to filter this high-frequency measurement noise when compared to the Kalman filter performance as shown in Figure 6.9c. This is expected as the Kalman observer filters the high frequency noise and was able to reduce the effect of the measurement uncertainty significantly.

Remark IV: If *the measurement is noisy as often the case in practical situation, then Kalman filter observer is preferable*.

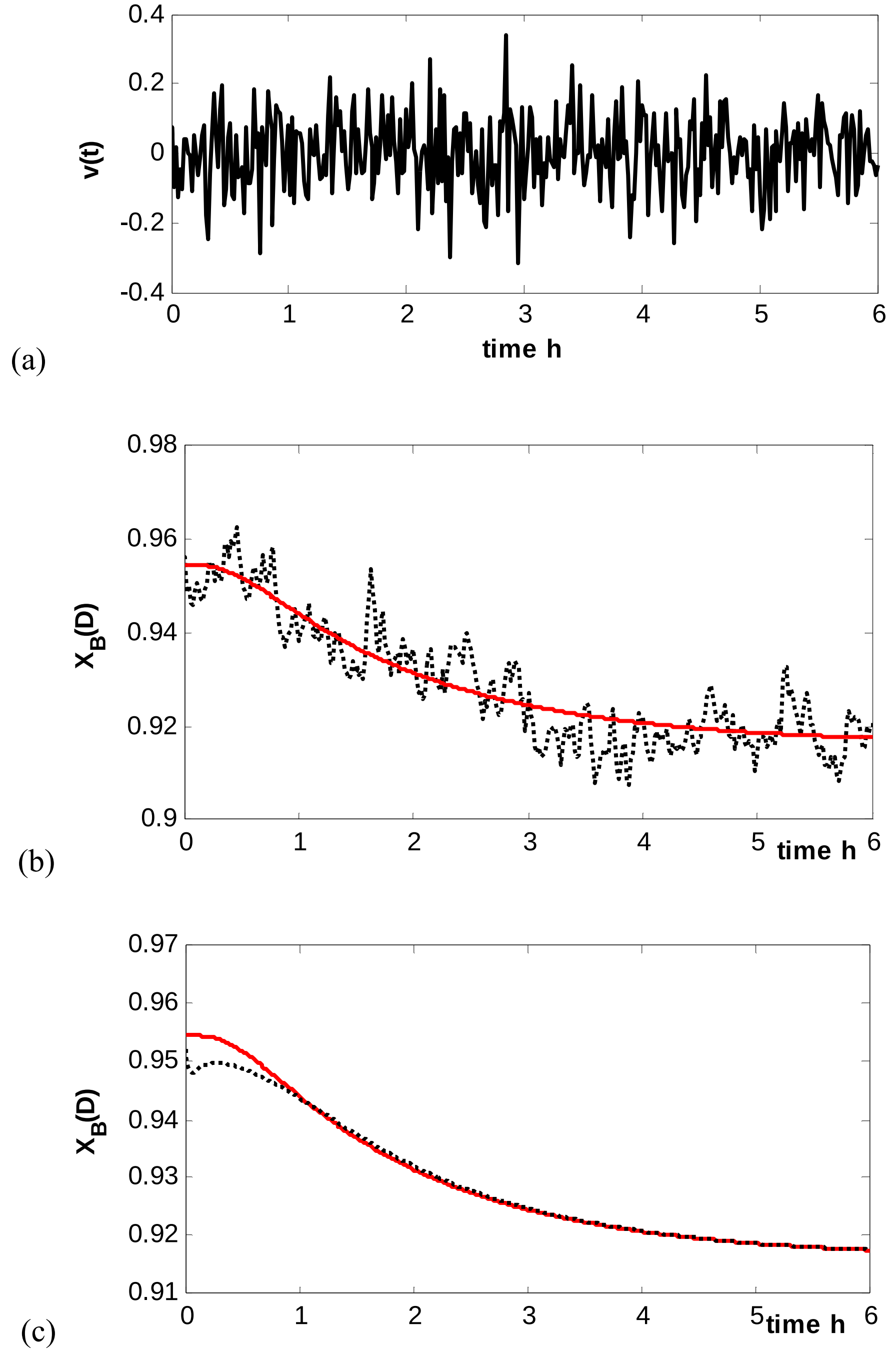

Figure 6.9 Effect of measurement noise on the performance of the estimators with a 10% F_B disturbance, (a) measurement noise; (b) response of the Luenberger observer; (c) response of the Kalman filter: (——) actual state profile; (----) estimated state profile.

6.5.4 Plant-model Mismatch

Studies in this section examine how the state estimators behave in presence of errors in estimator models. In the previous discussion, the state estimators were developed assuming largely the availability of an accurate estimator model with 0.1% standard deviation errors. The most common source of model errors is the complexity involved in providing accurate vapor-liquid equilibrium relation in modeling real distillation system [4]. As a result, we have considered the effect of the errors in the components relative volatilities, which in practice, are usually known with some uncertainty. Two set of the erroneous relative volatilities (i.e. $\hat{\alpha} = 4.2/2.2/8.2/1$ and $\hat{\alpha} = 4.4/2.4/8.4/1$), which are different from the actual relative volatility (i.e., $\hat{\alpha} = 4/2/8/1$) are used in the estimators models. Figure 6.10 shows the bottoms composition of reactant D, actual and as predicted by a Kalman filter and a Luenberger observer when the erroneous relative volatilities are used. The Kalman filter (KF) predictions are quite better than that of the Luenberger observer (LO), which indicates that KF observer is more robust toward plant-model mismatch than LO. The result also shows that an increase in the plant-model mismatch has a considerable effect on the performance of the state estimators.

Remark V: *Accurate models are a necessity for designing a good estimator. However, with proper adaptation of error covariance, the Kalman filter can efficiently cope with model uncertainties better than Luenberger observer.*

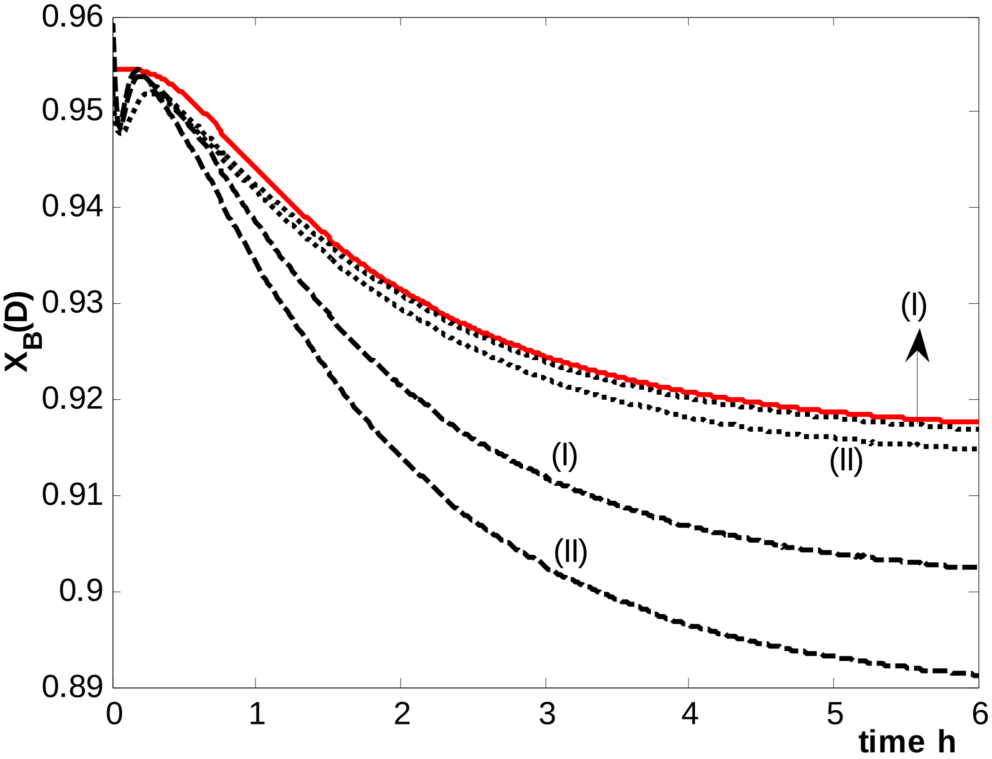

Figure 6.10 Effect of plant-model mismatch on the performance of the linear state estimators with a 10% F_B disturbance. (----) KF estimated state profile; (— —) LO estimated state profile; (——) actual state profile. (I) $\hat{\alpha} = 4.2/2.2/8.2/1$; (II) $\hat{\alpha} = 4.4/2.4/8.4/1$.

6.5.5 The Linear Estimators Using Measurement Data Predicted by the Nonlinear Equation

In all of the previous sections, the performance of the linear estimators is assessed by comparing the state estimates from the estimators to the states as predicted by the linear process model with the assumption that both the plant noise and measurement error could be described by Gaussian white noise. The linear output equation is employed to model the noisy measurement data. We have used these assumptions in order to achieve the first goal of the estimators that is, if a linear process model could describe accurately the actual plant process, the desired states of the system can be estimated accurately using the state estimators.

In a practical situation, the linearized process model will not be a perfect representation of the actual plant and the applicability of the linear estimators into a realistic system might be restricted (i.e. limited operating conditions and small magnitude of disturbance input). In order to investigate the feasibility of applying the linear estimators into a more practical system, the design of the two estimators is modified by using the measurement data predicted by nonlinear process model as an input into linear estimators. Therefore the measurement errors vector v will no longer be assumed to be Gaussian white noise but will be determined by the difference between the actual output data from the plant as predicted by nonlinear output equation and the linearized output equation used in the design of the estimators. This is given by

$$v = h(X(t)) - CX(t) \tag{6.27}$$

where $h(X(t))$ is a nonlinear function of output temperature measurement (from equation 6.5). By substituting equation 6.27 into equation 6.12, the new observation equation will now be given as:

$$Z = h(X(t)) \tag{6.28}$$

This simply means that the nonlinear output equation (i.e, the equation 6.28 which is the same as the equation 6.5) will be used to simulate the measurement data that would have been provided by the physical sensors in the real situation.

Figure 6.11 and 6.12 show the performance of the two estimators when the actual output data as predicted by nonlinear output model is used. The system is excited by a 10% increase in fresh feed flowrate of reactant B. The result presented in Figure 10A shows that the gains of Luenberger observer were tuned and updated by shifting the fifteen slowest eigenvalues of matrix A. On the figures, the plot termed “a” is the actual composition profiles as predicted by the nonlinear process model; “b” is the composition profiles as predicted by the estimators using the nonlinear equation for output data; while “c” is the composition as predicted by the observers using the linearized output equation for the measurement data. Both of the observers more or less give the same response when the measured temperatures are obtained from the nonlinear model.

Even though, the results give an indication of inadequate estimation from the observers when the magnitude of the excitation function is large, the results demonstrate a clear improvement in the performance of the observers toward estimating the actual plant states as predicted by the nonlinear process model when the output data to the linear estimators are modeled by nonlinear equation.

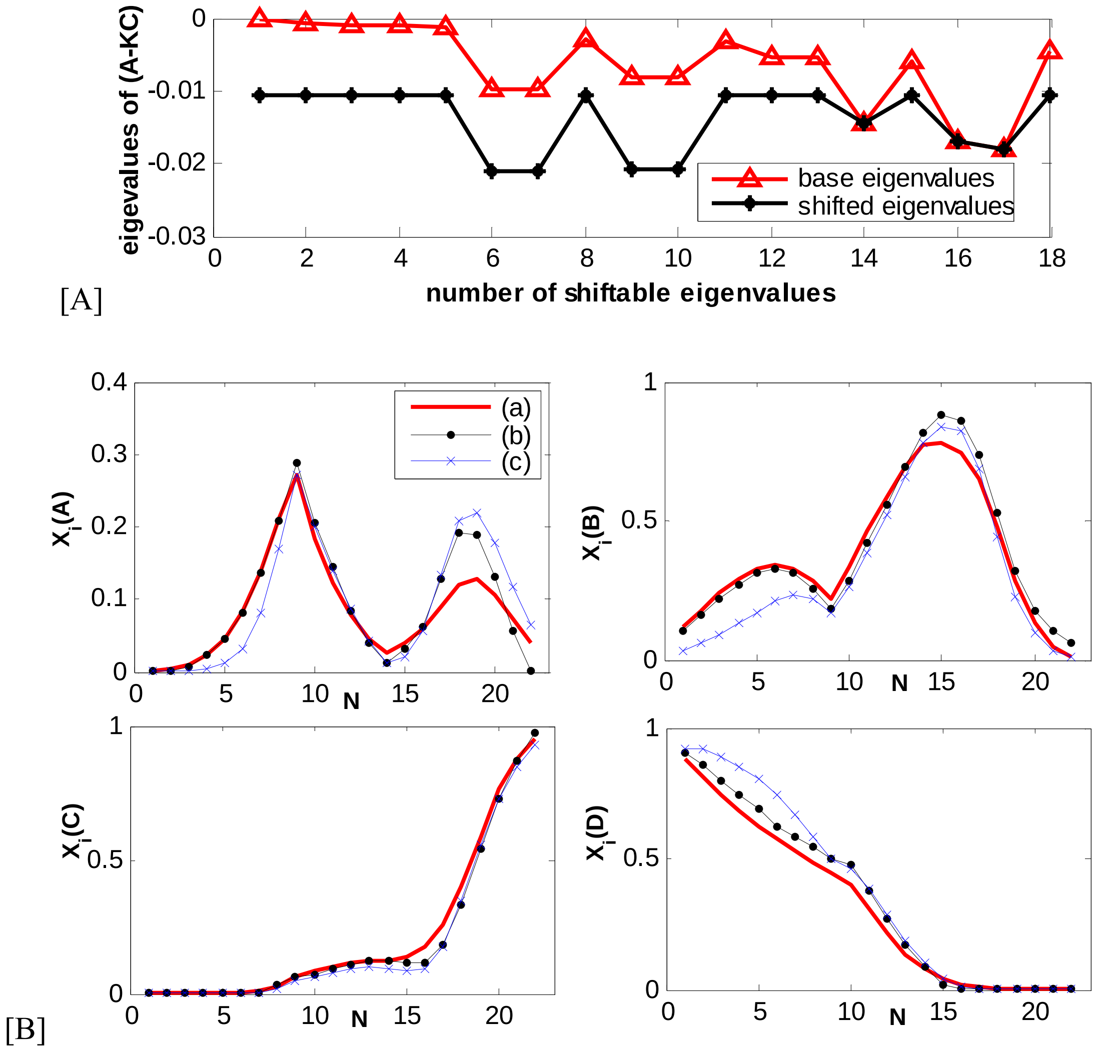

Figure 6.11 [A] The shifted eigenvalues for the Luenberger observer (LO) with a 10% F_B disturbance, [B] Steady state composition profiles from LO as: (a) predicted by nonlinear process model; (b) predicted by LO using nonlinear equation for measurement; (c) predicted by LO using linearized equation for measurement.

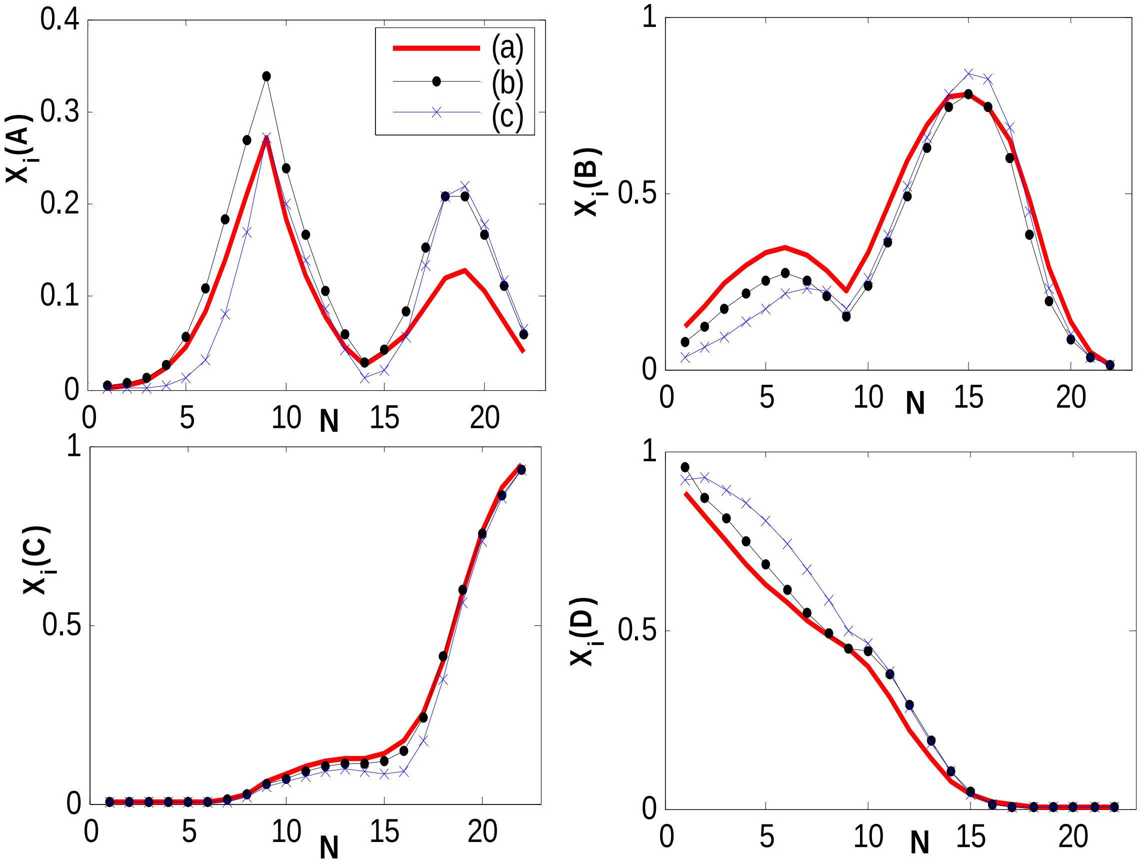

Figure 6.12 Steady state composition profiles from Kalman filter (KF) as: (a) predicted by nonlinear process model; (b) predicted by KF using nonlinear equation for measurement; (C) predicted by KF using linearized equation for measurement.

6.6 Conclusion

In this chapter, the design and application of a Luenberger observer and a Kalman filter in the composition estimation of reactive distillation are explored. A linear process model, which can approximate the actual plant model well, is ideally suited to designing a linear estimator. It is found that using *N/2* number of measurements is a sufficient condition to observe the whole states (liquid compositions) of reactive distillation. Though Luenberger observer requires less computational resources and the rate at which estimation error approaches zero can be set as a fast as desired, the Kalman filter demonstrates its ability to cope efficiently with erroneous initial conditions, corrupted measurements and model uncertainty.

In general, the linear estimators can be applied to estimate the states of the reactive distillation system using the actual output data from the process when: (1) the process is being operated under a small region of operating conditions where the system could be described by a linear process model, (2) accurate sensors are available where the effect of measurement noise may be negligible, and (3) the magnitude of the disturbance inputs is small.

6.7 References

[1] L. Ruokang and J. H. Olson, "Fault detection and diagnosis in a closed-loop nonlinear distillation process: application of extended Kalman filters," *Ind. Eng. Chem. Res.*, vol. 30, pp. 898-908, 1991.

[2] T. Mejdell and S. Skogestad, "Composition estimator in a pilot-plant distillation column using multiple temperatures," *Ind. Eng. Chem. Res.*, vol. 30, 1991.

[3] R. Baratti, A. Bertucco, D. Alessandro, and M. Morbidelli, "Development of a composition estimator for binary distillation columns. Application to a pilot plant," *Chem. Eng. Sci.*, vol. 50, pp. 1541-1550, 1995.

[4] R. Baratti, A. Bertucco, D. Alessandro, and M. Morbidelli, "A composition estimator for multicomponent distillation columns development and experimental test on ternary mixtures," *Chem. Eng. Sci.*, vol. 53, pp. 3601-3612, 1998.

[5] B. W. Bequette, "Nonlinear predictive control using multi-rate sampling," *The Can. J. Chem. Eng.*, vol. 69, pp. 136, 1991.

[6] M. Zeitz, "The extended Luenberger observer for nonlinear systems," *Syst. Control Lett.*, vol. 9, pp. 149, 1987.

[7] C.-T. Chen, *Linear system theory and design*. New York: Oxford University Press, 1999.

[8] E. Quintero-Marmol, L. W. Luyben, and C. Georgakis, "Application of an extended Luenberger observer to the control of multicomponent batch distillation," *Ind. Eng. Chem. Res*, vol. 30, pp. 1870-1879, 1991.

[9] D. G. Robertson, J. H. Lee, and R. J. B., "A moving horizon-based approach for least squares state estimation," *AIChE J.*, vol. 42, pp. 2209, 1996.

[10] M. J. Olanrewaju and M. A. Al-Arfaj, "Performance assessment of different control structures for generic reactive distillation using linear and nonlinear process models," *Ind. Eng. Chem. Res*, ASAP, 2005.

[11] B. W. Bequette and T. F. Edgar, "Non interacting control system design methods in distillation," *Comput. Chem. Engng*, vol. 13, pp. 641-650, 1989.

[12] C.-C. Yu and W. L. Luyben, "Control of multicomponent distillation columns using rigorous composition estimators," *Ind. Chem. E. Symp. Ser.*, vol. No. 104, pp. A29-A69, 1987.

[13] W. L. Luyben, "Control of distillation columns with sharp temperature profiles," *AIChE J.*, vol. 17, pp. 713-718, 1971.

[14] D. B. Whitehead and M. Parnis, "Computer control improves ethylene plant operation," *Hydrocarbon process*, pp. 105-108, 1987.

[15] H. W. Sorenson, "Kalman filtering: Theory and application." New York: IEEE Press, 1985.

CHAPTER 7

7 The State Estimator-Based Control of Reactive Distillation System

7.1 Introduction

Estimator-based control application has received considerable attention over the past several years. Basically, this is the problem of controlling a process where imperfect or limited information is available describing the states of the system that change considerably during the interval in which control is required. Al-Arfaj and Luyben [1] suggested that the state estimator could be a suitable alternative to an expensive and often unreliable composition analyzer when there is need to measure the internal composition of reactive distillation system for control purposes. In the same paper, Al-Arfaj and Luyben [1] summarized the literature on control of reactive distillation system. Since then, several other papers have appeared in the literature that discussed the closed-loop reactive distillation.

The main focus in this chapter is to demonstrate that a state estimator can be successfully designed and implemented in the feedback control of reactive distillation. The function of the state estimator is to estimate the desired state compositions that are required to be feedback into controller for necessary action. The control performance of the system that relies on the state estimator is examined and compared to that of the system which takes direct measurement from the process assuming the availability of perfect online analyzer. The effect of measurement errors, plant-model mismatch and erroneous initial conditions on the estimator-based system is investigated.

7.2 The Process

The process under consideration is the same reactive distillation system, which has been discussed in detail in the previous chapters. The reactive distillation column consists of 22 stages including a partial reboiler and a total condenser. The main column is further divided into three sections which are stripping section (7), reactive section (6) and rectifying section (7). A full-order linear process model presented in the previous chapter is considered to develop the state estimator-based system and is summarized in vector form as

$$\dot{X}(t) = AX(t) + BU(t) + Ed(t) \tag{7.1}$$

$$Y = CX(t) \tag{7.2}$$

where the n-dimensional vector X are state variables (liquid mole fractions in all the stages including partial reboiler and total condenser).

7.3 State Estimator Structure

The most important component of the control structure studied in this work is the underlying state estimator. A Kalman filter (KF), which has been the most popular estimation technique available in the literature is considered. We have equally shown (see Chapter 7) that a Kalman filter estimator is more robust and reliable than a Luenberger observer. The theory behind KF is well established and its applications have grown significantly in the academics and industry [2-4]. In the previous work, we presented the design procedure to develop this state estimator (KF). Therefore, the relevant equations describing the estimator are summarized as follows:

$$\hat{Y} = h(\hat{X}(t)) \tag{7.3}$$

$$Z = CX(t) + v(t) \tag{7.4}$$

$$\hat{X}(0) = X_0 + x_0 err \tag{7.5}$$

$$\dot{\hat{X}}(t) = A\hat{X}(t) + BU(t) + Ed(t) + K[Z(X(t)) - Y(\hat{X}(t))] \tag{7.6}$$

The equations 7.1 to 7.6 can be combined to for the estimator-based system as

$$\begin{bmatrix} \dot{X} \\ \dot{\hat{X}} \end{bmatrix} = \begin{bmatrix} A & \\ KC & A - KC \end{bmatrix} \begin{bmatrix} X \\ \hat{X} \end{bmatrix} + \begin{bmatrix} B \\ B \end{bmatrix} U + \begin{bmatrix} E \\ E \end{bmatrix} d + \begin{bmatrix} 0 \\ L \end{bmatrix} w \tag{7.7}$$

$$\begin{bmatrix} Z \\ \hat{Y} \end{bmatrix} = \begin{bmatrix} C & 0 \end{bmatrix} \begin{bmatrix} X \\ \hat{X} \end{bmatrix} + [\, G \ 0 \,] v \tag{7.8}$$

The state estimator has three inputs, which are U, d and Z and its output yields the estimated state vector $\hat{X}$. The *w* and *v* are vectors of the plant and measurement noise, and *L* and *G* are the matrices of their coefficients respectively. K is gain matrix of the sate estimator evaluated using the Kalman filtering algorithms [5]. In order to design a state estimator, it is necessary that the system is observable. Considerations based on simulated studies suggest that using not less than *N/2* temperature measurements uniformly distributed in the column is a sufficient condition to observe all the components liquid compositions of reactive distillation under study.

7.4 Control System Configuration

Al-Arfaj and Luyben [1] discussed many control schemes for the same system under study. In their study, it was assumed that perfect analyzer is available to measure the composition whenever it is needed for the control system. In this study, the control configuration of interest is the estimator-based control system, where the developed linear state estimator is implemented in the feedback control of reactive distillation column to estimate the inaccessible states. As shown in Figure 7.1, the estimates from the state estimator will serve as input to the controller and the decisions based on such feedback information are then implemented on the process. For illustration purposes, we considered the dual-end control structure shown in Figure 7.2 in which the purities of both products are measured and controlled. In the distillate product, the composition of component C is controlled by manipulating the reflux flowrate. In the bottoms, the composition of component D is controlled by manipulating the vapor boilup. The reflux-drum level is controlled by the distillate flowrate while the bottoms level is controlled by manipulating the bottoms flowrate.

Al-Arfaj and Luyben [1] stated the necessity to detect an internal composition of one of the reactants in two-reactant-two-product reactive distillation column so that feedbacks trim can balance the feeds stoichiometry. Therefore, the concentration of reactant A on the tray nf1 is measured and controlled by manipulating the fresh feed flowrate of component A. All of the composition controllers are PI except the internal composition controller which is P-only because it is aimed to only maintain the feeds stoichiometry. These loops are tuned by conducting relay-feedback tests to find ultimate gains and frequencies and then using the Tyreus-Luyben settings [6].

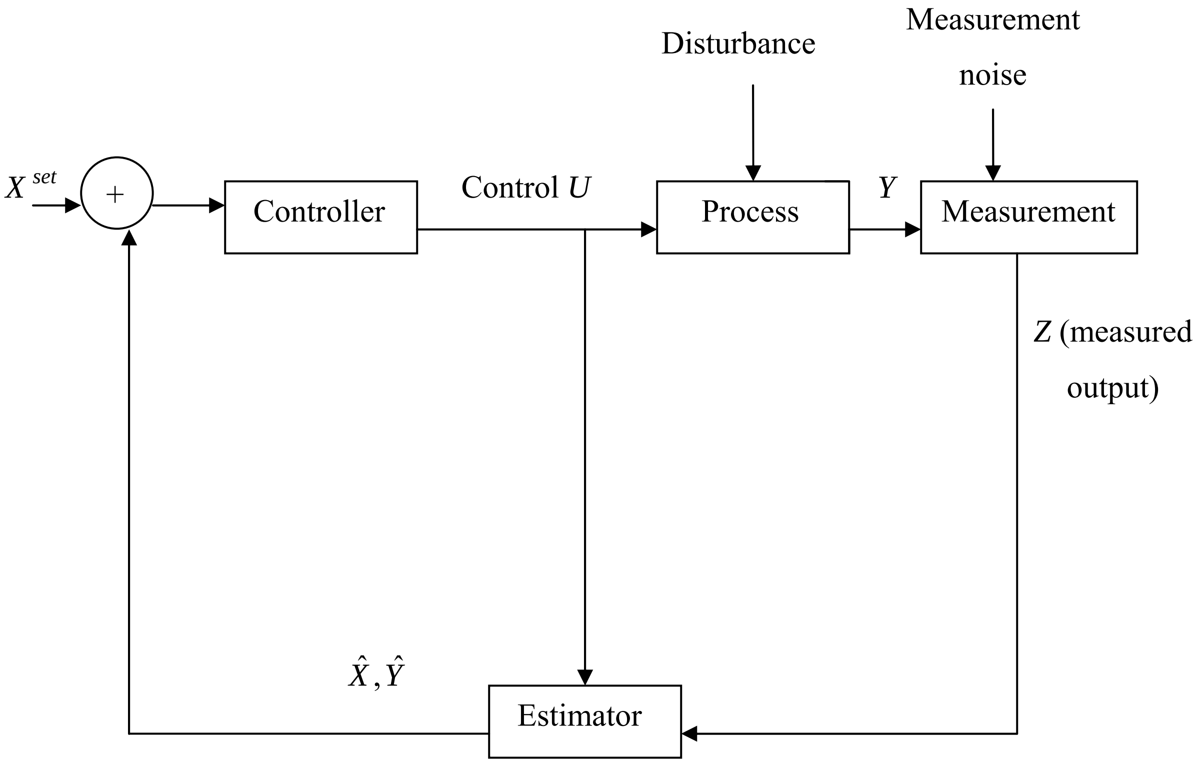
Disturbance
Measurement noise
X^{set}
+
Controller
Control U
Process
Y
Measurement
Z (measured output)
$\hat{X}, \hat{Y}$
Estimator

Figure 7.1 The estimator-based control system structure.

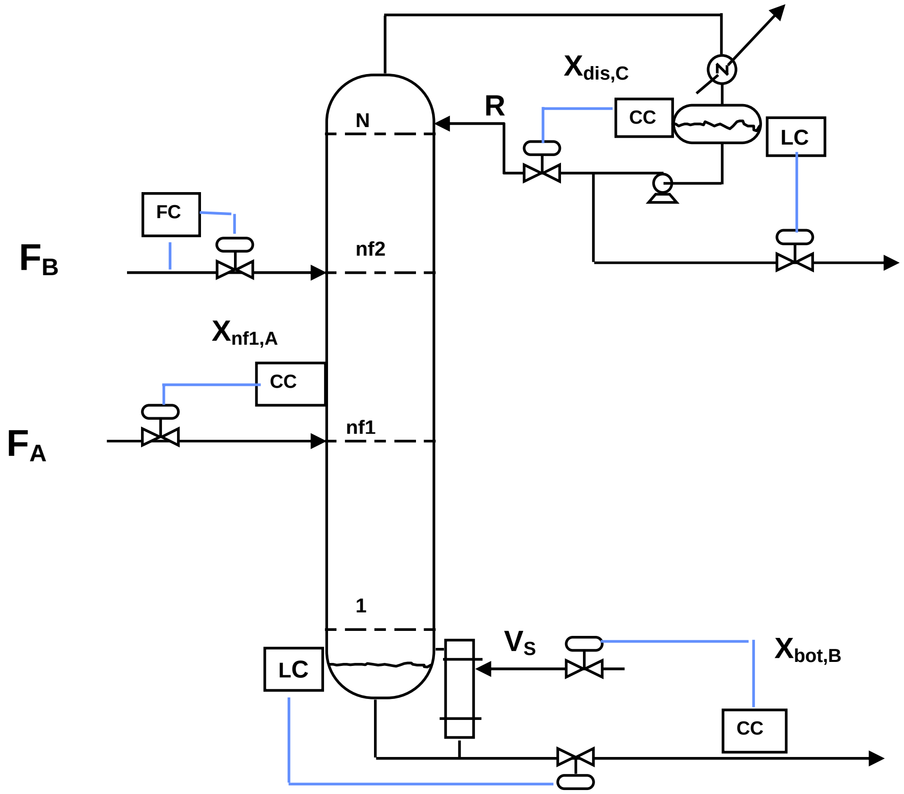
X_dis,C
R
CC
LC
N
FC
F_B
nf2
X_nf1,A
CC
F_A
nf1
1
V_S
X_bot,B
LC
CC

Figure 7.2 Dual-end control structure.

All of the control valves are designed to be half open at the initial steady state. Therefore, all of the manipulated variables cannot increase more than twice their steady state values.

In order to assess the performance of the estimator-based control system, two control configurations are developed and compared as follows:

(I) CS-Analyzer: In this control system, the desired states (liquid compositions) feed into the controllers are assumed to be perfectly available at any desired time using online analyzers. This control structure is considered in this work only to serve as a reference to which the performance of the estimator-based control system is compared. The three composition controllers' equations in CS-Analyzer are of the form

$$F_A = f_A(x_{nf1,A}) \tag{7.9}$$

$$Vs = f_v(x_{bot,D}) \tag{7.10}$$

$$R = f_R(x_{dis,C}) \tag{7.11}$$

Therefore, equations 7.1, 7.2 and 7.9-7.11 make the closed-loop system with perfect online analyzer available for composition measurements.

(II) CS-Estimator: This control structure is referred to as "the controller-estimator configuration". The states of the process are being estimated by the state estimator and are provided into the controllers for necessary decisions (see Figure 7.1). Therefore, equation 7.9-7.11 will be replaced the following equations:

$$F_A = f_A(\hat{x}_{nf1,A}) \tag{7.12}$$

$$Vs = f_v(\hat{x}_{bot,D}) \tag{7.13}$$

$$R = f_R(\hat{x}_{dis,C}) \tag{7.14}$$

where the $\hat{x}$ is the estimated state that comes from the estimator described by equation 7.3-7.6. Note that the equations 7.7, 7.8 and 7.12 - 7.14 make the CS-Estimator system.

7.5 Results and Discussion

A constant liquid holdup of 1 kmol in all of the trays and 10 kmol in both the partial reboiler and the total condenser are assumed throughout the simulation. Table 7.1 gives the summary of the steady state operating conditions of the system under study. In this work, temperature measurements are evenly located on 11 stages out of the 22 stages. The noise-contaminated temperature measurements from the process are available to the state estimator at every 30 sec. The differential equations of the model were integrated using Euler method with a step size of 1 sec. Because the process model used in the KF algorithm is not perfect due to some simplifying assumptions that have been made, plant noise ($\delta_p = 1\%$) was present in all the simulations. The base initial condition errors and the measurement noise ($\delta_m = 10\%$) used in the design and implementation of for the state estimator are shown in Figure 7.3. The initial conditions error is the deviation of the initial condition estimates for estimators from that of the real plant model.

7.5.1 Control Performance

In order to examine the performance of the estimator-based control system when compare to that when the perfect analyzers are used in the feedback system, the following sources of disturbance into the system are considered:

(1) ±10%, ±20%, step changes in feed flowrate of reactant B.

(2) A Pseudo Rectangular Random Sequence (PRRS) forcing function shown in Figure 7.4.

Table 7.1 Base steady state conditions

	variables	steady state values
column specifications	pressure (bar)	9
	stripping section (N_S)	7
	reactive section (N_{RX})	6
	rectifying section (N_R)	7
equilibrium data	Relative volatilities: A/B/C/D	4/2/8/1
flowrates (kmol/s)	Feed rate of reactant A	0.0126
	Feed rate of reactant B	0.0126
	Vapor boil up	0.0285
	Reflux rate	0.0331
	Distillate	0.0126
	Bottoms	0.0126
X_{dis}	A	0.0467
	B	0.0033
	C	0.9500
	D	0.0000
X_{bot}	A	0.0018
	B	0.0482
	C	0.0000
	D	0.9500

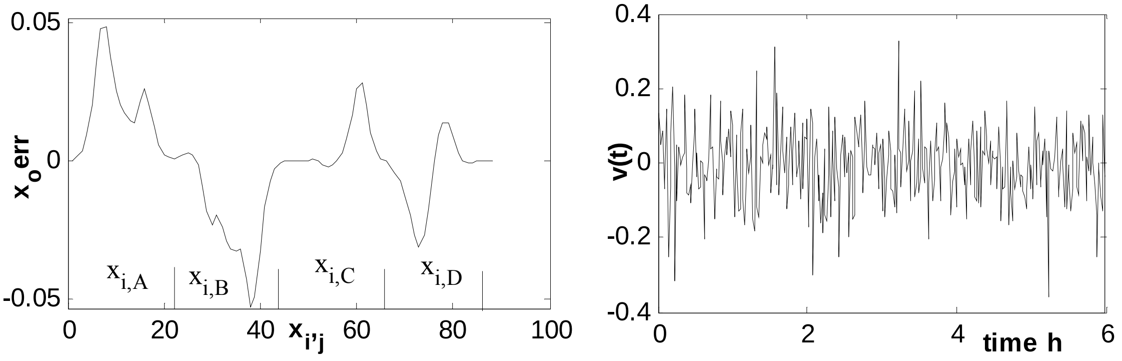

Figure 7.3 The base initial condition errors ($x_0 err$) and base measurement noise (v).

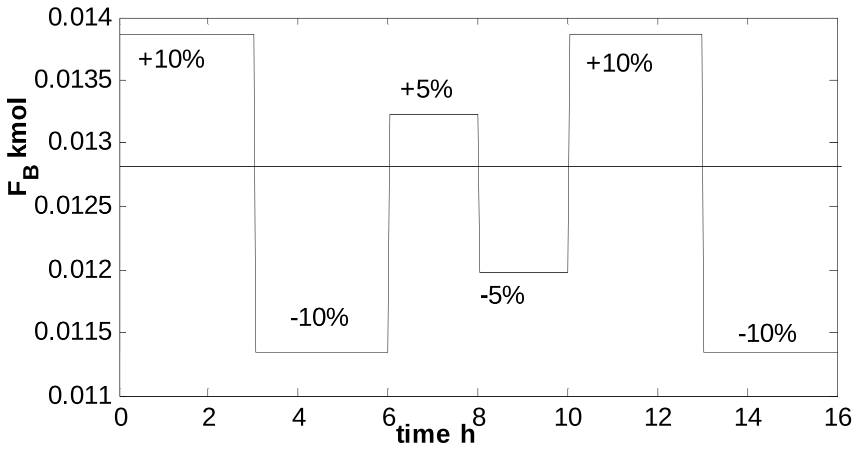

Figure 7.4 The Pseudo Rectangular Random Sequence (PRRS) forcing function on F_B.

Figure 7.5 compares the control performance of the system that relies on the state estimator (CS-Estimator) to that when perfect analyzer is assumed available (CS-Analyzer). The disturbance is a 10% increase and a 10% decrease in feed flowrate of reactant B. In this case, the composition of the component D in the bottoms, component C in the distillate and component A in the tray nf1 are being estimated (by the estimator) and feedback into the controllers for necessary actions. The results generally demonstrate that the controllers can successfully depend on the state estimates from the estimator for decision makings. The estimator-based system is able to reject the disturbance and drive the system to the desired operating specifications.

The control performance of the estimator-based system is seen to be relatively poor a few moment after the start up when compare to the control performance using direct measurement from the online analyzer. The reason for this is because of large estimation errors at the start up as a result of the errors in the initial conditions, measurement noise and plant-model uncertainties which will require some times to be compensated out. Because the gain matrix of the KF is calculated and updated online the response of the state estimator largely depends on system dynamics and the nature of disturbance input (i.e. large estimated errors at the early stage when -10% F_B is introduced). To further justify this and appreciate the use of the state estimator in the control system of reactive distillation, the system is excited by the function shown in Figure 7.4. The result of the CS-Estimator is compared to that of the CS-Analyzer in Figure 7.6. It can be seen clearly that after the state estimator overcomes the large estimation errors occurring at the early stage of the process, the response of the CS-

Estimator system gives an excellent matching with that of CS-Analyzer, which indicates good control performance.

It is interesting to note that the same trend of disturbance in the first 6 h (i.e. +10% F_B in the first 3 h and -10% F_B in the next 3 h of the operation was repeated between the time of 10 h to 16 h, but this time, the CS-Estimator responds adequately and the system is effectively controlled. This is because at the later time, the estimator has already overcome the effect of the initial estimate errors by updating the estimator gain based on the information from the updated estimated error covariance. Even if online analyzers are available and pose no problem in measuring the product composition at the two ends of the column, realistically the internal composition will be difficult to obtain using online analyzer and such a case could make the use of online estimator inevitable. Figure 7.7 illustrates that CS-Estimator performs well when the state estimator is used to estimate only the inaccessible internal composition for the internal composition controller. In this case, the product composition controllers use online perfect analyzers and the forcing function is a 20% increase and a 20% decrease in reactant B. The system generally demonstrates a better performance than when all the controllers depend on the state estimator.

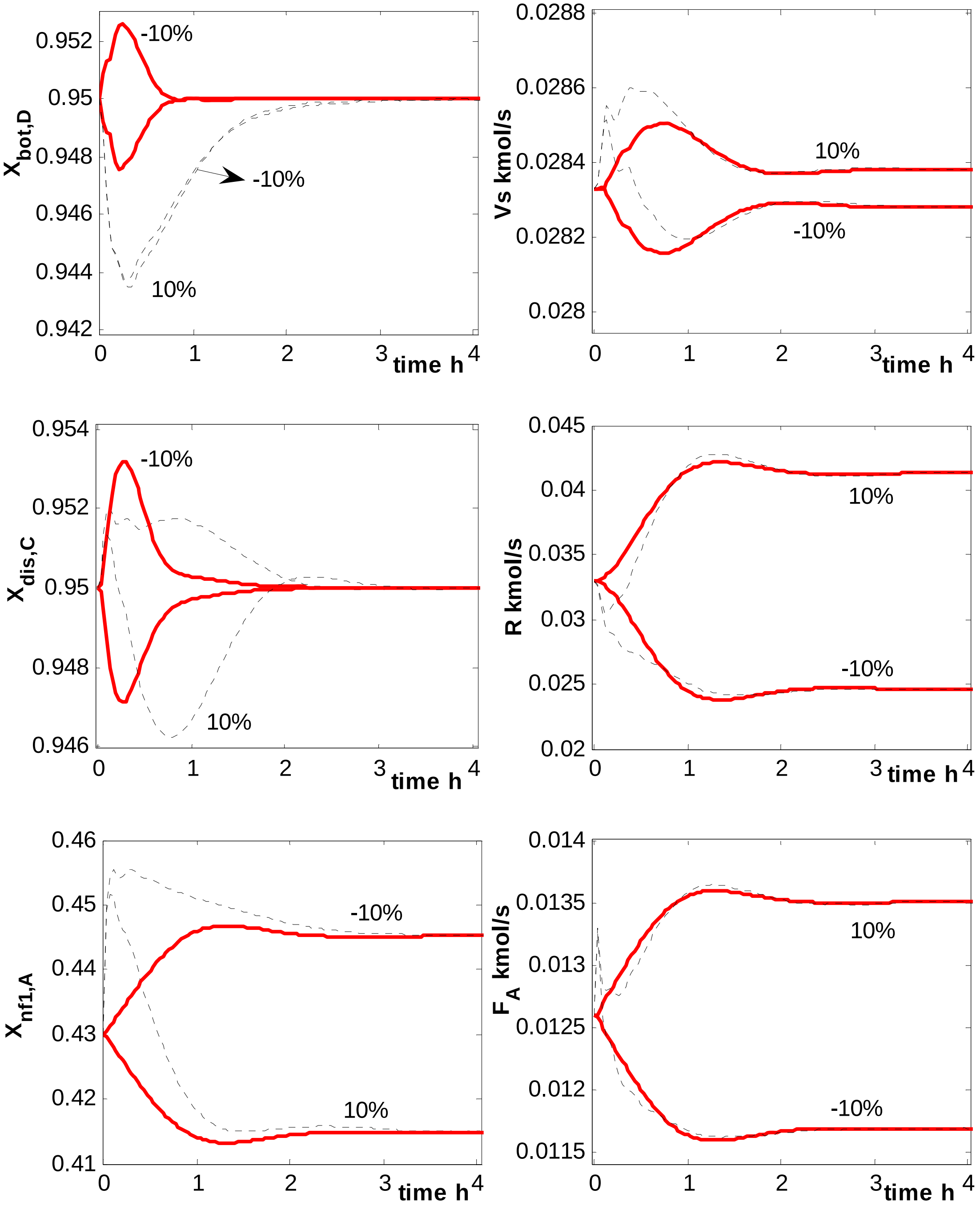

Figure 7.5 Control performance when all the composition controllers rely on the KF. The base initial condition errors, $\delta_m = 10\%$ and $\delta_p = 1\%$ are used for KF design. +10% and -10% F_B disturbance. (——) CS-Analyzer; (----) CS-Estimator.

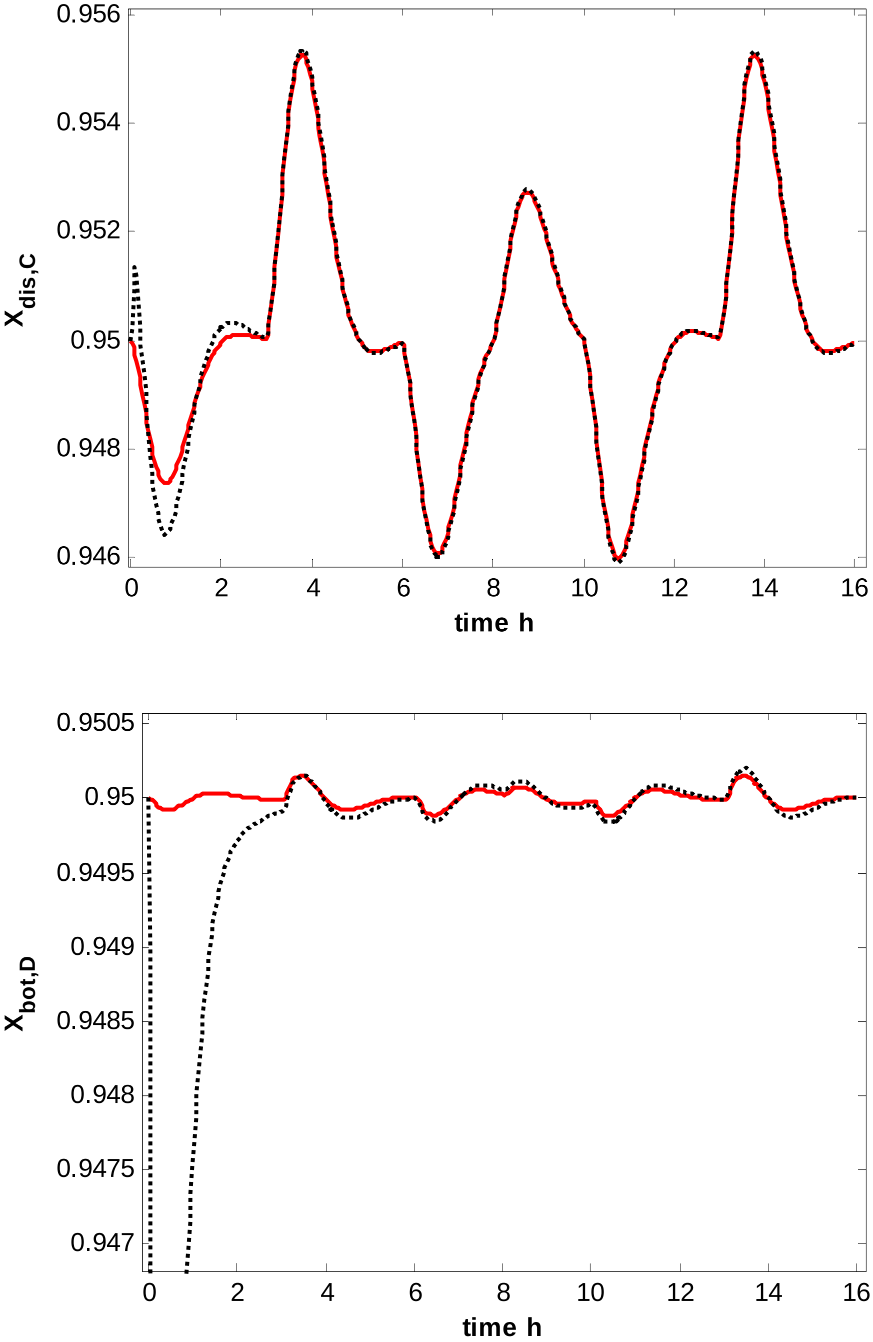

Figure 7.6 Control performance when all the composition controllers rely on the KF. The base initial condition errors, $\delta_m = 10\%$ and $\delta_p = 1\%$ are used for KF design. PRRS forcing function on F_B. (——) CS-Analyzer; (----) CS-Estimator.

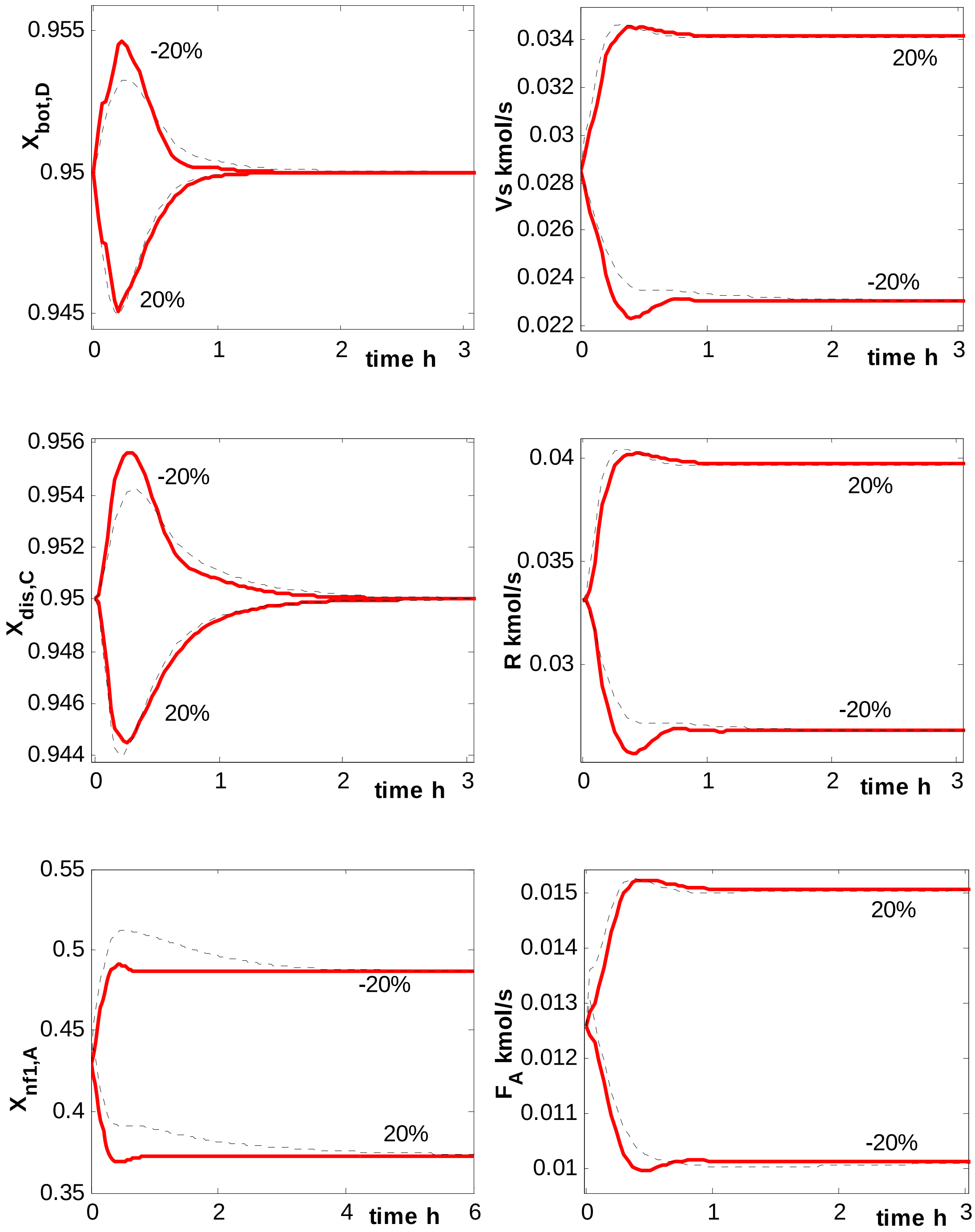

Figure 7.7 Control performances when the only internal composition controller relies on the KF: the base initial condition errors, $\delta_m = 10\%$ and $\delta_p = 1\%$ are used for KF design +20% and -20% F_B disturbance, (——) CS-Analyzer; (----) CS-Estimator.

7.5.2 Effect of Erroneous Initial Conditions

Because the actual initial conditions of the system is often not known in real situation, a state estimator must be designed to be able to converge to the actual column state on time when it is initialized with guessed initial conditions. In practice, what matter most are a few moments after a change is introduced into the system as the control system will intervene to reject introduced disturbance. In order to investigate the impact of erroneous initial conditions on the performance of the estimator and in turn, the control system as a whole, two set of erroneous initial conditions are tested as shown in Figure 7.8a. The first set of initial condition errors are taken to be four times in magnitude of the base initial condition errors ($4x_0err$), while the second set assumed an extreme case of equal composition of components in all stages (i.e. $\hat{X}(0) = 0.25/0.25/0.25/0.25$).

At first, the performance of the estimator in predicting the actual state is examined by simulating the open-loop dynamics of the system. This is to demonstrate that even though the estimator might be able to converge to the actual state at the long run using the worst set of initial conditions, the estimator accuracy at the early stage of the start up is important to the control system that relies on the state estimator. In the open-loop dynamics, all of the composition controllers are on manual, while the level controllers are automatic. In this test, the forcing function is a 10% increase in feed flowrate of reactant B. Figure 7.8 shows the performance of the state estimator to different set of initial conditions. Though, this result illustrates the capability of the state estimator to start from a guess or approximate initial conditions, however, it does show that the closer the initial estimates provided to the estimator, the better the performance.

The same set of initial conditions is then used to simulate the CS-Estimator system. Figure 7.9 shows the control performance of the CS-Estimator to different set of initial conditions. The CS-Estimator behaves predictably well in disturbance rejection when the first set of erroneous initial conditions are used. However, it can be seen clearly that in spite of the fact that the estimator is able to converge to the actual state in the open-loop dynamics case when equal composition of components is assumed at the initial point, the CS-Estimator behaves poorly and unable to control the system. The system that relies on such state estimator with worst initial conditions is unstable because the controllers use extremely poor estimated states at the early stage and as such could not control the system. Therefore, it is important to reduce the difference between the actual data and the estimated data in the short time possible following a disturbance so that the estimated data that the control system will use will be close to the actual plant data and thus an effective control could be achieved. One of the ways to do this is to use approximate initial conditions close enough to the true initial conditions of the actual system for the state estimators.

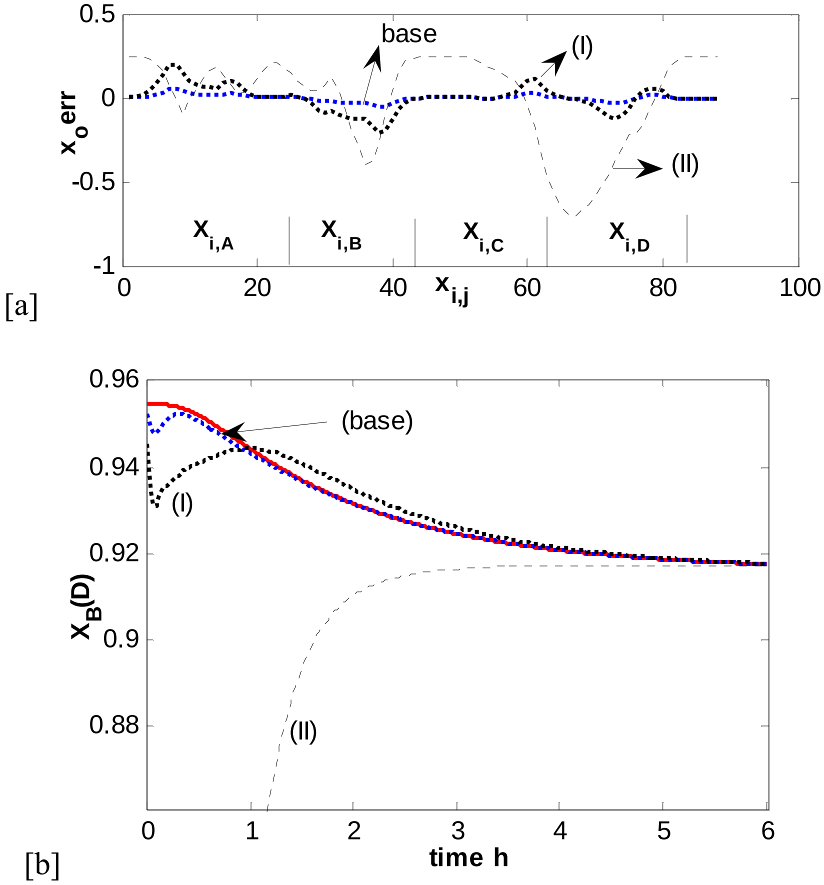

Figure 7.8 Effect of the erroneous initial conditions. [a] (I) $\hat{X}(0) = X_0 + 4x_0err$; (II) $\hat{X}(0) =$ 0.25/0.25/0.250.25. [b] Open-loop system response: 10% F_B disturbance, (——) actual state; (----) estimated state, $\delta_m = 10\%$ and $\delta_p = 1\%$ are used for KF design.

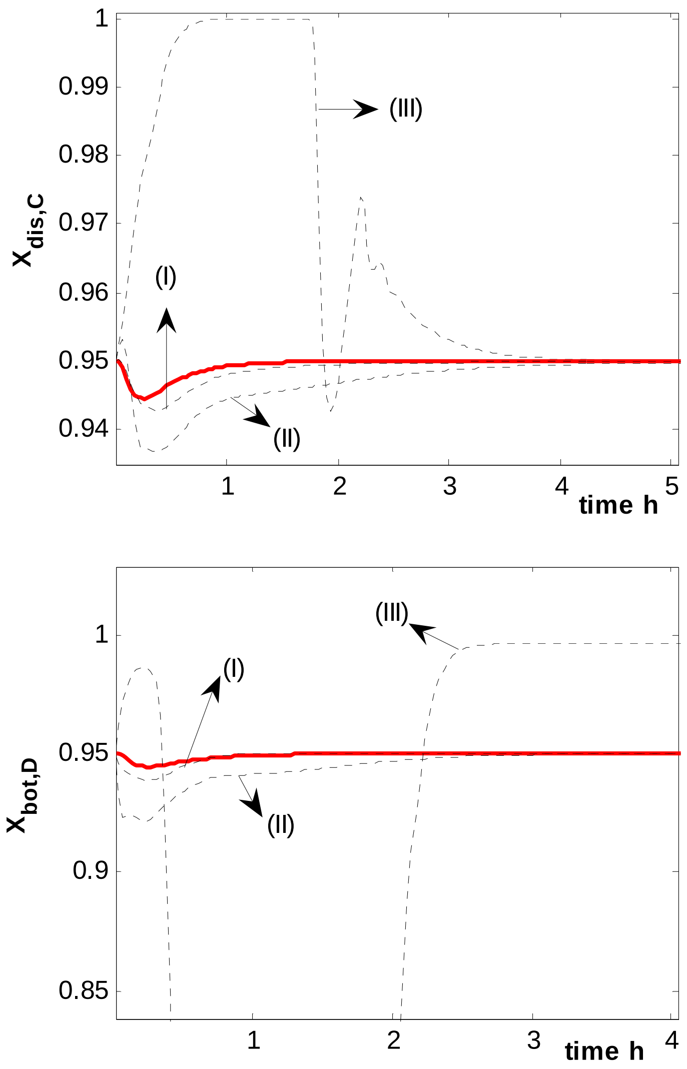

Figure 7.9 Effect of the erroneous initial conditions on the control performance: (I) $\hat{X}(0) = X_0 + x_0 err$; (II) $\hat{X}(0) = X_0 + 4x_0 err$;(III) $\hat{X}(0) =$ 0.25/0.25/0.25/0.25, 10% F_B disturbance, (——) CS-Analyzer; (----) CS-Estimator. $\delta_m = 10\%$ and $\delta_p = 1\%$ are used for KF design.

7.5.3 Effect of Measurement Error

In this Section, we are interested in assessing the effect of cyclical error in the temperature measurements. Unlike measurement noise, which is a stochastic and nondeterministic error of the sensors that cannot be predicted, cyclical errors are as a result of sensors imperfections and/or abnormal performance due to inaccurate settings. These types of errors are deterministic and repeatable. Figure 7.10 compares the control performance of CS-Estimator to that of CS-Analyzer when +1 ^{0}C and -1 ^{0}C measurement errors present in the sensors located in the reboiler, tray nf1 and the top plate. The forcing is a 10% increase in the feed flowrate of reactant B. The CS-Estimator performs reasonably well in resisting the effect of the disturbance with an acceptable error in the desired compositions.

Generally, the end effect of the sensors errors depends on the error type. This can be best explained when considering how well the estimator is able to predict the actual column temperature based on the noise contaminated temperature data supplied by the sensors. This is illustrated in Figure 7.11, by comparing the tray nf1 temperature measured by the sensor ($T_{measured}$) and as predicted by the state estimator ($T_{estimated}$) to the actual temperature profile (T_{actual}). It can be seen that the high frequency noise was effectively attenuated by the in built filter the state estimator, but the effect of the present 1^{0}C bias in the measurement data was only reduced. Because the control systems are designed to follow the feedback signal from the state estimator (including its estimated errors) as well as possible, deterministic errors will carry through, at least in part, to the control system and corrupt the response output. Therefore, much effort must be given to using accurate sensors with minimal cyclical errors in building the estimator.

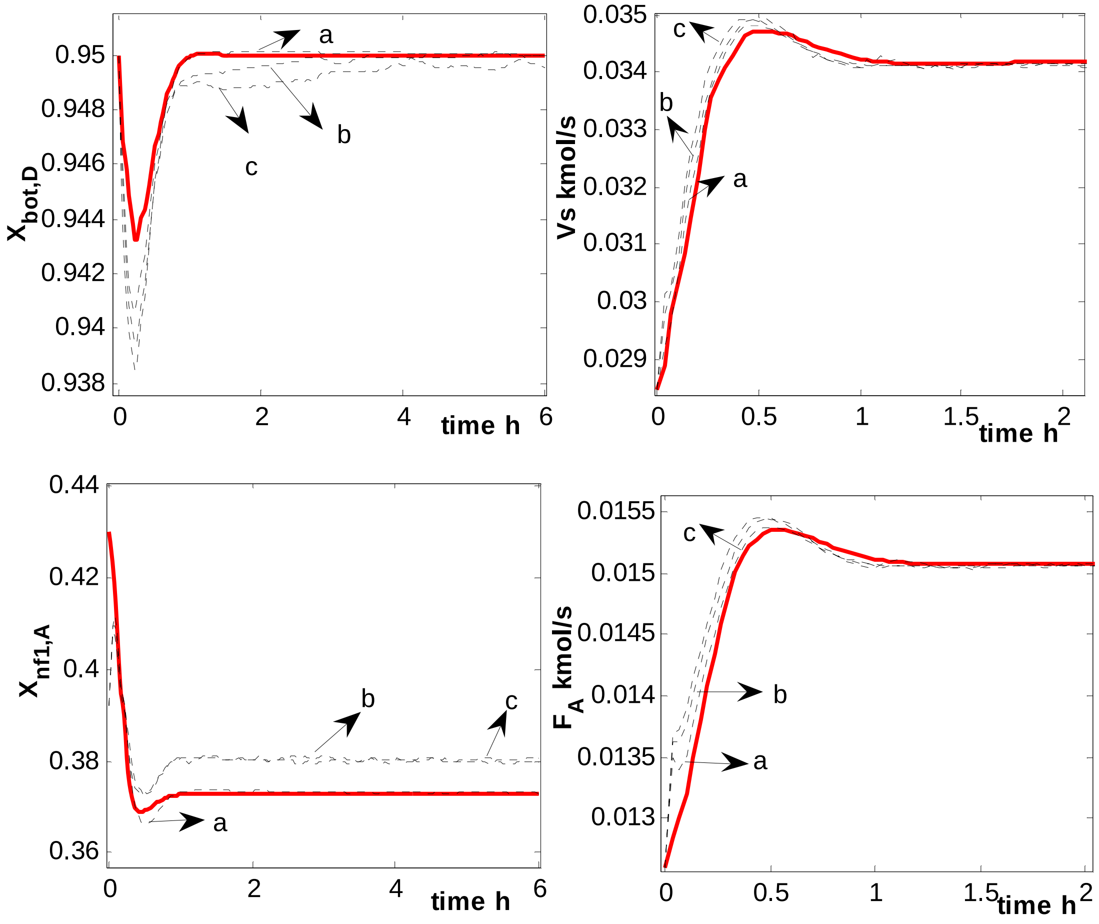

Figure 7.10 Effect of measurement error in the measurement data with a +10% F_B disturbance. The base initial condition errors, $\delta_m = 10\%$ and $\delta_p = 1\%$ are used for KF design. (——) CS-Analyzer; (----) CS-Estimator. (a) no error (b) +1 ^{0}C (c) -1 ^{0}C error located in 3 stages.

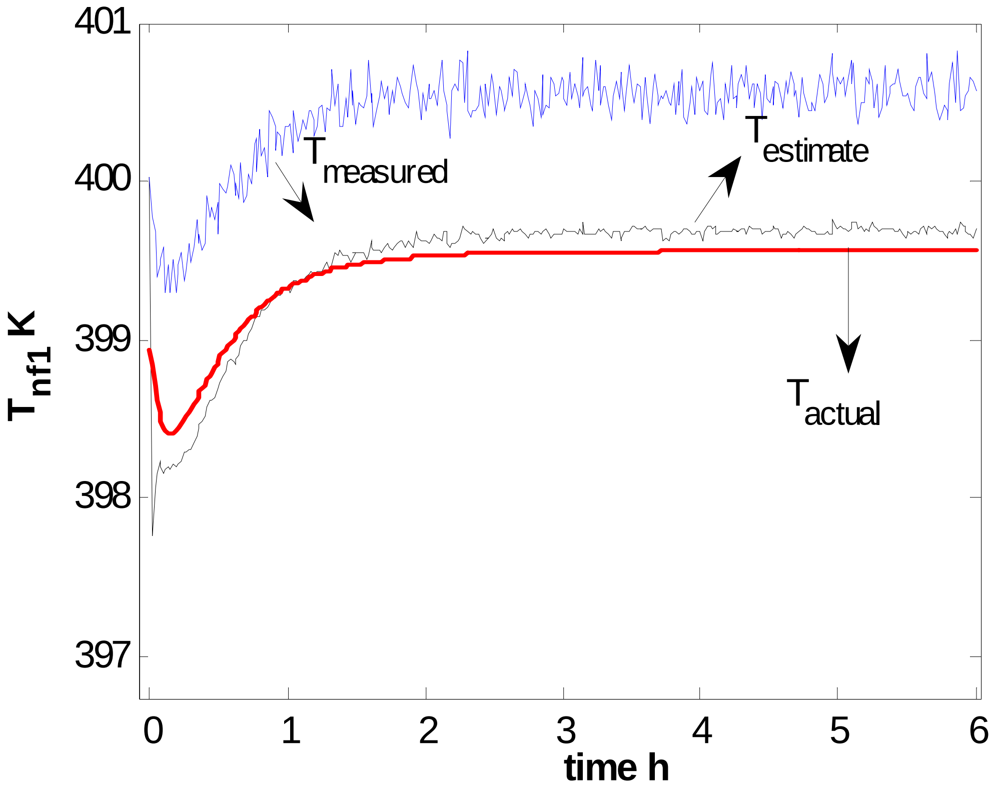

Figure 7.11 Temperature profile on tray nf1 of the CS-Estimator system. The measurement error of 1 ^{0}C present in the thermocouples located on the reboiler, the tray nf1 and the top plate. The base initial condition errors, $\delta_m = 10\%$ and $\delta_p = 1\%$ are used for KF design. +10% F_B disturbance.

7.5.4 Plant-Model mismatch

Though reactive distillation systems are generally known to have many advantages over the conventional multi-unit reaction/separation/recycle systems, they often possess complex dynamics and limited flexibility because of the interactive effect of reaction on separation. For a state estimator that relies heavily on such system dynamics, the effect of plant-model mismatch is essential to be investigated. Model mismatch has considerable effects on the performance of a closed-loop distillation system[7].

Uncertainties in relative volatility have significant effects on the design and performance of reactive distillation [8]. Therefore inaccurate modeling of the reaction kinetics and vapor-liquid equilibrium (VLE) relation can consequently affect the performance of the state estimators [2, 3, 8, 9]. To illustrate this, we have considered the effect of errors in the components relative volatilities, which in practice, are usually known with some uncertainties. The relative volatilities of the components in the real plant model are as given in Table 1. Two set of erroneous relative volatilities are tested as follows:

(I) $\hat{\alpha} = 3.9/1.9/7.9/1$, where the error of -0.1 is made in the component relative volatilities.

(II) $\hat{\alpha} = 4.1/2.1/8.1/1$, where the error of +0.1 is made in the component relative volatilities.

Using these set of relative volatilities in the estimator model means that the system dynamics has been altered by inaccurate vapor-liquid relationship parameters. The resulting control performance of CS-Estimator under the effect of erroneous relative volatilities is shown in Figure 7.12. It can be seen clearly that inaccurate vapor-liquid representation has a severe effects on the control performance of the CS-Estimator system. Therefore an adequate representation of the VLE relations is very important and a necessity to the successful application of the estimator in the control system of reactive distillation.

7.6 Conclusion

This chapter demonstrates that a state estimator can be successfully designed and implemented in the feedback control system of reactive distillation. The work of the state estimator is to provide the state compositions that are required to be used by the controller for necessary action. The control performance of the system that relies on the state estimator is examined and compared to that of the system which takes direct measurement from the process assuming the availability of perfect online analyzer. The robustness of the estimator-based system is investigated against measurement errors, model uncertainties and erroneous initial conditions.

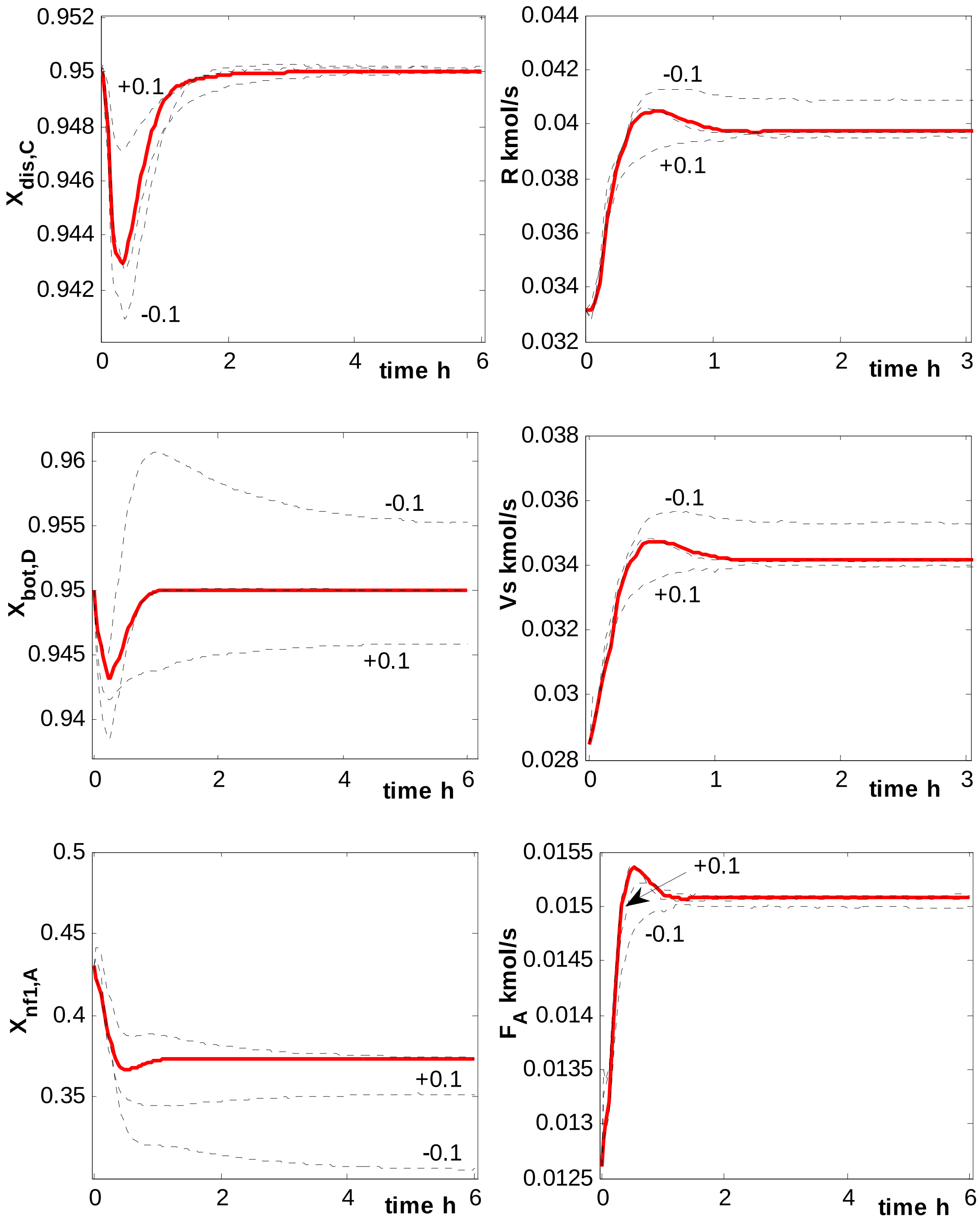

Figure 7.12 Effect of errors in relative volatility. The base initial condition errors, $\delta_m = 10\%$ and $\delta_p = 1\%$ are used for KF design. +10%F_B disturbance. (——) CS-Analyzer; (----) CS-Estimator.

7.7 References

[1] M. A. Al-Arfaj and W. L. Luyben, "Comparison of alternative control structures for an ideal two-product reactive distillation column," *Ind. Eng. Chem. Res.*, vol. 39, pp. 3298-3307, 2000.

[2] R. Baratti, A. Bertucco, D. Alessandro, and M. Morbidelli, "Development of a composition estimator for binary distillation columns. Application to a pilot plant," *Chem. Eng. Sci.*, vol. 50, pp. 1541-1550, 1995.

[3] R. Baratti, A. Bertucco, D. Alessandro, and M. Morbidelli, "A composition estimator for multicomponent distillation columns development and experimental test on ternary mixtures," *Chem. Eng. Sci.*, vol. 53, pp. 3601-3612, 1998.

[4] R. M. Oisiovici and S. L. Cruz, "State estimation of batch distillation columns using an extended Kalman filter," *Chem. Eng. Sci.*, vol. 55, pp. 4667-4680, 2000.

[5] H. W. Sorenson, "Kalman filtering: Theory and application." New York: IEEE Press, 1985.

[6] B. D. Tyreus and W. L. Luyben, "Tuning PI Controllers for integrator/dead time processes," *Ind. Eng. Chem. Res.*, vol. 31, pp. 2625-2628, 1992.

[7] L. Ruokang and J. H. Olson, "Fault detection and diagnosis in a closed-loop nonlinear distillation process: application of an extended Kalman filters," *Ind.Eng.Chem.Res.*, vol. 30, pp. 898-908, 1991.

[8] D. B. Kaymak and W. L. Luyben, "Effect of relative volatility on the quantitative comparison of reactive distillation and conventional multi-unit systems," *Ind. Eng. Chem. Res*, vol. 43, pp. 3151-3162, 2004.

[9] D. B. Kaymak and W. L. Luyben, "Effect of the chemical equilibrium constant on the design of reactive distillation columns," *Ind. Eng. Chem. Res*, vol. 43, pp. 3666-3671, 2004.

CHAPTER 8

8 Conclusions and Future Research Directions

8.1 Conclusions

The design and implementation of the linear state estimators and their applications in reactive distillation control are explored in this thesis work. A state estimator is required to infer the useful but inaccessible liquid composition in the reactive distillation column from the available process variables. The state estimates from the estimator are provided to the online controllers without the use of the unreliable composition analyzers.

First, a comprehensive formulation of the linear and nonlinear process models is presented for a generic two-reactant-two-product reactive distillation. The dynamic behavior of a linear process model is assessed by comparing its performance to that of a rigorous nonlinear process model. The impact of disturbance magnitudes and direction on the system dynamics are studied. It is found that operating two-reactant-two-product reactive distillation with excess of the heavy reactant enhances open-loop stability, but decreases the products purity. On the other hand, excess of more volatile reactant drifts the system to another state.

Second, the closed-loop performance of the three alternative control structures when based on a linear process model is compared to that when based on a nonlinear process model for a generic two-product reactive distillation. It is shown that an approximate linear model behaves essentially similar to a nonlinear model in a closed-loop system when the deviation of process variables resulting from the disturbance is within the region of the base steady state. It is found that the linear process model could be used in the design of a robust control system when the control valves are designed to handle the underestimation problem of the manipulated variables.

Third, two alternative state estimator design methods (i.e., a Kalman filter and a Luenberger observer) are explored and the accuracy of the developed state estimators is checked by comparing the state estimates with the actual states as predicted by the process model of the reactive distillation system. The robustness and reliability of the state estimators are demonstrated with respect to an erroneous initial condition, the measurement noise and plant-model uncertainties.

Lastly, it is demonstrated that a state estimator can be successfully designed and implemented in the feedback control system of reactive distillation. The work of the state estimator is to provide the state compositions that are required to be feedback into the controllers for the necessary actions. The control performance of the system that relies on the state estimator is examined and compared to that of the system which takes direct measurement from the process, assuming the availability of perfect online analyzer. The robustness of the estimator-based system is investigated against the measurement errors, model uncertainties and erroneous initial conditions.

8.2 Future Research Directions

New and challenging problems that have potential future research value are identified throughout this thesis work and are summarized as follows:

- **Developing more accurate but complex nonlinear process model for a reactive distillation:** In this work, we have used a simplified nonlinear process model to describe an ideal reactive distillation. Because the results in this work has shown us that the performance of a state estimator is a strong dependant of the process model from which it is developed, there is need to formulate more accurate nonlinear process models by removing some of the assumptions made in this work. For instance, nonideal vapor-liquid equilibrium relation, tray efficiency and energy balance equation should be considered in the modeling stage of a reactive distillation.
- **Development of a nonlinear state estimator from a nonlinear process model:** The complexity nature of a typical reactive distillation process and the desire to operate the system over a wide range of operating conditions will necessitate the study of nonlinear state estimators and their applicability in the reactive distillation control. The nonlinear state estimators can cope with the intrinsic nonlinearities when the system is operated under a wide range of operating conditions. Without doubt, the nonlinear estimators will severely increase the complexity of the system and demand effective computational resources.
- **The applicability of the developed estimator-based control system to a reactive distillation of a real chemical system:** Future research work is required to apply the developed state estimators in the composition estimation of reactive distillation for a specific chemical system, such as the production of MTBE, ETBE and TAME. In the real chemical systems, introducing the complex kinetics relations of a specific chemical reaction and vapor-liquid equilibrium relation will

add complexity to the reactive distillation model and pose more challenge in the design and implementation of a state estimator.

- **Development of an adaptive state estimator:** Although it is demonstrated that a Kalman filter is robust towards erroneous initial conditions, model uncertainties and measurement errors, it however assumes that the errors statistical characteristics are known. Thus future research is expected to focus on the design of “adaptive extended Kalman filter estimator” to take care of more practical situation of unknown errors statistics and disturbances.
- **Implementation of a state estimator on different types of control structures:** The developed estimators can be further tested by implementing them on other control structures such as: a state feedback control where all of the estimated states are used by the controllers, a single-end composition control structure, and a cascade control system.

NOMENCLATURE

A = reactant component

A = matrix of state variables of the linearized process

B = matrix of inputs of the linearized process

B = reactant component

B = bottoms flowrate (kmol/s)

C = matrix of outputs of the linearized process

C = product component

CC = composition controller

d = disturbance variables vector

D = distillate flowrate (kmol/s)

E = matrix of the disturbance input

F_A= fresh feed flowrate of reactant A (kmol/s)

F_B= fresh feed flowrate of reactant B (kmol/s)

FC = Flow controller

FT = Flow transmitter

I = gain matrix

I = unit matrix

K = gain matrix

K_F = specific reaction rate of the forward reaction ($kmol.s^{-1}.kmol^{-1}$)

K_B = specific reaction rate of the reverse reaction ($kmol.s^{-1}.kmol^{-1}$)

KF= Kalman filter

L = liquid flowrate (kmol/s)

LC = level controller

$\overline{L_i}$ = liquid flowrate at the steady state

LO= Luenberger observer

M_i = liquid holdup in all stages (kmol)

$\overline{M}_i$ = liquid holdup at the steady state

Nc = total number of components

N = total number of stages including reboiler and reflux drum

n= total states variable (n=N x Nc)

N_R = number of stages in rectifying section

N_{RX} = number of stages in reactive section

N_S = number of stages in striping section

nf1= first tray of reactive section (entrance of feed F_A)

nf2= last tray of reactive section (entrance of feed F_B)

P= covariance matrix for estimation error

$\hat{P}$ = estimated covariance matrix

P = column pressure.

q = number of output measurements

Q = model error covariance matrix.

R = reflux flowrate (kmol/s)

R_k = measurement error covariance matrix.

R_i = rate of production on tray i (kmol /s)

t = time (s)

T_i = temperature in stage i including reboiler (K)

T_{dev} = temperature in deviation form

TR = total reaction rate (kmol/s)

U= input variables vector

v = measurement noise

V_i = vapor flowrate from the reactive tray i (kmol/s)

V_S = vapor flowrate from reboiler (kmol/s)

w = plant noise

$x_{i,j}$ = liquid mole fraction of component j on tray i

X = state vector of the variables.

$\hat{X}$ = state estimate vector.

$X_{bot,D}$ = composition of D in the bottom

$X_{dis,C}$ = composition of C in the distillate

$X_{dev,A}$ = composition of A in deviation form

$X_{dev,B}$ = composition of B in deviation form

$X_{dev,C}$ = composition of C in deviation form

$X_{dev,D}$ = composition of D in deviation form

$X_{nf1,A}$ = composition of A on tray nf1

$X_{nf1,B}$ = composition of B on tray nf2

x_{ij} = liquid mole fraction of component j in tray i

X_0 = initial state vector

x' = liquid mole fraction in deviation form

$X_B(D)$ = composition of D in the bottoms

$X_D(C)$ = composition of C in the distillate

$X_{nf1}(A)$ = composition of A in tray nf1

X_0 = initial conditions of the plant model

$x_0 err$ =initial condition error vector

X^{set} = Vector of the controlled variables setpoint

Y = output vector

$\hat{Y}$ = observation vector

Y = vector of the outputs

Y' = output variables in deviation form

$y_{i,j}$ = vapor mole fraction of component j in tray i

Z = measured output vector

Z_a = composition of fresh feed F_A

Z_b = composition of fresh feed F_B

Greek letters

α_j = relative volatility of component j with respect to heavy component

$\hat{\alpha}$ = approximate relative volatilities

ΔH_V = heat of vaporization (cal/mol)

λ = heat of reaction (cal/mol)

δ = standard deviation

δ_m = of the measurement noise

δ_p = standard deviation of the plant noise

δ_{kj} = the Kronecter delta

θ = lumped model parameters.

β hydraulic time constant

α_j relative volatility of component j with respect to heavy component

ΔH_V heat of vaporization (cal/mol)

λ heat of reaction (cal/mol)

θ system constant parameters.

APPENDICES

Appendix A

Entries of Matrices A

State vector:

$$X = \left[x_{1,1}, x_{2,1} \ldots x_{N,1}, x_{1,2}, x_{2,2} \ldots x_{N,2}, x_{1,3}, x_{2,3}, \ldots x_{N,3}, x_{1,4}, x_{2,4}, \ldots x_{N,4,} M_1, M_2, \ldots M_N\right]^T$$

where the first subindex is the stage number and the second is the component number. The stages are numbered from bottom to top.

The $a_{i,j}$ elements of matrix A are given by:

A-1. Reboiler:

$$a_{11} = \frac{-L_2 + V_S\left(1 - dy_{1,11}\right)}{M_1} \qquad a_{1,N+1} = -\left({}^{V_S}\!/_{M_1}\right) dy_{1,12} \qquad a_{1,2N+1} = -\left({}^{V_S}\!/_{M_1}\right) dy_{1,13}$$

$$a_{1,3N+1} = -\left({}^{V_S}\!/_{M_1}\right) dy_{1,14} \qquad a_{12} = \frac{L_2}{M_1} \qquad a_{1,4N+2} = \frac{(x_{21} - x_{11})}{M_1 \beta}$$

$$a_{1,4N+1} = -\frac{\left[L_2\left(x_{21} - x_{11}\right) + V_S\left(x_{11} - y_{11}\right)\right]}{M_1^2} \qquad a_{N+1,N+1} = \frac{-L_2 + V_S\left(1 - dy_{1,22}\right)}{M_1}$$

$$a_{N+1,2N+1} = -\left({}^{V_S}\!/_{M_1}\right) dy_{1,23} \qquad a_{N+1,3N+1} = -\left({}^{V_S}\!/_{M_1}\right) dy_{1,24} \qquad a_{N+1,N+2} = \frac{L_2}{M_1}$$

$$a_{N+1,4N+2} = \frac{(x_{22} - x_{12})}{M_1 \beta} \qquad a_{N+1,4N+1} = -\frac{\left[L_2\left(x_{22} - x_{12}\right) + V_S\left(x_{12} - y_{12}\right)\right]}{M_1^2}$$

$$a_{2N+1,1} = -\left({}^{V_S}\!/_{M_1}\right) dy_{1,31} \qquad a_{2N+1,N+1} = -\left({}^{V_S}\!/_{M_1}\right) dy_{1,32} \qquad a_{2N+1,2N+1} = \frac{-L_2 + V_S\left(1 - dy_{1,33}\right)}{M_1}$$

$$a_{2N+1,3N+1} = -\left({}^{V_S}\!/_{M_1}\right) dy_{1,34} \qquad a_{2N+1,2N+2} = \frac{L_2}{M_1} \qquad a_{2N+1,4N+2} = \frac{(x_{23} - x_{13})}{M_1 \beta}$$

$$a_{2N+1,4N+1} = -\frac{\left[L_2\left(x_{23}-x_{13}\right)+V_S\left(x_{13}-y_{13}\right)\right]}{M_1^2} \qquad a_{3N+1,1} = -\left({}^{V_S}\!/\!{}_{M_1}\right)dy_{1,41}$$

$$a_{3N+1,N+1} = -\left({}^{V_S}\!/\!{}_{M_1}\right)dy_{1,42} \quad a_{3N+1,2N+1} = -\left({}^{V_S}\!/\!{}_{M_1}\right)dy_{1,43} \quad a_{3N+1,3N+1} = \frac{-L_2+V_S\left(1-dy_{1,44}\right)}{M_1}$$

$$a_{3N+1,3N+2} = \frac{L_2}{M_1} \quad a_{3N+1,4N+2} = \frac{\left(x_{24}-x_{14}\right)}{M_1\beta} \qquad a_{3N+1,4N+1} = -\frac{\left[L_2\left(x_{24}-x_{14}\right)+V_S\left(x_{14}-y_{14}\right)\right]}{M_1^2}$$

$$a_{4N+1,4N+2} = \frac{-2B}{M_1}, \qquad a_{4N+1,4N+1} = \frac{1}{\beta}$$

A-2. Stripping Section (Tray *i*):

$$a_{i,i-1} = \left({}^{V_S}\!/\!{}_{M_i}\right)dy_{i-1,11} \qquad a_{i,N+i-1} = \left({}^{V_S}\!/\!{}_{M_i}\right)dy_{i-1,12} \qquad a_{i,2N+i-1} = \left({}^{V_S}\!/\!{}_{M_i}\right)dy_{i-1,13}$$

$$a_{i,3N+i-1} = \left({}^{V_S}\!/\!{}_{M_i}\right)dy_{i-1,14} \quad a_{i,i} = \frac{-\left(L_{i+1}+V_S\,dy_{i,11}\right)}{M_i} \qquad a_{i,N+i} = -\left({}^{V_S}\!/\!{}_{M_i}\right)dy_{i,12}$$

$$a_{i,2N+i} = -\left({}^{V_S}\!/\!{}_{M_i}\right)dy_{i,13} \qquad a_{i,3N+i} = -\left({}^{V_S}\!/\!{}_{M_i}\right)dy_{i,14} \qquad a_{i,i+1} = \frac{L_{i+1}}{M_i}$$

$$a_{i,4N+i} = -\frac{\left[L_{i+1}\left(x_{i+1,1}-x_{i,1}\right)+V_S\left(y_{i-1,1}-y_{i,1}\right)\right]}{M_i^2} \qquad a_{i,4N+i+1} = \frac{\left(x_{i+1,1}-x_{i,1}\right)}{M_i\beta}$$

$$a_{N+i,i-1} = \left({}^{V_S}\!/\!{}_{M_i}\right)dy_{i-1,21} \qquad a_{N+i,N+i-1} = \left({}^{V_S}\!/\!{}_{M_i}\right)dy_{i-1,22} \qquad a_{N+i,2N+i-1} = \left({}^{V_S}\!/\!{}_{M_i}\right)dy_{i-1,23}$$

$$a_{N+i,3N+i-1} = \left({}^{V_S}\!/\!{}_{M_i}\right)dy_{i-1,24} \quad a_{N+i,i} = -\left({}^{V_S}\!/\!{}_{M_i}\right)dy_{i,21} \qquad a_{N+i,N+i} = \frac{-\left(L_{i+1}+V_S\,dy_{i,22}\right)}{M_i}$$

$$a_{N+i,2N+i} = -\left({}^{V_S}\!/\!{}_{M_i}\right)dy_{i,23} \qquad a_{N+i,3N+i} = -\left({}^{V_S}\!/\!{}_{M_i}\right)dy_{i,24} \qquad a_{N+i,N+i+1} = \frac{L_{i+1}}{M_i}$$

$$a_{N+i,4N+i} = -\frac{\left[L_{i+1}\left(x_{i+1,2}-x_{i,2}\right)+V_S\left(y_{i-1,2}-y_{i,2}\right)\right]}{M_i^2} \qquad a_{N+i,4N+i+1} = \frac{\left(x_{i+1,2}-x_{i,2}\right)}{M_i\beta}$$

$$a_{2N+i,i-1} = \left({}^{V_S}\!/\!{}_{M_i}\right)dy_{i-1,31} \quad a_{2N+i,N+i-1} = \left({}^{V_S}\!/\!{}_{M_i}\right)dy_{i-1,32} \quad a_{2N+i,2N+i-1} = \left({}^{V_S}\!/\!{}_{M_i}\right)dy_{i-1,33}$$

$$a_{2N+i,3N+i-1} = \left({}^{V_S}\!/\!{}_{M_i}\right)dy_{i-1,34} \quad a_{2N+i,i} = -\left({}^{V_S}\!/\!{}_{M_i}\right)dy_{i,31} \quad a_{2N+i,N+i} = -\left({}^{V_S}\!/\!{}_{M_i}\right)dy_{i,32}$$

$$a_{2N+i,2N+i} = \frac{-\left(L_{i+1} + V_S\, dy_{i,33}\right)}{M_i} \qquad a_{2N+i,3N+i} = -\left({}^{V_S}\!/_{M_i} \right) dy_{i,34} \qquad a_{2N+i,2N+i+1} = \frac{L_{i+1}}{M_i}$$

$$a_{2N+i,4N+i} = -\frac{\lfloor L_{i+1}\left(x_{i+1,3} - x_{i,3}\right) + V_S\,(y_{i-1,3} - y_{i,3})\rfloor}{M_i^2} \qquad a_{2N+i,4N+i+1} = \frac{(x_{i+1,3} - x_{i,3})}{M_i \beta}$$

$$a_{3N+i,i-1} = \left({}^{V_S}\!/_{M_i} \right) dy_{i-1,41} \qquad a_{3N+i,N+i-1} = \left({}^{V_S}\!/_{M_i} \right) dy_{i-1,42} \qquad a_{3N+i,2N+i-1} = \left({}^{V_S}\!/_{M_i} \right) dy_{i-1,43}$$

$$a_{3N+i,3N+i-1} = \left({}^{V_S}\!/_{M_i} \right) dy_{i-1,44} \qquad a_{3N+i,i} = -\left({}^{V_S}\!/_{M_i} \right) dy_{i,41} \qquad a_{3N+i,N+i} = -\left({}^{V_S}\!/_{M_i} \right) dy_{i,42}$$

$$a_{3N+i,2N+i} = -\left({}^{V_S}\!/_{M_i} \right) dy_{i,43} \qquad a_{3N+i,3N+i} = \frac{-\left(L_{i+1} + V_S\, dy_{i,44}\right)}{M_i} \qquad a_{3N+i,3N+i+1} = \frac{L_{i+1}}{M_i}$$

$$a_{3N+i,4N+i} = -\frac{\lfloor L_{i+1}\left(x_{i+1,4} - x_{i,4}\right) + V_S\,(y_{i-1,4} - y_{i,4})\rfloor}{M_i^2} \qquad a_{3N+i,4N+i+1} = \frac{(x_{i+1,4} - x_{i,4})}{M_i \beta}$$

$$a_{4N+i,4N+i} = -\frac{1}{\beta}, \qquad a_{4N+i,4N+i+1} = \frac{1}{\beta}$$

A-3. Reactive Section (tray *i*)

A-3.1. Feed tray for reactant A (*i* = nf1)

$$a_{i,i-1} = \left({}^{V_S}\!/_{M_i} \right) dy_{i-1,11} \qquad a_{i,N+i-1} = \left({}^{V_S}\!/_{M_i} \right) dy_{i-1,12}$$

$$a_{i,2N+i-1} = \left({}^{V_S}\!/_{M_i} \right) dy_{i-1,13} \qquad a_{i,3N+i-1} = \left({}^{V_S}\!/_{M_i} \right) dy_{i-1,14}$$

$$a_{N+i,i-1} = \left({}^{V_S}\!/_{M_i} \right) dy_{i-1,21} \qquad a_{N+i,N+i-1} = \left({}^{V_S}\!/_{M_i} \right) dy_{i-1,22}$$

$$a_{N+i,2N+i-1} = \left({}^{V_S}\!/_{M_i} \right) dy_{i-1,23} \qquad a_{N+i,3N+i-1} = \left({}^{V_S}\!/_{M_i} \right) dy_{i-1,24}$$

$$a_{2N+i,i-1} = \left({}^{V_S}\!/_{M_i} \right) dy_{i-1,31} \qquad a_{2N+i,N+i-1} = \left({}^{V_S}\!/_{M_i} \right) dy_{i-1,32}$$

$$a_{2N+i,2N+i-1} = \left({}^{V_S}\!/_{M_i} \right) dy_{i-1,33} \qquad a_{2N+i,3N+i-1} = \left({}^{V_S}\!/_{M_i} \right) dy_{i-1,34}$$

$$a_{3N+i,i-1} = \left(V_S \big/ M_i\right) dy_{i-1,41} \qquad a_{3N+i,N+i-1} = \left(V_S \big/ M_i\right) dy_{i-1,42}$$

$$a_{3N+i,2N+i-1} = \left(V_S \big/ M_i\right) dy_{i-1,43} \qquad a_{3N+i,3N+i-1} = \left(V_S \big/ M_i\right) dy_{i-1,44}$$

A-3.2. Reactive trays (for *i* ≠ nf1)

Subindex *k* is referring to reactive tray *i*.

For *k*= 1 to *i*-(Ns+2) . $\delta(k) = 0$ for all *k*, except when *k* =1 where $\delta(1) = 1$

$$a_{i,i-k} = \frac{\delta(k)V_{(i-k)}\left(dy_{i-1,11}\right) + \Delta V1_{(i-k)}(y_{i-1,1} - x_{i,1}) + \Delta V1_{(i-k)}(x_{i,1} - y_{i,1})}{M_i}$$

$$a_{i,N+i-k} = \frac{\delta(k)V_{(i-k)}\left(dy_{i-1,12}\right) + \Delta V2_{(i-k)}(y_{i-1,1} - x_{i,1}) + \Delta V2_{(i-k)}(x_{i,1} - y_{i,1})}{M_i}$$

$$a_{i,2N+i-k} = \frac{\delta(k)V_{(i-k)}\left(dy_{i-1,13}\right) + \Delta V3_{(i-k)}(y_{i-1,1} - x_{i,1}) + \Delta V3_{(i-k)}(x_{i,1} - y_{i,1})}{M_i}$$

$$a_{i,3N+i-k} = \frac{\delta(k)V_{(i-k)}\left(dy_{i-1,14}\right) + \Delta V4_{(i-k)}(y_{i-1,1} - x_{i,1}) + \Delta V4_{(i-k)}(x_{i,1} - y_{i,1})}{M_i}$$

$$a_{i,4N+i-k} = \frac{\Delta VM_{(i-k)}[(y_{i-1,1} - x_{i,1}) + (x_{i,1} - y_{i,1})]}{M_i}$$

$$a_{N+i,i-k} = \frac{\delta(k)V_{(i-k)}\left(dy_{i-1,21}\right) + \Delta V1_{(i-k)}(y_{i-1,2} - x_{i,2}) + \Delta V1_{(i-k)}(x_{i,2} - y_{i,2})}{M_i}$$

$$a_{N+i,N+i-k} = \frac{\delta(k)V_{(i-k)}\left(dy_{i-1,22}\right) + \Delta V2_{(i-k)}(y_{i-1,2} - x_{i,2}) + \Delta V2_{(i-k)}(x_{i,2} - y_{i,2})}{M_i}$$

$$a_{N+i,2N+i-k} = \frac{\delta(k)V_{(i-k)}\left(dy_{i-1,23}\right) + \Delta V3_{(i-k)}(y_{i-1,2} - x_{i,2}) + \Delta V3_{(i-k)}(x_{i,2} - y_{i,2})}{M_i}$$

$$a_{N+i,3N+i-k} = \frac{\delta(k)V_{(i-k)}\left(dy_{i-1,24}\right) + \Delta V4_{(i-k)}(y_{i-1,2} - x_{i,2}) + \Delta V4_{(i-k)}(x_{i,2} - y_{i,2})}{M_i}$$

$$a_{N+i,4N+i-k} = \frac{\Delta VM_{(i-k)}[(y_{i-1,2} - x_{i,2}) + (x_{i,2} - y_{i,2})]}{M_i}$$

$$a_{2N+i,i-k} = \frac{\delta(k)V_{(i-k)}\left(dy_{i-1,31}\right) + \Delta V1_{(i-k)}(y_{i-1,3} - x_{i,3}) + \Delta V1_{(i-k)}(x_{i,3} - y_{i,3})}{M_i}$$

$$a_{2N+i,N+i-k} = \frac{\delta(k)V_{(i-k)}\left(dy_{i-1,32}\right) + \Delta V2_{(i-k)}(y_{i-1,3} - x_{i,3}) + \Delta V2_{(i-k)}(x_{i,3} - y_{i,3})}{M_i}$$

$$a_{2N+i,2N+i-k} = \frac{\delta(k)V_{(i-k)}\left(dy_{i-1,33}\right) + \Delta V3_{(i-k)}(y_{i-1,3} - x_{i,3}) + \Delta V3_{(i-k)}(x_{i,3} - y_{i,3})}{M_i}$$

$$a_{2N+i,3N+i-k} = \frac{\delta(k)V_{(i-k)}\left(dy_{i-1,34}\right) + \Delta V4_{(i-k)}(y_{i-1,3} - x_{i,3}) + \Delta V4_{(i-k)}(x_{i,3} - y_{i,3})}{M_i}$$

$$a_{2N+i,4N+i-k} = \frac{\Delta VM_{(i-k)}[(y_{i-1,3} - x_{i,3}) + (x_{i,3} - y_{i,3})]}{M_i}$$

$$a_{3N+i,i-k} = \frac{\delta(k)V_{(i-k)}\left(dy_{i-1,41}\right) + \Delta V1_{(i-k)}(y_{i-1,4} - x_{i,4}) + \Delta V1_{(i-k)}(x_{i,4} - y_{i,4})}{M_i}$$

$$a_{3N+i,N+i-k} = \frac{\delta(k)V_{(i-k)}\left(dy_{i-1,42}\right) + \Delta V2_{(i-k)}(y_{i-1,4} - x_{i,4}) + \Delta V2_{(i-k)}(x_{i,4} - y_{i,4})}{M_i}$$

$$a_{3N+i,2N+i-k} = \frac{\delta(k)V_{(i-k)}\left(dy_{i-1,43}\right) + \Delta V3_{(i-k)}(y_{i-1,4} - x_{i,4}) + \Delta V3_{(i-k)}(x_{i,4} - y_{i,4})}{M_i}$$

$$a_{3N+i,3N+i-k} = \frac{\delta(k)V_{(i-k)}\left(dy_{i-1,44}\right) + \Delta V4_{(i-k)}(y_{i-1,4} - x_{i,4}) + \Delta V4_{(i-k)}(x_{i,4} - y_{i,4})}{M_i}$$

$$a_{3N+i,4N+i-k} = \frac{\Delta VM_{(i-k)}[(y_{i-1,4} - x_{i,4}) + (x_{i,4} - y_{i,4})]}{M_i}$$

A-3.3. Reactive trays (tray *i*)

$F_i = 0$ except in *i* = nf1 where $F_i = F_A$ and $z(j) = Z_{a,j}$, and in the *i* = nf2 where $F_i = F_B$, $z(j) = Z_{b,j}$

$$a_{i,i} = \frac{-L_{i+1} - V_{i-1} + V_i\left(1 - dy_{i,11}\right) + \Delta V1_i(x_{i,1} - y_{i,1}) + stoich(1)\Delta R1_i - F_i}{M_i}$$

$$a_{i,N+i} = \frac{\Delta V2_i\, x_{i,1} - \left(V_i dy_{i,12} + \Delta V2_i\, y_{i,1}\right) + stoich(1)\Delta R2_i}{M_i}$$

$$a_{i,2N+i} = \frac{\Delta V3_i\, x_{i,1} - \left(V_i dy_{i,13} + \Delta V3_i\, y_{i,1}\right) + stoich(1)\Delta R3_i}{M_i}$$

$$a_{i,3N+i} = \frac{\Delta V4_i\, x_{i,1} - \left(V_i dy_{i,14} + \Delta V4_i\, y_{i,1}\right) + stoich(1)\Delta R4_i}{M_i}$$

$$a_{i,i+1} = \frac{L_{i+1}}{M_i} \qquad a_{i,4N+i+1} = \frac{(x_{i+1,1} - x_{i,1})}{M_i \beta}$$

$$a_{i,4N+i} = -\frac{\left\lfloor L_{i+1}\left(x_{i+1,1} - x_{i,1}\right) + V_{i-1}\left(y_{i-1,1} - x_{i,1}\right) + V_{i-1}\left(x_{i,1} - y_{i,1}\right) + F_i\,(z(1) - x_{i,1})\right\rfloor}{M_i^2}$$

$$a_{N+i,i} = \frac{\Delta V1_i\, x_{i,1} - \left(V_i dy_{i,21} + \Delta V1_i\, y_{i,2}\right) + stoich(2)\Delta R1_i}{M_i}$$

$$a_{N+i,N+i} = \frac{-L_{i+1} - V_{i-1} + V_i\left(1 - dy_{i,22}\right) + \Delta V2_i\,(x_{i,2} - y_{i,2}) + stoich(2)\Delta R2_i - F_i}{M_i}$$

$$a_{N+i,2N+i} = \frac{\Delta V3_i\, x_{i,2} - \left(V_i dy_{i,23} + \Delta V3_i\, y_{i,2}\right) + stoich(2)\Delta R3_i}{M_i}$$

$$a_{N+i,3N+i} = \frac{\Delta V4_i\, x_{i,2} - \left(V_i dy_{i,24} + \Delta V4_i\, y_{i,2}\right) + stoich(2)\Delta R4_i}{M_i}$$

$$a_{N+i,N+i+1} = \frac{L_{i+1}}{M_i} \qquad a_{N+i,4N+i+1} = \frac{(x_{i+1,2} - x_{i,2})}{M_i \beta}$$

$$a_{N+i,4N+i} = -\frac{\left\lfloor L_{i+1}\left(x_{i+1,2} - x_{i,2}\right) + V_{i-1}\left(y_{i-1,2} - x_{i,2}\right) + V_{i-1}\left(x_{i,2} - y_{i,2}\right) + F_i\,(z(2) - x_{i,2})\right\rfloor}{M_i^2}$$

$$a_{2N+i,i} = \frac{\Delta V1_i\, x_{i,3} - \left(V_i dy_{i,31} + \Delta V1_i\, y_{i,3}\right) + stoich(3)\Delta R1_i}{M_i}$$

$$a_{2N+i,N+i} = \frac{\Delta V2_i\, x_{i,3} - \left(V_i dy_{i,32} + \Delta V2_i\, y_{i,3}\right) + stoich(3)\Delta R2_i}{M_i}$$

$$a_{2N+i,2N+i} = \frac{-L_{i+1} - V_{i-1} + V_i\left(1 - dy_{i,33}\right) + \Delta V3_{(i)}\,(x_{i,3} - y_{i,3}) + stoich(3)\Delta R3_i - F_i}{M_i}$$

$$a_{2N+i,3N+i} = \frac{\Delta V4_i\, x_{i,3} - \left(V_i dy_{i,34} + \Delta V4_i\, y_{i,3}\right) + stoich(3)\Delta R4_i}{M_i}$$

$$a_{2N+i,2N+i+1} = \frac{L_{i+1}}{M_i} \qquad a_{2N+i,4N+i+1} = \frac{(x_{i+1,3} - x_{i,3})}{M_i \beta}$$

$$a_{2N+i,4N+i} = -\frac{\left\lfloor L_{i+1}\left(x_{i+1,3} - x_{i,3}\right) + V_{i-1}\left(y_{i-1,3} - x_{i,3}\right) + V_i\left(x_{i,3} - y_{i,3}\right) + F_i\,(z(3) - x_{i,3})\right\rfloor}{M_i^2}$$

$$a_{3N+i,i} = \frac{\Delta V1_i\, x_{i,4} - \left(V_i dy_{i,41} + \Delta V1_i\, y_{i,4}\right) + stoich(4)\Delta R1_i}{M_i}$$

$$a_{3N+i,N+i} = \frac{\Delta V2_i\, x_{i,4} - \left(V_i dy_{i,42} + \Delta V2_i\, y_{i,4}\right) + stoich(4)\Delta R2_i}{M_i}$$

$$a_{3N+i,2N+i} = \frac{\Delta V3_i\, x_{i,4} - \left(V_i dy_{i,43} + \Delta V3_i\, y_{i,4}\right) + stoich(4)\Delta R3_i}{M_i}$$

$$a_{3N+i,3N+i} = \frac{-L_{i+1} - V_{i-1} + V_i\left(1 - dy_{i,44}\right) + \Delta V4_i\,(x_{i,4} - y_{i,4}) + stoich(4)\Delta R4_i - F_i}{M_i}$$

$$a_{3N+i,3N+i+1} = \frac{L_{i+1}}{M_i} \qquad a_{3N+i,4N+i+1} = \frac{(x_{i+1,4} - x_{i,4})}{M_i\beta}$$

$$a_{3N+i,4N+i} = -\frac{\left[L_{i+1}\left(x_{i+1,4} - x_{i,4}\right) + V_{i-1}\left(y_{i-1,4} - x_{i,4}\right) + V_{i-1}\left(x_{i,4} - y_{i,4}\right) + F_i\,(z(4) - x_{i,4})\right]}{M_i^2}$$

$$a_{4N+i,4N+i} = -(\frac{1}{\beta} + \frac{\lambda}{\Delta H_v}\Delta Rm_i) \qquad a_{4N+i,4N+i+1} = \frac{1}{\beta} \qquad a_{4N+i,i} = \frac{-\lambda}{\Delta H_v}\Delta R1_i$$

$$a_{4N+i,N+i} = \frac{-\lambda}{\Delta H_v}\Delta R2_{i,} \qquad a_{4N+i,2N+i} = \frac{-\lambda}{\Delta H_v}\Delta R3_i \qquad a_{4N+i,3N+i} = \frac{-\lambda}{\Delta H_v}\Delta R4_i$$

A-4. Rectifying Section

A-4.1 Tray *i*: (*i* = nf2+1)

$$a_{i,N+i-1} = \left(\frac{V_{i-1}dy_{i-1,12} + \Delta V2_{(i-1)}(y_{i-1,1} - y_{i,1})}{M_i}\right) \qquad a_{i,i-1} = \left(\frac{V_{i-1}dy_{i-1,11} + \Delta V1_{(i-1)}(y_{i-1,1} - y_{i,1})}{M_i}\right)$$

$$a_{i,2N+i-1} = \left(\frac{V_{i-1}dy_{i-1,13} + \Delta V3_{(i-1)}(y_{i-1,1} - y_{i,1})}{M_i}\right) \qquad a_{i,3N+i-1} = \left(\frac{V_{i-1}dy_{i-1,14} + \Delta V4_{(i-1)}(y_{i-1,1} - y_{i,1})}{M_i}\right)$$

$$a_{N+i,i-1} = \left(\frac{V_{i-1}dy_{i-1,21} + \Delta V1_{(i-1)}(y_{i-1,2} - y_{i,2})}{M_i}\right) \qquad a_{N+i,N+i-1} = \left(\frac{V_{i-1}dy_{i-1,22} + \Delta V2_{(i-1)}(y_{i-1,2} - y_{i,2})}{M_i}\right)$$

$$a_{N+i,2N+i-1} = \left(\frac{V_{i-1}dy_{i-1,23} + \Delta V3_{(i-1)}(y_{i-1,2} - y_{i,2})}{M_i}\right) \qquad a_{N+i,3N+i-1} = \left(\frac{V_{i-1}dy_{i-1,24} + \Delta V4_{i-1}(y_{i-1,2} - y_{i,2})}{M_i}\right)$$

$$a_{2N+i,i-1}=\left(\frac{V_{i-1}dy_{i-1,31}+\Delta V1_{i-1}(y_{i-1,3}-y_{i,3})}{M_i}\right)\qquad a_{2N+i,N+i-1}=\left(\frac{V_{i-1}dy_{i-1,32}+\Delta V2_{i-1}(y_{i-1,3}-y_{i,3})}{M_i}\right)$$

$$a_{2N+i,2N+i-1}=\left(\frac{V_{i-1}dy_{i-1,33}+\Delta V3_{i-1}(y_{i-1,3}-y_{i,3})}{M_i}\right)\qquad a_{2N+i,3N+i-1}=\left(\frac{V_{i-1}dy_{i-1,34}+\Delta V4_{i-1}(y_{i-1,3}-y_{i,3})}{M_i}\right)$$

$$a_{3N+i,i-1}=\left(\frac{V_n dy_{i-1,41}+\Delta V1_n(y_{i-1,4}-y_{i,4})}{M_i}\right)\qquad a_{3N+i,N+i-1}=\left(\frac{V_n dy_{i-1,42}+\Delta V2_n(y_{i-1,4}-y_{i,4})}{M_i}\right)$$

$$a_{3N+i,2N+i-1}=\left(\frac{V_n dy_{i-1,43}+\Delta V3_n(y_{i-1,4}-y_{i,4})}{M_i}\right)\qquad a_{3N+i,3N+i-1}=\left(\frac{V_n dy_{i-1,44}+\Delta V4_n(y_{i-1,4}-y_{i,4})}{M_i}\right)$$

A-4.2. Tray *i*: (*i* = nf2+2: N-1)

$$a_{i,i-1}=\left({}^{V_n}\!/_{M_i}\right)dy_{i-1,11}\qquad a_{i,N+i-1}=\left({}^{V_n}\!/_{M_i}\right)dy_{i-1,12}\qquad a_{i,2N+i-1}=\left({}^{V_n}\!/_{M_i}\right)dy_{i-1,13}$$

$$a_{i,3N+i-1}=\left({}^{V_n}\!/_{M_i}\right)dy_{i-1,14}\qquad a_{N+i,i-1}=\left({}^{V_n}\!/_{M_i}\right)dy_{i-1,21}\qquad a_{N+i,N+i-1}=\left({}^{V_n}\!/_{M_i}\right)dy_{i-1,22}$$

$$a_{N+i,2N+i-1}=\left({}^{V_n}\!/_{M_i}\right)dy_{i-1,23}\qquad a_{N+i,3N+i-1}=\left({}^{V_n}\!/_{M_i}\right)dy_{i-1,24}\qquad a_{2N+i,i-1}=\left({}^{V_n}\!/_{M_i}\right)dy_{i-1,31}$$

$$a_{2N+i,N+i-1}=\left({}^{V_n}\!/_{M_i}\right)dy_{i-1,32}\qquad a_{2N+i,2N+i-1}=\left({}^{V_n}\!/_{M_i}\right)dy_{i-1,33}\qquad a_{2N+i,3N+i-1}=\left({}^{V_n}\!/_{M_i}\right)dy_{i-1,34}$$

$$a_{3N+i,i-1}=\left({}^{V_n}\!/_{M_i}\right)dy_{i-1,41}\qquad a_{3N+i,N+i-1}=\left({}^{V_n}\!/_{M_i}\right)dy_{i-1,42}\qquad a_{3N+i,2N+i-1}=\left({}^{V_n}\!/_{M_i}\right)dy_{i-1,43}$$

$$a_{3N+i,3N+i-1}=\left({}^{V_n}\!/_{M_i}\right)dy_{i-1,44}$$

A-4.3. Tray *i*: (*i* = nf2+1: N-1)

for k = 1 to Nrx

$$a_{i,Ns+1+k}=(y_{i-1,1}-y_{i,1})\Delta V1_{Ns+1+k}\qquad a_{i,N+Ns+1+k}=(y_{i-1,1}-y_{i,1})\Delta V2_{Ns+1+k}$$

$$a_{i,2N+Ns+1+k}=(y_{i-1,1}-y_{i,1})\Delta V3_{Ns+1+k}\qquad a_{i,3N+Ns+1+k}=(y_{i-1,1}-y_{i,1})\Delta V4_{Ns+1+k}$$

$$a_{i,4N+Ns+1+k}=(y_{i-1,1}-y_{i,1})\Delta VM_{Ns+1+k}\qquad a_{N+i,Ns+1+k}=(y_{i-1,2}-y_{i,2})\Delta V1_{Ns+1+k}$$

$$a_{N+i,N+Ns+1+k}=(y_{i-1,2}-y_{i,2})\Delta V2_{Ns+1+k}\qquad a_{N+i,2N+Ns+1+k}=(y_{i-1,2}-y_{i,2})\Delta V3_{Ns+1+k}$$

$$a_{N+i,3N+Ns+1+k} = (y_{i-1,2} - y_{i,2})\Delta V4_{Ns+1+k} \qquad a_{N+i,4N+Ns+1+k} = (y_{i-1,2} - y_{i,2})\Delta VM_{Ns+1+k}$$

$$a_{2N+i,Ns+1+k} = (y_{i-1,3} - y_{i,3})\Delta V1_{Ns+1+k} \qquad a_{2N+i,N+Ns+1+k} = (y_{i-1,3} - y_{i,3})\Delta V2_{Ns+1+k}$$

$$a_{2N+i,2N+Ns+1+k} = (y_{i-1,3} - y_{i,3})\Delta V3_{Ns+1+k} \qquad a_{2N+i,3N+Ns+1+k} = (y_{i-1,3} - y_{i,3})\Delta V4_{Ns+1+k}$$

$$a_{2N+i,4N+Ns+1+k} = (y_{i-1,3} - y_{i,3})\Delta VM_{Ns+1+k} \qquad a_{3N+i,Ns+1+k} = (y_{i-1,4} - y_{i,4})\Delta V1_{Ns+1+k}$$

$$a_{3N+i,N+Ns+1+k} = (y_{i-1,4} - y_{i,4})\Delta V2_{Ns+1+k} \qquad a_{3N+i,2N+Ns+1+k} = (y_{i-1,4} - y_{i,4})\Delta V3_{Ns+1+k}$$

$$a_{3N+i,3N+Ns+1+k} = (y_{i-1,4} - y_{i,4})\Delta v4_{Ns+1+k} \qquad a_{4N+i,4N+Ns+1+k} = (y_{i-1,4} - y_{i,4})\Delta VM_{Ns+1+k}$$

$$a_{i,i} = \frac{-\left(L_{i+1} + V_n dy_{i,11}\right)}{M_i} \qquad a_{i,N+i} = -\left({}^{V_n}\!\big/_{M_i}\right)dy_{i,12} \qquad a_{i,2N+i} = -\left({}^{V_n}\!\big/_{M_i}\right)dy_{i,13}$$

$$a_{i,3N+i} = -\left({}^{V_n}\!\big/_{M_i}\right)dy_{i,14} \qquad a_{i,i+1} = \frac{L_{i+1}}{M_i} \qquad a_{i,4N+i+1} = \frac{(x_{i+1,1} - x_{i,1})}{M_i\beta}$$

$$a_{i,4N+i} = -\frac{\left[L_{i+1}\left(x_{i+1,1} - x_{i,1}\right) + V\left(y_{i-1,1} - y_{i,1}\right)\right]}{M_i^2}$$

$$a_{N+i,i} = -\left({}^{V_n}\!\big/_{M_i}\right)dy_{i,21} \qquad a_{N+i,N+i} = \frac{-\left(L_{i+1} + V_n dy_{i,22}\right)}{M_i} \qquad a_{N+i,2N+i} = -\left({}^{V_n}\!\big/_{M_i}\right)dy_{i,23}$$

$$a_{N+i,3N+i} = -\left({}^{V_n}\!\big/_{M_i}\right)dy_{i,24} \qquad a_{N+i,N+i+1} = \frac{L_{i+1}}{M_i} \qquad a_{N+i,4N+i+1} = \frac{(x_{i+1,2} - x_{i,2})}{M_i\beta}$$

$$a_{N+i,4N+i} = -\frac{\left[L_{i+1}\left(x_{i+1,2} - x_{i,2}\right) + V_{i-1}(y_{i-1,2} - y_{i,2})\right]}{M_i^2}$$

$$a_{2N+i,i} = -\left({}^{V_n}\!\big/_{M_i}\right)dy_{i,31} \qquad a_{2N+i,N+i} = -\left({}^{V_n}\!\big/_{M_i}\right)dy_{i,32} \qquad a_{2N+i,2N+i} = \frac{-\left(L_{i+1} + V_n dy_{i,33}\right)}{M_i}$$

$$a_{2N+i,3N+i} = -\left({}^{V_n}\!\big/_{M_i}\right)dy_{i,34} \qquad a_{2N+i,2N+i+1} = \frac{L_{i+1}}{M_i} \qquad a_{2N+i,4N+i+1} = \frac{(x_{i+1,3} - x_{i,3})}{M_i\beta}$$

$$a_{2N+i,4N+i} = -\frac{\left[L_{i+1}\left(x_{i+1,3} - x_{i,3}\right) + V_{i-1}(y_{i-1,3} - y_{i,3})\right]}{M_i^2}$$

$$a_{3N+i,i} = -\left({}^{V_n}\!\big/_{M_i}\right)dy_{i,41} \qquad a_{3N+i,N+i} = -\left({}^{V_n}\!\big/_{M_i}\right)dy_{i,42} \qquad a_{3N+i,2N+i} = -\left({}^{V_n}\!\big/_{M_i}\right)dy_{i,43}$$

$$a_{3N+i,3N+i} = \frac{-\left(L_{i+1} + V_n dy_{i,44}\right)}{M_i} \qquad a_{3N+i,3N+i+1} = \frac{L_{i+1}}{M_i} \qquad a_{3N+i,4N+i+1} = \frac{(x_{i+1,4} - x_{i,4})}{M_i\beta}$$

$$a_{3N+i,4N+i} = -\frac{\lfloor L_{i+1}\left(x_{i+1,4} - x_{i,4}\right) + V_{i-1}(y_{i-1,4} - y_{i,4})\rfloor}{M_i^2}$$

A-5. Reflux drum (stage N):

for $k = 1$ to Nrx

$a_{N,Ns+1+k} = (y_{N-1,1} - x_{N,1})\Delta V1_{Ns+1+k}$ $a_{N,N+Ns+1+k} = (y_{N-1,1} - x_{N,1})\Delta V2_{Ns+1+k}$

$a_{N,2N+Ns+1+k} = (y_{N-1,1} - x_{N,1})\Delta V3_{Ns+1+k}$ $a_{N,3N+Ns+1+k} = (y_{N-1,1} - x_{N,1})\Delta V4_{Ns+1+k}$

$a_{N,4N+Ns+1+k} = (y_{N-1,1} - x_{N,1})\Delta VM_{Ns+1+k}$ $a_{2N,Ns+1+k} = (y_{N-1,2} - x_{N,2})\Delta V1_{Ns+1+k}$

$a_{2N,N+Ns+1+k} = (y_{N-1,2} - x_{N,2})\Delta V2_{Ns+1+k}$ $a_{2N,2N+Ns+1+k} = (y_{N-1,2} - x_{N,2})\Delta V3_{Ns+1+k}$

$a_{2N,3N+Ns+1+k} = (y_{N-1,2} - x_{N,2})\Delta V4_{Ns+1+k}$ $a_{2N,4N+Ns+1+k} = (y_{N-1,2} - x_{N,2})\Delta VM_{Ns+1+k}$

$a_{2N,Ns+1+k} = (y_{N-1,2} - x_{N,2})\Delta V1_{Ns+1+k}$ $a_{2N,N+Ns+1+k} = (y_{N-1,2} - x_{N,2})\Delta V2_{Ns+1+k}$

$a_{2N,2N+Ns+1+k} = (y_{N-1,2} - x_{N,2})\Delta V3_{Ns+1+k}$ $a_{2N,3N+Ns+1+k} = (y_{N-1,2} - x_{N,2})\Delta V4_{Ns+1+k}$

$a_{2N,4N+Ns+1+k} = (y_{N-1,2} - x_{N,2})\Delta VM_{Ns+1+k}$ $a_{4N,Ns+1+k} = (y_{N-1,4} - x_{N,4})\Delta V1_{Ns+1+k}$

$a_{4N,N+Ns+1+k} = (y_{N-1,4} - x_{N,4})\Delta V2_{Ns+1+k}$ $a_{4N,2N+Ns+1+k} = (y_{N-1,4} - x_{N,4})\Delta V3_{Ns+1+k}$

$a_{4N,3N+Ns+1+k} = (y_{N-1,4} - x_{N,4})\Delta R4_{Ns+1+k}$ $a_{4N,4N+Ns+1+k} = (y_{N-1,4} - x_{N,4})\Delta VM_{Ns+1+k}$

$a_{5N,Ns+1+k} = \Delta V1_{Ns+1+k}$ $a_{5N,N+Ns+1+k} = \Delta V2_{Ns+1+k}$

$a_{5N,2N+Ns+1+k} = \Delta V3_{Ns+1+k}$ $a_{5N,3N+Ns+1+k} = \Delta V4_{Ns+1+k}$ $a_{5N,4N+Ns+1+k} = \dfrac{\lambda}{\Delta H}\Delta Rm_{Ns+1+k}$

$a_{N,N-1} = \left({}^{V_n}\!\big/_{M_N}\right)dy_{N-1,11}$ $a_{N,2N-1} = \left({}^{V_n}\!\big/_{M_N}\right)dy_{N-1,12}$ $a_{N,3N-1} = \left({}^{V_n}\!\big/_{M_N}\right)dy_{N-1,13}$

$a_{N,4N-1} = \left({}^{V_n}\!\big/_{M_N}\right)dy_{N-1,14}$ $a_{N,N} = -\dfrac{V_N}{M_N}$ $a_{N,5N} = -\dfrac{\lfloor V_n\left(y_{N-1,1} - x_{N1}\right)\rfloor}{M_N^2}$

$a_{2N,N-1} = \left({}^{V_n}\!\big/_{M_N}\right)dy_{N-1,21}$ $a_{2N,2N-1} = \left({}^{V_n}\!\big/_{M_N}\right)dy_{N-1,22}$ $a_{2N,3N-1} = \left({}^{V_n}\!\big/_{M_N}\right)dy_{N-1,23}$

$a_{2N,4N-1} = \left({}^{V_n}\!\big/_{M_N}\right)dy_{N-1,24}$ $a_{2N,2N} = -\dfrac{V_n}{M_N}$ $a_{2N,5N} = -\dfrac{\lfloor V_n\left(y_{N-1,2} - x_{N2}\right)\rfloor}{M_N^2}$

$a_{3N,N-1} = \left({}^{V_n}\!\big/_{M_N}\right)dy_{N-1,31}$ $a_{3N,2N-1} = \left({}^{V_n}\!\big/_{M_N}\right)dy_{N-1,32}$ $a_{3N,3N-1} = \left({}^{V_n}\!\big/_{M_N}\right)dy_{N-1,33}$

$$a_{3N,4N-1} = \left({}^{V_n}\!\big/_{M_N} \right) dy_{N-1,34} \qquad a_{3N,3N} = -\frac{V_N}{M_N} \qquad a_{3N,5N} = -\frac{\left\lfloor V_n \left(y_{N-1,3} - x_{N3} \right) \right\rfloor}{M_N^2}$$

$$a_{4N,N-1} = \left({}^{V_n}\!\big/_{M_N} \right) dy_{N-1,41} \qquad a_{4N,2N-1} = \left({}^{V_n}\!\big/_{M_N} \right) dy_{N-1,42} \qquad a_{4N,3N-1} = \left({}^{V_n}\!\big/_{M_N} \right) dy_{N-1,43}$$

$$a_{4N,4N-1} = \left({}^{V_n}\!\big/_{M_N} \right) dy_{N-1,44} \qquad a_{4N,4N} = -\frac{V_N}{M_N} \qquad a_{4N,5N} = -\frac{\left\lfloor V_n \left(y_{N-1,4} - x_{N4} \right) \right\rfloor}{M_N^2}$$

$$a_{5N-1,5N-1} = -\frac{1}{\beta} \qquad a_{5N,5N} = \frac{-2D}{M_N}$$

$$\Delta T_{i,1}^{x} = \frac{\partial T_i}{\partial x_{i,1}} = -\frac{B_{vp,1}\alpha_1}{G(i)\left(A_{vp,1} - In\left({}^{\alpha_1 P}\!\big/_{G(i)} \right) \right)^2}$$

$$\Delta T_{i,2}^{x} = \frac{\partial T_i}{\partial x_{i,2}} = -\frac{B_{vp,1}\alpha_2}{G(i)\left(A_{vp,1} - In\left({}^{\alpha_1 P}\!\big/_{G(i)} \right) \right)^2}$$

$$\Delta T_{i,3}^{x} = \frac{\partial T_i}{\partial x_{i,3}} = -\frac{B_{vp,1}\alpha_3}{G(i)\left(A_{vp,1} - In\left({}^{\alpha_1 P}\!\big/_{G(i)} \right) \right)^2}$$

$$\Delta T_{i,4}^{x} = \frac{\partial T_i}{\partial x_{i,4}} = -\frac{B_{vp,1}\alpha_4}{G(i)\left(A_{vp,1} - In\left({}^{\alpha_1 P}\!\big/_{G(i)} \right) \right)^2} \qquad \text{where } G(i) = \sum_{k=1}^{Nc} \alpha_k x_{ik}$$

$$\Delta k_{F,i}^{T} = \frac{dk_{F,i}}{dT_i} = \frac{a_F E_F}{R_i T_i^2} e^{-{}^{E_F}\!/_{RT_i}} \qquad \Delta k_{B,i}^{T} = \frac{dk_{B,i}}{dT_i} = \frac{a_B E_B}{R_i T_i^2} e^{-{}^{E_B}\!/_{RT_i}}$$

$$\Delta k_{Fi,1}^{x} = \frac{\partial K_{Fi}}{\partial x_{i,1}} = \Delta k_{F,i}^{T} \Delta T_{i,1}^{x} \qquad \Delta k_{Fi,2}^{x} = \frac{\partial K_{Fi}}{\partial x_{i,2}} = \Delta k_{F,i}^{T} \Delta T_{i,2}^{x}$$

$$\Delta k_{Fi,3}^{x} = \frac{\partial K_{Fi}}{\partial x_{i,3}} = \Delta k_{F,i}^{T} \Delta T_{i,3}^{x} \qquad \Delta k_{Fi,4}^{x} = \frac{\partial K_{Fi}}{\partial x_{i,4}} = \Delta k_{F,i}^{T} \Delta T_{i,4}^{x}$$

$$\Delta k_{Bi,1}^{x} = \frac{\partial K_{Bi}}{\partial x_{i,1}} = \Delta k_{B,i}^{T} \Delta T_{i,1}^{x} \qquad \Delta k_{Bi,2}^{x} = \frac{\partial K_{Bi}}{\partial x_{i,2}} = \Delta k_{B,i}^{T} \Delta T_{i,2}^{x}$$

$$\Delta k_{Bi,3}^{x} = \frac{\partial K_{Bi}}{\partial x_{i,3}} = \Delta k_{B,i}^{T} \Delta T_{i,3}^{x} \qquad \Delta k_{Bi,4}^{x} = \frac{\partial K_{Bi}}{\partial x_{i,4}} = \Delta k_{B,i}^{T} \Delta T_{i,4}^{x}$$

$$\Delta R1_i = \frac{dR_i}{dx_{i,1}} = M_i\left(k_{F,i}x_{i,2} + x_{i,1}x_{i,2}\Delta k_{Fi,1}^{x} - x_{i,3}x_{i,4}\Delta k_{Bi,1}^{x}\right)$$

$$\Delta R2_i = \frac{dR_i}{dx_{i,2}} = M_i\left(k_{F,i}x_{i,1} + x_{i,1}x_{i,2}\Delta k_{Fi,2}^{x} - x_{i,3}x_{i,4}\Delta k_{Bi,2}^{x}\right)$$

$$\Delta R3_i = \frac{dR_i}{dx_{i,3}} = M_i\left(x_{i,1}x_{i,2}\Delta k_{Fi,3}^{x} - k_{B,i}x_{i,4} - x_{i,3}x_{i,4}\Delta k_{Bi,3}^{x}\right)$$

$$\Delta R4_i = \frac{dR_i}{dx_{i,4}} = M_i\left(x_{i,1}x_{i,2}\Delta k_{Fi,4}^{x} - k_{B,i}x_{i,3} - x_{i,3}x_{i,4}\Delta k_{Bi,4}^{x}\right)$$

$$\Delta Rm_i = \frac{dR_i}{dM_i} = \left(k_{F,i}x_{i,1}x_{i,2} - k_{B,i}x_{i,3}x_{i,4}\right)$$

$$\Delta V1_i = \frac{\partial V_i}{\partial x_{i,1}} = \frac{\lambda}{\Delta H_v}\Delta R1_i \qquad \Delta V2_i = \frac{\partial V_i}{\partial x_{i,2}} = \frac{\lambda}{\Delta H_v}\Delta R2_i$$

$$\Delta V3_i = \frac{\partial V_i}{\partial x_{i,3}} = \frac{\lambda}{\Delta H_v}\Delta R3_i \qquad \Delta V4_i = \frac{\partial V_i}{\partial x_{i,4}} = \frac{\lambda}{\Delta H_v}\Delta R4_i$$

$$\Delta VM_i = \frac{\partial V_i}{\partial M_i} = \frac{\lambda}{\Delta H_v}\Delta Rm_i$$

$$dy_{i,11} = \frac{\partial y_{i1}}{\partial x_{i1}} = \frac{\alpha_1\left(\alpha_2 x_{i2} + \alpha_3 x_{i3} + \alpha_4 x_{i4}\right)}{G(i)^2} \qquad dy_{i,12} = \frac{\partial y_{i1}}{\partial x_{i2}} = \frac{-\alpha_1 x_{i1}\alpha_2}{G(i)^2}$$

$$dy_{i,13} = \frac{\partial y_{i1}}{\partial x_{i3}} = \frac{-\alpha_1 x_{i1}\alpha_3}{G(i)^2} \qquad dy_{i,14} = \frac{\partial y_{i1}}{\partial x_{i4}} = \frac{-\alpha_1 x_{i1}\alpha_4}{G(i)^2}$$

$$\frac{\partial y_{i2}}{\partial x_{i1}} = dy_{i,21} = \frac{-\alpha_2 x_{i2}\alpha_1}{G(i)^2} \qquad dy_{i,22} = \frac{\partial y_{i2}}{\partial x_{i2}} = \frac{\alpha_2\left(\alpha_1 x_{i1} + \alpha_3 x_{i3} + \alpha_4 x_{i4}\right)}{G(i)^2}$$

$$dy_{i,23} = \frac{\partial y_{i2}}{\partial x_{i3}} = \frac{-\alpha_2 x_{i2}\alpha_3}{G(i)^2} \qquad dy_{i,24} = \frac{\partial y_{i2}}{\partial x_{i4}} = \frac{-\alpha_2 x_{i2}\alpha_4}{G(i)^2}$$

$$dy_{i,31} = \frac{\partial y_{i3}}{\partial x_{i1}} = \frac{-\alpha_3 x_{i3}\alpha_1}{G(i)^2} \qquad dy_{i,32} = \frac{\partial y_{i3}}{\partial x_{i2}} = \frac{-\alpha_3 x_{i3}\alpha_2}{G(i)^2}$$

$$dy_{i,33} = \frac{\partial y_{i3}}{\partial x_{i3}} = \frac{\alpha_3\left(\alpha_1 x_{i1} + \alpha_2 x_{i2} + \alpha_3 x_{i3}\right)}{G(i)^2} \qquad dy_{i,34} = \frac{\partial y_{i3}}{\partial x_{i4}} = \frac{-\alpha_3 x_{i3}\alpha_4}{G(i)^2}$$

$$dy_{i,41} = \frac{\partial y_{i4}}{\partial x_{i1}} = \frac{-\alpha_4 x_{i4} \alpha_1}{G(i)^2} \qquad dy_{i,42} = \frac{\partial y_{i4}}{\partial x_{i2}} = \frac{-\alpha_4 x_{i4} \alpha_2}{G(i)^2}$$

$$dy_{i,43} = \frac{\partial y_{i4}}{\partial x_{i3}} = \frac{-\alpha_4 x_{i4} \alpha_3}{G(i)^2} \qquad dy_{i,44} = \frac{\partial y_{i4}}{\partial x_{i4}} = \frac{\alpha_4 \left(\alpha_1 x_{i1} + \alpha_2 x_{i2} + \alpha_3 x_{i3}\right)}{G(i)^2}$$

Appendix B

Entries of Matrix B

Input variable Vector: $U = [V_S, R,]^T$

Dimension: (5N X 2)

B-1. Reboiler:

$$b_{1,1} = \frac{\left(x_{1,1} - y_{1,1}\right)}{M_1} \qquad b_{N-1,2} = \frac{\left(x_{N-2,1} - x_{N-1,1}\right)}{M_{N-1}} \qquad b_{N+1,1} = \frac{\left(x_{1,2} - y_{1,2}\right)}{M_1}$$

$$b_{2N-1,2} = \frac{\left(x_{N-2,2} - x_{N-1,2}\right)}{M_{N-1}} \qquad b_{2N+1,1} = \frac{\left(x_{1,3} - y_{1,3}\right)}{M_1} \qquad b_{3N-1,2} = \frac{\left(x_{N-2,3} - x_{N-1,3}\right)}{M_{N-1}}$$

$$b_{3N+1,1} = \frac{\left(x_{1,4} - y_{1,4}\right)}{M_1} \qquad b_{4N-1,2} = \frac{\left(x_{N-2,3} - x_{N-1,3}\right)}{M_{N-1}} \qquad b_{4N+1,1} = -1 \qquad b_{5N,2} = -1$$

B-2. Stripping Section :($2 \le i \le Ns + 1$)

$$b_{i,1} = \frac{\left(y_{i-1,1} - y_{i,1}\right)}{M_i} \qquad b_{N+i,1} = \frac{\left(y_{i-1,2} - y_{i,2}\right)}{M_i} \qquad b_{2N+i,1} = \frac{\left(y_{i-1,3} - y_{i,3}\right)}{M_i} \qquad b_{3N+i,1} = \frac{\left(y_{i-1,4} - y_{i,4}\right)}{M_i}$$

B-3. Reactive Section: ($Ns + 2 \le i \le Ns + Nrx + 1$)

$$b_{i,1} = \frac{\left(y_{i-1,1} - x_{i,1}\right) + \left(x_{i,1} - y_{i,1}\right)}{M_i} \qquad b_{N+i,1} = \frac{\left(y_{i-1,2} - x_{i,2}\right) + \left(x_{i,2} - y_{i,2}\right)}{M_i}$$

$$b_{2N+i,1} = \frac{\left(y_{i-1,3} - x_{i,3}\right) + \left(x_{i,3} - y_{i,3}\right)}{M_i} \qquad b_{3N+i,1} = \frac{\left(y_{i-1,4} - x_{i,4}\right) + \left(x_{i,4} - y_{i,4}\right)}{M_i}$$

B-4. Rectifying Section ($Ns + Nrx + 2 \le i \le Ns + Nrx + Nr + 1$)

$$b_{i,1} = \frac{\left(y_{i-1,1} - y_{i,1}\right)}{M_i} \quad b_{N+i,1} = \frac{\left(y_{i-1,2} - y_{i,2}\right)}{M_i} \quad b_{2N+i,1} = \frac{\left(y_{i-1,3} - y_{i,3}\right)}{M_i} \quad b_{3N+i,1} = \frac{\left(y_{i-1,4} - y_{i,4}\right)}{M_i}$$

B-5. Condenser (N-stage)

$$b_{N,1} = \frac{\left(y_{N-1,1} - x_{N,1}\right)}{M_i} \quad b_{2N,1} = \frac{\left(y_{N-1,2} - x_{N,2}\right)}{M_i} \quad b_{3N,1} = \frac{\left(y_{N-1,3} - x_{N,3}\right)}{M_i}$$

$$b_{4N,1} = \frac{\left(y_{N-1,4} - x_{N,4}\right)}{M_i} \quad b_{5N,1} = 1$$

Appendix C

Entries of Matrix C

Output variables Vector:

C-1. If output variables are considered to be composition of C in distillate and D in the bottom: $Y = \left[x_{1,4}, x_{N,3}\right]^T$, q = 2

Dimension: (q × 5N)

$C_{1,3N+1} = 1$, while $C_{1,i} = 0$ for $i \neq 3N+1$

$C_{2,3N} = 1$, while $C_{1,i} = 0$ for $i \neq 3N+1$

C-2. For temperature as out variables:

$Y = \left[T_1, T_2, \ldots T_{N-1}\right]^T$, q = N-1

Dimension: (q × 5N)

$C_{i,i} = \Delta T1_i$

$C_{i,N+i} = \Delta T2_i$

$C_{i,2N+i} = \Delta T3_i$

$C_{i,3N+i} = \Delta T4_i$

Appendix D

Entries of Matrix E

Disturbance vector: $d = \left[Z_{a,1}, Z_{a,2}, Z_{a,3}, Z_{a,4}, Z_{b,1}, Z_{b,2}, Z_{b,3}, Z_{b,4}, F_A, F_B\right]^T$

Dimension : (5N X 2Nc+2)

$$e_{nf1,1} = \frac{F_A}{M_{nf1}} \qquad e_{N+nf1,2} = \frac{F_A}{M_{nf1}} \qquad e_{2N+nf1,3} = \frac{F_A}{M_{nf1}}$$

$$e_{3N+nf1,4} = \frac{F_A}{M_{nf1}} \qquad e_{nf1,2Nc+1} = \frac{\left(Z_{a,1} - x_{nf1,1}\right)}{M_{nf1}} \qquad e_{N+nf1,2Nc+1} = \frac{\left(Z_{a,2} - x_{nf1,2}\right)}{M_{nf1}}$$

$$e_{4N+nf1,2Nc+1} = 1 \qquad e_{2N+nf1,2Nc+1} = \frac{\left(Z_{a,3} - x_{nf1,3}\right)}{M_{nf1}} \qquad e_{3N+nf1,2Nc+1} = \frac{\left(Z_{a,4} - x_{nf1,4}\right)}{M_{nf1}}$$

$$e_{nf2,Nc+1} = \frac{F_B}{M_{nf2}} \qquad e_{N+nf2,Nc+2} = \frac{F_B}{M_{nf2}} \qquad e_{2N+nf2,Nc+3} = \frac{F_B}{M_{nf2}}$$

$$e_{3N+nf2,Nc+4} = \frac{F_B}{M_{nf2}} \qquad e_{nf2,2Nc+2} = \frac{\left(Z_{b,1} - x_{nf2,1}\right)}{M_{nf2}} \qquad e_{N+nf2,2Nc+2} = \frac{\left(Z_{b,2} - x_{nf2,2}\right)}{M_{nf2}}$$

$$e_{4N+nf2,2Nc+2} = 1 \qquad e_{2N+nf2,2Nc+2} = \frac{\left(Z_{b,3} - x_{nf2,3}\right)}{M_{nf2}} \qquad e_{3N+nf2,2Nc+2} = \frac{\left(Z_{b,4} - x_{nf2,4}\right)}{M_{nf2}}$$

VITA

Name	Olanrewaju, Moshood Jide
Nationality	Nigeria
Date of birth	April 5th, 1975
Education	Bachelors Degree in Chemical Engineering from Federal University of Technology, Minna, Nigeria, in December 2000.